ELSEVIER

ICRP Publication 106

Annals of the ICRP

Radiation Dose to Patients from Radiopharmaceuticals

Addendum 3 to ICRP Publication 53

ICRP Publication 106

Approved by the Commission in October 2007

Abstract–In this report, the Commission provides biokinetic and dosimetric models for 33 radiopharmaceuticals, as well as recommendations related to breast feeding for mothers who have undergone a nuclear medicine investigation. The report is based on Addenda 3–9 to *Publication 53*. Addenda 3–7 have been available on the ICRP website (www.icrp.org) as interim reports. The work has been carried out by a Joint Task Group of ICRP Committees 2 and 3.

This publication provides biokinetic models, absorbed doses, and effective doses for the following radiopharmaceuticals: ^{11}C-acetate; ^{11}C-amino acids; ^{11}C-brain receptor substances; ^{11}C-methionine; ^{18}F-amino acids; ^{18}F-FET; ^{18}F-FDG; ^{111}In-monoclonal antibodies/fragments; ^{123}I-fatty acids (BMIPP, IPPA); ^{123}I-monoclonal antibodies/fragments; ^{131}I-monoclonal antibodies/fragments; and ^{201}Tl-ion. The publication also provides realistic maximum models for ^{11}C- and ^{18}F-substances, for which no specific models are available.

Keywords: Radiopharmaceuticals; Biokinetics; Dosimetry; Breast feeding

ELSEVIER

ICRP Publication 106

Annals of the ICRP

Guest Editorial

MORE THAN THREE DECADES OF WORK OF ICRP IN THE ASSESSMENT OF DOSE TO PATIENTS FROM RADIOPHARMACEUTICALS

As early as 1971, i.e., more than three decades ago, ICRP started work on doses to patients from radiopharmaceuticals (*Publication 17*; ICRP, 1971). *Publication 17* was intended to be a compilation of published data and estimates on absorbed doses from a total of 92 compounds used at the time in nuclear medicine, to give guidance to the nuclear medicine physician and the medical physicist in protecting the patient in radionuclide investigations. Later, *Publications 53* (ICRP, 1987) and *62* (ICRP, 1991), on absorbed doses and effective dose equivalents and on effective doses, respectively, per unit activity administered, considered radiopharmaceuticals which had been introduced into regular use since 1987.

This series of ICRP reports takes account of new radiopharmaceuticals and has introduced, in *Publication 62*, an age-related bladder voiding model. It is most important that the assessment of age-dependent effective doses provides an opportunity to express, by means of a single value, the radiation-induced risk to patients of various ages (reference patients) undergoing different radiodiagnostic procedures. These estimates also provide guidance to ethics committees when deciding upon research projects involving the use of radioactive substances on volunteers who receive no individual benefit from the study.

In view of the importance of absorbed and effective dose estimates in nuclear medicine, early in the 1980s, a Task Group of ICRP Committee 2, later converted to a Joint Task Group together with Committee 3, on Radiation Dose to Patients from Radiopharmaceuticals was appointed:

- to provide biokinetic models, absorbed doses, and effective doses using ICRP dosimetry for current and new radiopharmaceuticals which have come into use since *Publication 17* (ICRP, 1971); and
- to supply estimated absorbed and effective doses to patients, including the range of variation to be expected in pathological states, for adults, children, and the embryo and fetus.

The present report, constituting Addendum 3 to *Publication 53* (ICRP, 1987), covers 33 different substances in addition to Addenda 1 and 2 in *Publications 62* and *80*. Together with *Publication 80* (ICRP, 1998), the present *Publication 106* will cover most of the pharmaceuticals in current use in diagnostic nuclear medicine.

Consequently, as in the past, the report will support the nuclear physician in her/his responsibility of optimising the use of various radiodiagnostic techniques.

However, due to the need for more detailed and patient-specific dosimetry and dose planning in tumour therapy using radionuclides, the data are not intended for therapeutic applications of radionuclides. Likewise, as in earlier reports, amounts of administered radiopharmaceuticals, i.e. activities, required for a particular investigation are not given, since the report does not imply any recommendation regarding the use of a radiopharmaceutical.

Recommendations are also given for the protection of infants on breast-feeding interruptions, and for the protection of personnel on radiation exposure of hands in radiopharmacies.

As a former member of the Task Group on Absorbed Dose to Patients from Radiopharmaceuticals which prepared *Publication 53* (ICRP, 1987), and Chairman of ICRP Committee 2 for several years, I wish to congratulate the Task Group for the extremely valuable work they have done over the years. I wish to close by repeating the plea made in 1971 in *Publication 17* to secure the maximum information possible from any investigation in the future:

'The particular information needed for dose calculations includes fractional long-term retention of radionuclides and labelled compounds, turnover of the radiopharmaceutical and its metabolites, and distribution of radionuclides within different organs.'

This means that those who are involved in diagnostic and therapeutic administration of radionuclides to patients or volunteers are requested to collect such information as completely as possible, as a basis for future advanced internal dosimetry in nuclear medicine.

Alexander Kaul

References

ICRP, 1971. Protection of the Patient in Radionuclide Investigations. ICRP Publication 17. Pergamon Press, Oxford, UK.

ICRP, 1987. Radiation dose to patients from radiopharmaceuticals. ICRP Publication 53. Ann. ICRP 18 (1–4).

ICRP, 1991. Radiation dose to patients from radiopharmaceuticals. Addendum 1 to ICRP Publication 53. ICRP Publication 62. Ann. ICRP 22(3).

ICRP, 1998. Radiation dose to patients from radiopharmaceuticals. Addendum 2 to ICRP Publication 53. ICRP Publication 80. Ann. ICRP 28(3).

CONTENTS

ABSTRACT 1

GUEST EDITORIAL 3

CONTENTS 5

PREFACE 7

1. INTRODUCTION 11

2. SELECTION OF RADIOPHARMACEUTICALS 13

3. SELECTION OF ORGANS AND TISSUES FOR DOSE CALCULATIONS 15

4. BIOKINETIC MODELS AND DATA 17

5. METHODS FOR CALCULATING ABSORBED DOSE 21
   5.1. Calculation of absorbed dose 21
   5.2. Calculation of cumulated activity 22
   5.3. Uncertainities in absorbed dose estimates 24

6. EFFECTIVE DOSE 25
   6.1. Use of effective dose in nuclear medicine 25
   6.2. Calculation of effective dose 27

7. DOSE TO EMBRYO AND FETUS 29

8. REFERENCES FOR THE MAIN TEXT 31

ANNEX A. SPECIAL BIOKINETIC AND DOSIMETRIC MODELS 35

ANNEX B. EXPLANATIONS 47

ANNEX C. BIOKINETIC MODELS AND DOSE TABLES 51

ANNEX D. RECOMMENDATIONS ON BREAST-FEEDING INTERRUPTIONS 163

ANNEX E. RADIATION EXPOSURE OF HANDS IN RADIOPHARMACIES: MONITORING OF DOSES AND OPTIMISATION OF PROTECTION 167

FULL BIBLIOGRAPHY 185

PREFACE

In 1987, the International Commission on Radiological Protection (ICRP), referred to below as 'the Commission', published a report entitled 'Radiation dose to patients from radiopharmaceuticals' (*Publication 53*; ICRP, 1987). This report contained calculations of absorbed doses per unit activity administered for some 120 radiopharmaceuticals in regular use at the time. The calculations were based on biokinetic models and best estimates of biokinetic data for individual radiopharmaceuticals.

A first addendum to *Publication 53* was published (as ICRP (1991b; included in *Publication 62*). This contained biokinetic and dosimetric data for six new radiopharmaceuticals, and a table of effective doses per unit administered activity for those radiopharmaceuticals that had been discussed in *Publication 53*.

In the second addendum to *Publication 53* (ICRP, 1998; included in *Publication 80*), the Joint Task Group on Radiopharmaceuticals of ICRP Committees 2 and 3 presented biokinetic and dosimetric data on 10 new radiopharmaceuticals, and recalculations of dose data for 19 of the most frequently used radiopharmaceuticals in *Publication 53*. A number of minor corrections and recalculations of older data were also provided at that time.

In this third printed amendment to *Publication 53*, dosimetric and biokinetic data are provided for 33 further radiopharmaceuticals in current use. The report also includes recommendations relating to breast feeding for mothers who have undergone nuclear medicine procedures.

In addition, Annex E comprises recommendations concerning radiation exposure of hands in radiopharmacies, drafted by a Working Party of ICRP Committee 3.

The membership of the Task Group that prepared this report, except for Annex E, was:

S. Mattsson (Chair)	L. Johansson (Secretary)	J. Liniecki
D. Noßke	M. Stabin	S. Leide-Svegborn
D. Taylor		

The corresponding members were:

S. Carlsson	K. Norrgren	B. Nosslin
S. Valind		

The membership of the Working Party that prepared Annex E was:

J. Liniecki (Chair)	J. Jankowski	C. Martin
S. Mattsson		

The membership of Committees 2 and 3 during the period of preparation was:

Committee 2 (2001–2005)

C. Streffer (Chair)
A. Bouville
J. Inaba
H.-G. Menzel
A.S. Pradhan
Y.-Z. Zhou
M. Balonov
G. Dietze
I.A. Liktharev
H. Métivier
J.W. Stather (Vice-Chair)
B.B. Boecker
K.F. Eckerman
J.L. Lipsztein
H. Paretzke
D.M. Taylor (Secretary)

Committee 2 (2005–2009)

H.-G. Menzel (Chair, 2007–)
W.E. Bolch
K.F. Eckerman
P. Jacob (2006–)
H. Paretzke (–2006)
C. Streffer (Chair, –2007)
M. Balonov
A. Bouville
J.D. Harrison (Secretary)
J.L. Lipsztein
A.S. Pradhan
Y.-Z. Zhou
V. Berkovski
G. Dietze
N. Ishigure
F. Paquet
J.W. Stather (Vice-Chair, –2008)

Committee 3 (2001–2005)

F.A. Mettler, Jr (Chair)
M.J. Guiberteau
M. Hiraoka
P. Ortiz Lopez
H. Ringertz
E. Vañó
J.-M. Cosset
I.A. Gusev
J. Liniecki (Vice-Chair)
L.V. Pinillos-Ashton
M. Rosenstein
W. Yin
C. Cousins
L.K. Harding (Secretary)
S. Mattsson
M.M. Rehani
C. Sharp

Committee 3 (2005–2009)

C. Cousins (Chair, 2005–)
J.W. Hopewell (2006–)
P. Ortiz Lopez
H. Ringertz
Y. Yonekura
J.-M. Cosset (Vice-Chair)
Y. Li
S. Mattsson
M. Rosenstein
I.A. Gusev
J. Liniecki
L.V. Pinillos-Ashton
E. Vañó (Secretary)

The report was approved for publication by Committee 3 at its meeting in Berlin, Germany in October 2007, by delegation of authority from the Commission with respect to reports on doses to patients from radiopharmaceuticals.

References

ICRP, 1987. Radiation dose to patients from radiopharmaceuticals. ICRP Publication 53. Ann. ICRP 18(1–4).

ICRP, 1991b. Radiation dose to patients from radiopharmaceuticals. Addendum 1 to ICRP Publication 53, in: Radiological protection in biomedical research. ICRP Publication 62. Ann. ICRP 22(3).

ICRP, 1998. Radiation dose to patients from radiopharmaceuticals. Addendum 2 to ICRP Publication 53. ICRP Publication 80. Ann. ICRP 28(3).

1. INTRODUCTION

(1) The administration of radioactive substances to humans for diagnosis, therapy, or research purposes is a well-established and developing branch of medical practice, and is, in most countries, recognised under the name of 'nuclear medicine and molecular imaging'. New methods and new radiopharmaceuticals are being introduced continually. Reasonably accurate dosimetry for representative groups of patients for each specific investigation is needed in order to optimise use of the various alternative radiodiagnostic techniques, and to estimate the collective radiation exposure and risk from nuclear medicine investigations. The limited, but increasing, use of radiopharmaceuticals for therapy requires even more detailed and patient-specific dosimetry and dose planning, including both tumour and normal tissue. The data presented in this report are intended for diagnostic nuclear medicine and not for therapeutic applications.

(2) With regard to dose calculations for radiopharmaceuticals for diagnostic purposes, important material has been published previously by the Commission. In 1987, *Publication 53* (ICRP, 1987) was published containing dose estimates for approximately 120 substances and superseding *Publication 17* (ICRP, 1971). In 1991, dose data for six additional substances were published in *Publication 62* (ICRP, 1991b), and data for another 10 substances were published within *Publication 80* (ICRP, 1998). Most of the further work of the Task Group on Radiation Dose to Patients from Radiopharmaceuticals has been available on the ICRP's website (www.icrp.org), and open for comments and corrections. This material, covering 33 different substances in current use, is published in the present report. Together with *Publication 80*, this will cover most of the pharmaceuticals in current use in diagnostic nuclear medicine.

(3) Important material regarding dose calculations from radiopharmaceuticals has also been published in reports from the International Commission on Radiation Units and Measurements, especially ICRU Reports 32 and 67 (ICRU, 1979, 2002). At national level, several absorbed dose catalogues for radiopharmaceuticals and collections of published values have also appeared (Roedler et al., 1978; NCRP, 1982; Johansson et al., 1992; ARSAC, 2006). Of particular importance is the work of the Medical Internal Radiation Dose (MIRD) Committee of the United States Society of Nuclear Medicine, and the dosimetry work performed at the Radiation Internal Dose Information Center at Oak Ridge Associated Universities in Oak Ridge, TN, USA (now disbanded), and the Radiation Dose Assessment Resource (RADAR) (www.doseinfo-radar.com).

(4) A personal computer software code called 'MIRDOSE' has been developed (Stabin, 1996) to facilitate automated and standardised internal dose calculations for nuclear medicine applications. This code has been completely rewritten and renamed 'OLINDA' (Organ Level INternal Dose Assessment) (Stabin et al., 2005). The OLINDA/EXM code (EXM stands for EXponential Modelling) allows users to fit data to one, two, or three exponential functions. The OLINDA/EXM code uses the same technical basis (phantoms, organ masses, equations, relationships assumed, and other details) as the MIRDOSE code and the RADAR system.

(5) Important basic material regarding reference biokinetic and dosimetric models and reference data for workers and members of the public exposed to radionuclides have been published by the Commission, giving dose coefficients for intake of radionuclides by inhalation and ingestion (ICRP, 1973, 1979, 1980, 1981, 1993, 1994, 1996).

(6) The Task Group has made extensive use of the information and material available from these sources.

2. SELECTION OF RADIOPHARMACEUTICALS

(7) Certain general principles were followed in establishing the list of radiopharmaceuticals for inclusion in this report. A radiopharmaceutical that has been described in the literature and proposed for use in humans has been included if there is evidence that it has been in, or is coming into, common use, provided that acceptable and sufficient metabolic data for making absorbed dose calculations are available. The list of radiopharmaceuticals covers not only those used in the practice of nuclear medicine, but also some of those used in clinical research.

(8) It is important to note that the inclusion of a radiopharmaceutical in this report does not imply any recommendation regarding its use. For this reason, the amounts of administered radiopharmaceutical required for a particular investigation are not given. The list is based on the judgement of the Task Group regarding their past, present, or potential future application in nuclear medicine procedures. Data relating to these substances were obtained by an extensive search of the literature. Some of the information had been published in scientific journals covering subjects other than nuclear medicine.

(9) Complete radionuclide and radiochemical purity is assumed in all absorbed dose calculations.

3. SELECTION OF ORGANS AND TISSUES FOR DOSE CALCULATIONS

(10) Absorbed doses are calculated for a large number of organs and tissues (called the 'target organs and tissues'). These absorbed doses may arise as a result of radioactive decays occurring in other regions (called the 'source regions'). Thus, absorbed doses in a particular organ or tissue are typically the sum of contributions from various sources, usually including the target organ or tissue itself. Two groups of target organs and tissues are included in the calculation of absorbed dose (Table 3.1):

- target organs and tissues, for which the absorbed dose is always calculated (Group 1); and
- other organs and tissues which, for some reason, receive significantly higher absorbed doses than the average to the rest of the body, or which are of special interest in the investigation (included as appropriate) (Group 2).

(11) The absorbed dose to organs and tissues not included in the table can usually be approximated by using the absorbed dose quoted for 'Other tissues', e.g. muscle. The absorbed doses given in Table 3.1 are the mean absorbed doses to an organ or region. In general, these mean absorbed doses are calculated assuming uniform distribution of the radionuclide in the source regions.

Table 3.1. Organs and tissues for which absorbed dose is calculated.

Group 1	Group 2
Adrenals	Lachrymal glands
Bone surfaces	Salivary glands
Breast	Spinal cord
Brain	
Gallbladder wall	
Gastrointestinal tract	
Stomach wall	
Small intestine wall	
Large intestine wall	
Heart wall	
Kidneys	
Liver	
Lungs	
Oesophagus	
Other tissues*	
Ovaries	
Pancreas	
Red bone marrow	
Skin	
Spleen	
Testes	
Thymus	
Thyroid	
Urinary bladder wall	
Uterus	

* Mainly muscle tissues.

(12) An exception is made to this assumption in the case of the kidneys, where non-uniform distribution of radionuclides may be taken into consideration. However, even in this case, absorbed doses to other organs and tissues are calculated under the assumption that the radionuclide is distributed uniformly throughout both kidneys; this is justified because, in practice, use of a non-uniform distribution when calculating the absorbed doses to these other organs and tissues would only result in very small changes (<10%) in the results obtained.

(13) Discussions were held regarding whether or not to calculate doses to regions of the brain that will receive doses considerably higher than the average dose, such as the putamen and nucleus caudatus from fluoropropyl-carbomethoxy-iodophenyl-tropan (FP-CIT). As S-values for the calculation of regional doses in this case have been published (Bouchet et al., 1999), the decision was made to include the absorbed dose to the region of the brain that receives the highest absorbed dose as a footnote to the dose table. However, this dose is not used in calculation of the effective dose for these radiopharmaceuticals. It is important to stress that the doses are small, even if the central regions of the brain receive doses 10 times the average; this is still far from levels where known deterministic effects can be observed.

(14) The lens of the eye is considered as a tissue at risk in *Publication 60* (ICRP, 1991a) because of the possibility of inducing opacities that may interfere with vision. The radionuclides in radiopharmaceuticals currently used in nuclear medicine do not concentrate in the tissues of the healthy human eye, with the possible exception of iodo-amphetamine which is utilised in the synthesis of melanin (Winchell et al., 1980). For this reason, the lens is not included in the list of target organs and tissues.

4. BIOKINETIC MODELS AND DATA

(15) The Task Group has encountered several problems in finding good biokinetic information from measurements on man. In general, published data are scarce, especially with regard to quantitative measurements. The clinician is often only interested in the initial distribution and metabolism of a test substance, whereas for dosimetry calculations, long-term retention is of prime importance.

(16) The Task Group wishes to repeat the pleas made in *Publications 17* and *53* (ICRP, 1971, 1987) for securing the maximum information possible from any investigation. The particular information needed for dose calculations includes fractional long-term retention of radionuclides and labelled compounds, turnover of the radiopharmaceutical and its metabolites, fractional gastrointestinal absorption values for orally administered compounds, distribution of radionuclides within different organs, and their excretion pathways. Collection of such data should be encouraged by professional and scientific societies and by regulatory authorities, and the data should be made available by publication and by storage in accessible databases. The editors and referees of scientific journals are encouraged to request such information in papers on new radiopharmaceuticals.

(17) For each compound, the Task Group has agreed upon a biokinetic model giving quantitative estimates for the distribution and metabolism of the radiopharmaceutical in the body. The literature on which this model is based is referenced. In appropriate cases, the range of pathological variation expected in the metabolic data is also indicated.

(18) Some models have been developed within a generic framework for application to a class of radiopharmaceutical, e.g. monoclonal antibodies and brain receptor substances. Each of the generic model frameworks is a compromise between biological realism and practical considerations regarding the amount and quality of information available to determine parameter values for specific compounds.

(19) Worst-case models have been developed for substances labelled with very-short-lived radionuclides, often used for positron emission tomography investigations.

(20) For absorbed dose calculations, knowledge of the time–activity curve in different organs and tissues of the body after administration of a radiopharmaceutical is needed. The best way to get this information is by pharmacokinetic analysis, which includes the use of knowledge about mechanisms affecting radionuclide localisation by listing the physiological assumptions regarding its behaviour in body tissues. On the basis of this knowledge, a model is defined, delineating the detailed distribution and flow, or transfer, of the radionuclide.

(21) This model, in turn, allows the derivation of a mathematical model, consisting of differential and/or integral equations for the variation with time of the amounts of radionuclide in different parts of the body. The model may be either compartmental or non-compartmental. Knowledge of the values for compartment sizes, flow rates, and other physiological parameters allows numerical solution of the equations, giving activity–time relationships for all parts of the system which are then integrated to obtain the cumulated activities needed for calculations of absorbed dose.

(22) The method outlined above could, in principle, be applied to derive absorbed doses in those disease states leading to quantitative changes in the normal physiological processes. However, this is not generally possible since, with some exceptions, there is insufficient information to define a complete model including all pools or compartments as well as flow rates in or out of the system and between the parts of the system. For absorbed dose calculations, only the time–activity curves are needed; these can be established in alternative ways, as discussed in detail in ICRU Reports 32 and 67 (ICRU, 1979, 2002) and the MIRD primer (Loevinger et al., 1991).

(23) For example, a simple approach might involve modification of the bone dose in younger individuals in whom bone growth is assumed to result in higher uptakes and thus doses. In these tissues, the absorbed dose may be higher by a factor of approximately two to five for ^{99m}Tc-phosphonates (Gelfand et al., 1983; Kaul et al., 1985) compared with the mean absorbed dose to the bone surfaces, which is the target tissue considered in this report. Similar ratios can be derived for ^{67}Ga-citrate from data reported by Gelfand et al. (1983). Thus, in these cases, the use of the same biokinetic model for both children and adults underestimates radiation doses to a particular part of the skeleton, although the mean absorbed dose to bone surfaces is not likely to be substantially underestimated. In calculations of absorbed doses to children, age-dependent data are used for organ mass, blood distribution, and S-values.

(24) The influence of pathological changes on absorbed dose has also been studied. Variations of absorbed dose in disease states can generally be calculated using the same model as for the healthy state, but with appropriate data for organ or tissue mass, uptake, and retention. Separate absorbed dose estimates are presented in cases where such variations lead to significant changes in these absorbed doses.

(25) The models and absorbed dose values presented are intended for use in diagnostic nuclear medicine and clinical research with radionuclides, and should not be used in radionuclide therapy.

(26) Some radiopharmaceuticals administered to breast-feeding women may be excreted in the breast milk and thus transferred to the breast-fed child. This problem is dealt with in Annex D of the present publication. Excretion in breast milk in connection with occupational exposure is dealt with in *Publication 95* (ICRP, 2004).

(27) In the case of radionuclides such as ^{67}Ga, ^{111}In, ^{125}I, and ^{201}T1, administered in forms which result in their uptake in cell nuclei, the minor fraction of the energy carried by Auger electrons may have a disproportionately large effect, owing to their very short range in tissue (Stepanek et al., 1996; Bingham et al., 2000; Taylor, 2000c; Kassis, 2004). The assumption made here, that the absorbed dose is distributed uniformly within the cell, may therefore result in underestimation of the risk.

(28) This problem has been discussed in earlier publications (ICRP, 1979, 1991a, 2003), and by a large number of other authors, of which only a few are referred to here as an example (Hofer, 1996; Gardin et al., 1999; Bingham et al., 2000; Feinendegen and Neumann, 2004). MIRD has given detailed advice and presented S-values for the cellular level (Goddu et al., 1994, 1997). It is still, however, difficult to estab-

lish the intracellular distribution of the radionuclides of interest so that such detailed S-values can be used effectively.

(29) It is usually assumed that daughter radionuclides produced within the body stay with, and behave metabolically like, their parent nuclide. This may be an oversimplification in some cases, and if specific information to the contrary is available, the dose estimates presented here should be modified appropriately.

(30) For some substances, such as iodine-labelled compounds, pertechnetate, and some radiopharmaceuticals used for renal studies, blocking agents may be administered in advance or simultaneously (e.g. to induce competitive inhibition of uptake in specific organs). In such circumstances, including blocking of the thyroid, total inhibition of radionuclide uptake has been assumed, although this may be difficult to achieve in practice.

(31) It is often possible to reduce the absorbed dose to a patient by increasing the rate of elimination of the radionuclide from the body, for example by more frequent emptying of the urinary bladder (with hydration, diuretics, and catheterisation), the bowel (with laxatives and enema), and the gallbladder (with a meal of high fat content and cholecystokinin).

5. METHODS FOR CALCULATING ABSORBED DOSE

5.1. Calculation of absorbed dose

(32) The mean absorbed dose D_T to a target organ or tissue T is the sum of the contributions, $D(T \leftarrow S)$, arising from nuclear transformations of the radionuclide in various source organs S, i.e.:

$$D_T = \sum_S D(T \leftarrow S) \tag{5.1}$$

(33) Several methods of calculating the absorbed dose to an organ from radioactive sources in the same organ and in other organs have been proposed and used. For a review of these methods, the reader is referred to ICRU Reports 32 and 67 (ICRU, 1979, 2002), *Publication 30* (ICRP, 1979), and NCRP Report 84 (NCRP, 1985). The most common method currently in use in nuclear medicine was originally developed from an approach by Loevinger and Berman (1968) using tabulated data on absorbed fractions of energy in a target tissue from a specific source region (Snyder et al., 1969; Loevinger et al., 1991). This method was later improved by Snyder et al. who introduced the 'S-value' (Snyder et al., 1975), which also contains all necessary physical information for a specific radionuclide.

(34) With this more straightforward method, the absorbed dose in T from a radionuclide in a single source organ S is given by:

$$D(T \leftarrow S) = \widetilde{A}_S \times S(T \leftarrow S) \tag{5.2}$$

where $\widetilde{A}$ is the time-integrated or cumulated activity, equal to the total number of nuclear transformations in S, and $S(T \leftarrow S)$ is the absorbed dose in T per unit cumulated activity in S.

(35) The value of $S(T \leftarrow S)$ depends on the radiation type, the energy emitted per transformation, the mass of the target organ, and the geometry of the mathematical phantoms representing the adult and children of various ages. When the source organ is the total body less the organs already listed in the biokinetic data table, a common approximation is to use the S-value calculated on the basis of 'total body' as a source. However, a formally correct S-value for this case can be derived (Cloutier et al., 1973; Roedler and Kaul, 1976; Coffey and Watson, 1979), and it is this latter method which is used in this report.

(36) If S-values were not available, the absorbed dose per nuclear transformation was calculated using the absorbed fraction φ, derived from Snyder et al. (1978):

$$S(T \leftarrow S) = \frac{c}{M_T} \sum_i E_i Y_i \varphi_i \tag{5.3}$$

where M_T is the mass of the target organ or tissue (see Table A.1), E_i is the mean energy of radiation type i, Y_i is the yield of radiation type i per transformation, φ_i is the absorbed fraction of energy of radiation type i, and c is a constant, the value of which depends on the units of the included quantities (for E in joules, M_T in kg, and $c = 1$, the absorbed dose per transformation, S, will be in gray).

5.2. Calculation of cumulated activity

(37) For a more detailed description of the mathematical analysis of biokinetic models, reference should be made to MIRD Pamphlet No. 12 (Berman, 1977) and ICRU Report 32 (ICRU, 1979). The following text only serves as a short account of the calculation of cumulated activity in selected cases.

(38) The cumulated activity $\widetilde{A}_S$ in a source organ or tissue S depends on the administered activity, A_0, the physical half-life, T, and the biokinetics of the radiopharmaceutical. $\widetilde{A}_S$ which represents the number of disintegrations occurring in source region S is obtained by integrating the time-dependent activity:

$$\widetilde{A}_S(t) = \int_0^t A_S(u)du \tag{5.4}$$

where $A_S(u)$ is the activity at time u in the source organ or tissue considered. Due to the relatively short physical half-life of radionuclides used in nuclear medicine, the upper integration limit, t, can be taken as infinity.

(39) Although the mechanisms by which radionuclides are distributed within, or excreted from, the body are not necessarily well represented by first-order kinetic models, such models are generally adequate for representing overall uptake and retention of radionuclides in individual organs and tissues. Since this is all that is required for dosimetric calculations, these models are used extensively in this report.

(40) A general first-order kinetic model can be represented as a system of n compartments, interlinked with constant rate coefficients. In such a system, the rate of change of the amount of material (q_i) in compartment i is given by:

$$\frac{dq_i}{dt} = -\lambda_{ii}q_i(t) - \lambda_p q_i(t) + \sum_{\substack{j=1 \\ j\neq i}}^{n} \lambda_{ij}q_j(t) \tag{5.5}$$

where λ_{ii} is the fraction of the amount of material in compartment i leaving per unit time, λ_{ij} is the fraction of the amount of material in compartment j flowing to compartment i per unit time, and λ_p is the radioactive decay constant, as appropriate.

(41) A direct correspondence between compartments and anatomical regions of the body does not usually exist. However, for absorbed dose calculations, it is necessary to know the amount of substance in different regions of the body. Therefore, for practical reasons, specific organs and tissues are considered instead of compartments. The activity in an organ or tissue can usually be described sufficiently accurately by a sum of exponentials:

$$A_S(t) = \sum_{i=1}^{n} k_i e^{-(\lambda_i+\lambda_p)t} \tag{5.6}$$

where k_i is a constant, and λ_i is the biological elimination constant of the exponential component i.

(42) The constants in this equation are often derived directly from measurements. Expressed in terms of fractional distributions to the organ or tissue, fractions of

organ or tissue contents and half-lives, which are given in the biokinetic data tables of this report, A_S is given by:

$$\frac{\widetilde{A}_S}{A_0} = F_S \sum_{j=n+1}^{n+m} a_j \sum_{i=1}^{n} \left\{ a_i \frac{T_i}{T_i - T_j} \left[\exp\left(\frac{-\ln(2)}{T_{i,eff}} t \right) - \exp\left(\frac{-\ln(2)}{T_{j,eff}} t \right) \right] \right\} \tag{5.7}$$

where F_S is the fractional distribution to organ or tissue S, i.e. the fraction of the administered substance that would arrive in source organ or tissue S over all time if there were no radioactive decay; a_i is the fraction of F_S eliminated with a biological half-life T_i ($\Sigma a_i = 1$); a_j is the fraction of F_S taken up with a biological half-life T_j (marked by a minus sign in the biokinetic data tables) ($\Sigma a_j = 1$); n is the number of elimination components; m is the number of uptake components; and $T_{j,eff}$ and $T_{i,eff}$ are the elimination and uptake effective half-lives, respectively. Eq. (5.7) is, under certain constraints, a solution to Eq. (5.5).

(43) The effective half-life can be calculated from the corresponding biological half-life T_i and the functional physical half-life T_p:

$$\frac{1}{T_{i,eff}} = \frac{1}{T_i} + \frac{1}{T_p} \tag{5.8}$$

(44) Eq. (5.7) describes the build-up and subsequent decline of activity. If $T_i = T_j$ for some combination of i and j, the corresponding term in the sum in Eq. (5.7) becomes:

$$a_i \frac{\ln(2)}{T_i} t \exp\left(\frac{-\ln(2)}{T_{i,eff}} t \right) \tag{5.9}$$

(45) A special case, which often occurs, is that immediate uptake in the organ is assumed. Eq. (5.7) then reduces to:

$$\frac{A_S(t)}{A_0} = F_S \sum_{i=1}^{n} a_i \exp\left(\frac{-\ln(2)}{T_{i,eff}} t \right) \tag{5.10}$$

Integrating Eq. (5.7) over time up to infinity gives the normalised cumulated activity:

$$\frac{\widetilde{A}_S}{A_0} = F_S \sum_{j=n+1}^{n+m} a_j \sum_{i=1}^{n} \left[a_i \frac{T_i}{T_i - T_j} \left(\frac{T_{i,eff}}{\ln(2)} - \frac{T_{j,eff}}{\ln(2)} \right) \right] \tag{5.11}$$

or, if Eq. (5.10) is integrated:

$$\frac{\widetilde{A}_S}{A_0} = F_S \sum_{i=1}^{n} a_i \frac{T_{i,eff}}{\ln(2)} \tag{5.12}$$

In cases when the retention function cannot be described by a sum of exponential functions, the cumulated activities are derived directly from the metabolic model.

(46) For absorbed dose calculations in nuclear medicine, it has often been assumed that the effective half-life in an organ equals the physical half-life. The reason for this approximation is that the substance, in these cases, is labelled with a radionuclide with a physical half-life which is short in comparison with the biological half-life.

For short-lived radionuclides, a slow biological excretion may not be apparent and, for absorbed dose calculations, the approximation is sufficiently accurate. However, this assumption has the consequence that infinite biological half-lives are given in the tables and this is not strictly correct. This should be kept in mind when biokinetic data are used.

5.3. Uncertainties in absorbed dose estimates

(47) The uncertainty in the estimate of the mean absorbed dose for an organ or tissue in a reference person reflects uncertainties in the cumulated activity and the S-value. Differences between planned and actual administered activity are considered to be minor contributors to the total uncertainty if regular quality control is performed (IAEA, 2006). Variation in mass of the target organ and, for photon radiation, variation in the distance between the source and target organs are the major contributors to the uncertainty in S-values, whereas physical data, for example the yield and energy deposition in the target organs, are not considered to be major contributors to the uncertainty. Experimental validation of calculated absorbed doses have indicated agreement within 20–60%, the latter for patients who differed considerably from the body size and shape assumed in the calculations, i.e. the uncertainty for the dose to the reference person would be considerably lower. For a review, see Roedler (1980).

(48) Variation in the estimated cumulated activity largely arises from uncertainties in the quantitative description of uptake, distribution, and retention of the radiopharmaceutical in tissues (Norrgren et al., 2003; Jönsson et al., 2005). Functional impairment of an organ can introduce considerable variation in these factors. Variation in the body's retention of radionuclides administered as radiopharmaceuticals is limited by the short radioactive half-life of these radionuclides; thus, variation in the uptake and distribution of the radiopharmaceutical among the organs and tissues is often the major contributor to uncertainties in cumulated activity.

(49) Calculations have shown (Roedler, 1980; Zanzonico, 2000) that estimates of absorbed dose to different organs will not generally deviate from actual absorbed doses in patients by more than a factor of three. The deviation is even less for substances labelled with short-lived radionuclides such as ^{99m}Tc. The effective dose is less sensitive to variations in the distribution pattern than organ doses, and may vary within a factor of two.

6. EFFECTIVE DOSE

6.1. Use of effective dose in nuclear medicine

(50) Radiation exposure of the different organs and tissues in the body results in different probabilities of harm and different severities. The Commission calls the combination of probability and severity of harm 'detriment', meaning health detriment.

(51) The detriment depends on the type of radiation or, more specifically, the ionisation density. This is accounted for by introducing the concept of equivalent dose. The mean equivalent dose H_T in a target organ or tissue T is given by (ICRP 1991a):

$$H_T = \sum_R w_R D_{T,R} \tag{6.1}$$

where $D_{T,R}$ is the mean absorbed dose from radiation R in tissue or organ T, and w_R is the radiation weighting factor. For all types of radiation used in diagnostic nuclear medicine, w_R equals 1.0 (even if this value may not be appropriate for Auger emitters).

(52) To reflect the combined detriment from stochastic effects due to the equivalent doses in all the organs and tissues of the body, the equivalent dose in each organ and tissue is multiplied by a tissue weighting factor, and the results are summed over the whole body to give the effective dose. The special unit for effective dose is the sievert (Sv).

(53) The effective dose was developed primarily for radiation protection of occupationally exposed persons (ICRP, 1977, 1991a). It attributes weighting factors w_T to organs or tissues, representing the fraction of the total stochastic risk (i.e. fatal cancer and serious inherited disorders) resulting from the irradiation of that organ or tissue T when the whole body is irradiated uniformly. The effective dose is calculated by adding the weighted organ or tissue mean dose equivalents, H_T, i.e.:

$$E = \sum_T w_T H_T \tag{6.2}$$

where E is the effective dose, w_T is the relative radiation sensitivity of organ or tissue T (see Table 6.1.), and H_T is the mean equivalent dose in target organ or tissue T. For the radionuclides used in diagnostic nuclear medicine, it is numerically equal to that of the mean absorbed dose, since the radiation weighting factor w_R is taken as unity for these radionuclides.

(54) If the body is irradiated uniformly, all the H_Ts are the same and the equivalent dose at any point in the body is equal to the effective dose E.

(55) The weighting factors used in computing this quantity are appropriate to a population of workers and also valid for the general population.

(56) Many readers will be aware that the Commission recently issued its 2007 Recommendations (ICRP, 2007), superseding the 1990 Recommendations, and that these include updated and amended tissue weighting factors (and radiation weighting factors). Currently, work is in progress within ICRP to generate correspondingly

Table 6.1. Weighting factors for calculation of the effective dose E according to the Commission's 1990 Recommendations (ICRP, 1991a).

Tissue	w_T
Gonads	0.20
Colon	0.12
Lung	0.12
Red bone marrow	0.12
Stomach	0.12
Bladder	0.05
Breast	0.05
Liver	0.05
Oesophagus	0.05
Thyroid	0.05
Skin	0.01
Bone surfaces	0.01
Remainder*	0.05

* Adrenals, brain, small intestine, kidney, muscle, pancreas, spleen, thymus, and uterus.

updated dose coefficients for the calculation of doses to workers and members of the public due to intake of radioactive substances, and ultimately these are expected to be integrated into regulatory systems. In due course, doses to patients from intake of radiopharmaceuticals will also be calculated accordingly. However, pending the availability of such updated information, the present data should be used.

(57) The concept of effective dose to patients can also be useful in nuclear medicine and other medical investigations using ionising radiation.

(58) Effective dose can be of practical value for comparing the relative doses related to stochastic effects from: different diagnostic examinations and interventional procedures; the use of similar technologies and procedures in different hospitals and countries; and the use of different technologies for the same medical examination provided that the representative patients or patient populations for which the effective doses are derived are similar with regard to age and gender. However, comparisons of effective doses are inappropriate when there are significant dissimilarities between the age and gender distributions of the representative patients or patient populations being compared (e.g. children, all females, elderly populations) and the Commission's reference distribution of both genders and all ages. This is a consequence of the fact that the magnitudes of risk for stochastic effects are dependent on age and gender.

(59) The effective dose should not be used to assess risks of stochastic effects in retrospective situations for exposures in identified individuals, nor should it be used in epidemiological evaluations of human exposure. The Commission has made judgements on the relative severity of various components of radiation risk in the derivation of 'detriment' for the purpose of defining tissue weighting factors. Such risks for stochastic effects are, as mentioned above, dependent on age. The age distributions for workers and the general population (for which the effective dose is derived) can be quite different from the overall age distribution for the population undergoing

medical procedures using ionising radiation, and will also differ from one type of medical procedure to another, depending on the prevalence of the ages and genders of individuals for the medical condition being evaluated.

(60) For these reasons, risk assessment for medical uses of ionising radiation is best evaluated using appropriate risk values for the individual tissues at risk, and for the age and gender distribution of the population groups undergoing the medical procedures.

(61) For the exposure of young children, the risk would be higher, perhaps by a factor of two or three (ICRP, 1991a, Annex C). For many common types of diagnostic examination, the higher risk will be offset by the reduction in administered activity relative to that to an adult. For an age at exposure of approximately 60 years, the risk would be lower, perhaps by a factor of three. At higher ages at exposure, the risks are even less (ICRP, 1991a, Annex C). The specific demographics of the medically exposed population present obstacles to applying the concept of effective dose as a tool for comparing doses from medical irradiation with other sources of exposure to humans.

6.2. Calculation of effective dose

(62) The organs and tissues considered for calculation of the effective dose equivalent are listed in Table 6.1. Those with specific weighting factors are always included in the calculation. For the gonads, the arithmetic mean of the absorbed doses to ovaries and testes is used in conjunction with the weighting factor of 0.20. Absorbed doses to blood and blood vessels are not included in the calculation.

(63) The definition of 'colon' or 'large intestine' follows that given in *Publication 67* (ICRP, 1993, Para. 14). The weighting factor is applied to the mass average of the equivalent dose in the walls of the upper and lower large intestine of the gastrointestinal tract. Since the ratio between the masses of the walls of the upper large intestine (ULI) and lower large intestine (LLI) is independent of age, the equivalent dose to the colon H_{colon} is given as:

$$H_{\text{colon}} = 0.57H_{\text{ULI}} + 0.43H_{\text{LLI}} \tag{6.3}$$

where H_{ULI} and H_{LLI} are the equivalent doses in the walls of the ULI and LLI, respectively.

(64) The biokinetic model presented here contains no information on uptake and retention of radionuclides in the oesophagus. Since the transit time of materials through the oesophagus is normally quite rapid in comparison with the physical half-life, only the absorbed dose from penetrating radiation emitted from other source regions is considered. In the absence of absorbed fraction values for the oesophagus, the dose to the thymus has been used previously as a surrogate (ICRP, 1991b) and this method is utilised in the present report.

(65) The weighting factor for the remainder, 0.05, is applied on the mass-weighted average dose of those organs listed in the footnote of Table 6.1. In those cases in which a single remainder tissue or organ receives an equivalent dose which exceeds the dose to any other organ, a weighting factor of 0.025 should be applied to that

organ, and 0.025 to the average dose in the rest of the remainder tissues or organs as defined above. This 'rule' may also apply for any other organ that is recognised as radiation sensitive.

(66) As many radiopharmaceuticals are excreted rapidly in urine, the absorbed dose to the wall of the urinary bladder is often large compared with the absorbed dose to other organs and tissues in the same study, and may contribute considerably to the effective dose. In cases where the contribution is more than 50%, a note at the foot of the dosimetry table states the actual contribution.

(67) The presence of chemical forms of the radionuclide other than that intended may change the distribution and kinetics of the radionuclide. This may lead to a different distribution of the absorbed dose to some organs and tissues.

(68) In this report, complete radiochemical purity has been assumed, unless otherwise stated.

7. DOSE TO EMBRYO AND FETUS

(69) The absorbed dose to the uterus, which is included in the dose tabulations, may be used as a substitute for the absorbed dose to the embryo if the subject is in the first 2–3 months of pregnancy. Similarly, the absorbed dose to the fetus from radioactive substances without placental transfer is expected to be in the same range as the dose to the uterus. For radioactive substances with placental transfer, the absorbed dose to organs and tissues of the mother may, as a first approximation, be taken as representative of the absorbed dose to the corresponding organs and tissues of the fetus.

(70) More detailed radiation dose estimates for the fetus from administration of a number of radiopharmaceuticals to women at various stages of pregnancy are given by Russell et al. (1997). Their data illustrate that the majority of studies will probably involve fetal doses <10 mGy. Only studies using ^{131}I-iodide, ^{201}Tl-chloride, and ^{67}Ga-citrate appear to result in fetal doses >10 mGy, according to present knowledge. Therapeutic administrations are routinely contraindicated in the case of pregnancy or breast feeding as they may result in very high fetal doses. In addition, beyond 10–13 weeks of gestation, the fetal thyroid may receive extremely high doses in cases of therapy using ^{131}I-iodide (Watson et al., 1989; Berg et al., 1998). For substances in their ionic form, a comprehensive compilation of doses to the embryo and fetus is found in *Publication 88* (ICRP, 2001a).

8. REFERENCES FOR THE MAIN TEXT

ARSAC, 2006. Notes for Guidance on the Clinical Administration of Radiopharmaceuticals and Use of Sealed Radioactive Sources. Administration of Radioactive Substances Advisory Committee, Health Protection Agency, UK.

Berg, G., Nyström, E., Jacobsson, L., et al., 1998. Radioiodine treatment of hyperthyroidism in a pregnant woman. J. Nucl. Med. 39, 357–361.

Berman, M., 1977. Kinetic Models for Absorbed Dose Calculation. Medical Internal Radiation Committee (MIRD) Pamphlet No. 12. Society of Nuclear Medicine, New York, NY.

Bingham, D., Gardin, I., Hoyes, K.P., 2000. The problem of Auger emitters for radiological protection. Radiat. Prot. Dosim. 92, 219–228.

Bouchet, L.G., Bolch, W.E., Weber, D.A., Atkins, H.L., Poston Sr., J.W., 1999. Radionuclide S-values in a revised dosimetric model of the adult head and brain. MIRD Pamphlet No. 15. J. Nucl. Med. 40, 62S–101S.

Cloutier, R.J., Watson, E.E., Rohrer, R.H., Smith, E.M., 1973. Calculating the radiation dose to an organ. J. Nucl. Med. 14, 53–55.

Coffey, J.L., Watson, E.E., 1979. Calculating doses from remaining body activity. A comparison of two methods. Med. Phys. 6, 307–308.

Feinendegen, L.E., Neumann, R.D., 2004. Dosimetry and risk from low- versus high-LET radiation of Auger events and the role of nuclide carriers. Int. J. Radiat. Biol. 80, 813–822.

Gardin, I., Faraggi, M., Le Guludec, D., Bok, B., 1999. Cell irradiation caused by diagnostic nuclear medicine procedures: dose heterogeneity and biological consequences. Eur. J. Nucl. Med. 26, 1617–1626.

Gelfand, M.J., Thomas, S.R., Kereiakes, J.G., 1983. Absorbed radiation dose from routine imaging of the skeleton in children. Ann. Radiol. 26, 421–423.

Goddu, S.M., Howell, R.W., Rao, D.V., 1994. Cellular dosimetry: absorbed fractions for monoenergetic electron and alpha particle sources and S-values for radionuclides uniformly distributed in different cell compartments. J. Nucl. Med. 35, 303–316.

Goddu, S.M., Howell, R.W., Bouchet, L.G., Bolch, W.E., Rao, D., 1997. MIRD Cellular S Values. Society of Nuclear Medicine, Inc, Reston, VA.

Hofer, K.G., 1996. Biophysical aspects of Auger processes. A review. Acta Oncol. 35, 789–796.

IAEA, 2006. Quality Assurance for Radioactivity Measurement in Nuclear Medicine. Technical Report Series No. 454. International Atomic Energy Agency, Vienna.

ICRP, 1971. Protection of the Patient in Radionuclide Investigations. ICRP Publication 17. Pergamon Press, Oxford.

ICRP, 1973. Alkaline Earth Metabolism in Adult Man. ICRP Publication 20. Pergamon Press, Oxford.

ICRP, 1977. Recommendations of the International Commission on Radiological Protection. ICRP Publication 26. Pergamon Press, Oxford.

ICRP, 1979. Limits for intakes of radionuclides by workers. ICRP Publication 30, Part 1. Ann. ICRP 2(3/4).

ICRP, 1980. Limits for intakes of radionuclides by workers. ICRP Publication 30, Part 2. Ann. ICRP 4(3/4).

ICRP, 1981. Limits for intakes of radionuclides by workers. ICRP Publication 30, Part 3. Ann. ICRP 6(2/3).

ICRP, 1987. Radiation dose to patients from radiopharmaceuticals. ICRP Publication 53. Ann. ICRP 18(1–4).

ICRP, 1991a. 1990 Recommendations of the International Commission on Radiological Protection. ICRP Publication 60. Ann. ICRP 21(1–3).

ICRP, 1991b. Radiation dose to patients from radiopharmaceuticals. Addendum 1 to ICRP Publication 53. ICRP Publication 62. Ann. ICRP 22(3).

ICRP, 1993. Age-dependent doses to members of the public from intake of radionuclides. Part 2: ingestion dose coefficients. ICRP Publication 67. Ann. ICRP 23(3/4).

ICRP, 1994. Dose coefficients for intake of radionuclides by workers. ICRP Publication 68. Ann. ICRP 24(4).

ICRP, 1996. Age-dependent doses to members of the public from intake of radionuclides. Part 5. ICRP Publication 72. Ann. ICRP 26(1).

ICRP, 1998. Radiation dose to patients from radiopharmaceuticals. Addendum 2 to ICRP Publication 53. ICRP Publication 80. Ann. ICRP 28(3).

ICRP, 2001a. Doses to the embryo and fetus from intake of radionuclides by the mother. ICRP Publication 88. Ann. ICRP 31(1–3).

ICRP, 2003. Relative biological effectiveness (RBE), quality factor (Q) and radiation weighting factor (w_R). ICRP Publication 92. Ann. ICRP 33(4).

ICRP, 2004. Doses to infants from ingestion of radionuclides in mothers' milk. ICRP Publication 95. Ann. ICRP 34(3/4).

ICRP, 2007. The 2007 Recommendations of the International Commission on Radiological Protection. ICRP Publication 103. Ann. ICRP 37(1–3).

ICRU, 1979. Methods of Assessment of Absorbed Dose in Clinical Use of Radionuclides. ICRU Report 32. International Commission on Radiation Units and Measurements, Bethesda, MD.

ICRU, 2002. Absorbed-dose specification in nuclear medicine. ICRU Report 67. J. ICRU 2, 1–110.

Johansson, L., Mattsson, S., Nosslin, B., Leide-Svegborn, S., 1992. Effective dose from radiopharmaceuticals. Eur. J. Nucl. Med. 19, 933–938.

Jönsson, L., Ljungberg, M., Strand, S.E., 2005. Evaluation of accuracy in activity calculations for the conjugate view method from Monte Carlo simulated scintillation camera images using experimental data in an anthropomorphic phantom. J. Nucl. Med. 46, 1679–1686.

Kassis, A.M., 2004. The amazing world of Auger electrons. Int. J. Radiat. Biol. 80, 789–903.

Kaul, A., Krauss, O., Petrausch, G., 1985. Strahlenexposition durch Tc-99m-Methylendiphosphonat — lokale Dosisverteilung in Wachstum zonen des kindlichen Skelett und Organdosen. In: Poretti, G. (Ed.), Medizinische Physik. Deutsche Gesellschaft für medizinische Physik, Bern.

Loevinger, R., Berman, M., 1968. A schema for absorbed-dose calculations for biologically distributed radionuclides. MIRD Pamphlet No. 1. J. Nucl. Med. 9 (Suppl. 1), 7–14.

Loevinger, R., Budinger, T.F., Watson, E.E., 1991. MIRD Primer for Absorbed Dose Calculations. Revised edition. Society of Nuclear Medicine, New York, NY.

NCRP, 1982. Nuclear Medicine – Factors Influencing the Choice and Use of Radionuclides in Diagnosis and Therapy. NCRP Report No. 70. National Council on Radiation Protection and Measurements, Bethesda, MD.

NCRP, 1985. General Concepts for the Dosimetry of Internally Deposited Radionuclides. NCRP Report No. 84. National Council on Radiation Protection and Measurements, Bethesda, MD.

Norrgren, K., Svegborn, S.L., Areberg, J., Mattsson, S., 2003. Accuracy of the quantification of organ acticity from planar gamma camera images. Cancer Biother. Radiopharm., 18.

Roedler, H.D., 1980. Accuracy of Internal Dose Calculations with Special Consideration of Radiopharmaceutical Biokinetics. Third International Radiopharmaceutical Dosimetry Symposium, Oak Ridge, TN. HHS Publication (FDA 81-8166). Department of Health and Human Welfare, Bureau of Radiological Health, Rockville, MD.

Roedler, H.D., Kaul, A., 1976. Dose to Target Organs from Remaining Body Activity: Results of the Formally Exact and Approximate Solution. Radiopharmaceutical Dosimetry Symposium, Oak Ridge, TN. HEW Publication (FDA 76-8044). pp. 155–163.

Roedler, H.D., Kaul, A., Hine, G.J., 1978. Internal Radiation Dose in Diagnostic Nuclear Medicine. Hoffman, Berlin.

Russell, J.R., Stabin, M.G., Sparks, R.B., Watson, E.E., 1997. Radiation absorbed dose to the embryo/fetus from radiopharmaceuticals. J. Nucl. Med. 73, 756–769.

Snyder, W.S., Ford, M.R., Warner, G.G., 1978. Estimates of Specific Absorbed Fractions for Photon Sources Uniformly Distributed in Various Organs of a Heterogeneous Phantom. Medical Internal Radiation Dose Committee (NM/MIRD) Pamphlet No. 5, revised. Society of Nuclear Medicine, New York, NY.

Snyder, W.S., Ford, M.R., Warner, G.G., Fisher Jr, H.R., 1969. Estimates of absorbed fractions for monoenergetic photon sources uniformly distributed in various organs of a heterogeneous phantom. MIRD Pamphlet No. 5. J. Nucl. Med. 10 (Suppl. 3).

Snyder, W.S., Ford, M.R., Warner, G.G., Watson, S.B., 1975. "S" Absorbed Dose per Unit Cumulated Activity for Selected Radionuclides and Organs. MIRD Pamphlet No. 11. Society of Nuclear Medicine, New York, NY.

Stabin, M.G., 1996. MIRDOSE: Personal computer software for internal dose assessment in nuclear medicine. J. Nucl. Med. 37, 538–546.

Stabin, M.G., Sparks, R.B., Crowe, E., 2005. OLINDA/EXM: the second-generation personal computer software for internal dose assessment in nuclear medicine. J. Nucl. Med. 46, 1023–1027.

Stepanek, J., Larsson, B., Weinreich, R., 1996. Auger-electron spectra of radionuclides for therapy and diagnostics. Acta Oncol. 35, 863–868.

Taylor, D.M., 2000c. Subcellular distribution of gallium-67 and other Auger-emitting radionuclides in human and animal tissues. Radiat. Prot. Dosim. 92, 229–231.

Watson, E.E., Stabin, M.G., Eckerman, K.F., 1989. A model of the peritoneal cavity for use in internal dosimetry. J. Nucl. Med. 30, 2002–2011.

Winchell, H.S., Horst, W.D., Braun, L., Oldendorf, W.H., Hattner, R., Parker, H., 1980. N-Isopropyl (^{123}I)*p*-iodoamphetamine: single-pass brain uptake and washout; binding to brain synaptosomes; and localisation in dog and monkey brain. J. Nucl. Med. 21, 947–952.

Zanzonico, P.B., 2000. Internal radionuclide radiation dosimetry: a review of basic concepts and recent developments. J. Nucl. Med. 41, 297–308.

ANNEX A. SPECIAL BIOKINETIC AND DOSIMETRIC MODELS

A.1. Organ and tissue masses for different ages

(A 1) The masses of the organs and tissues are inherent in the S-values used (Stabin and Siegel, 2003; Stabin et al., 2005). The masses of the phantoms used for calculation of the S-values are those presented by Stabin and Siegel (2003) (Table A.1). The phantoms were produced by Cristy and Eckerman (1987), based predominantly on data in *Publication 23* (ICRP, 1975). Since the masses refer to the phantoms used, they may deviate somewhat from those in *Publications 23* (ICRP, 1975) and *89* (ICRP, 2002).

A.2. Blood volume and blood flow models

(A 2) Substances that remain largely in the blood are assumed to be distributed according to the relative blood volume of the different organs. An example of such substances are labelled blood cells and radionuclides attached to macro-molecules, but this blood distribution model has also been used, where appropriate, for other substances. This model requires information on blood volumes in different organs and tissues. These data were taken from Leggett and Williams (1991) and Williams and Leggett (1989), and were also proposed by the Commission in *Publication 89* (ICRP, 2002). The haematocrit, or fractional red cell content of the blood, has been considered constant for blood circulating through all tissues. The data are presented in Table A.2 and refer to adults. The fractional blood volumes used for children have been calculated assuming that the blood content in an organ or tissue per unit mass of tissue relative to that of the total body is independent of age. The total blood volume in children is taken from *Publication 89* (ICRP, 2002) and is presented in Table A.1.

(A 3) In the biokinetic models used in this report, the term 'uptake' or 'content' of a radionuclide in an organ or tissue usually includes the radioactivity in blood in that organ or tissue. However, when the blood distribution model is used, a specified fraction of the activity is associated with the blood. In this case, the activity in blood in an organ or tissue has been added to the activity in that organ or tissue for purposes of dose calculations.

(A 4) Table A.2 also presents the fractional cardiac output to different organs and tissues. These fractions, which are also proposed in *Publication 89* (ICRP, 2002), were taken from Leggett and Williams (1995). These data have been applied as a model for the activity distribution of radionuclides with very short physical half-lives (seconds up to a few minutes), e.g. a number of positron emitters.

A.3. Gastrointestinal tract model

(A 5) The model presented in *Publication 30* (ICRP, 1979) for the gastrointestinal tract has been used for adults and children aged 1–15 years. The model, shown in

Table A.1. Masses (g) of models of selected organs and tissues at different ages* (years).

Organ	Adult	15	10	5	1	Newborn
Adrenals	16.3	10.5	7.22	5.27	3.52	5.83
Brain	1420	1410	1360	1260	884	352
Breasts	351	361	2.6	1.51	0.732	0.107
Gallbladder contents	55.7	49	38.5	19.7	4.81	2.12
Gallbladder wall	10.5	9.27	7.28	3.73	0.91	0.408
Gastrointestinal tract						
LLI contents	143	109	61.7	36.6	18.3	6.98
LLI wall	167	127	70	41.4	20.6	7.96
SI contents	1100	838	465	275	138	52.9
Stomach contents	260	195	133	75.1	36.2	10.6
Stomach wall	158	118	85.1	49.1	21.8	6.41
ULI contents	232	176	97.5	57.9	28.7	11.2
ULI wall	220	168	93.4	55.2	27.8	10.5
Heart contents	454	347	219	134	72.7	36.5
Heart wall	316	241	151	92.8	50.6	25.4
Kidneys	299	248	173	116	62.9	22.9
Liver	1910	1400	887	584	292	121
Lungs	1000	651	453	290	143	50.6
Muscle†	28,000	15,500	7000	2000	1000	760
Ovaries	8.71	10.5	3.13	1.73	0.714	0.328
Pancreas	94.3	64.9	30	23.6	10.3	2.8
Remaining tissues†	51,800	40,000	23,100	13,300	6400	2360
Skeleton						
Active marrow	1120	1050	610	320	150	47
Cortical bone	4000	3220	1580	875	299	0
Trabecular bone	1000	806	396	219	200	140
Skin	3010	2150	888	538	271	118
Spleen	183	123	77.4	48.3	25.5	9.11
Testes	39.1	15.5	1.89	1.63	1.21	0.843
Thymus	20.9	28.4	31.4	29.6	22.9	11.3
Thyroid	20.7	12.4	7.93	3.45	1.78	1.29
Urinary bladder contents	211	160	103	64.7	32.9	12.4
Urinary bladder wall	47.6	35.9	23.2	14.5	7.7	2.88
Uterus	79	79	4.16	2.7	1.45	3.85
Whole body	73,700	56,800	33,200	19,800	9720	3600
Blood volume, males (ml)‡	5300	4500	2400	1400	500	270
Blood volume, females (ml)‡	3900	3300	2400	1400	500	270

LLI, lower large intestine; SI, small intestine; ULI, upper large intestine.

* Stabin and Siegel (2003).

† 'Remaining tissue' is defined as the part of the phantom remaining when all defined organs except muscles have been removed. The muscle mass is taken from *Publication 23* (ICRP, 1975).

‡ Data from *Publication* 89 (ICRP, 2002).

Fig. A.1, consists of four compartments: stomach, small intestine (SI), upper large intestine (ULI), and lower large intestine (LLI). Immediate mixing within each compartment is assumed. The recently introduced model for the human alimentary tract (HAT model; ICRP, 2006) and *Publication 89* (ICRP, 2002) present a more detailed

Table A.2. Adult values for blood content and blood flow in different organs.

Organ	Fractional blood volume %	Fractional cardiac output %
Adrenals	0.06	0.3
Brain	1.2	12
Gastrointestinal tract		
Stomach wall	1.0	1.0
Small intestine	3.8	10
Large intestine	2.2	4.0
Heart contents	9.0	
Heart wall	1.0	4.0
Kidneys	2.0	19
Liver	10	25.5
Lungs	12.5	2.5
Ovaries	0.02	0.02
Pancreas	0.6	1.0
Skeleton		
Red marrow	4.0	3.0
Cortical bone	0.8	0.6
Trabecular bone	1.2	0.9
Skin	3.0	5.0
Spleen	1.4	3.0
Testes	0.04	0.1
Thyroid	0.06	1.5

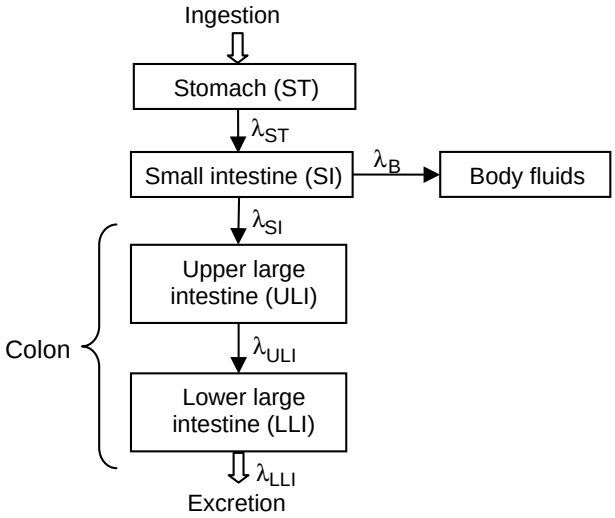

Fig. A.1. Compartment model used to describe the kinetics of radionuclides in the gastrointestinal tract.

model for the gastrointestinal tract, but this has not been implemented for calculations in the present report.

(A 6) For substances included in this report, the Task Group does not generally consider the deviations in effective dose caused by using the *Publication 30* model

Table A.3. Parameters used for calculating absorbed dose to the gastrointestinal tract.

Section of gastrointestinal tract	Mass of walls* (g)	Mass of contents* (g)	Mean residence time (h)	λ (/h)
Stomach	150	250	1	1
Small intestine	640	400	4	0.25
Upper large intestine	210	220	13	0.077
Lower large intestine	160	135	24	0.042

* From *Publication 23* (ICRP, 1975).

instead of the HAT model as significant. An example of a large deviation case arises when the activity is distributed in the stomach. Using the HAT model, the mean residence time in the stomach contents is considerably longer than that using the *Publication 30* model. This results in an absorbed dose to the stomach wall that is 30–40% larger with the HAT model compared with the *Publication 30* model.

(A 7) The same biological half-lives are used for both children and adults (see Table A.3). In fact, the mean transit time in the small and large intestine together is somewhat less in children than that in adults (ICRP, 2002, 2006); 36 h compared with 41 h in this model. The assumption of a transit time of 41 h in children will affect estimates of the absorbed dose to different parts of the gastrointestinal tract, depending upon the physical half-life of the radionuclide. Long half-life radionuclides will result in overestimates and short half-life radionuclides will result in underestimates. For newborn babies, however, it is not recommended to use the same gastrointestinal transit time as for adults. For substances for which the dose is calculated for newborn babies, further details about data for the transit time through the intestine are given in the biokinetic model, where applicable.

(A 8) A modified model is used for non-absorbable inert markers intended for studying different aspects of the physiology of the gastrointestinal tract, e.g. gastric emptying, intestinal transport and transit time, abnormal intestinal permeability, etc. These substances are usually labelled with ^{99m}Tc or ^{111}In. Small quantities of non-absorbable markers (i.e. up to a few percent) may be absorbed into the blood. For the purposes of this report, the amounts absorbed are considered to have a negligible effect on the dose calculations. The modification to the standard ICRP model is that the gastric residence time is changed to 0.5 h for fluids and 1.5 h for solids (ICRP, 2002, 2006).

A.4. Kidney–bladder model

(A 9) This model is applied to all substances used for kidney function tests, and to other substances if urinary excretion results in a significant absorbed dose to the bladder wall. In all these cases, the bladder is a separate entry in the biokinetic data tables.

(A 10) It is assumed that the fraction of the total excretion which passes through the kidneys and bladder is known. Activity excreted via this route passes through the kidneys with a transit time established from other clinical studies, and subsequently enters the bladder in urine where it remains until the bladder is emptied and the radioactive contents leave the body.

(A 11) The rate at which a radionuclide is excreted is determined from knowledge of the amount of activity in the total body, A_{TB}, which is assumed to be described by the sum of a series of exponential functions:

$$A_{TB} = \sum_{i=1}^{n} a_i \exp(-(\lambda_i + \lambda_p)t)$$

where λ_i is the biological elimination constant for component I, λ_p is the radioactive decay constant, and a_i is the fraction of the administered activity associated with component *i*.

The cumulated activity in the kidneys from the excretion process, $\widetilde{A}_K$, is given by:

$$\widetilde{A}_K = f_r \frac{1 - \exp(-\lambda_p \overline{T}_K)}{\lambda_p} \sum_{i=1}^{n} a_i \frac{\lambda_i}{\lambda_i + \lambda_p}$$

where f_r is the fraction of excreted activity which is eliminated through the kidneys, and $\overline{T_K}$ is the mean transit time through the kidneys appropriate for the given radiopharmaceutical and physiological status; unless otherwise stated, this is assumed to be 5 min.

(A 12) The expression is approximate, since f_r may differ for the individual components of whole-body clearance. However, for practical application, this approximation is judged to be adequate. The cumulated activity in the kidneys given in the biokinetic data tables for the individual substances is the sum of the cumulated activity from the excretion process and a contribution from activity distributed uniformly in the remaining organs and tissues, which can include the kidneys.

(A 13) The cumulated activity in bladder contents, $\widetilde{A}_B$, is given by:

$$\widetilde{A}_B = f_r \sum_{i=1}^{1} a_i \left[\frac{1 - \exp(-\lambda_p t_v)}{\lambda_p} - \frac{1 - \exp(-(\lambda_i + \lambda_p)t_v)}{\lambda_i + \lambda_p} \right] \times \left[\frac{1}{1 - \exp(-(\lambda_p + \lambda_p)t_v} \right]$$

where t_v, is the bladder filling and voiding interval, which for the purpose of the present model is assumed to be constant and equal to 3.5 h for adults and children aged $\geqslant$10 years; the average urinary cycle in humans (Syed, 1976). The first voiding is assumed to occur at time t_v after administration of the radiopharmaceutical to the patient. In the equations above, the effect of kidney residence time has been neglected since it is usually much shorter than the physical half-life of the radionuclide; if this is not the case, this equation should be multiplied by $\exp(-\lambda_p \overline{T_K})$.

(A 14) Calculating the radiation absorbed dose to the bladder wall involves consideration of a complex relationship between urine flow rate, voiding period, and the urine volume initially present in the bladder when the radiopharmaceutical is administered, and is critically dependent on the model used to describe the geometrical relationships between the wall of the bladder and its contents. Such a model was developed by Snyder and Ford (1976) to investigate the effects of the above physiological variables on absorbed dose to the bladder wall, and was extended by Smith

Table A.4. Parameters used for calculating absorbed dose to the urinary bladder wall.

Age (years)	Adult	15	10	5	1	Newborn
Voiding period (h)	3.5	3.5	3.5	3.0	2.0	2.0
Mass of wall* (g)	40–50	35–40	25	16	9	4
Mass of wall used (g)	47.6	35.9	23.2	14.5	7.7	2.88
Volume (ml)	211	160	103	64.7	32.9	12.4
Excretion (ml/day)*	1200–1600	1200	700	500	400	300

* The lower limit of the interval applies for females and the upper limit applies for males. Data from *Publication 89* (ICRP, 2002).

et al. (1982) to examine these effects for any radiopharmaceutical. The MIRD Committee has published a dynamic bladder model (Thomas et al., 1999) incorporating more physiologically realistic features providing for a varying bladder volume, varying initial content and voiding interval, and a night gap in the voiding pattern.

(A 15) Within the ranges of urine flow rate of 0.5–2 l/day, voiding period of 0.5–8 h, and initial bladder contents of 0–300 ml, the predicted bladder wall dose varies over a range of about 25 times for radiopharmaceuticals that are cleared rapidly by the renal system (e.g. ^{99m}Tc-MAG3), reducing to a range of about five times for substances that are cleared more slowly (e.g. ^{131}I-iodide). For voiding periods of $\geqslant$3.5 h, the bladder dose predicted by the simplified method used in this report lies within the spread of doses obtained using the above ranges of parameter values, but may be as much as five times lower than the highest values. As the voiding period decreases, the simple method leads to a further underestimate of the dose, which, for a period of 0.5 h, may be of the order of 25 times.

(A 16) An age-related bladder voiding model is used. The voiding periods are based upon urinary production rates as described in *Publication 89* (ICRP, 2002) and volume of the content as described by Stabin and Siegel (2003). The voiding periods are presented in Table A.4.

(A 17) The S-values used for calculation of the absorbed dose to the bladder wall relate to the contents and the wall of the bladder as the source and target tissue, respectively. It should be noted that the S-values, which for electrons and beta particles represent a surface dose to the bladder wall, are based on fixed average bladder contents (Table A.4). These S-values have been used in the present report in conjunction with cumulated activities in the bladder contents estimated for an age-dependent bladder voiding interval presented in Table A.4. This method does not allow for the variation in dose rate to the wall as the bladder fills with urine containing radionuclides.

A.5. Model for radiopharmaceuticals used to measure glomerular filtration rate

(A 18) For a variety of labelled inulin and inulin-like radiopharmaceuticals used for the measurement of glomerular filtration rate, the following biokinetic model has been used. After intravenous administration and initial rapid distribution in extracellular fluid, it is assumed that the radionuclide is excreted exclusively by the kidneys according to the kidney–bladder model. In the normal case, total body

retention is described by a mono-exponential function with a half-time of 100 min, fraction excreted by the kidneys of 1.0, and renal transit time of 5 min.

(A 19) For chelated compounds (DTPA, EDTA) and the contrast medium sodium iothalamate, there is evidence of a small degree of in-vivo dissociation of the radioactive label, leading to longer retention of approximately 1% of the administered radionuclide. This fraction is assumed to be distributed uniformly and to be eliminated with a half-time of 7 days. This is a simplifying approximation, since the dissociated label will exhibit specific biokinetics depending upon its chemical form. Nevertheless, it is considered adequate for estimating the contributions to absorbed dose from this dissociated label, provided that the examinations are conducted with a blocked thyroid for those radiopharmaceuticals for which the dissociated label would concentrate preferentially in the thyroid.

(A 20) In the abnormal case, it is assumed that the retention half-time of the major component is increased to 1000 min and that the renal transit time is increased to 20 min.

A.6. Models for bone-seeking radionuclides administered as radiopharmaceuticals

(A 21) For calculation of effective dose, the radiation-sensitive part of bone tissues has been identified as a 10-μm-thick layer on bone surfaces, representing endosteal and periosteal cells (ICRP, 1991a). The Task Group are aware that this figure is subject to revision, and that future dose estimates should be based on an extended bone surface volume (Gössner et al., 2000). However, for the present report, the dose estimates were produced using the earlier established method.

(A 22) The mean absorbed dose to bone surfaces and red marrow is presented in this report. Calculation of the absorbed dose for these tissues is a complex task since they comprise an intricate mixture of soft tissues and bone. For the present report, the calculations are based on S-values derived by Stabin and Siegel (2003), based on methods for calculating the absorbed fraction for the non-penetrating radiation developed by Eckerman and Stabin (2000) and Bouchet et al. (2000). The S-values from bone tissues to bone surfaces and red marrow are dependent on the distribution of activity within the bone. Two different cases can be distinguished:

- surface-deposited activity in trabecular and cortical bone ('bone surface seekers'); and
- activity deposited uniformly throughout the entire volume of the mineral bone in trabecular and cortical bone ('bone volume seekers').

(A 23) In *Publication 30* (ICRP, 1979), a general rule concerning short-lived radionuclides was introduced and used for various elements: 'radionuclides with a physical half-life less than 15 days are assumed to be surface deposited.' The same general rule, extended to apply to the effective half-time, is adopted in the present report. Thus, for the absorbed dose calculations, substances with an effective half-time of <15 days have been assumed to be surface deposited, and those with a effective half-time >15 days have been assumed to be volume distributed, unless

otherwise stated. In cases with two or more biological excretion half-times, the different components are considered separately, thus a fraction excreted slowly from the skeleton may be considered to be volume deposited, while the remaining part is surface deposited, provided that the physical half-life is sufficiently long.

(A 24) If nothing is known about the distribution of cumulated activity between cortical and trabecular bone, it is assumed to be distributed uniformly on surfaces or throughout the volume, as appropriate.

(A 25) The distribution of activity thus follows the surface area or mass distribution of mineral bone. For adults, the mass ratio cortical:trabecular bone, according to *Publication 89*, is 80:20 and the surface area ratio is 40:60 (ICRP, 2002). Since no reference values for the distribution between cortical and trabecular bone for children are available, and since the information on this matter in the open literature is very scarce, the Task Group has also adopted these values for 15- and 10-year-old children. For 5- and 1-year-old children, the mass ratio cortical:trabecular bone used for the calculations is assumed to be 60:40 and the surface area ratio is assumed to be 30:70.

(A 26) A few radiopharmaceuticals are concentrated to a significant extent in the metaphyseal growth plates of children's bones. This factor is not taken into account in the dose calculations given herein. Thus, radiation doses to this part of the skeleton may be underestimated for children. However, the mean absorbed dose to bone surfaces is not likely to be underestimated substantially.

A.7. Model for colloids taken up preferentially in the liver, spleen, and red bone marrow

(A 27) Colloids of ^{99m}Tc-sulphur and ^{198}Au were discussed in MIRD Report Nos. 3 and 4, respectively (Atkins et al., 1975; Cloutier et al., 1975). The colloids were assumed to be taken up preferentially in the liver, spleen, and red bone marrow, with a uniform distribution of any residue in the remainder of the body. Uptake fractions were given for three patient categories: normal liver condition, early to intermediate diffuse parenchymal liver disease, and intermediate to advanced diffuse parenchymal liver disease. These categories differ not only in biokinetics, but also with regard to liver and spleen mass. In the normal case, the uptake in liver, spleen, and red marrow was set at 85, 7, and 5% for sulphur colloid and 90, 3, and 7% for gold colloid, respectively. These values were estimates based on clinical studies, but no details about the methods used for calculating the percentages were given. However, the values are in good agreement with results obtained from animal studies.

(A 28) Studies on man have shown a decreased uptake of colloids with increasing degree of liver disease, with corresponding increases in uptake for other organs (Herzog et al., 1987; Groshar et al., 2002). The change in uptake depends on the particle size of the administered colloid.

(A 29) The Task Group has adopted the same view as the MIRD Committee with regard to choice of patient categories, definition of organs with an active uptake, organ masses, and biokinetic differences between large and small colloids. The uptake values used are based on the report by Herzog et al. (1987), which contains results of quantitative measurements with conjugate view whole-body counting and double-

window regional counting over liver and spleen. For all types of colloid, immediate uptake is assumed. The biological half-time is assumed to be long compared with the physical half-life of the radionuclide, except for iodine-labelled albumin micro-aggregates. For these substances, the metabolic breakdown of the particles is assumed to be represented by biological half-times (fraction) of 3 h (0.8) and 5 days (0.2).

(A 30) The organ masses for different patient categories and uptake data for different sizes of colloid are presented in Tables A.5–A.7. For further details, the reader is referred to the biokinetic data on the individual substances.

A.8. Model for liver and biliary excretion

(A 31) This model is intended for substances that are actively taken up in hepatocytes and excreted, via the biliary tract, to the intestine. Typical examples are a large

Table A.5. Organ mass (kg): based on Atkins et al. (1975).

Organ	Condition		
	1*	2†	3‡
Total body	70	70	70
Liver	1.8	2.4	1.4
Spleen	0.17	0.25	0.4
Red marrow	1.5	1.5	1.5

* Normal liver.
† Early to intermediate diffuse parenchymal liver disease.
‡ Intermediate to advanced diffuse parenchymal liver disease.

Table A.6. Uptake values (fractions) for large colloids (100–1000 nm diameter).*

Organ	Condition†		
	1	2	3
Liver	0.70	0.50	0.30
Spleen	0.10	0.20	0.30
Red marrow	0.10	0.15	0.25
Remaining	0.10	0.15	0.15

* Examples: ^{99m}Tc micro-aggregated albumin, ^{99m}Tc-phytate.
† See footnote to Table A.3.

Table A.7. Uptake values (fractions) for small colloids (<100 nm diameter).*

Organ	Condition†		
	1	2	3
Liver	0.70	0.50	0.30
Spleen	0.10	0.20	0.30
Red marrow	0.15	0.25	0.30
Remaining	0.05	0.15	0.10

* Examples: ^{99m}Tc mini-/micro-aggregated albumin.
† See footnote to Table A.3.

group of technetium-labelled iminodiacetic acid (IDA) derivatives (e.g. BIDA, HIDA, EIDA, PIPIDA, PBIDA, and DISIDA).

(A 32) Several biokinetic models have been presented in the literature for technetium-labelled IDA derivatives (Ryan et al., 1977; Wistow et al., 1977; Taavitsainen et al., 1980; Brown et al., 1981, 1982; Wu et al., 1984). The substance is assumed to be rapidly taken up in the liver from the blood and then excreted, via the biliary tract, partly to the gallbladder for temporary storage and partly directly to the intestine. A minor portion of the radiopharmaceutical is excreted in the urine. In pathological states (liver disease, occlusion of the biliary tract, congenial biliary atresia), the same model is used but with different kinetic data (transfer factors). The compartmental model is shown in Fig. A.2.

(A 33) Similar models have been used for all substances that undergo biliary excretion. For each substance, the fraction and half-time for movement between compartments are specified in the biokinetic data table. Unless otherwise stated in the model, it is assumed that 65% of the activity entering the liver is transferred directly from the liver to the small intestine, and 35% goes to the gallbladder (Wu et al., 1984).

(A 34) The gallbladder empties at intervals on stimulation by food. It is assumed to empty in an identical manner for all substances. The first emptying is after 3 h, during which time 75% of the radioactive material present in the bile is assumed to be excreted to the small intestine. The second emptying is after 9 h, again associated with the excretion of 75% of the radioactive material in the bile. For the dose estimation, the third and final emptying is assumed to occur after 24 h when all the radioactive material is excreted. Earlier emptying can be induced by a meal of high fat content or by cholecystokinin.

(A 35) The final excretion from the body follows the models for the gastrointestinal tract and for the kidney–bladder system (see above).

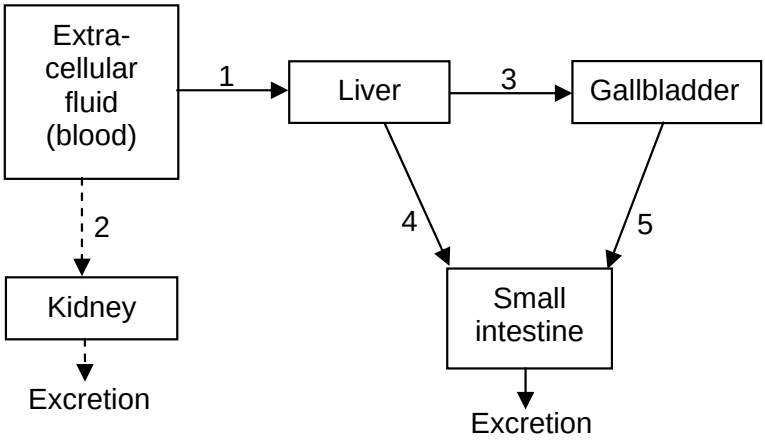

Fig. A.2. Model for liver and biliary excretion. The flows are defined as follows: 1, uptake in liver; 2, uptake in kidney; 3, excretion from liver to gallbladder; 4, excretion from liver directly to small intestine; 5, emptying of gallbladder to small intestine.

A.9. Salivary glands

(A 36) Some substances are actively taken up in the salivary glands. In those cases, an approximate absorbed dose in the salivary glands is estimated and included in the dose table. This organ is not included in the presently used tables of S-values. Johansson (1996) presented S-values for self-irradiation of the salivary glands for ^{99m}Tc. The calculation method lined up in this report has also been used by the Task Group for other radionuclides, utilising the unit density sphere model in the formerly freely available MIRDOSE3 program (Stabin, 1996). The S-values have been calculated considering the three pairs of salivary glands (parotid, submaxillary, and sublingual) with masses according to *Publication 23* (ICRP, 1975). Those masses do not deviate significantly from those reported in the updated version, *Publication 89* (ICRP, 2002). To estimate the absorbed dose from source in other organs, the brain is used as a substitute target organ, except in cases when the brain is also a source.

A.10. References for Annex A

Atkins, H.L., Cloutier, R.J., Lathrop, K.A. et al., 1975. Technetium-99m-sulfur colloid in various liver conditions. MIRD Dose Estimate Report No. 3. J. Nucl. Med. 16, 108A–108B.

Bouchet, L.G., Bolch, W.E., Howell, R.W., Rao, D.V., 2000. S values for radionuclides localized within the skeleton. J. Nucl. Med. 41, 189–212.

Brown, P.H., Krishnamurthy, G.T., Bobba, V.R., Kingston, E., 1981. Radiation-dose calculation for Tc-99m HIDA in health and disease. J. Nucl. Med. 22, 177–183.

Brown, P.H., Krishnamurthy, G.T., Bobba, V.R., Kingston, E., Turner, F.E., 1982. Radiation-dose calculation for five Tc-99m IDA hepatobiliary agents. J. Nucl. Med. 23, 1025–1030.

Cloutier, R.J., Freeman, L.M., McAfee, J.G. et al., 1975. Summary of current radiation dose estimates to humans with various liver conditions from ^{198}Au colloidal gold. MIRD Dose Estimate Report No. 4. J. Nucl. Med. 16, 173–174.

Cristy, M., Eckerman, K., 1987. Specific Absorbed Fractions of Energy at Various Ages from Internal Photon Sources. Oak Ridge National Laboratory, Oak Ridge, TN.

Eckerman, K.F., Stabin, M.G., 2000. Electron absorbed fractions and dose conversion factors for marrow and bone by skeletal region. Health Phys. 78, 199–214.

Gössner, W., Masse, R., Stather, J.W., 2000. Cells at risk for dosimetric modelling relevant to bone tumour induction. Radiat. Prot. Dosim. 92, 209–213.

Groshar, D., Slobodin, G., Zuckerman, E., 2002. Quantitation of liver and spleen uptake of 99mTc-phytate colloid using SPECT: detection of liver cirrhosis. J. Nucl. Med. 43, 312–317.

Herzog, H., Spohr, G., Notohamiprodjo, G., Feinendegen, L.E., 1987. Absolute quantification of pharmacokinetic distribution of RES colloids in individuals with normal liver function. Nucl. Med. Commun. 8, 157–175.

ICRP, 1975. Report of the Task Group on Reference Man. ICRP Publication 23. Pergamon Press, Oxford.

ICRP, 1979. Limits for intakes of radionuclides by workers. ICRP Publication 30, Part 1. Ann. ICRP 2(3/4).

ICRP, 1991a. 1990 Recommendations of the International Commission on Radiological Protection. ICRP Publication 60. Ann. ICRP 21(1–3).

ICRP, 2002. Basic anatomical and physiological data for use in radiological protection: reference values. ICRP Publication 89. Ann. ICRP 31(3/4).

ICRP, 2006. Human alimentary tract model for radiological protection. ICRP Publication 100. Ann. ICRP 35(1/2).

Johansson, L., 1996. Absorbed dose in the salivary glands from technetium-99m labeled radiopharmaceuticals, in: Schlafke-Stelson, A., Stabin, M.G., Sparks, R.B.. Sixth International Radiopharmaceutical Dosimetry Symposium, Oak Ridge Institute for Science and Education, Gatlinburg, TN, pp 513–521.

Leggett, R.W., Williams, L.R., 1991. Suggested reference values for regional blood volumes in humans. Health Phys. 60, 139–154.

Leggett, R.W., Williams, L.R., 1995. A proposed blood circulation model for reference man. Health Phys. 69, 187–201.

Ryan, J., Cooper, M., Loberg, M., Harvey, E., Sikorski, S., 1977. Technetium-99m-labelled N-(2,6-dimethylphenyl carbamoylmethyl)-iminodiacetic acid (Tc99mHIDA): a new radiopharmaceutical for hepatobiliary imaging studies. J. Nucl. Med. 18, 997–1004.

Smith, T., Veall, N., Wootton, R., 1982. Bladder wall dose from administered radiopharmaceuticals: the effect of variation in urine flow rate, voiding interval and initial bladder content. Radiat. Prot. Dosim. 2, 183–189.

Snyder, W.S., Ford, M.R., 1976. Estimation of doses to the urinary bladder and to the gonads, in: Cloutier, R.J., Coffey, J.L., Snyder, W.S., et al. (Eds.), Radiopharmaceutical Dosimetry Symposium, Oak Ridge, TN. HEW Publication (FDA 76-8044). Department of Health, Education and Welfare, Bureau of Radiological Health, Rockville, MD, pp. 313–349.

Stabin, M.G., 1996. MIRDOSE: personal computer software for internal dose assessment in nuclear medicine. J. Nucl. Med. 37, 538–546.

Stabin, M.G., Siegel, J.A., 2003. Physical models and dose factors for use in internal dose assessment. Health Phys. 83, 294–310.

Stabin, M.G., Sparks, R.B., Crowe, E., 2005. OLINDA/EXM: the second-generation personal computer software for internal dose assessment in nuclear medicine. J. Nucl. Med. 46, 1023–1027.

Syed, I.B., 1976. Dosimetry of indium-113m radiopharmaceuticals with special attention to the urinary bladder, in: Cloutier, R.J., Coffey, J.L., Snyder, W.S., et al. (Eds.), Radiopharmaceutical Dosimetry Symposium, Oak Ridge, TN. HEW Publication (FDA 76-8044). Department of Health, Education and Welfare, Bureau of Radiological Health, Rockville, MD, pp. 360–369.

Taavitsainen, M., Riihimäki, E., Tähti, E., 1980. Body disappearance and liver mean transit time of 99m-Tc-diethyl-IDA. Eur. J. Nucl. Med. 5, 147–150.

Thomas, S.R., Stabin, M.G., Chen, C.-T., Samaratunga, R.C., 1999. A dynamic urinary bladder model for radiation dose calculations. MIRD Pamphlet No. 14, revised. J. Nucl. Med. 40, 102S–123S.

Williams, L.R., Leggett, R.W., 1989. Reference values for resting blood flow to organs of man. Clin. Phys. Physiol. Meas. 10, 187–217.

Wistow, B.W., Subramanian, G., Van Heertum, R.L. et al., 1977. An evaluation on ^{99m}Tc-labeled hepatobiliary agents. J. Nucl. Med. 18, 455–461.

Wu, R.K., Siegel, J.A., Rattner, Z., Malmud, L.S., 1984. Tc-99m HIDA dosimetry in patients with various hepatic disorders. J. Nucl. Med. 25, 905–912.

ANNEX B. EXPLANATIONS

B.1. Where can the most recent ICRP information about a specific substance be found?

Radiopharmaceutical	This publication	*Publication 80*	*Publication 53*
^{3}H-neutral fat, free fatty acids		x	
^{11}C-acetate	x		
^{11}C-amino acids (generic model)	x		
^{11}C-brain receptor substances (generic model)	x		
^{11}C-methionine	x		
^{11}C-thymidine		x	
^{11}C (realistic maximum model)	x		
^{14}C-neutral fat, free fatty acids		x	
^{14}C-urea		x	
^{15}O-water	x		
^{18}F-amino acids (generic model)	x		
^{18}F-brain receptor substances (generic model)	x		
^{18}F-FDG	x		
^{18}F-L-dopa	x		
^{18}F (realistic maximum model)	x		
^{51}Cr-EDTA		x	
^{67}Ga-citrate		x	
^{68}Ga-EDTA		x	
^{75}Se-amino acids	x		
^{75}Se-HCAT		x	
^{99m}Tc-apticide	x		
^{99m}Tc-colloids (small)	x		
^{99m}Tc-EC	x		
^{99m}Tc-ECD	x		
^{99m}Tc-furifosmin	x		
^{99m}Tc-HIG		x	
^{99m}Tc-HM-PAO		x	
^{99m}Tc-IDA derivatives		x	
^{99m}Tc-MAA		x	
^{99m}Tc-MAG3		x	
^{99m}Tc-markers, non-absorbable		x	
^{99m}Tc-MIBI		x	
^{99m}Tc-monoclonal antibodies/fragments	x		
^{99m}Tc-pertechnegas		x	
^{99m}Tc-pertechnetate		x	
^{99m}Tc-phosphates and phosphonates		x	
^{99m}Tc-RBC		x	x
^{99m}Tc-Technegas		x	
^{99m}Tc-tetrofosmin (rest/exercise)	x		
^{99m}Tc-WBC		x	
^{111}In-HIG		x	

Radiopharmaceutical	This publication	*Publication 80*	*Publication 53*
^{111}In-monoclonal antibodies/fragments	x		
^{111}In-octreotide		x	
^{123}I-iodide			x
^{123}I-fatty acids (BMIPP/IPPA)	x		
^{123}I-brain receptor substances (generic model)	x		
^{123}I-iodo hippurate		x	
^{123}I-MIBG		x	
^{123}I-monoclonal antibodies/fragments	x		
^{124}I-iodide			x
^{125}I-iodide			x
^{131}I-iodide			x
^{131}I-iodo hippurate		x	
^{131}I-monoclonal antibodies/fragments	x		
^{131}I-norcholesterol		x	
^{201}Tl-ion	x		

B.2. Presentation of data

(B 1) The data on each substance are presented in three subsections: biokinetic model, biokinetic data, and table of absorbed dose per unit of activity administered. Unless otherwise stated, the model refers to intravenous administration.

(B 2) The rate of the biological process, for example uptake, metabolism, and excretion, is usually given as the half-time of the corresponding exponential function. If the process is assumed to be multi-exponential, the fraction of the organ content belonging to each exponential component is given in brackets immediately after the half-time figure. When rates are given as fractions per time unit (k) as reported in cited publications, they are transformed into half-times according to the formula $T = 0.693/k$.

(B 3) The following abbreviations have been used:

S	Source organ or tissue
F_s	Fractional distribution to organ or tissue S
T	Biological half-time for an uptake or elimination component
a	Fraction of F_s taken up or eliminated with the corresponding half-time. A minus sign indicates uptake
$\widetilde{A}_s/A_o$	Cumulated activity in organ or tissue S per unit of administered activity

(B 4) The tables sometimes contain empty spaces under the headings T and *a*, usually because the kinetics are described by complex exponential, or non-exponential, expressions, which cannot easily be defined in the table. This is the case for activity in the gastrointestinal tract, the gallbladder, and the urinary bladder. In these cases, the tables only present the cumulated activities together with the fractional distribution.

(B 5) The relative cumulated activities are presented in hours (h). Average organ or tissue absorbed doses are given as milligrays (mGy) per megabecquerel (MBq). The effective dose is given as millisieverts (mSv) per megabecquerel. All dose values are given in exponential notation (e.g. $2.6E-02 = 2.6 \times 10^{-2}$ or 0.026 and $4.9E+01 = 4.9 \times 10^{+1}$ or 49). The calculations have been performed without rounding, but the final result is given with two digits.

(B 6) Dose calculations have been performed for adults and 15-, 10-, 5-, and 1-year-old children. The organs (or tissues) are presented in alphabetical order except 'Remaining organs', which is placed at the end. The dose to organs or tissues not mentioned in the table can usually be approximated with the value given for 'Remaining organs'.

ANNEX C. BIOKINETIC MODELS AND DOSE TABLES

C.1. [1-^{11}C]-acetate

^{11}C

C.1.1. Biokinetic model

(C 1) Acetate labelled with ^{11}C in the carboxyl position, [1-^{11}C]-acetate, is used for dynamic positron emission tomography (PET) studies of myocardial metabolism (Armbrecht et al., 1990; van den Hoff et al., 1996; Sun et al., 1997), and in renal (Shreve et al., 1995), pancreatic (Shreve and Gross, 1997), and nasopharyngeal disease (Yeh et al., 1999).

(C 2) In most tissues, after extraction from the blood, [1-^{11}C]-acetate is activated to acetyl co-enzyme A (CoA) and enters the tricarboxylic acid (TCA) cycle. From the TCA cycle, the label is lost mainly in the form of $^{11}CO_2$ (Armbrecht et al., 1990). In resting myocardium, the behaviour of [1-^{11}C]-acetate can be summarised as follows (Armbrecht et al., 1990):

- extraction of approximately two-thirds of the activity in a single capillary transit;
- a very rapid initial washout phase ($T_{1/2} < 5$ s);
- activation of [1-^{11}C]-acetate to [1-^{11}C]-acetyl-CoA within a few seconds;
- labelling of TCA cycle intermediates takes several minutes;
- onset of rapid $^{11}CO_2$ release after 2–3 min; and
- $^{11}CO_2$ release is bi-exponential.

(C 3) In all the tissues studied, peak uptake appears to be reached within less than 3 min. After 3–5 min, 50% of the tissue activity is present as $^{11}CO_2$, 24% as non-ionised species, and 13% each as acetate and TCA-amino acid intermediates (Sun et al., 1997). The rate of metabolism of the radiopharmaceutical reflects the rate of oxidative metabolism in the tissue, and thus the oxygen supply.

(C 4) Clinical studies indicate that in both myocardium and kidney parenchyma, the initial uptake is complete by 2.5–3 min post injection, and that between 3 and 30 min, the ^{11}C is lost from the tissues with a half-time of approximately 10 min. In normal pancreas, the uptake is also complete in 3 min, and up to 30 min, at least, the activity is lost from the tissue with a half-time of 38 min. In the liver, uptake is again rapid, peaking at approximately 3 min; thereafter, loss of ^{11}C from the tissue follows a tri-exponential clearance, with 35% being cleared with a half-time of 10 min and the remainder with half-times of 1 (30%) and 2 h (35%).

(C 5) Few data on the fractional deposition of [1-^{11}C]-acetate in human tissues appear to be available in the literature. However, since there is a high extraction rate for [1-^{11}C]-acetate in most tissues and its rate of metabolism reflects the tissue oxygen supply, the rate of blood flow, expressed as a fraction of cardiac output, in the tissue may be used as an approximation of the tissue uptake of [1-^{11}C]-acetate. Leggett and

Williams (1995) have tabulated blood flow data for most human tissues, and these values have been used to construct the biokinetic model illustrated below. In this model, uptake in all tissues is assumed to be rapid with a half-time of 1 min.

C.1.2. References for [1-^{11}C]-acetate

Armbrecht, J.J., Burton, D.B., Schelbert, H.R., 1990. Validation of [1-^{11}C]acetate as a tracer for non-invasive assessment of oxidative metabolism with positron emission tomography in normal, ischemic, postischemic and hyperaemic canine myocardium. Circulation 81, 1594–1605.

Leggett, R.W., Williams, L.R., 1995. A proposed blood circulation model for reference man. Health Phys. 69, 187–201.

Shreve, P.D., Gross, M.D., 1997. Imaging of the pancreas and related diseases with PET carbon-11-acetate. J. Nucl. Med. 38, 1305–1310.

Shreve, P., Chiao, P.C., Humes, H.D., Schwaiger, M., Gross, M.D., 1995. Carbon-11-acetate PET imaging in renal disease. J. Nucl. Med. 36, 1595–1601.

Sun, K.T., Chen, K., Huang, S-C., Buxton, D.B., et al., 1997. Compartment model for measuring myocardial oxygen consumption using [1-^{11}C]acetate. J. Nucl. Med. 38, 459–466.

van den Hoff, J., Burchert, W., Wolpers, H.G., Meyer, G.J., Hundeshagen, H., 1996. A kinetic model for cardiac PET with [1-^{11}C]acetate. J. Nucl. Med. 37, 521–529.

Yeh, S.H., Liu, R.S., Wu, L.C., Yen, S.H., Chang, C.W., Chen, K.Y., 1999. ^{11}C-acetate clearance in nasopharyngeal carcinoma. Nucl. Med. Commun 20, 131–134.

C.1.3. Biokinetic data for [1-^{11}C]-acetate

Organ (S)	F_s	T (h)	a	$\widetilde{A}_s/A_0$(h)
Blood	1.0	0.017	1.0	0.023
Heart wall	0.045	−0.017	1.0	0.014
		0.17	0.50	
		8.0	0.50	
Kidneys	0.19	−0.017	1.0	0.059
		0.17	0.50	
		24	0.50	
Liver	0.25	−0.017	1.0	0.075
		0.17	0.35	
		1.0	0.30	
		2.0	0.35	
Pancreas	0.01	−0.017	1.0	0.0035
		0.67	0.50	
		2.0	0.50	
Other organs and tissues	0.505	−0.017	1.0	0.15
		0.17	0.50	
		8.0	0.50	

This biokinetic model is not applicable for ^{14}C.

C.1.4. Absorbed doses for [1-^{11}C]-acetate

^{11}C 20.4 min

Organ	Absorbed dose per unit activity administered (mGy/MBq)				
	Adult	15 years	10 years	5 years	1 year
Adrenals	3.4E-03	4.3E-03	6.6E-03	1.0E-02	1.8E-02
Bladder	1.2E-03	1.4E-03	2.3E-03	3.9E-03	7.0E-03
Bone surfaces	1.5E-03	1.9E-03	3.0E-03	4.8E-03	9.6E-03
Brain	9.8E-04	1.2E-03	2.1E-03	3.5E-03	6.6E-03
Breasts	1.2E-03	1.5E-03	2.5E-03	4.0E-03	7.6E-03
Gallbladder	3.4E-03	3.9E-03	5.5E-03	8.7E-03	1.6E-02
Gastrointestinal tract					
Stomach	2.0E-03	2.4E-03	3.9E-03	6.0E-03	1.1E-02
Small intestine	1.7E-03	2.2E-03	3.5E-03	5.6E-03	1.0E-02
Colon	1.6E-03	1.9E-03	3.2E-03	5.0E-03	9.5E-03
(Upper large intestine	1.8E-03	2.2E-03	3.7E-03	5.7E-03	1.1E-02)
(Lower large intestine	1.3E-03	1.5E-03	2.5E-03	4.1E-03	7.5E-03)
Heart	1.3E-02	1.7E-02	2.6E-02	4.1E-02	7.4E-02
Kidneys	5.2E-02	6.3E-02	8.8E-02	1.3E-01	2.3E-01
Liver	1.3E-02	1.8E-02	2.7E-02	4.0E-02	7.5E-02
Lungs	2.4E-03	3.1E-03	4.8E-03	7.6E-03	1.5E-02
Muscles	1.3E-03	1.7E-03	2.6E-03	4.2E-03	8.0E-03
Oesophagus	1.5E-03	1.9E-03	2.8E-03	4.4E-03	8.1E-03
Ovaries	1.4E-03	1.8E-03	2.8E-03	4.6E-03	8.6E-03
Pancreas	1.2E-02	1.6E-02	3.3E-02	4.2E-02	9.1E-02
Red marrow	1.8E-03	2.2E-03	3.3E-03	5.1E-03	9.2E-03
Skin	1.0E-03	1.2E-03	2.0E-03	3.3E-03	6.4E-03
Spleen	2.9E-03	3.6E-03	5.8E-03	8.9E-03	1.6E-02
Testes	1.0E-03	1.3E-03	2.0E-03	3.2E-03	6.4E-03
Thymus	1.5E-03	1.9E-03	2.8E-03	4.4E-03	8.1E-03
Thyroid	1.2E-03	1.6E-03	2.6E-03	4.4E-03	8.5E-03
Uterus	1.4E-03	1.7E-03	2.8E-03	4.5E-03	8.4E-03
Remaining organs	1.4E-03	1.7E-03	2.7E-03	4.4E-03	8.1E-03
Effective dose (mSv/MBq)	3.5E-03	4.3E-03	6.5E-03	9.9E-03	1.8E-02

C.2. ^{11}C-labelled amino acids (generic model)

^{11}C

C.2.1. Biokinetic model

(C 6) The methionine analogue [^{75}Se]-selenomethionine has been used in nuclear medicine for many years (ICRP, 1987), and more recently, a number of other amino acids labelled with ^{11}C or ^{18}F have been utilised, or proposed, for clinical applications such as L-[methyl-^{11}C]-methionine (Deloar et al., 1998b), L-[2-^{18}F]-fluorotyrosine (Coenen et al., 1989; Cottrall et al., 1973; Taylor and Cottrall, 1973), [^{18}F]-*p*-fluorophenylalanine (Cottrall et al., 1973), 6-[^{18}F]-fluorotryptophan (Atkins et al., 1972; Taylor and Cottrall, 1973), *cis*-4-[^{18}F]-fluoroproline and *trans*-4-[^{18}F]-fluoroproline (Wester et al., 1999a,b), and L-3-[^{18}F]-fluoro-α-methyl tyrosine (Inoue et al., 1996).

(C 7) The Commission has only published biokinetic models for [^{75}Se]-selenomethionine (ICRP, 1987) and L-[methyl-^{11}C]-methionine (ICRP, 2001b). Taylor (2000b) developed the generic biokinetic model described below for use in assessment of the internal dose received by human subjects injected intravenously with amino acids labelled with ^{11}C, ^{18}F, or ^{75}Se. Comparison of the radiation doses to adults calculated using this generic model with those calculated using compound-specific models for [^{11}C]-labelled and [^{18}F]-labelled amino acids and for [^{75}Se]-selenomethionine indicated that, in general, the effective doses, as well as the organ and tissue doses, calculated using the generic model agreed within a factor of two or less with those calculated using compound-specific models. It was further noted that the generic model tended to overestimate, rather than underestimate, the organ and tissue doses. It was concluded that for [^{11}C]-, [^{18}F]-, and [^{75}Se]-labelled amino acids or their analogues, the generic biokinetic model could be applied for general radiation protection purposes.

(C 8) The generic model assumes that, following entry of a labelled amino acid into the blood stream, the radiopharmaceutical is taken up instantaneously by the organs and tissues. This is followed by a phase of rapid elimination of that fraction of the injected material which goes directly into the excretory pathways or is excreted following early metabolism, a second phase which represents loss due to metabolic breakdown of labelled proteins and other compounds with relatively rapid turnover times, and a final phase representing elimination of the small fraction of the radionuclide which had been incorporated into structural proteins or other body components with very slow turnover.

(C 9) In the model, elimination of the radionuclide from the various organs and tissues is assumed to approximate a three-component exponential relationship with biological half-times of 0.5, 50, and 5000 days. The long biological half-time assigned to the small final component of the model reflects the evidence that ^{14}C incorporated into structural tissues such as bone is retained with a very long half-time (Stenhouse and Baxter, 1977; Stenström et al., 1996).

(C 10) The generic model assumes that 20% of the administered activity is excreted directly from the blood to the urinary bladder with biological half-times of 0.2 h

(0.25) and 6 h (0.75) in the blood. It has also been assumed that 3% of the injected activity is excreted into the small intestine, half with a biological half-time of 6 h and half with a biological half-time of 12 h. Since labelled amino acids are potentially important for studies of protein synthesis in the brain (Bergmann et al., 1995; Schmidt et al., 1997; Shoup et al., 1999), it was assumed that 1.5% of the injected activity deposits in brain, from where it is released back to the circulation with biological half-times of 50 (70%) and 5000 days (30%). The parameters of this generic model are shown in the biokinetic data table.

(C 11) Taylor (2000b) pointed out that the biokinetic data from humans or animals that were used to derive both the compound-specific and the generic models are subject to quite large uncertainties (coefficients of variation ranging from approximately 20% to approximately 80%); therefore, when comparing doses calculated by the generic and compound-specific biokinetic models, differences in individual tissue or organ doses of a factor of two, or even three, should be regarded as good agreement.

(C 12) This agreement appears to be close enough for the single generic biokinetic model to be used for normal prospective radiation dosimetry, and for general assessment of the risk from the use of amino acids labelled with ^{11}C, ^{18}F, or ^{75}Se. In situations where compound-specific retrospective dosimetry is necessary, for example in the case of accidental intake of a large amount of a radionuclide compound, it might reasonably be expected that some subject- and compound-specific biokinetic information would be available upon which a more accurate person-specific dose assessment could be based.

> This model is not appropriate for the interpretation of bio-assay data following intake of ^{14}C-labelled amino acids.

C.2.2. References for ^{11}C-labelled amino acids

Atkins, H.L., Christman, D.R., Fowler, J.S., et al., 1972. Organic Radiopharmaceuticals Labeled with Isotopes of Short Half-Life. V. 18F-Labeled 5- and 6-Fluorotryptophan. J. Nucl. Med. 13, 713–719.

Bergmann, R., Brust, P., Kampf, G., Coenen, H.H., Stöcklin, G., 1995. Evaluation of radioselenium labeled selenomethionine, a potential tracer for brain protein synthesis by PET. Nucl. Med. Biol. 22, 475–481.

Coenen, H.H., Kling, P., Stöcklin, G., 1989. Cerebral metabolism of l-[2-^{18}F]fluorotyrosine, a new PET tracer of protein synthesis. J. Nucl. Med. 30, 1367–1372.

Cottrall, M.F., Taylor, D.M., McElwain, T.J., 1973. Investigations of ^{18}F-p-fluorophenylalanine for pancreas scanning. Br. J. Radiol. 46, 277–288.

Deloar, H.M., Fujiwara, T., Nakamura, T., Itoh, M., Imai, D., Miyake, M., Watanuki, S., 1998b. Estimation of internal absorbed dose of l-[methyl-^{11}C] methionine using whole body positron emission tomography. Eur. J. Nucl. Med. 25, 629–633.

ICRP, 1987. Radiation dose to patients from radiopharmaceuticals. ICRP Publication 53. Ann. ICRP 18, 149–150.

Inoue, T., Tomiyoshi, K., Higuichi, T., Ahmed, K., Sarwar, M., Aoyagi, K., Amano, S., Alyafei, S., Zhang, H., Endo, K., 1996. Biodistribution studies on l-3-[fluorine-18]fluoro-α-methyl tyrosine: a potential tumor-detecting agent. J. Nucl. Med. 39, 663–667.

Schmidt, D., Langen, K-J., Herzog, H., Wirths, J., Holschbach, M., Kiwit, J.C.W., Ziemons, K., Coenen, H.H., Müller-Gärtner, H.W., 1997. Whole-body kinetics and dosimetry of l-3-[^{123}I]iodo-α-methyltyrosine. Eur. J. Nucl. Med. 24, 1162–1166.

Shoup, T.M., Olson, J., Hoffman, J.M., Votaw, J., Eshima, D., Eshima, L., Camp, M., Stabin, M., Votaw, D., Goodman, M., 1999. Synthesis and evaluation of [^{18}F]1-amino-3-fluorocyclobutane-1-carboxylic acid to image brain tumours. J. Nucl. Med. 40, 331–338.

Stenhouse, M.J., Baxter, M.S., 1977. Bomb ^{14}C as a biological tracer. Nature (Lond.) 267, 828–832.

Stenström, K., Leide-Svegborn, S., Erlandsson, B., Hellborg, R., Mattsson, S., Nilsson, L-E., Nosslin, B., Skog, G., Wiebert, A., 1996. Application of accelerator mass spectrometry (AMS) for high-sensitivity measurements of $^{14}CO_2$ in long-term studies of fat metabolism. Appl. Radiat. Isot. 47, 417–422.

Taylor, D.M., 2000b. Generic models for radionuclide dosimetry: ^{11}C, ^{18}F or ^{75}Se-labelled amino acids. Appl. Radiat. Isot. 52, 911–922.

Taylor, D.M., Cottrall, M.F., 1973. Evaluation of amino acids labelled with ^{18}F for pancreas scanningRadiopharmaceuticals and Labelled Compounds, Vol. I. IAEA, Vienna, pp. 441–443.

Wester, H.J., Herz, M., Senkowitsch-Schmidtke, R., Schwaiger, M., Stöcklin, G., Hamacher, K., 1999a. Preclinical evaluation of 4-[^{18}F]fluoroprolines: diasteromeric effect on metabolism and uptake in mice. Nucl. Med. Biol. 26, 259–265.

Wester, H.J., Herz, M., Weber, W., Heiss, P., Senkowitsch-Schmidtke, R., Schwaiger, M., Stöcklin, G., 1999b. Synthesis and radiopharmacology of O-(2-[^{18}F]fluoroethyl)-L-tyrosine for tumor imaging. J. Nucl. Med. 40, 205–212.

C.2.3. Biokinetic data for ^{11}C-labelled amino acids

Organ (S)	F_s	T (h)	a	$\widetilde{A}_s/A_0$(h)
Blood	0.20	0.2	0.25	0.079
		6	0.75	
Brain	0.015	1200	0.70	0.0073
		∞	0.30	
Thyroid	0.0007	1200	0.70	0.00034
		∞	0.30	
Lungs	0.02	12	0.10	0.0098
		1200	0.85	
		∞	0.05	
Kidneys	0.02	12	0.15	0.0098
		1200	0.80	
		∞	0.05	
Kidney excretion	0.20			0.0030
Liver	0.08	12	0.40	0.039
		1200	0.55	
		∞	0.05	
Spleen	0.004	12	0.33	0.0019
		1200	0.67	
Pancreas	0.03	12	0.85	0.014
		1200	0.15	
Small intestine wall	0.03	6	0.50	0.014
		12	0.50	
Ovaries	0.0002	1200	0.70	0.000098
		∞	0.30	
Testes	0.00092	1200	0.70	0.00045
		∞	0.30	
Muscle	0.24	12	0.15	0.12
		1200	0.45	
		∞	0.40	
Other organs and tissues	0.359	12	0.15	0.18
		1200	0.45	
		∞	0.40	
Urinary bladder contents	0.20			
Adult, 15 years, 10 years				0.016
5 years				0.016
1 year				0.016

For L-[methyl-^{11}C]-methionine, the compound-specific data should be used.

C.2.4. Absorbed doses for ^{11}C-labelled amino acids

^{11}C 20.4 min

Organ	Absorbed dose per unit activity administered (mGy/MBq)				
	Adult	15 years	10 years	5 years	1 year
Adrenals	4.5E-03	5.4E-03	8.4E-03	1.3E-02	2.4E-02
Bladder	1.3E-02	1.6E-02	2.4E-02	3.8E-02	7.1E-02
Bone surfaces	3.1E-03	3.7E-03	5.7E-03	8.8E-03	1.9E-02
Brain	2.3E-03	2.4E-03	2.9E-03	3.7E-03	5.9E-03
Breasts	2.3E-03	2.6E-03	4.0E-03	6.2E-03	1.2E-02
Gallbladder	4.1E-03	4.7E-03	7.3E-03	1.1E-02	2.0E-02
Gastrointestinal tract					
Stomach	3.5E-03	3.9E-03	5.9E-03	9.0E-03	1.7E-02
Small intestine	7.3E-03	9.0E-03	1.5E-02	2.4E-02	4.8E-02
Colon	3.4E-03	3.8E-03	5.9E-03	9.1E-03	1.7E-02
(Upper large intestine	3.6E-03	4.0E-03	6.2E-03	9.7E-03	1.8E-02)
(Lower large intestine	3.2E-03	3.5E-03	5.5E-03	8.3E-03	1.5E-02)
Heart	6.0E-03	7.4E-03	1.1E-02	1.8E-02	3.3E-02
Kidneys	1.4E-02	1.7E-02	2.5E-02	3.8E-02	6.9E-02
Liver	9.0E-03	1.2E-02	1.8E-02	2.7E-02	5.2E-02
Lungs	6.3E-03	8.6E-03	1.3E-02	2.1E-02	4.1E-02
Muscles	2.3E-03	3.4E-03	6.5E-03	1.7E-02	2.9E-02
Oesophagus	2.8E-03	3.2E-03	4.8E-03	7.3E-03	1.4E-02
Ovaries	4.7E-03	4.7E-03	1.1E-02	1.9E-02	4.2E-02
Pancreas	4.1E-02	5.8E-02	1.2E-01	1.5E-01	3.4E-01
Red marrow	3.6E-03	4.1E-03	6.3E-03	9.6E-03	1.8E-02
Skin	2.1E-03	2.3E-03	3.6E-03	5.5E-03	1.1E-02
Spleen	6.3E-03	8.6E-03	1.3E-02	2.1E-02	3.9E-02
Testes	4.3E-03	9.2E-03	6.4E-02	7.4E-02	1.0E-01
Thymus	2.8E-03	3.2E-03	4.8E-03	7.3E-03	1.4E-02
Thyroid	5.2E-03	7.9E-03	1.2E-02	2.6E-02	5.0E-02
Uterus	3.6E-03	4.1E-03	6.5E-03	9.9E-03	1.9E-02
Remaining organs	2.6E-03	3.8E-03	6.8E-03	1.4E-02	2.2E-02
Effective dose (mSv/MBq)	5.6E-03	7.5E-03	1.8E-02	2.5E-02	4.5E-02

C.3. ^{11}C-labelled brain receptor substances (generic model)

^{11}C

C.3.1. Biokinetic model

(C 13) A large number of radiopharmaceuticals labelled with ^{11}C are being developed for PET studies of different types of receptor in the human brain. For most of these agents, the available biokinetic data are insufficient to construct realistic compound-specific biokinetic models for calculating the internal radiation dose delivered to persons undergoing investigation. A generic model for brain receptor substances that predicts the internal dose with sufficient accuracy for general radiation protection purposes has, therefore, been developed (Nosslin et al., 2003).

(C 14) Biokinetic data for 13 ^{11}C radiopharmaceuticals used clinically for imaging different brain receptors indicate that, despite differences in chemical structure, their uptake and retention in the human brain and other tissues is broadly similar. The adopted model assumes instantaneous deposition of 5% of the injected activity in the brain, with the remaining activity being distributed rapidly and uniformly throughout all other tissues. Elimination from all tissues is assumed to occur with a half-time of 2 h. It is further assumed that 75% of the injected ^{11}C is excreted in urine, and 25% via the gallbladder, with a half-time of 2 h.

Table C.1. Brain receptor substances – comparison of ^{11}C retention in brain up to approximately 90 min.

Substance	Brain			Other tissues	Reference
	Uptake (%)	T_{max} (h)	T_b (h)		
Acetylcholine esterase receptor agents					
N-Methylpiperidyl-acetate N-Methylpiperidyl-propionate	5	0.2	0.1–∞	No human information but some animal data	Mulholland et al., 1995; Iyo et al., 1997; Tanaka et al., 2001
Benzodiazepine receptor agents					
Flumazenil	7	0.1	~0.5	No human data for [^{11}C]flumazenil, dosimetry based on data for [^{123}I]flumazenil	Pappata et al., 1988; Persson et al., 1989; Verhoeff et al., 1993; Westera et al., 1996
Dopamine receptor agents					
Raclopride	1.5	0.4	~3	No human data, data from positron emission tomography imaging in monkeys	Farde et al., 1986; Herscovitch et al., 1997
FLB-457	5	0.3	0.5–12	No human data	Votaw et al., 1995; Farde et al., 1997; Olsson et al., 1999
Epidepride	n.a.	n.a.		Human data for [^{123}I]epidepride	
Spiperone	1	0.5	~0.5	Human data for [^{76}Br]spiperone, mouse data for [^{11}C]methylspiperone	Burns et al., 1984; ICRP, 1987
Dopamine transporter agents					
Methylphenidate	9	0.1–0.2	1.25+	No human data	Volkow et al., 1995
Opiate receptor agents					
Carfentanil	3	0.1	1–2	Human data for plasma clearance of fentanyl	McClain and Hug, 1980; Frost et al., 1990; Kim et al., 1997
Serotonin receptor agents					
OMeWAY-100634	9	0.1	~1	Human plasma clearance data	Osman et al., 1996; Pike et al., 1995; Wilson et al., 1998
COWAY	3-4	0.1	0.05–3	Human plasma clearance data	Houle et al., 2000a
McN-5652	3	0.2	3+	No human data	Szabo et al., 1999
DASB	8		0.8–1.8	No human data	Houle et al., 2000b

n.a., not available.

C.3.2. References and further reading for ^{11}C-labelled brain receptor substances

Burns, H.D., Dannals, R.F., Langström, B., Ravert, H.T., Zemyan, S.E., Duelfer, T., Wong, D.F., Frost, J.J., Kuhar, M.J., Wagner, H.N., 1984. 3-N-[^{11}C]methylspiperone, a ligand binding to dopamine receptors: radiochemical synthesis and biodistribution studies in mice. J. Nucl. Med. 25, 1222–1227.

Farde, L., Hall, H., Ehrin, E., Sedvall, G., 1986. Quantitative analysis of D2 dopamine receptor binding in the living human brain. Science 231, 258–261.

Farde, L., Suhara, T., Nyberg, S., Karlsson, P., Nakashima, Y., Hietala, J., Halldin, C., 1997. A PET study of [^{11}C]FLB 457 binding to extrastriatal D_2-dopamine receptors in healthy subjects and antipsychotic drug-treated patients. Psychopharmacology 133, 394–404.

Frost, J.J., Mayberg, H.S., Sadzot, B., Dannals, R.F., Lever, J.R., Ravert, H.T., Wilson, A.A., Wagner Jr., H.N., Links, J.M., 1990. Comparison of [^{11}C]diprenorphine and [^{11}C]carfentanil binding to opiate receptors in humans by positron emission tomography. J. Cereb. Blood Flow Metab. 10, 484–492.

Herscovitch, P., Schmall, B., Doudet, D., Carson, R., Eckelman, W., 1997. Biodistribution and radiation dose estimates for [^{11}-C]raclopride (abstract). J. Nucl. Med. 5 (Suppl.), 224.

Houle, S., DaSilva, J.N., Wilson, A.A., 2000a. Imaging the 5-HT_{1A} receptors with PET: WAY-100635 and analogues. Nucl. Med. Biol. 27, 463–466.

Houle, S., Ginovart, N., Hussey, D., Meyer, J.H., Wilson, A.A., 2000b. Imaging the serotonin transporter system with positron emission tomography: initial human studies with [^{11}C]DAPP and [^{11}C]DASB. Eur. J. Nucl. Med. 27, 1719–1722.

ICRP, 1987. Radiation dose to patients from radiopharmaceuticals. ICRP Publication 53. Ann. ICRP 18 (1–4).

Iyo, M., Namba, H., Fukushi, K., Shinotoh, H., Nagatsuka, S., Suhara, T., Sudo, Y., Suzuki, K., Irie, T., 1997. Measurement of acetylcholinesterase by positron emission tomography in the brains of healthy controls and patients with Alzheimer's disease. Lancet 349, 1805–1809.

Kim, S., Wagner Jr., H.N., Villemagne, V.L., Kao, P-F., Dannals, R.F., Ravert, H.T., Joh, T., Dixon, R.B., Civelik, A.C., 1997. Longer occupancy of opioid receptors by nalmefene compared to naloxone as measured in vivo by a dual detector system. J. Nucl. Med. 38, 1726–1731.

McClain, D.A., Hug Jr., C.C., 1980. Intravenous fentanyl kinetics. Clin. Pharmacol. Ther. 28, 106–114.

Mulholland, G.K., Kilbourn, M.R., Sherman, P., Carey, J.E., Frey, K.A., Koeppe, R.A., Kuhl, D.E., 1995. Synthesis, in vivo biodistribution and dosimetry of [^{11}C]N-methylpiperidyl benzilate ([^{11}C]NMPB), a muscarinic acetylcholine receptor antagonist. Nucl. Med. Biol. 22, 13–17.

Nosslin, B., Johansson, L., Leide-Svegborn, S., Liniecki, J., Mattsson, S., Taylor, D., 2003. A generic model for 11C-labelled radiopharmaceuticals for imaging receptors in the human brain, Presented at Workshop of Internal Dosimetry of Radionuclides in Oxford, 9–12 September 2002. Rad. Prot. Dosim. 105, 587–591.

Olsson, H., Halldin, C., Swahn, G., Farde, L., 1999. Quantification of [^{11}C]FLB 457 binding to extrastriatal dopamine receptors in the human brain. J. Cereb. Blood Flow Metab. 19, 1164–1173.

Osman, S., Lundkvist, C., Pike, V.W., Halldin, C., McCarron, J.A., Swahn, C-G., Ginovart, N., Luthra, S.K., Bench, C.J., Grasby, P.M., Wikström, H., Barf, T., Cliffe, I.A., Fletcher, A., Farde, L., 1996. Characterization of the radioactive metabolites of the 5-HT_{1A} receptor radioligand, [O-methy-^{11}C]-WAY-100635, in monkey and human plasma by HPLC: comparison of the behaviour of an identified radioactive metabolite with parent radioligand in monkey using PET. Nucl. Med. Biol. 23, 627–634.

Pappata, S., Samson, Y., Chavoix, C., Prenant, C., Mazière, M., Baron, J.C., 1988. Regional specific binding of [^{11}C]RO 15 1788 to central type benzodiazepine receptors in human brain: quantitative evaluation by PET. J. Cereb. Blood Flow Metab. 8, 304–313.

Persson, A., Pauli, S., Swahn, C.G., Halldin, C., Sedvall, G., 1989. Cerebral uptake of ^{11}C-Ro 15 1788 and its acid metabolite ^{11}C-Ro 15 3890: PET study in human volunteers. Human Psychopharmacol. 4, 215–220.

Pike, V.W., McCarron, J.A., Hume, S.P., Ashworth, S., Opacka-Juffry, J., Osman, S., Lammertsma, A.A., Poole, K.G., Fletcher, A., White, A.C., Cliffe, I.A., 1995. Preclinical development of a radioligand for studies of central 5-HT1A receptors in vivo – [^{11}C]WAY-100635. Med. Chem. Res. 5, 208–227.

Szabo, Z., Scheffel, U., Mathews, W.B., Ravert, H.T., Szabo, K., Kraut, M., Palmon, S., Ricaurte, G.A., Dannals, R.F., 1999. Kinetic analysis of [^{11}C]McN5652: a serotonin transporter radioligand. J. Cereb. Blood Flow Metab. 19, 967–981.

Tanaka, N., Fukushi, K., Shinotoh, H., Nagatsuka, S., Namba, H., Iyo, M., Aotsuka, A., Ota, T., Tanada, S., Irie, T., 2001. Positron emission tomographic measurement of brain acetylcholinesterase activity using N-[^{11}C]methylpiperidin-4-yl acetate without arterial blood sampling: methodology of shape analysis and its diagnostic power for Alzheimer's disease. J. Cereb. Blood Flow Metab. 21, 295–306.

Verhoeff, N.P., Buseman Sokole, E.B., Hengst, D., Stubbs, J.B., van Royen, E.A., 1993. Dosimetry of iodine-123 iomazenil in humans. Eur. J. Nucl. Med. 20, 580–584.

Volkow, N.D., Ding, Y.-S., Fowler, J.S., Wang, G.-J., Logan, J., Gatley, S.J., Schlyer, D.J., Pappas, N., 1995. A new PET ligand for the dopamine transporter: studies in human brain. J. Nucl. Med. 36, 2162–2168.

Votaw, J.R., Ansari, M.S., Scott Mason, N., Schmidt, D., de Paulis, T., Holburn, G., Clanton, J.A., Votlaw, D.B., Manning, R.G., Kessler, R.M., 1995. Dosimetry of iodine-123-epidepride: a dopamine D2 receptor ligand. J. Nucl. Med. 36, 1316–1321.

Westera, G., Buck, A., Burger, C., Leenders, K.L., von Schultness, G.K., Schubiger, A.P., 1996. Carbon-11 and iodine-123 labelled iomazenil: a direct PET-SPECT comparison. Eur. J. Nucl. Med. 23, 5–12.

Wilson, A.A., Inaba, T., Fischer, N., Dixon, L.M., Nobrega, J., DaSilva, J.N., Houle, S., 1998. Derivatives of WAY 100635 as potential imaging agents for 5-HT1A receptors: syntheses, radiosyntheses, and in vitro and in vivo evaluation. Nucl. Med. Biol. 25, 769–776.

C.3.3. Biokinetic data for ^{11}C-labelled brain receptor substances

Organ (S)	F_s	T (h)	a	$\widetilde{A}_s/A_0$(h)
Brain	0.05	2.0	1.0	0.021
Other organs and tissues	0.95	2.0	1.0	0.40
Gallbladder contents	0.0875			0.0062
Gastrointestinal tract contents				
Small intestine	0.25			0.010
Upper large intestine	0.25			0.0012
Urinary bladder contents	0.75			
Adult, 15 years, 10 years				0.045
5 years				0.044
1 year				0.042

C.3.4. Absorbed doses for ^{11}C-labelled brain receptor substances

^{11}C 20.4 min

Organ	Absorbed dose per unit activity administered (mGy/MBq)				
	Adult	15 years	10 years	5 years	1 year
Adrenals	2.8E-03	3.6E-03	5.7E-03	9.5E-03	1.8E-02
Bladder	3.2E-02	4.1E-02	6.3E-02	9.7E-02	1.7E-01
Bone surfaces	2.8E-03	3.5E-03	5.5E-03	8.9E-03	1.7E-02
Brain	5.2E-03	5.3E-03	5.6E-03	6.5E-03	9.2E-03
Breasts	2.1E-03	2.8E-03	4.3E-03	7.2E-03	1.5E-02
Gallbladder	1.7E-02	1.9E-02	2.5E-02	4.6E-02	1.6E-01
Gastrointestinal tract					
Stomach	2.8E-03	3.5E-03	5.6E-03	9.2E-03	1.8E-02
Small intestine	4.4E-03	5.6E-03	9.5E-03	1.5E-02	2.9E-02
Colon	3.3E-03	4.1E-03	6.6E-03	1.0E-02	1.9E-02
(Upper large intestine	3.2E-03	4.0E-03	6.4E-03	1.0E-02	1.9E-02)
(Lower large intestine	3.5E-03	4.2E-03	6.9E-03	1.1E-02	2.0E-02)
Heart	2.7E-03	3.5E-03	5.7E-03	9.1E-03	1.8E-02
Kidneys	2.8E-03	3.5E-03	5.6E-03	9.3E-03	1.8E-02
Liver	2.8E-03	3.6E-03	5.6E-03	9.4E-03	1.8E-02
Lungs	2.5E-03	3.2E-03	5.1E-03	8.3E-03	1.6E-02
Muscles	2.6E-03	3.3E-03	5.3E-03	8.7E-03	1.7E-02
Oesophagus	2.5E-03	3.3E-03	5.2E-03	8.5E-03	1.7E-02
Ovaries	3.6E-03	4.5E-03	7.1E-03	1.1E-02	2.1E-02
Pancreas	3.0E-03	3.8E-03	6.2E-03	1.0E-02	1.9E-02
Red marrow	2.7E-03	3.5E-03	5.4E-03	8.4E-03	1.6E-02
Skin	2.1E-03	2.6E-03	4.3E-03	7.2E-03	1.4E-02
Spleen	2.7E-03	3.4E-03	5.5E-03	9.2E-03	1.8E-02
Testes	2.8E-03	3.7E-03	6.1E-03	9.7E-03	1.9E-02
Thymus	2.5E-03	3.3E-03	5.2E-03	8.5E-03	1.7E-02
Thyroid	2.6E-03	3.3E-03	5.4E-03	8.9E-03	1.8E-02
Uterus	4.3E-03	5.4E-03	8.6E-03	1.4E-02	2.5E-02
Remaining organs	2.8E-03	3.6E-03	5.6E-03	8.5E-03	1.5E-02
Effective dose (mSv/MBq)	4.3E-03	5.5E-03	8.6E-03	1.4E-02	2.6E-02

C.4. L-[Methyl-^{11}C]-methionine

^{11}C

C.4.1. Biokinetic model

(C 15) The amino acid L-[methyl-^{11}C]-methionine can be applied in tumour diagnosis and to the study of protein synthesis using PET. Deloar et al. (1998b) reported quantitative PET studies on the distribution of L-[methyl-^{11}C]-methionine in five healthy, male volunteers, aged 22–40 years. The data suggested that approximately 90% of the activity was lost from all tissues during the first 90 min after injection, with biological half-times of approximately 20–30 min. Thereafter, the activity appeared to be lost more slowly, with a half-time that could be considered to be long in relation to the physical half-life of ^{11}C.

(C 16) The biokinetic model presented below was developed on the basis of the human data of Deloar et al. (1998b). In the study of Deloar et al., the uptake of L-[methyl-^{11}C]-methionine into the brains of the five volunteers was estimated to be $2.8 \pm 0.7\%$ of the injected activity; some seven times higher than the value of 0.4% previously estimated by Comar et al. (1976).

C.4.2. References for L-[methyl-^{11}C]-methionine

Comar, D., Catron, J.C., Maziere, M., Marazanop, C., 1976. Labelling and metabolism of methionine-methyl-^{11}C. Eur. J. Nucl. Med. 1, 11–14.

Deloar, H.M., Fujiwara, T., Nakamura, T., Itoh, M., Imai, D., Miyake, M., Watanuki, S., 1998b. Estimation of internal absorbed dose of L-[methyl-^{11}C]-methionine using whole body positron emission tomography. Eur. J Nucl. Med. 25, 629–633.

C.4.3. Biokinetic data for L-[methyl-^{11}C]-methionine

Organ (S)	F_s	T (h)	a	$\widetilde{A}_s/A_0$(h)
Brain	0.030	0.4	0.90	0.0086
		12	0.10	
Lungs	0.050	0.4	0.90	0.014
		12	0.10	
Kidneys	0.022	0.4	0.90	0.0063
		12	0.10	
Kidney excretion				0.026
Liver	0.22	0.4	0.90	0.063
		12	0.10	
Spleen	0.010	0.4	0.90	0.0029
		12	0.10	
Pancreas	0.016	0.4	0.90	0.0046
		12	0.10	
Other organs and tissues	0.652	0.4	0.90	0.19
		12	0.10	
Gallbladder contents	0.077			0.0033
Gastrointestinal tract contents				
Small intestine	0.22			0.0055
Upper large intestine	0.22			0.00064
Lower large intestine	0.22			0.000024
Urinary bladder contents	0.78			
Adult, 15 years, 10 years				0.13
5 years				0.13
1 year				0.13

This biokinetic model is not applicable for ^{14}C.

C.4.4. Absorbed doses for L-[methyl-^{11}C]-methionine

^{11}C 20.4 min

Organ	Absorbed dose per unit activity administered (mGy/MBq)				
	Adult	15 years	10 years	5 years	1 year
Adrenals	2.9E-03	3.7E-03	5.7E-03	9.0E-03	1.6E-02
Bladder	1.1E-01	1.4E-01	2.1E-01	3.3E-01	6.0E-01
Bone surfaces	1.8E-03	2.2E-03	3.5E-03	5.5E-03	1.1E-02
Brain	2.2E-03	2.2E-03	2.4E-03	2.8E-03	4.0E-03
Breasts	1.3E-03	1.7E-03	2.7E-03	4.5E-03	8.9E-03
Gallbladder	1.1E-02	1.2E-02	1.6E-02	2.9E-02	9.6E-02
Gastrointestinal tract					
Stomach	2.2E-03	2.6E-03	4.3E-03	6.9E-03	1.3E-02
Small intestine	3.4E-03	4.5E-03	7.4E-03	1.2E-02	2.2E-02
Colon	3.0E-03	3.8E-03	5.9E-03	9.2E-03	1.6E-02
(Upper large intestine	2.7E-03	3.4E-03	5.5E-03	8.8E-03	1.6E-02)
(Lower large intestine	3.4E-03	4.3E-03	6.4E-03	9.7E-03	1.6E-02)
Heart	1.9E-03	2.5E-03	4.0E-03	6.3E-03	1.2E-02
Kidneys	3.0E-02	3.6E-02	5.1E-02	7.5E-02	1.4E-01
Liver	1.1E-02	1.5E-02	2.3E-02	3.4E-02	6.5E-02
Lungs	4.5E-03	6.7E-03	9.5E-03	1.5E-02	2.9E-02
Muscles	2.0E-03	2.5E-03	4.0E-03	6.4E-03	1.2E-02
Oesophagus	1.5E-03	1.9E-03	3.0E-03	4.9E-03	9.5E-03
Ovaries	3.7E-03	4.8E-03	7.1E-03	1.1E-02	1.9E-02
Pancreas	1.4E-02	2.0E-02	4.1E-02	5.3E-02	1.2E-01
Red marrow	2.0E-03	2.6E-03	3.8E-03	5.6E-03	1.0E-02
Skin	1.3E-03	1.7E-03	2.7E-03	4.5E-03	8.8E-03
Spleen	5.8E-03	8.2E-03	1.3E-02	2.0E-02	3.6E-02
Testes	2.7E-03	3.8E-03	6.6E-03	1.0E-02	1.9E-02
Thymus	1.5E-03	1.9E-03	3.0E-03	4.9E-03	9.5E-03
Thyroid	1.3E-03	1.7E-03	2.8E-03	4.7E-03	9.3E-03
Uterus	6.5E-03	7.7E-03	1.3E-02	1.9E-02	3.3E-02
Remaining organs	2.4E-03	3.2E-03	5.1E-03	8.2E-03	1.4E-02
Effective dose (mSv/MBq)	8.4E-03	1.1E-02	1.7E-02	2.6E-02	4.7E-02

Bladder wall contributes 65% of the effective dose.

C.5. ^{11}C-labelled substances (realistic maximum)

^{11}C

C.5.1. Biokinetic model

(C 17) It is assumed that 50% of the decays occur while the substance passes the bladder, and the remaining 50% of the disintegrations occur when it is distributed homogeneously within the whole body.

C.5.2. Biokinetic data for ^{11}C-labelled substances (realistic maximum)

Organ (S)	F_s	T (h)	a	$\widetilde{A}_s/A_0$(h)
Other organs and tissues	0.50			0.25
Urinary bladder contents	0.50			
Adult, 15 years, 10 years				0.25
5 years				0.25
1 year				0.25

C.5.3. Absorbed doses for ^{11}C-labelled substances (realistic maximum)

^{11}C 20.4 min

Organ	Absorbed dose per unit activity administered (mGy/MBq)				
	Adult	15 years	10 years	5 years	1 year
Adrenals	1.7E-03	2.2E-03	3.5E-03	5.7E-03	1.1E-02
Bladder	1.7E-01	2.1E-01	3.2E-01	5.0E-01	9.5E-01
Bone surfaces	1.9E-03	2.4E-03	3.7E-03	5.8E-03	1.1E-02
Brain	1.3E-03	1.7E-03	2.8E-03	4.6E-03	8.8E-03
Breasts	1.3E-03	1.7E-03	2.6E-03	4.3E-03	8.4E-03
Gallbladder	2.0E-03	2.4E-03	4.0E-03	6.2E-03	1.2E-02
Gastrointestinal tract					
Stomach	1.8E-03	2.2E-03	3.5E-03	5.7E-03	1.1E-02
Small intestine	3.0E-03	4.0E-03	6.2E-03	9.7E-03	1.8E-02
Colon	3.7E-03	4.7E-03	7.2E-03	1.1E-02	1.8E-02
(Upper large intestine	2.7E-03	3.4E-03	5.4E-03	8.7E-03	1.5E-02)
(Lower large intestine	5.1E-03	6.4E-03	9.6E-03	1.4E-02	2.3E-02)
Heart	1.6E-03	2.1E-03	3.3E-03	5.3E-03	1.0E-02
Kidneys	1.8E-03	2.2E-03	3.6E-03	5.9E-03	1.1E-02
Liver	1.7E-03	2.1E-03	3.5E-03	5.8E-03	1.1E-02
Lungs	1.5E-03	1.9E-03	3.0E-03	4.8E-03	9.4E-03
Muscles	2.3E-03	2.8E-03	4.5E-03	7.1E-03	1.3E-02
Oesophagus	1.5E-03	1.9E-03	3.1E-03	4.9E-03	9.5E-03
Ovaries	4.9E-03	6.3E-03	9.1E-03	1.4E-02	2.4E-02
Pancreas	1.8E-03	2.3E-03	3.7E-03	6.1E-03	1.2E-02
Red marrow	2.1E-03	2.7E-03	4.0E-03	5.9E-03	1.0E-02
Skin	1.5E-03	1.9E-03	3.0E-03	5.0E-03	9.5E-03
Spleen	1.7E-03	2.2E-03	3.3E-03	5.5E-03	1.1E-02
Testes	3.7E-03	5.3E-03	9.2E-03	1.4E-02	2.6E-02
Thymus	1.5E-03	1.9E-03	3.1E-03	4.9E-03	9.5E-03
Thyroid	1.5E-03	1.9E-03	3.1E-03	5.1E-03	9.8E-03
Uterus	9.2E-03	1.1E-02	1.8E-02	2.7E-02	4.6E-02
Remaining organs	2.3E-03	2.8E-03	4.3E-03	6.4E-03	1.2E-02
Effective dose (mSv/MBq)	1.1E-02	1.4E-02	2.1E-02	3.3E-02	6.1E-02

Bladder wall contributes 79% of the effective dose.

C.6. ^{15}O-water

^{15}O

C.6.1. Biokinetic model

(C 18) Water labelled with ^{15}O is widely used to evaluate regional cerebral blood flow using PET, and has been proposed for blood flow measurement in other organs and tissues. Early biokinetic models based on equilibrium tracer distribution in body water are inaccurate for use with ^{15}O-water. On account of the short half-life of ^{15}O (2.04 min), uniform radionuclide concentration in body water is not attained; consequently, such models underestimate dose values for this substance.

(C 19) A more satisfactory method of kinetic modelling is based on organ blood flow rates. Using this model, the concentration of ^{15}O-water in a given organ is derived by convolution of the arterial blood concentration (arterial input function) and the transit time function (impulse response) of the organ. The latter is given by $\exp[-(F/V_d + \lambda)t]$, where F (ml min^{-1}g^{-1}) is the organ blood flow, V_d (ml g tissue^{-1}/ml $\times$ ml blood^{-1}) is its relative water distribution space, and λ (min^{-1}) is the radioactive decay constant of ^{15}O. Thus, following intravenous administration of ^{15}O-water and measurement of the arterial blood concentration, a retention equation can be derived for organs for which values of F and V_d are known.

(C 20) In practice, a measured amount of ^{15}O-water activity is injected via a forearm vein, and the arterial blood concentration is monitored continuously from the other forearm. Residence time (min) in a given organ is calculated as the product of the areas under the curves of the arterial input function (min ml^{-1} normalised per administered MBq) and the organ transit time function (min), multiplied by the total blood flow to the organ (ml min^{-1}). The latter is given by $F \times M$, where M is the mass (g) of the organ. The table lists organ residence times that lead to organ doses equal to the mean values that have been estimated using the blood flow model at four different centres (Berridge et al., 1991; Herscovitch et al., 1993; Brihaye et al., 1995; Eichling et al., 1997). Direct measurements of the retention in some organs by PET (Smith et al., 1994) have shown good agreement with the model for brain, heart, liver, and spleen.

C.6.2. References for ^{15}O-water

Berridge, M.S., Adler, L.P., Rao, P.S., 1991. Radiation absorbed dose for O-15-butanol and O-15 water estimated by positron emission tomography. J. Nucl. Med. 32, 1043.

Brihaye, C., Depresseux, J.C., Comar, D., 1995. Radiation dosimetry for bolus administration of oxygen-15 water. J. Nucl. Med. 36, 651–656.

Eichling, J.O., Bergman, S.R., Schwarz, S.W., Siegel, B.A. 1997. Equivalent dose estimates in adults for intravenously administered O-15 water. Unpublished; personal communication through S. Schwarz..

Herscovitch, P., Carson, R.E., Stabin, M., et al., 1993. A new kinetic approach to estimate the radiation dosimetry of flow-based radiotracers. J. Nucl. Med. 34, 155P.

Smith, T., Tong, C., Lammertsma, A.A., et al., 1994. Dosimetry of intravenously administered oxygen-15 labelled water in man: a model based on experimental human data from 21 subjects. Eur. J. Nucl. Med. 21, 1126–1134.

C.6.3. Biokinetic data for ^{15}O-water

Organ (S)	$\widetilde{A}_s/A_0$(h)
Adrenals	0.000044
Brain	0.0036
Bone	0.0012
Gastrointestinal tract	
Stomach wall	0.00047
Small intestine wall	0.0018
Upper large intestine wall	0.00061
Lower large intestine wall	0.00047
Heart contents	0.0015
Heart wall	0.00067
Kidneys	0.0010
Liver	0.0053
Lungs	0.0031
Muscles	0.011
Ovaries*	0.000014
Pancreas	0.00025
Red marrow	0.0016
Spleen	0.00056
Testes*	0.000056
Thyroid	0.000064
Other organs and tissues	0.016

* For adults, the ratio between cumulated activity in the gonads and that in the total body is proportional to the ratio of gonad weight and total body weight. For children, the same assumption is made.

C.6.4. Absorbed doses for ^{15}O-water

^{15}O 2.04 min

Organ	Absorbed dose per unit activity administered (mGy/MBq)				
	Adult	15 years	10 years	5 years	1 year
Adrenals	1.4E-03	2.2E-03	3.1E-03	4.3E-03	6.6E-03
Bladder	2.6E-04	3.1E-04	5.0E-04	8.4E-04	1.5E-03
Bone surfaces	6.3E-04	8.0E-04	1.3E-03	2.3E-03	5.5E-03
Brain	1.3E-03	1.3E-03	1.4E-03	1.6E-03	2.2E-03
Breasts	2.8E-04	3.5E-04	6.0E-04	9.9E-04	2.0E-03
Gallbladder	4.5E-04	5.5E-04	8.6E-04	1.4E-03	2.7E-03
Gastrointestinal tract					
Stomach	1.7E-03	2.2E-03	3.1E-03	5.3E-03	1.2E-02
Small intestine	1.3E-03	1.7E-03	3.0E-03	5.0E-03	9.9E-03
Colon	1.6E-03	2.1E-03	3.7E-03	6.2E-03	1.2E-02
(Upper large intestine	1.6E-03	2.1E-03	3.7E-03	6.2E-03	1.2E-02)
(Lower large intestine	1.6E-03	2.1E-03	3.7E-03	6.2E-03	1.2E-02)
Heart	1.9E-03	2.4E-03	3.8E-03	6.0E-03	1.1E-02
Kidneys	1.7E-03	2.1E-03	3.0E-03	4.5E-03	8.1E-03
Liver	1.6E-03	2.1E-03	3.2E-03	4.8E-03	9.3E-03
Lungs	1.6E-03	2.4E-03	3.4E-03	5.2E-03	1.0E-02
Muscles	2.9E-04	3.7E-04	6.1E-04	1.0E-03	2.0E-03
Oesophagus	3.3E-04	4.2E-04	6.7E-04	1.1E-03	2.1E-03
Ovaries	8.5E-04	1.1E-03	1.8E-03	2.8E-03	5.8E-03
Pancreas	1.4E-03	2.0E-03	4.2E-03	5.4E-03	1.2E-02
Red marrow	8.9E-04	9.7E-04	1.6E-03	3.0E-03	6.1E-03
Skin	2.5E-04	3.1E-04	5.2E-04	8.8E-04	1.8E-03
Spleen	1.6E-03	2.3E-03	3.7E-03	5.8E-03	1.1E-02
Testes	7.4E-04	9.3E-04	1.5E-03	2.6E-03	5.1E-03
Thymus	3.3E-04	4.2E-04	6.7E-04	1.1E-03	2.1E-03
Thyroid	1.5E-03	2.5E-03	3.8E-03	8.5E-03	1.6E-02
Uterus	3.5E-04	4.4E-04	7.2E-04	1.2E-03	2.3E-03
Remaining organs	4.0E-04	5.6E-04	9.4E-04	1.7E-03	2.9E-03
Effective dose (mSv/MBq)	1.1E-03	1.4E-03	2.3E-03	3.8E-03	7.7E-03

C.7. ^{18}F-labelled amino acids (generic model)

^{18}F

C.7.1. Biokinetic model

(C 21) The generic biokinetic model for ^{18}F-labelled amino acids is the same as the generic biokinetic model for ^{11}C-labelled amino acids (see Section C.2.1).

C.7.2. Further reading for ^{18}F-labelled amino acids

Coenen, H.H., Kling, P., Stöcklin, G., 1989. Cerebral metabolism of l-[2-^{18}F]Fluorotyrosine, a new PET tracer of protein synthesis. J. Nucl. Med. 30, 1367–1372.

Cottrall, M.F., Taylor, D.M., McElwain, T.J., 1973. Investigations of ^{18}F-p-fluorophenylalanine for pancreas scanning. Br. J. Radiol. 46, 277–288.

ICRP, 1987. Radiation dose to patients from radiopharmaceuticals. ICRP Publication 53. Ann. ICRP 18 (1–4), 149–150.

ICRP, 2001b. Radiation dose to patients from radiopharmaceuticals. Addendum 4 to ICRP Publication, 53.

Inoue, T., Tomiyoshi, K., Higuichi, T., Ahmed, K., Sarwar, M., Aoyagi, K., Amano, S., Alyafei, S., Zhang, H., Endo, K., 1996. Biodistribution studies on l-3-[Fluorine-18]fluoro-α-methyl tyrosine: a potential tumor-detecting agent. J. Nucl. Med. 39, 663–667.

Schmidt, D., Langen, K-J., Herzog, H., Wirths, J., Holschbach, M., Kiwit, J.C.W., Ziemons, K., Coenen, H.H., Müller-Gärtner, H.W., 1997. Whole-body kinetics and dosimetry of l-3-[^{123}I]iodo-α-methyltyrosine. Eur. J. Nucl. Med. 24, 1162–1166.

Shoup, T.M., Olson, J., Hoffman, J.M., Votaw, J., Eshima, D., Eshima, L., Camp, M., Stabin, M., Votaw, D., Goodman, M., 1999. Synthesis and evaluation of [^{18}F]1-Amino-3-fluorocyclobutane-1-carboxylic acid to image brain tumours. J. Nucl. Med. 40, 331–338.

Stenhouse, M.J., Baxter, M.S., 1977. Bomb ^{14}C as a biological tracer. Nature (Lond.) 267, 828–832.

Stenström, K., Leide-Svegborn, S., Erlandsson, B., Hellborg, R., Mattsson, S., Nilsson, L-E., Nosslin, B., Skog, G., Wiebert, A., 1996. Application of accelerator mass spectrometry (AMS) for high-sensitivity measurements of $^{14}CO_2$ in long-term studies of fat metabolism. Appl. Radiat. Isot. 47, 417–422.

Taylor, D.M., 2000b. Generic models for radionuclide dosimetry: ^{11}C, ^{18}F or ^{75}Se-labelled amino acids. Appl. Radiat. Isot. 52, 911–922.

Taylor, D.M., Cottrall, M.F., 1973. Evaluation of amino acids labelled with ^{18}F for pancreas scanningRadiopharmaceuticals and Labelled Compounds, Vol. I. IAEA, Vienna, pp. 441–443.

Wester, H.J., Herz, M., Senkowitsch-Schmidtke, R., Schwaiger, M., Stöcklin, G., Hamacher, K., 1999a. Preclinical evaluation of 4-[^{18}F]fluoroprolines: diasteromeric effect on metabolism and uptake in mice. Nucl. Med. Biol. 26, 259–265.

Wester, H.J., Herz, M., Weber, W., Heiss, P., Senkowitsch-Schmidtke, R., Schwaiger, M., Stöcklin, G., 1999b. Synthesis and radiopharmacology of O-(2-[^{18}F]fluoroethyl)-L-tyrosine for tumor imaging. J. Nucl. Med. 40, 205–212.

C.7.3. Biokinetic data for ^{18}F-labelled amino acids

Organ (S)	F_s	T (h)	a	$\widetilde{A}_s/A_0$(h)
Blood	0.20	0.2	0.25	0.32
		6.0	0.75	
Brain	0.015	1200	0.70	0.040
		∞	0.30	
Thyroid	0.0007	1200	0.70	0.0019
		∞	0.30	
Lungs	0.02	12	0.10	0.052
		1200	0.85	
		∞	0.05	
Kidneys	0.02	12	0.15	0.052
		1200	0.80	
		∞	0.05	
Kidney excretion	0.20			0.0066
Liver	0.08	12	0.40	0.20
		1200	0.55	
		∞	0.05	
Spleen	0.004	12	0.33	0.010
		1200	0.67	
Pancreas	0.03	12	0.85	0.070
		1200	0.15	
Small intestine wall	0.03	6	0.50	0.065
		12	0.50	
Ovaries	0.0002	1200	0.70	0.00053
		∞	0.30	
Testes	0.00092	1200	0.70	0.0024
		∞	0.30	
Muscle	0.24	12	0.15	0.62
		1200	0.45	
		∞	0.40	
Other organs and tissues	0.359	12	0.15	0.93
		1200	0.45	
		∞	0.40	
Urinary bladder contents	0.20			
Adult, 15 years, 10 years				0.13
5 years				0.12
1 year				0.086

C.7.4. Absorbed doses for ^{18}F-labelled amino acids

^{18}F 1.83 h

Organ	Absorbed dose per unit activity administered (mGy/MBq)				
	Adult	15 years	10 years	5 years	1 year
Adrenals	1.9E-02	2.2E-02	3.4E-02	5.2E-02	9.5E-02
Bladder	7.4E-02	9.4E-02	1.4E-01	2.0E-01	2.8E-01
Bone surfaces	1.3E-02	1.5E-02	2.3E-02	3.5E-02	7.0E-02
Brain	9.6E-03	1.0E-02	1.2E-02	1.5E-02	2.4E-02
Breasts	9.5E-03	1.1E-02	1.6E-02	2.5E-02	4.9E-02
Gallbladder	1.9E-02	2.1E-02	3.3E-02	4.8E-02	8.8E-02
Gastrointestinal tract					
Stomach	1.5E-02	1.7E-02	2.6E-02	3.9E-02	7.3E-02
Small intestine	2.7E-02	3.3E-02	5.5E-02	8.7E-02	1.7E-01
Colon	1.5E-02	1.7E-02	2.7E-02	4.0E-02	7.2E-02
(Upper large intestine	1.6E-02	1.8E-02	2.8E-02	4.3E-02	7.8E-02)
(Lower large intestine	1.4E-02	1.6E-02	2.5E-02	3.7E-02	6.5E-02)
Heart	2.2E-02	2.7E-02	4.1E-02	6.2E-02	1.1E-01
Kidneys	4.9E-02	5.9E-02	8.5E-02	1.3E-01	2.3E-01
Liver	3.5E-02	4.6E-02	6.9E-02	1.0E-01	1.9E-01
Lungs	2.3E-02	3.1E-02	4.6E-02	7.2E-02	1.4E-01
Muscles	1.0E-02	1.5E-02	2.7E-02	6.5E-02	1.1E-01
Oesophagus	1.2E-02	1.4E-02	2.0E-02	3.1E-02	5.9E-02
Ovaries	2.0E-02	2.1E-02	4.5E-02	7.5E-02	1.6E-01
Pancreas	1.4E-01	2.0E-01	4.1E-01	5.2E-01	1.1E+00
Red marrow	1.4E-02	1.6E-02	2.4E-02	3.6E-02	6.7E-02
Skin	8.4E-03	9.4E-03	1.4E-02	2.2E-02	4.4E-02
Spleen	2.5E-02	3.3E-02	5.1E-02	8.0E-02	1.5E-01
Testes	1.6E-02	3.3E-02	2.1E-01	2.5E-01	3.4E-01
Thymus	1.2E-02	1.4E-02	2.0E-02	3.1E-02	5.9E-02
Thyroid	2.1E-02	3.3E-02	5.1E-02	1.1E-01	2.0E-01
Uterus	1.7E-02	2.0E-02	3.2E-02	4.8E-02	8.3E-02
Remaining organs	1.1E-02	1.6E-02	2.7E-02	5.2E-02	8.4E-02
Effective dose (mSv/MBq)	2.3E-02	3.1E-02	6.6E-02	9.3E-02	1.6E-01

C.8. ^{18}F-labelled brain receptor substances (generic model)

^{18}F

C.8.1. Biokinetic model

(C 22) A large number of radiopharmaceuticals labelled with ^{18}F and ^{123}I have been developed for PET and single photon emission computer tomographic (SPECT) studies of different types of receptor in the human brain. For many of these substances, the available biokinetic data are insufficient to construct realistic compound-specific biokinetic models for the calculation of absorbed dose to persons undergoing an investigation. Therefore, a generic model for radionuclide-labelled brain receptor substances that would predict the internal radiation dose with sufficient accuracy for general radiation protection purpose has been developed.

(C 23) A generic model for ^{11}C-labelled brain receptor substances has been published previously (Nosslin et al., 2003). A review of the literature has identified biokinetic and dosimetric data for five ^{18}F-labelled and 15 ^{123}I-labelled compounds considered to be potential substances for the clinical imaging of brain receptors, e.g. acetylcholinesterase receptors, benzodiazepine receptors, dopamine receptors, dopamine transporters, and serotonin receptors. These data indicate that despite fairly large differences in chemical structure, the patterns of uptake in the human brain, and other tissues for which information is available, appear to be sufficiently similar to justify a generic model for each radionuclide.

(C 24) For some compounds, the published data on the dosimetry of ^{18}F- and ^{123}I-labelled receptor radiopharmaceuticals were derived from PET and SPECT studies in humans, and for other compounds, the biokinetic models were derived, at least in part, from studies of biodistribution in experimental animals.

(C 25) The generic model adopted for ^{18}F-labelled substances assumes that fractions of 0.07, 0.08, 0.05, 0.02, 0.02, and 0.002 of the administered activity are distributed instantaneously to the brain, liver, lungs, kidneys, stomach wall, and thyroid, respectively, from where they are excreted with a biological half-time of 10 h. The remaining activity is assumed to be distributed uniformly throughout the rest of the body and eliminated with a biological half-time of 10 h. A biological half-time of 10 h means that approximately 98% of the ^{18}F will decay in the tissue of interest. It is assumed that of the activity entering the liver, 30% would be eliminated via the gallbladder and the remainder would pass directly into the small intestine. A total of 60% of the administered activity is assumed to be excreted in the urine and 40% via the gastrointestinal tract.

C.8.2. References and further reading for ^{18}F-labelled brain receptor substances

Booij, J., Sokole, E.B., Stabin, M.G., Janssen, A.G.M., de Bruin, K., van Royen, E.A., 1998. Human biodistribution and dosimetry of [^{123}I]FP-CIT: a potent radioligand for imaging of dopamine transporters. Eur. J. Nucl. Med. 25, 24–30.

Booij, J., Sokole, E.B., Stabin, M.G., Janssen, A.G.M., de Bruin, K., van Royen, E.A., 1998. Human biodistribution and dosimetry of [^{123}I]FP-CIT: a potent radioligand for imaging of dopamine transporters: erratum. Eur. J. Nucl. Med. 25, 458.

Boundy, K.L., Barnden, L.R., Rowe, C.C., Reid, M., Kassiou, M., Katsifis, A.G., Lambrecht, R.L., 1995. Human dosimetry and biodistribution of iodine-123-iododexetimide: a SPECT imaging agent for cholinergic muscarinic neuroreceptors. J. Nucl. Med. 36, 1332–1338.

Deterding, T.A., Votaw, J.R., Wang, C.K., Eshima, D., Eshima, L., Keil, R., Malveaux, E., Kilts, C.D., Goodman, M.M., Hoffman, J.M., 2001. Biodistribution and radiation dosimetry of the dopamine transporter ligand [^{18}F]FECNT. J. Nucl. Med. 42, 376–381.

Gründer, G., Siessmeier, T., Lange-Asschenfeldt, C., Vernaleken, I., Buchholz, H.-G., Stoeter, P., Drzezga, A., Lüddens, H., Rösch, F., Bartenstein, P., 2001. [^{18}F]Fluoroethylflumaazenil: a novel tracer for PET imaging of human benzodiazepine receptors. Eur. J. Nucl. Med. 28, 1463–1470.

Gründer, G., Siessmeier, T., Piel, M., Vernaleken, I., Buchholz, H.-G., Zhou, Y., Hiemke, C., Wong, D.P., Rösch, F., Bartenstein, P., 2003. Quantification of D_2-like dopamine receptors in the human brain with [^{18}F]-desmethoxyfallypride. J. Nucl. Med. 44, 109–116.

Kauppinen, T.A., Bergström, K.A., Heikman, P., Hiltunen, J., Ahonen, A.K., 2003. Biodistribution and radiation dosimetry of [^{123}I]ADAM in healthy human subjects: preliminary results. Eur. J. Nucl. Med. 30, 132–136.

Kuikka, J.T., Bergström, K.A., Ahonen, A., Länsimies, E., 1994. The dosimetry of iodine-123 labelled 2β-carbomethoxy-3β-(4-iodophenyl)tropane. Eur. J. Nucl. Med. 21, 53–56.

Mitterhauser, M., Wadsak, W., Wabnegger, L., Mien, L-K., Tögel, S., Langer, O., Sieghart, W., Viernstein, H., Kletter, K., Dudczak, R., 2004. Biological evaluation of 2′-[^{18}F]fluoroflumazenil ([^{18}F]FFMZ): a potential GABA receptor ligand for PET. Nucl. Med. Biol. 31, 291–295.

Mozley, P.D., Stubbs, J.T., Kim, H-J., McElgin, W., Chumpradit, S., Kung, M-P., Romaniallo, G., Kung, H.F., 1995. Dosimetry of a D2/D3 dopamine receptor antagonist that can be used with PET or SPECT. J. Nucl. Med. 36, 1322–1331.

Mozley, P.D., Stubbs, J.T., Kim, H-J., McElgin, W., Kung, M-P., Meegalla, S., Kung, H.F., 1996. Dosimetry of an iodine-123-labeled tropane to image dopamine transporters. J. Nucl. Med. 37, 151–159.

Nosslin, B., Johansson, L., Leide-Svegborn, S., Liniecki, J., Mattsson, S., Taylor, D.M., 2003. A generic model for [^{11}C]-labelled radiopharmaceuticals for imaging receptors in the human brain. Rad. Prot. Dosim. 105, 587–591.

Taylor, D.M., 2000a. Unpublished assessments.

van de Wiele, C., De Vos, F., De Sutter, J., Dumont, F., Slegers, G., Dierkx, R.A., Thierens, H., 1999. Biokinetics and dosimetry of (iodine-123)-iodomethyl-N,N-dimethyltamoxifen, an (anti)oestrogen receptor radioligand. Eur. J. Nucl. Med. 26, 1259–1264.

Verhoeff, N.P., Sokole, E.B., Stabin, M., Hengst, D., Kung, H.F., Van Royen, E.A., Janssen, A.G., 1993. Dosimetry of iodine-123 iodobenzamide in healthy volunteers. Eur. J. Nucl. Med. 20, 747–752.

Verhoeff, N.P., Busemann Sokole, E., Hengst, D., Stubbs, J.B., van Royen, E.A., 1993. Dosimetry of iodine-123 iomazenil in humans. Eur. J. Nucl. Med. 20, 580–584.

Versijpt, J., Dumont, F., Thierens, H., Jansen, H., De Vos, F., Slegers, G., Santens, P., Dierckx, R.A., Korf, J., 2000. Biodistribution and dosimetry of [^{123}I]iodo-PK 11195: a potential agent for SPET imaging of the peripheral benzodiazepine receptor. Eur. J. Nucl. Med. 27, 1326–1333.

Volkow, N.D., Ding, Y.S., Fowler, J.S., Wang, G.J., Logan, J., Gatley, S.J., Schlyer, D.J., Pappas, N., 1995. A new PET ligand for the dopamine transporter: studies in human brain. J. Nucl. Med. 36, 2162–2168.

Votaw, J.R., Ansari, M.S., Scott Mason, N., Schmidt, D., de Paulis, T., Holburn, G., Clanton, J.A., Votlaw, D.B., Manning, R.G., Kessler, R.M., 1995. Dosimetry of iodine-123-epidepride: a dopamine D2 receptor ligand. J. Nucl. Med. 36, 1316–1321.

Waterhouse, R.N., Stabin, M.G., Page, J.G., 2003. Preclinical acute toxicity studies and rodent-based dosimetry estimates of the novel sigma-1 receptor radiotracer [^{18}F]FPS. Nucl. Med. Biol. 30, 555–563.

C.8.3. Biokinetic data for ^{18}F-labelled brain receptor substances

Organ (S)	F_s	T (h)	a	$\widetilde{A}_s/A_0$(h)
Brain	0.07	10	1.0	0.16
Thyroid	0.002	10	1.0	0.0045
Lungs	0.05	10	1.0	0.11
Kidneys	0.02	10	1.0	0.045
Kidney excretion	0.90			0.011
Liver	0.08	10	1.0	0.18
Stomach wall	0.02	10	1.0	0.045
Other organs and tissues	0.758	10	1.0	1.7
Gallbladder contents	0.024			0.080
Gastrointestinal tract contents				
Stomach	0.02			0.0022
Small intestine	0.10			0.019
Upper large intestine	0.10			0.011
Lower large intestine	0.10			0.0020
Urinary bladder contents	0.90			
Adult, 15 years, 10 years				0.20
5 years				0.17
1 year				0.12

C.8.4. Absorbed doses for ^{18}F-labelled brain receptor substances

^{18}F 1.83 h

Organ	Absorbed dose per unit activity administered (mGy/MBq)				
	Adult	15 years	10 years	5 years	1 year
Adrenals	1.1E-02	1.3E-02	2.0E-02	3.0E-02	5.0E-02
Bladder	1.1E-01	1.3E-01	2.0E-01	2.7E-01	3.5E-01
Bone surfaces	6.9E-03	8.4E-03	1.2E-02	1.8E-02	3.3E-02
Brain	2.8E-02	2.9E-02	3.0E-02	3.4E-02	4.8E-02
Breasts	3.7E-03	4.6E-03	8.4E-03	1.3E-02	2.3E-02
Gallbladder	1.4E-01	1.6E-01	2.1E-01	3.8E-01	1.4E+00
Gastrointestinal tract					
Stomach	5.5E-02	7.2E-02	1.0E-01	1.7E-01	3.6E-01
Small intestine	4.7E-02	6.1E-02	1.1E-01	1.7E-01	3.3E-01
Colon	1.7E-02	2.1E-02	3.2E-02	5.1E-02	8.2E-02
(Upper large intestine	2.0E-02	2.4E-02	3.8E-02	6.2E-02	1.0E-01)
(Lower large intestine	1.4E-02	1.6E-02	2.4E-02	3.6E-02	5.7E-02)
Heart	7.4E-03	9.7E-03	1.4E-02	2.2E-02	3.7E-02
Kidneys	4.3E-02	5.2E-02	7.4E-02	1.1E-01	1.9E-01
Liver	3.0E-02	3.9E-02	5.8E-02	8.6E-02	1.6E-01
Lungs	2.5E-02	3.7E-02	5.2E-02	8.0E-02	1.6E-01
Muscles	1.7E-02	2.6E-02	5.2E-02	1.4E-01	2.4E-01
Oesophagus	6.5E-03	8.2E-03	1.2E-02	1.8E-02	3.1E-02
Ovaries	1.4E-02	1.8E-02	2.7E-02	4.1E-02	6.7E-02
Pancreas	1.2E-02	1.5E-02	2.4E-02	3.7E-02	6.2E-02
Red marrow	7.8E-03	9.6E-03	1.3E-02	1.8E-02	2.8E-02
Skin	4.4E-03	5.2E-03	7.6E-03	1.2E-02	2.1E-02
Spleen	8.5E-03	1.1E-02	1.6E-02	2.5E-02	4.2E-02
Testes	7.1E-03	9.5E-03	1.6E-02	2.3E-02	3.7E-02
Thymus	6.5E-03	8.2E-03	1.2E-02	1.8E-02	3.1E-02
Thyroid	4.2E-02	6.7E-02	1.0E-01	2.2E-01	4.3E-01
Uterus	1.7E-02	2.1E-02	3.4E-02	4.9E-02	7.7E-02
Remaining organs	1.8E-02	2.8E-02	5.1E-02	1.0E-01	1.7E-01
Effective dose (mSv/MBq)	2.8E-02	3.7E-02	5.4E-02	8.7E-02	1.8E-01

C.9. 2-[^{18}F]Fluoro-2-deoxy-D-glucose (FDG)
^{18}F

C.9.1. Biokinetic model

(C 26) ^{18}FDG is a glucose analogue used in the characterisation of glucose metabolism for diagnosis or follow-up of cancer diseases, and for investigation of myocardial and cerebral glucose metabolism. Following intravenous administration, most of the radiopharmaceutical is cleared rapidly from the circulation with a half-time of less than 1 min as it mixes within a large distribution space, although there are longer-term components with half-times of up to 1.5 h. Data from Hays et al. (2002) together with data obtained by Deloar et al. (1998a) are used in this biokinetic model for the dose assessments to patients administered with ^{18}F-FDG. These data confirm the assumption in *Publication 53* (ICRP, 1987) of an uptake of 0.04 to the heart wall, while the uptake to the brain seems to be higher (0.07–0.1) than was given in the *Publication 53* model (0.06).

(C 27) Additionally, there are indications of significant uptake in the liver and the lungs. For liver uptake, values of approximately 0.05 were derived by Deloar et al. (1998a) and Meija et al. (1991). The model of Hays and Segall (1999) predicts a larger uptake in the liver but it decreases rapidly to similar values. For uptake in the lungs, results range from 0.009 (Meija et al., 1991) to 0.029 (Deloar et al., 1998a). Here again, the model by Hays and Segall (2002) indicates a higher uptake followed by a rapid decrease. There are indications that there is a slight increase in activity in the heart and brain, and a steep decrease in activity in the lungs and liver (Meija et al., 1991; Hays and Segall, 1999). It is assumed that all activity is excreted in urine.

(C 28) Based on this information, the following biokinetic model is derived. There is an initial uptake of ^{18}F-FDG in heart (0.04), brain (0.08), liver (0.05), lungs (0.03), and all other tissues (0.8). The retention in the specified source organs is considered to be infinite (without consideration of a delayed uptake). A fraction of 0.3 of the activity in other organs and tissues is considered to be excreted in urine with biological half-times of 12 min (25%) and 1.5 h (75%), according to the kidney–bladder model.

C.9.2. References and further reading for ^{18}F-FDG

Deloar, H.M., Fujiwara, T., Shidahara, M., Nakamura, T., Watabe, H., Narita, Y., Itoh, M., Miyake, M., Watanuki, S., 1998a. Estimation of absorbed dose for 2-[F-18]fluoro-2-deoxy-D-glucose using whole-body positron emission tomography and magnetic resonance imaging. Eur. J. Nucl. Med. 25, 565–574.

Hays, M.T., Segall, G.M., 1999. A mathematical model for the distribution of fluorodeoxyglucose in humans. J. Nucl. Med. 40, 1358–1366.

Hays, M.T., Watson, E.E., Thomas, S.R., Stabin, M., 2002. Radiation absorbed dose estimates from ^{18}F-FDG. MIRD Dose Estimate Report No. 19. J. Nucl. Med. 43, 210–214.

ICRP, 1987. Radiation dose to patients from radiopharmaceuticals. ICRP Publication 53. Ann. ICRP 18 (1–4).
ICRP, 1998. Radiation dose to patients from radiopharmaceuticals. Addendum 2 to ICRP Publication 53. ICRP Publication 80. Ann. ICRP 28(3).
Meija, A.A., Nakamura, T., Masatoshi, I., Hatazawa, J., Mazaki, M., Watanuki, S., 1991. Estimation of absorbed doses in humans due to intraveneous administration of fluorine-18-fluorodeoxyglucose in PET studies. J. Nucl. Med. 32, 699–706.

C.9.3. Biokinetic data for ^{18}F-FDG

Organ (S)	F_s	T (h)	a	$\widetilde{A}_s/A_0$(h)
Brain	0.08	∞	1.0	0.21
Heart wall	0.04	∞	1.0	0.11
Lungs	0.03	∞	1.0	0.079
Liver	0.05	∞	1.0	0.13
Other organs and tissues	0.80	0.20	0.075	1.7
		1.5	0.225	
		∞	0.70	
Urinary bladder contents	0.24			
Adult, 15 years, 10 years				0.26
5 years				0.23
1 year				0.16

C.9.4. Absorbed doses for ^{18}F-FDG

^{18}F 1.83 h

Organ	Absorbed dose per unit activity administered (mGy/MBq)				
	Adult	15 years	10 years	5 years	1 year
Adrenals	1.2E-02	1.6E-02	2.4E-02	3.9E-02	7.1E-02
Bladder	1.3E-01	1.6E-01	2.5E-01	3.4E-01	4.7E-01
Bone surfaces	1.1E-02	1.4E-02	2.2E-02	3.4E-02	6.4E-02
Brain	3.8E-02	3.9E-02	4.1E-02	4.6E-02	6.3E-02
Breasts	8.8E-03	1.1E-02	1.8E-02	2.9E-02	5.6E-02
Gallbladder	1.3E-02	1.6E-02	2.4E-02	3.7E-02	7.0E-02
Gastrointestinal tract					
Stomach	1.1E-02	1.4E-02	2.2E-02	3.5E-02	6.7E-02
Small intestine	1.2E-02	1.6E-02	2.5E-02	4.0E-02	7.3E-02
Colon	1.3E-02	1.6E-02	2.5E-02	3.9E-02	7.0E-02
(Upper large intestine	1.2E-02	1.5E-02	2.4E-02	3.8E-02	7.0E-02)
(Lower large intestine	1.4E-02	1.7E-02	2.7E-02	4.1E-02	7.0E-02)
Heart	6.7E-02	8.7E-02	1.3E-01	2.1E-01	3.8E-01
Kidneys	1.7E-02	2.1E-02	2.9E-02	4.5E-02	7.8E-02
Liver	2.1E-02	2.8E-02	4.2E-02	6.3E-02	1.2E-01
Lungs	2.0E-02	2.9E-02	4.1E-02	6.2E-02	1.2E-01
Muscles	1.0E-02	1.3E-02	2.0E-02	3.3E-02	6.2E-02
Oesophagus	1.2E-02	1.5E-02	2.2E-02	3.5E-02	6.6E-02
Ovaries	1.4E-02	1.8E-02	2.7E-02	4.3E-02	7.6E-02
Pancreas	1.3E-02	1.6E-02	2.6E-02	4.0E-02	7.6E-02
Red marrow	1.1E-02	1.4E-02	2.1E-02	3.2E-02	5.9E-02
Skin	7.8E-03	9.6E-03	1.5E-02	2.6E-02	5.0E-02
Spleen	1.1E-02	1.4E-02	2.1E-02	3.5E-02	6.6E-02
Testes	1.1E-02	1.4E-02	2.4E-02	3.7E-02	6.6E-02
Thymus	1.2E-02	1.5E-02	2.2E-02	3.5E-02	6.6E-02
Thyroid	1.0E-02	1.3E-02	2.1E-02	3.4E-02	6.5E-02
Uterus	1.8E-02	2.2E-02	3.6E-02	5.4E-02	9.0E-02
Remaining organs	1.2E-02	1.5E-02	2.4E-02	3.8E-02	6.4E-02
Effective dose (mSv/MBq)	1.9E-02	2.4E-02	3.7E-02	5.6E-02	9.5E-02

C.10. [^{18}F]Fluoro-L-DOPA
^{18}F

C.10.1. Biokinetic model

(C 29) The amino acid analogue 6-fluoro-L-dopa (L-DOPA) is taken up rapidly into the human brain and transformed into the important catecholamine neurotransmitter dopamine (Luxen et al., 1992; Pauwels et al., 1994). After labelling with the positron-emitting radioisotope ^{18}F, the resulting ^{18}F-L-DOPA can be used for the scintigraphic investigation of normal and pathological dopamine metabolism in the human brain and tumours (Luxen et al., 1992; Meyer et al., 1995; Heiss et al., 1996), and for the quantitative assessment of dopaminergic function in Parkinson's disease and other conditions.

(C 30) Studies in normal human volunteers and dogs after administration of ^{18}F-L-DOPA have shown that the activity is more or less uniformly distributed throughout the body tissues, and is removed by a bi-exponential process with biological half-times of approximately 12 h (67–94%) and 1.7–3.9 h (6–33%) (Harvey et al., 1985; Boyes et al., 1986). Both these half-times appear to be age-dependent (Harvey et al., 1985). The ^{18}F is excreted through the kidneys; 50% with a half-time of 0.7 h and 50% with a half-time of approximately 12 h (Harvey et al., 1985).

(C 31) On the basis of the biokinetic data given by Harvey et al. (1985) and Dhawan et al. (1996), the biokinetic model for ^{18}F-L-DOPA illustrated in the biokinetic data table was developed. This model assumes that 100% of the ^{18}F is distributed homogeneously in the body and eliminated through the kidneys with biological half-times of 1 h (50%) and 12 h (50%). This model was, in spite of observations cited above, assumed to be independent of age.

(C 32) Human studies have shown that the uptake of ^{18}F-L-DOPA in the striatum and cerebellum can be increased approximately two-fold by administration of the amino decarboxylase inhibitor carbidopa (Melega et al., 1990; Hoffman et al., 1992; Brown et al., 1998).

C.10.2. References and further reading for ^{18}F-L-DOPA

Boyes, R.E., Cumming, P., Martin, W.R.W., McGeer, E.G., 1986. Determination of plasma [^{18}F]-6-fluorodopa during positron emission tomography; elimination and metabolism in carbidopa treated subjects. Life Sci. 39, 2243–2252.

Brown, W.D., Oakes, T.R., DeJesus, O.T., Taylor, M.D., Roberts, A.D., Nickles, R.J., Holden, J.E., 1998. Fluorine-18-fluoro-L-DOPA dosimetry with carbidopa pretreatment. J. Nucl. Med. 39, 1884–1891.

Dhawan, V., Belakhlef, A., Robeson, W., Ishikawa, T., Margouleff, C., Takikawa, S., Chaly, T., Kazumata, K., Margouleff, D., Eidelberg, D., 1996. Bladder wall radiation dose in humans from fluorine-18-FDOPA. J. Nucl Med. 37, 1850–1852.

Harvey, J., Firnau, G., Garnett, E.S., 1985. Estimation of the radiation dose in man due to 6-[^{18}F]fluoro-L-dopa. J. Nucl. Med. 26, 931–935.

Heiss, W.D., Wienhard, K., Wagner, R., Lanfermann, H., Thiel, A., Herhoiz, K., Pietrak, U., 1996. F-DOPA as an amino acid tracer to detect brain tumors. J Nucl. Med. 37, 1180–1182.

Hoffman, J.M., Melega, W.P., Hawk, T.C., Grafton, S.C., Luxen, A., Mahoney, D.K., Bardo, J.R., Huang, S.-C., Mazziotta, J.C., Phelps, M.E., 1992. The effects of carbidopa administration of 6-[^{18}F]fluoro-L-DOPA kinetics in positron emission tomography. J. Nucl. Med. 33, 1472–1477.

Lu, E., Meyer, E., Kuwabara, H., Ma, Y., Shiraishi, M., Evans, A.C., 1995. Reduction of radiation absorbed dose in F-18-DOPA PET studies by hydration-induced voiding. J. Nucl. Med. 36 (Suppl.), 98P.

Luxen, A., Guillaume, M., Melega, W.P., Pike, V.W., Solin, O., Wagner, R., 1992. Production of 6[^{18}F]fluoro-L-DOPA and its metabolism in vivo – a critical review. Nucl. Med. Biol. 19, 149–158.

Melega, W.P., Hoffman, J.M., Luxen, A., Nissenson, C.H.K., Phelps, M.E., Barrio, J.P., 1990. The effects of carbidopa on the metabolism of 6-[^{18}F]fluoro-L-dopa in rats, monkeys and humans. Life Sci. 47, 149–157.

Meyer, G.-J., Waters, S.L., Coenen, H.H., Luxen, A., Maziere, B., Långström, B., 1995. PET radiopharmaceuticals in Europe: current use and data relevant for the formulation of summaries of product characteristics (SPCs). Eur. J. Nucl. Med. 22, 1420–1432.

Pauwels, T., Dethy, S., Goldman, S., Monclus, M., Luxen, A., 1994. Effect of catechol-O-methyl transferase inhibition on peripheral and central metabolism of 6-[^{18}F]Fluoro-L-DOPA. Eur. J Pharmacol. 257, 53–58.

C.10.3. Biokinetic data for ^{18}F-L-DOPA

Organ (S)	F_s	T (h)	a	$\widetilde{A}_s/A_0$(h)
Total body	1.0	1.0	0.50	1.6
		12	0.50	
Kidney excretion	1.0			0.032
Urinary bladder contents	1.0			
Adult, 15 years, 10 years				0.60
5 years				0.53
1 year				0.37

C.10.4. Absorbed doses for ^{18}F-L-DOPA

^{18}F 1.83 h

Organ	Absorbed dose per unit activity administered (mGy/MBq)				
	Adult	15 years	10 years	5 years	1 year
Adrenals	9.9E-03	1.3E-02	1.9E-02	3.1E-02	5.5E-02
Bladder	3.0E-01	3.8E-01	5.7E-01	7.8E-01	1.0E+00
Bone surfaces	9.6E-03	1.2E-02	1.8E-02	2.8E-02	5.1E-02
Brain	7.1E-03	8.8E-03	1.5E-02	2.4E-02	4.4E-02
Breasts	6.7E-03	8.5E-03	1.3E-02	2.1E-02	3.9E-02
Gallbladder	1.0E-02	1.3E-02	2.0E-02	2.9E-02	5.0E-02
Gastrointestinal tract					
Stomach	9.5E-03	1.2E-02	1.8E-02	2.8E-02	5.0E-02
Small intestine	1.3E-02	1.7E-02	2.6E-02	3.9E-02	6.5E-02
Colon	1.5E-02	1.8E-02	2.7E-02	4.1E-02	6.3E-02
(Upper large intestine	1.2E-02	1.5E-02	2.3E-02	3.6E-02	5.9E-02)
(Lower large intestine	1.8E-02	2.2E-02	3.3E-02	4.7E-02	6.9E-02)
Heart	8.9E-03	1.1E-02	1.8E-02	2.8E-02	5.0E-02
Kidneys	3.1E-02	3.7E-02	5.2E-02	7.8E-02	1.4E-01
Liver	9.1E-03	1.2E-02	1.8E-02	2.9E-02	5.2E-02
Lungs	7.9E-03	1.0E-02	1.6E-02	2.5E-02	4.6E-02
Muscles	9.9E-03	1.2E-02	1.9E-02	3.0E-02	5.1E-02
Oesophagus	8.2E-03	1.0E-02	1.6E-02	2.5E-02	4.7E-02
Ovaries	1.7E-02	2.2E-02	3.3E-02	4.7E-02	7.4E-02
Pancreas	1.0E-02	1.3E-02	2.0E-02	3.1E-02	5.6E-02
Red marrow	9.8E-03	1.2E-02	1.9E-02	2.7E-02	4.7E-02
Skin	7.0E-03	8.5E-03	1.4E-02	2.2E-02	4.0E-02
Spleen	9.5E-03	1.2E-02	1.8E-02	2.9E-02	5.3E-02
Testes	1.3E-02	1.8E-02	3.0E-02	4.5E-02	7.0E-02
Thymus	8.2E-03	1.0E-02	1.6E-02	2.5E-02	4.7E-02
Thyroid	8.1E-03	1.0E-02	1.7E-02	2.7E-02	5.0E-02
Uterus	2.8E-02	3.3E-02	5.3E-02	7.5E-02	1.1E-01
Remaining organs	1.0E-02	1.3E-02	1.9E-02	3.0E-02	5.2E-02
Effective dose (mSv/MBq)	2.5E-02	3.2E-02	4.9E-02	7.0E-02	1.0E-01

Bladder wall contributes 51% of the effective dose.

C.11. ^{75}Se-labelled amino acids (generic model)
^{75}Se

C.11.1. Biokinetic model

(C 33) The generic biokinetic model for ^{75}Se-labelled amino acids is the same as the generic biokinetic model for ^{11}C-labelled amino acids (see Section C.2.1).

C.11.2. Further reading for ^{75}Se-labelled amino acids

Bergmann, R., Brust, P., Kampf, G., Coenen, H.H., Stöcklin, G., 1995. Evaluation of radioselenium labeled selenomethionine, a potential tracer for brain protein synthesis by PET. Nucl. Med. Biol. 22, 475–481.

Coenen, H.H., Kling, P., Stöcklin, G., 1989. Cerebral metabolism of l-[2-^{18}F]fluorotyrosine, a new PET tracer of protein synthesis. J. Nucl. Med. 30, 1367–1372.

Cottrall, M.F., Taylor, D.M., McElwain, T.J., 1973. Investigations of ^{18}F-p-fluorophenylalanine for pancreas scanning. Br. J. Radiol. 46, 277–288.

Deloar, H.M., Fujiwara, T., Nakamura, T., Itoh, M., Imai, D., Miyake, M., Watanuki, S., 1998b. Estimation of internal absorbed dose of l-[methyl-^{11}C] methionine using whole body positron emission tomography. Eur. J. Nucl. Med. 25, 629–633.

ICRP, 1987. Radiation dose to patients from radiopharmaceuticals. ICRP Publication 53. Ann. ICRP 18 (1–4), 149–150.

ICRP, 2001b. Radiation dose to patients from radiopharmaceuticals. Addendum 4 to ICRP Publication, 53.

Inoue, T., Tomiyoshi, K., Higuichi, T., Ahmed, K., Sarwar, M., Aoyagi, K., Amano, S., Alyafei, S., Zhang, H., Endo, K., 1996. Biodistribution studies on l-3-[Fluorine-18]fluoro-α-methyl tyrosine: a potential tumor-detecting agent. J. Nucl. Med. 39, 663–667.

Schmidt, D., Langen, K-J., Herzog, H., Wirths, J., Holschbach, M., Kiwit, J.C.W., Ziemons, K., Coenen, H.H., Müller-Gärtner, H-W., 1997. Whole-body kinetics and dosimetry of l-3-[^{123}I]iodo-α-methyltyrosine. Eur. J. Nucl. Med. 24, 1162–1166.

Shoup, T.M., Olson, J., Hoffman, J.M., Votaw, J., Eshima, D., Eshima, L., Camp, M., Stabin, M., Votaw, D., Goodman, M., 1999. Synthesis and evaluation of [^{18}F]1-amino-3-fluorocyclobutane-1-carboxylic acid to image brain tumours. J. Nucl. Med. 40, 331–338.

Stenhouse, M.J., Baxter, M.S., 1977. Bomb ^{14}C as a biological tracer. Nature (Lond.) 267, 828–832.

Stenström, K., Leide-Svegborn, S., Erlandsson, B., Hellborg, R., Mattsson, S., Nilsson, L-E., Nosslin, B., Skog, G., Wiebert, A., 1996. Application of accelerator mass spectrometry (AMS) for high-sensitivity measurements of $^{14}CO_2$ in long-term studies of fat metabolism. Appl. Radiat. Isot. 47, 417–422.

Taylor, D.M., 2000b. Generic models for radionuclide dosimetry: 11C, 18F or 75Se-labelled amino acids. Appl. Radiat. Isot. 52, 911–922.

Taylor, D.M., Cottrall, M.F., 1973. Evaluation of amino acids labelled with ^{18}F for pancreas scanning. In: Radiopharmaceuticals and Labelled Compounds, Vol. I. IAEA, Vienna, pp. 441–443.

Wester, H.J., Herz, M., Senkowitsch-Schmidtke, R., Schwaiger, M., Stöcklin, G., Hamacher, K., 1999a. Preclinical evaluation of 4-[^{18}F]fluoroprolines: diasteromeric effect on metabolism and uptake in mice. Nucl. Med. Biol. 26, 259–265.

Wester, H.J., Herz, M., Weber, W., Heiss, P., Senkowitsch-Schmidtke, R., Schwaiger, M., Stöcklin, G., 1999b. Synthesis and radiopharmacology of O-(2-[^{18}F]fluoroethyl)-L-tyrosine for tumor imaging. J. Nucl. Med. 40, 205–212.

C.11.3. Biokinetic data for ^{75}Se-labelled amino acids

Organ (S)	F_s	T (h)	a	$\widetilde{A}_s/A_0$(h)
Blood	0.20	0.2	0.25	1.3
		6	0.75	
Brain	0.015	1200	0.70	31
		∞	0.30	
Thyroid	0.0007	1200	0.70	1.4
		∞	0.30	
Lungs	0.02	12	0.10	25
		1200	0.85	
		∞	0.05	
Kidneys	0.02	12	0.15	24
		1200	0.80	
		∞	0.05	
Kidney excretion	0.20			0.017
Liver	0.08	12	0.40	70
		1200	0.55	
		∞	0.05	
Spleen	0.004	12	0.33	3.3
		1200	0.67	
Pancreas	0.03	12	0.85	5.9
		1200	0.15	
Small intestine wall	0.03	6	0.50	0.39
		12	0.50	
Ovaries	0.0002	1200	0.70	0.41
		∞	0.30	
Testes	0.00092	1200	0.70	1.9
		∞	0.30	
Muscle	0.24	12	0.15	520
		1200	0.45	
		∞	0.40	
Other organs and tissues	0.359	12	0.15	780
		1200	0.45	
		∞	0.40	
Urinary bladder contents	0.20			
Adult, 15 years, 10 years				0.44
5 years				0.37
1 year				0.24

For [^{75}Se]-selenomethionine, the compound-specific data (ICRP, 1987) should be used.

C.11.4. Absorbed doses for ^{75}Se-labelled amino acids

^{75}Se 119.8 days

Organ	Absorbed dose per unit activity administered (mGy/MBq)				
	Adult	15 years	10 years	5 years	1 year
Adrenals	2.6E+00	3.1E+00	4.6E+00	6.7E+00	1.2E+01
Bladder	2.0E+00	2.6E+00	3.6E+00	5.3E+00	9.0E+00
Bone surfaces	2.9E+00	3.3E+00	4.7E+00	6.8E+00	1.2E+01
Brain	1.7E+00	1.7E+00	2.0E+00	2.7E+00	3.9E+00
Breasts	1.3E+00	1.6E+00	2.2E+00	3.4E+00	6.4E+00
Gallbladder	2.7E+00	3.3E+00	5.2E+00	7.4E+00	1.0E+01
Gastrointestinal tract					
Stomach	2.3E+00	2.8E+00	4.2E+00	5.9E+00	1.0E+01
Small intestine	2.0E+00	2.4E+00	3.6E+00	5.5E+00	9.5E+00
Colon	2.1E+00	2.6E+00	3.9E+00	6.0E+00	1.0E+01
(Upper large intestine	2.1E+00	2.6E+00	3.7E+00	6.1E+00	9.8E+00)
(Lower large intestine	2.2E+00	2.6E+00	4.1E+00	5.9E+00	1.1E+01)
Heart	2.3E+00	2.8E+00	4.0E+00	5.7E+00	1.0E+01
Kidneys	3.8E+00	4.6E+00	6.3E+00	9.2E+00	1.6E+01
Liver	3.0E+00	3.8E+00	5.6E+00	7.7E+00	1.4E+01
Lungs	2.1E+00	2.8E+00	3.9E+00	5.7E+00	1.0E+01
Muscles	1.7E+00	2.3E+00	3.6E+00	6.6E+00	1.2E+01
Oesophagus	2.0E+00	2.4E+00	3.5E+00	5.2E+00	9.4E+00
Ovaries	2.7E+00	3.0E+00	5.4E+00	8.8E+00	1.7E+01
Pancreas	3.6E+00	4.7E+00	7.8E+00	1.1E+01	2.0E+01
Red marrow	1.9E+00	2.2E+00	3.2E+00	4.5E+00	7.6E+00
Skin	1.2E+00	1.3E+00	2.0E+00	3.1E+00	5.7E+00
Spleen	2.2E+00	2.9E+00	4.3E+00	6.4E+00	1.1E+01
Testes	2.3E+00	3.9E+00	1.7E+01	2.0E+01	2.8E+01
Thymus	2.0E+00	2.4E+00	3.5E+00	5.2E+00	9.4E+00
Thyroid	2.8E+00	4.0E+00	6.1E+00	1.1E+01	2.1E+01
Uterus	2.3E+00	2.7E+00	4.2E+00	6.5E+00	1.1E+01
Remaining organs	1.8E+00	2.3E+00	3.4E+00	5.3E+00	8.8E+00
Effective dose (mSv/MBq)	2.2E+00	2.9E+00	5.3E+00	7.6E+00	1.3E+01

For [^{75}Se]-selenomethionine, the compound-specific data (ICRP, 1987) should be used.

C.12. ^{99m}Tc-apcitide

^{99m}Tc

C.12.1. Biokinetic model

(C 34) Apcitide is a peptide that binds to the GP IIb/IIIa receptor on the surface of activated platelets; a major component of active thrombus formation. Apcitide is used for the detection and localisation of acute venous thrombosis in the lower extremities. A biokinetic model with distribution in circulating blood and an effective half-time equal to the physical half-time is assumed.

C.12.2. Further reading for ^{99m}Tc-apcitide

Taillefer, R., Edell, S., Innes, G., Lister-James, J., 2000. Acute thromboscintigraphy with (99m)Tc-apcitide: results of the phase 3 multicenter clinical trial comparing 99mTc-apcitide scintigraphy with contrast venography for imaging acute DVT. Multicenter trial investigators. J. Nucl. Med. 41, 1214–1223.

C.12.3. Biokinetic data for ^{99m}Tc-apcitide

Organ (S)	F_s	T (h)	a	$\widetilde{A}_s/A_0$(h)
Blood	1.0	∞	1.0	8.7

C.12.4. Absorbed doses for ^{99m}Tc-apcitide

^{99m}Tc 6.01 h

Organ	Absorbed dose per unit activity administered (mGy/MBq)				
	Adult	15 years	10 years	5 years	1 year
Adrenals	5.3E-03	6.6E-03	9.8E-03	1.5E-02	2.7E-02
Bladder	5.3E-03	7.3E-03	1.0E-02	1.5E-02	2.7E-02
Bone surfaces	8.0E-03	9.4E-03	1.4E-02	2.1E-02	3.7E-02
Brain	3.8E-03	4.8E-03	7.8E-03	1.2E-02	2.2E-02
Breasts	3.2E-03	4.0E-03	5.8E-03	9.2E-03	1.8E-02
Gallbladder	5.6E-03	7.5E-03	1.2E-02	1.8E-02	2.2E-02
Gastrointestinal tract					
Stomach	5.0E-03	6.6E-03	1.1E-02	1.5E-02	2.6E-02
Small intestine	5.6E-03	7.0E-03	1.0E-02	1.6E-02	2.8E-02
Colon	5.4E-03	7.0E-03	1.0E-02	1.6E-02	2.8E-02
(Upper large intestine	5.4E-03	7.1E-03	1.0E-02	1.6E-02	2.7E-02)
(Lower large intestine	5.4E-03	6.9E-03	1.1E-02	1.6E-02	2.9E-02)
Heart	5.1E-03	6.4E-03	9.5E-03	1.4E-02	2.5E-02
Kidneys	4.9E-03	6.0E-03	9.2E-03	1.4E-02	2.5E-02
Liver	4.9E-03	6.1E-03	9.5E-03	1.4E-02	2.5E-02
Lungs	4.5E-03	5.7E-03	8.5E-03	1.3E-02	2.3E-02
Muscles	4.1E-03	5.1E-03	7.8E-03	1.2E-02	2.2E-02
Oesophagus	4.5E-03	5.7E-03	8.5E-03	1.3E-02	2.4E-02
Ovaries	5.7E-03	7.1E-03	1.0E-02	1.6E-02	2.9E-02
Pancreas	5.6E-03	7.1E-03	1.0E-02	1.6E-02	2.8E-02
Red marrow	4.4E-03	5.4E-03	8.3E-03	1.2E-02	2.2E-02
Skin	2.9E-03	3.5E-03	5.5E-03	8.9E-03	1.7E-02
Spleen	4.9E-03	6.1E-03	9.5E-03	1.4E-02	2.5E-02
Testes	4.1E-03	5.0E-03	7.4E-03	1.2E-02	2.1E-02
Thymus	4.5E-03	5.7E-03	8.5E-03	1.3E-02	2.4E-02
Thyroid	4.6E-03	5.8E-03	9.2E-03	1.5E-02	2.6E-02
Uterus	5.8E-03	7.1E-03	1.1E-02	1.6E-02	2.9E-02
Remaining organs	4.2E-03	5.2E-03	8.0E-03	1.2E-02	2.3E-02
Effective dose (mSv/MBq)	4.7E-03	6.0E-03	9.1E-03	1.4E-02	2.5E-02

C.13. ^{99m}Tc-ethylenedicysteine (EC)
^{99m}Tc

C.13.1. Biokinetic model

(C 35) The substance ^{99m}Tc-ethylenedicysteine (EC) is used for renal studies. The biokinetic behaviour of the substance is very similar to that of hippuran with a half-time in the total body of 25 min (ICRP, 1987). The cumulated amount found in urine at different times is as follows: 40 min, 70%; 60 min, 80%; 90 min, 95% (Liniecki, 1998). The clearance is approximately 70% of that of hippuran.

C.13.2. References and further reading for ^{99m}Tc-EC

ICRP, 1987. Radiation dose to patients from radiopharmaceuticals. ICRP Publication 53. Ann. ICRP 18 (1–4).

Liniecki, J., 1998. Private communication. Department of Nuclear Medicine, Medical University of Lodz, Lodz..

Surma, M.J., 1998a. Verification of ^{99m}Tc-ethylenedicysteine (^{99m}Tc-EC) distribution model in the organism. Nucl. Med. Rev. 1, 29–32.

Surma, M.J., 1998b. ^{99m}Tc-Ethylenedicysteine (^{99m}Tc-EC) renal clearance determination error for the multiple- and single-sample methods. Nucl. Med. Rev. 1, 33–40.

Surma, M.J., Wiewiora, J., Liniecki, J., 1994. Usefulness of ^{99m}Tc-N,N′-ethylene-1-dicysteine complex for dynamic kidney investigations. Nucl. Med. Comm. 15, 628–635.

C.13.3. Biokinetic data for ^{99m}Tc-EC

Organ (S)	F_s	T (h)	a	$\widetilde{A}_s/A_0$(h)
Normal renal function				
Total body (excl. bladder contents)	1.0	0.42	1.0	0.56
Kidney excretion	1.0			0.062
Urinary bladder contents	1.0			
Adult, 15 years, 10 years				2.3
5 years				2.0
1 year				1.3
Abnormal renal function				
Total body (excl. bladder contents)	1.0	4.2	1.0	3.6
Kidney excretion	1.0			0.20
Liver	0.04	4.2	1.0	0.14
Urinary bladder contents	1.0			
Adult, 15 years, 10 years				1.0
5 years				0.86
1 year				0.58
Acute unilateral renal blockage				
Total body (excl. bladder contents)	1.0	0.42	0.5	4.4
		120	0.5	
Abnormal kidney	0.5	120	1.0	4.1
Normal kidney excretion	1.0			0.033
Urinary bladder contents	1.0			
Adult, 15 years, 10 years				1.2
5 years				1.0
1 year				0.66

C.13.4. Absorbed doses for ^{99m}Tc-EC

Normal renal function

^{99m}Tc 6.01 h

Organ	Absorbed dose per unit activity administered (mGy/MBq)				
	Adult	15 years	10 years	5 years	1 year
Adrenals	5.3E-04	6.8E-04	1.1E-03	1.7E-03	3.0E-03
Bladder	9.5E-02	1.2E-01	1.7E-01	2.2E-01	2.6E-01
Bone surfaces	1.4E-03	1.7E-03	2.5E-03	3.4E-03	4.8E-03
Brain	2.2E-04	2.8E-04	4.5E-04	7.3E-04	1.3E-03
Breasts	2.0E-04	2.6E-04	4.1E-04	7.0E-04	1.3E-03
Gallbladder	7.0E-04	1.0E-03	2.4E-03	2.4E-03	3.1E-03
Gastrointestinal tract					
Stomach	5.2E-04	6.5E-04	1.3E-03	1.9E-03	2.9E-03
Small intestine	2.2E-03	2.8E-03	4.5E-03	6.0E-03	7.2E-03
Colon	3.2E-03	4.0E-03	6.2E-03	7.8E-03	8.8E-03
(Upper large intestine	1.7E-03	2.2E-03	3.7E-03	5.3E-03	6.3E-03)
(Lower large intestine	5.2E-03	6.3E-03	9.6E-03	1.1E-02	1.2E-02)
Heart	3.3E-04	4.3E-04	6.6E-04	1.0E-03	1.9E-03
Kidneys	3.4E-03	4.1E-03	5.9E-03	8.5E-03	1.4E-02
Liver	4.5E-04	5.9E-04	1.0E-03	1.7E-03	2.6E-03
Lungs	2.8E-04	3.8E-04	5.8E-04	9.1E-04	1.7E-03
Muscles	1.4E-03	1.6E-03	2.4E-03	3.2E-03	4.1E-03
Oesophagus	2.7E-04	3.5E-04	5.4E-04	8.6E-04	1.5E-03
Ovaries	4.9E-03	6.2E-03	9.0E-03	1.1E-02	1.2E-02
Pancreas	5.5E-04	6.8E-04	1.2E-03	1.9E-03	3.1E-03
Red marrow	9.6E-04	1.2E-03	1.8E-03	2.1E-03	2.4E-03
Skin	5.0E-04	6.1E-04	1.0E-03	1.4E-03	2.0E-03
Spleen	5.0E-04	6.5E-04	1.1E-03	1.7E-03	2.8E-03
Testes	3.4E-03	4.8E-03	8.4E-03	1.1E-02	1.3E-02
Thymus	2.7E-04	3.5E-04	5.4E-04	8.6E-04	1.5E-03
Thyroid	2.7E-04	3.4E-04	5.5E-04	8.9E-04	1.6E-03
Uterus	1.1E-02	1.3E-02	2.0E-02	2.4E-02	2.6E-02
Remaining organs	1.4E-03	1.7E-03	2.3E-03	2.7E-03	3.4E-03
Effective dose (mSv/MBq)	6.3E-03	8.0E-03	1.2E-02	1.5E-02	1.8E-02

Bladder wall contributes 76% of the effective dose.

Abnormal renal function
^{99m}Tc 6.01 h

Organ	Absorbed dose per unit activity administered (mGy/MBq)				
	Adult	15 years	10 years	5 years	1 year
Adrenals	2.6E-03	3.3E-03	5.0E-03	7.4E-03	1.3E-02
Bladder	4.4E-02	5.6E-02	8.1E-02	1.0E-01	1.3E-01
Bone surfaces	3.6E-03	4.3E-03	6.4E-03	9.2E-03	1.6E-02
Brain	1.5E-03	1.8E-03	3.0E-03	4.8E-03	8.5E-03
Breasts	1.3E-03	1.6E-03	2.3E-03	3.7E-03	7.0E-03
Gallbladder	2.7E-03	3.6E-03	5.9E-03	8.3E-03	1.0E-02
Gastrointestinal tract					
Stomach	2.2E-03	2.9E-03	4.7E-03	6.5E-03	1.1E-02
Small intestine	3.1E-03	3.9E-03	6.0E-03	8.8E-03	1.4E-02
Colon	3.4E-03	4.4E-03	6.7E-03	9.6E-03	1.4E-02
(Upper large intestine	2.8E-03	3.7E-03	5.6E-03	8.6E-03	1.3E-02)
(Lower large intestine	4.3E-03	5.3E-03	8.2E-03	1.1E-02	1.6E-02)
Heart	2.1E-03	2.6E-03	3.9E-03	5.8E-03	1.0E-02
Kidneys	1.1E-02	1.3E-02	1.8E-02	2.6E-02	4.5E-02
Liver	2.8E-03	3.5E-03	5.3E-03	7.5E-03	1.3E-02
Lungs	1.8E-03	2.3E-03	3.4E-03	5.2E-03	9.5E-03
Muscles	2.1E-03	2.6E-03	4.0E-03	5.8E-03	1.0E-02
Oesophagus	1.8E-03	2.2E-03	3.3E-03	5.2E-03	9.3E-03
Ovaries	4.3E-03	5.4E-03	7.9E-03	1.1E-02	1.6E-02
Pancreas	2.6E-03	3.3E-03	4.9E-03	7.4E-03	1.3E-02
Red marrow	2.1E-03	2.6E-03	4.0E-03	5.6E-03	9.3E-03
Skin	1.3E-03	1.6E-03	2.5E-03	3.9E-03	7.0E-03
Spleen	2.3E-03	3.0E-03	4.6E-03	6.8E-03	1.2E-02
Testes	2.9E-03	3.9E-03	6.4E-03	9.2E-03	1.4E-02
Thymus	1.8E-03	2.2E-03	3.3E-03	5.2E-03	9.3E-03
Thyroid	1.8E-03	2.2E-03	3.6E-03	5.7E-03	1.0E-02
Uterus	6.9E-03	8.3E-03	1.3E-02	1.7E-02	2.2E-02
Remaining organs	2.2E-03	2.8E-03	4.2E-03	6.4E-03	1.1E-02
Effective dose (mSv/MBq)	4.6E-03	5.9E-03	8.8E-03	1.2E-02	1.8E-02

Acute unilateral renal blockage

^{99m}Tc 6.01 h

Organ	Absorbed dose per unit activity administered (mGy/MBq)				
	Adult	15 years	10 years	5 years	1 year
Adrenals	1.1E-02	1.5E-02	2.3E-02	3.3E-02	5.7E-02
Bladder	4.9E-02	6.2E-02	9.1E-02	1.2E-01	1.4E-01
Bone surfaces	3.1E-03	4.1E-03	6.0E-03	8.9E-03	1.7E-02
Brain	1.1E-04	1.4E-04	2.4E-04	4.0E-04	7.9E-04
Breasts	4.0E-04	5.3E-04	1.1E-03	1.7E-03	3.1E-03
Gallbladder	6.4E-03	7.5E-03	1.1E-02	1.6E-02	2.3E-02
Gastrointestinal tract					
Stomach	4.0E-03	4.6E-03	7.3E-03	9.7E-03	1.3E-02
Small intestine	4.3E-03	5.5E-03	8.8E-03	1.2E-02	1.9E-02
Colon	3.8E-03	4.8E-03	7.4E-03	1.0E-02	1.4E-02
(Upper large intestine	4.0E-03	5.1E-03	7.8E-03	1.1E-02	1.6E-02)
(Lower large intestine	3.5E-03	4.4E-03	6.8E-03	9.4E-03	1.2E-02)
Heart	1.4E-03	1.7E-03	2.8E-03	4.2E-03	6.3E-03
Kidneys	2.0E-01	2.4E-01	3.4E-01	4.8E-01	8.4E-01
Liver	4.6E-03	5.6E-03	8.4E-03	1.2E-02	1.7E-02
Lungs	1.1E-03	1.7E-03	2.6E-03	4.0E-03	7.4E-03
Muscles	2.2E-03	2.7E-03	3.8E-03	5.5E-03	8.8E-03
Oesophagus	3.9E-04	5.6E-04	8.8E-04	1.6E-03	2.3E-03
Ovaries	3.6E-03	4.7E-03	7.2E-03	1.0E-02	1.4E-02
Pancreas	7.7E-03	9.3E-03	1.4E-02	1.9E-02	2.9E-02
Red marrow	3.0E-03	3.6E-03	5.1E-03	6.4E-03	8.4E-03
Skin	8.2E-04	1.0E-03	1.6E-03	2.3E-03	4.2E-03
Spleen	1.0E-02	1.3E-02	1.9E-02	2.7E-02	4.1E-02
Testes	1.8E-03	2.5E-03	4.5E-03	6.1E-03	8.4E-03
Thymus	3.9E-04	5.6E-04	8.8E-04	1.6E-03	2.3E-03
Thyroid	1.8E-04	2.4E-04	4.7E-04	9.6E-04	1.7E-03
Uterus	6.5E-03	7.9E-03	1.2E-02	1.6E-02	2.0E-02
Remaining organs	2.2E-03	2.7E-03	3.7E-03	4.6E-03	6.8E-03
Effective dose (mSv/MBq)	9.9E-03	1.2E-02	1.8E-02	2.4E-02	3.7E-02

C.14. ^{99m}Tc-ECD

^{99m}Tc

C.14.1. Biokinetic model

(C 36) N,N′-1,2-ethylenediylbis-L-cysteinediethylester (ECD, Neurolite), labelled with ^{99m}Tc, is a neutral lipophilic complex that crosses the intact blood–brain barrier rapidly and is retained in the brain for a long time, making it possible to perform detailed tomographic studies of the regional cerebral blood flow.

(C 37) Kinetic data from humans (Holman et al., 1989; Vallabhajosula et al., 1989; Léveillé et al., 1992) have shown that the substance is cleared rapidly from the blood after intravenous injection. Uptake in the brain reaches a maximum of 4.9–6.5% within 1 min and remains relatively constant over several hours. Early whole-body imaging also shows uptake in lungs, liver, kidneys, and thyroid.

(C 38) In the model, it is assumed that there is immediate cellular uptake of the substance in the brain (0.06), lungs (0.06), liver (0.20), kidneys (0.10), and thyroid (0.003). The activity in the brain is cleared bi-exponentially with half-times of 1 h (0.40) and 1.5 days (0.60). At 48 h, approximately 80% has been excreted in urine and 20% in faeces. Activity in the liver is assumed to be excreted through the intestines, partly via the gallbladder, according to the model described in Section A.9 in *Publication 53* (ICRP, 1987). The rest of the activity is assumed to be excreted via the kidneys and urinary bladder.

(C 39) For children, the fractional uptake in the brain is higher due to the relative weight of the brain (Barthel et al., 1997).

C.14.2. References for ^{99m}Tc-ECD

Barthel, H., Wiener, M., Dannenberg, C., Bettin, S., Sattler, B., Knapp, W.H., 1997. Age-specific cerebral perfusion in 4- to 15-year-old children: a high-resolution brain SPET study using ^{99m}Tc-ECD. Eur. J. Nucl. Med. 24, 1245–1252.

Holman, B.L., Hellman, R.S., Goldsmith, S.J., Mena, I., Leveille, J., Gherardi, P.G., Moretti, J.L., Bischof-Delaloye, A., Hill, T.C., Rigo, P.M., Van Heertum, R.L., Ell, P.J., Buell, U., De Roo, M.C., Morgan, R.A., 1989. Biodistribution, dosimetry and clinical evaluation of technetium-99m ethyl cysteinate dimer in normal subjects and in patients with chronic cerebral infarction. J. Nucl. Med. 30, 1018–1024.

ICRP, 1987. Radiation dose to patients from radiopharmaceuticals. ICRP Publication 53. Ann. ICRP 18 (1–4).

Léveillé, J., Demonceau, G., Walovitch, R.C., 1992. Intrasubject comparison between technetium-99m-ECD and technetium-99m-HMPAO in healthy human subjects. J. Nucl. Med. 33, 480–484.

Vallabhajosula, S., Zimmerman, R.E., Picard, M., Stritzke, P., Mena, I., Hellman, R.S., Tikofsky, R.S., Stabin, M.G., Morgan, R.A., Goldsmith, S.J., 1989. Technetium-99m ECD: a new brain imaging agent: in vivo kinetics and biodistribution studies in normal human subjects. J. Nucl. Med. 30, 599–604.

C.14.3. Biokinetic data for ^{99m}Tc-ECD

Organ (S)	F_s	T (h)	a	$\widetilde{A}_s/A_0$(h)
Brain		1.0	0.4	
		36	0.6	
Adult	0.06			0.30
15 years	0.10			0.50
10 years	0.17			0.84
5 years	0.23			1.1
1 year	0.28			1.4
Thyroid	0.003	1.0	0.7	0.0093
		36	0.3	
Lungs	0.06	0.25	0.8	0.082
		10	0.2	
Kidneys	0.10	0.50	0.9	0.13
		36	0.1	
Liver	0.20	0.50	0.9	0.27
		36	0.1	
Other organs and tissues		1.0	0.7	
		36	0.3	
Adult	0.577			1.8
15 years	0.537			1.7
10 years	0.467			1.5
5 years	0.407			1.3
1 year	0.357			1.1
Gallbladder contents	0.07			0.19
Gastrointestinal tract contents				
Small intestine	0.20			0.44
Upper large intestine	0.20			0.58
Lower large intestine	0.20			0.28
Urinary bladder contents	0.80			
Adult				1.2
15 years				1.2
10 years				1.1
5 years				0.92
1 year				0.58

C.14.4. Absorbed doses for ^{99m}Tc-ECD

^{99m}Tc 6.01 h

Organ	Absorbed dose per unit activity administered (mGy/MBq)				
	Adult	15 years	10 years	5 years	1 year
Adrenals	2.5E-03	3.1E-03	4.5E-03	6.5E-03	1.1E-02
Bladder	5.0E-02	6.2E-02	8.7E-02	1.1E-01	1.3E-01
Bone surfaces	3.5E-03	4.3E-03	6.4E-03	9.4E-03	1.5E-02
Brain	4.9E-03	8.0E-03	1.4E-02	1.9E-02	3.1E-02
Breasts	8.9E-04	1.1E-03	1.6E-03	2.4E-03	4.3E-03
Gallbladder	2.8E-02	3.2E-02	4.2E-02	7.3E-02	2.4E-01
Gastrointestinal tract					
Stomach	2.7E-03	3.5E-03	5.6E-03	8.3E-03	1.3E-02
Small intestine	1.2E-02	1.6E-02	2.5E-02	3.8E-02	6.8E-02
Colon	2.1E-02	2.6E-02	4.3E-02	6.7E-02	1.2E-01
(Upper large intestine	2.3E-02	2.9E-02	4.8E-02	7.5E-02	1.4E-01)
(Lower large intestine	1.8E-02	2.2E-02	3.6E-02	5.6E-02	1.0E-01)
Heart	1.6E-03	2.0E-03	2.9E-03	4.2E-03	7.2E-03
Kidneys	8.7E-03	1.0E-02	1.5E-02	2.1E-02	3.5E-02
Liver	5.0E-03	6.3E-03	9.5E-03	1.4E-02	2.4E-02
Lungs	2.1E-03	2.9E-03	4.0E-03	5.9E-03	1.1E-02
Muscles	2.2E-03	2.7E-03	3.8E-03	5.4E-03	8.7E-03
Oesophagus	1.2E-03	1.5E-03	2.0E-03	3.0E-03	5.1E-03
Ovaries	7.9E-03	9.9E-03	1.4E-02	1.9E-02	2.9E-02
Pancreas	2.9E-03	3.7E-03	6.0E-03	9.0E-03	1.4E-02
Red marrow	2.4E-03	3.0E-03	4.2E-03	5.5E-03	8.9E-03
Skin	1.1E-03	1.3E-03	2.0E-03	3.0E-03	5.2E-03
Spleen	2.0E-03	2.6E-03	3.9E-03	5.7E-03	9.5E-03
Testes	2.7E-03	3.6E-03	5.8E-03	7.9E-03	1.1E-02
Thymus	1.2E-03	1.5E-03	2.0E-03	3.0E-03	5.1E-03
Thyroid	6.1E-03	9.6E-03	1.5E-02	3.1E-02	5.8E-02
Uterus	9.2E-03	1.1E-02	1.7E-02	2.2E-02	2.9E-02
Remaining organs	2.8E-03	3.8E-03	6.8E-03	1.3E-02	2.1E-02
Effective dose (mSv/MBq)	7.7E-03	9.9E-03	1.5E-02	2.2E-02	4.0E-02

C.15. ^{99m}Tc-furifosmin (Q12)

^{99m}Tc

C.15.1. Biokinetic model

(C 40) [Trans-1,2-bis(dihydro-2,2,5,5-tetramethyl-3(2H)furanone-4- methylene-imino ethane)bis tris(3-methoxy-1propyl)–phosphine] technetium (III)-99m is a non-reducible complex of Tc(III). Technetium(III)-99m-Q12 is prepared from a freeze-dried kit (TechneCard) and is used for studies of myocardial perfusion.

(C 41) ^{99m}Tc-Q12 accumulates in viable myocardial tissue in proportion to regional blood flow in a manner similar to thallous chloride. After intravenous injection, the substance is cleared rapidly from the blood (<5% left by 20 min) and taken up predominantly in muscular tissues (including heart), liver, and kidneys. Biodistribution is generally similar to that of ^{99m}Tc-MIBI (Cardiolite; ICRP, 1991b) and ^{99m}Tc-tetrofosmin (Myoview; ICRP, 1998), but there are some differences which have a bearing on diagnostic technique. ^{99m}Tc-Q12 shows a heart uptake of 1.2–2.4%. It is cleared rapidly from the liver (<6.5% left by 1 h), and lung uptake is low (4%). More than 50% of the substance has entered excretory pathways by 24 h and the faecal: urinary excretion ratio is 60:40.

(C 42) It is assumed that the fractions of the substance taken up by the liver and kidneys are excreted in faeces and urine, respectively. When the substance is injected in conjunction with an exercise stress test, there is little change in heart uptake, and biodistribution is similar to that observed at rest. The initial rate of urinary clearance is lower than at rest, and the same faecal:urinary excretion ratio is assumed.

(C 43) The quantitative figures for uptake and excretion in man, presented in the table below, are based on the rest and exercise studies of Rossetti et al. (1994) with supplementary information from Gerson et al. (1994). Substance excreted by the hepatobiliary system is assumed to leave the body via the intestinal tract according to the ICRP model for the gastrointestinal tract (ICRP, 1979).

(C 44) The biodistribution and excretion data used to derive this model were based on a small number of subjects (seven at rest and three after exercise), with the result that significant differences between rest and exercise data could not be established. The difference between the biokinetic data tables presented for rest and exercise studies is therefore largely based on experience of models for similar ^{99m}Tc-labelled myocardial perfusion imaging agents such as MIBI and tetrofosmin.

C.15.2. References for ^{99m}Tc-furifosmin

Gerson, M.C., Lukes, J., Deutsch, E., Biniakiewicz, D., Rohe, R.C., Washburn, L.C., Fortman, C., Walsh, R.A., 1994. Comparison of technetium 99m Q12 and thallium 201 for detection of angiographically documented coronary artery disease in humans. J. Nucl. Cardiol. 1, 499–508.

ICRP, 1979. Limits for intakes of radionuclides by workers. ICRP Publication 30, Part 1. Ann. ICRP 2 (3/4).

ICRP, 1991b. Radiation dose to patients from radiopharmaceuticals. Addendum 1 to ICRP Publication 53, in: Radiological protection in biomedical research. ICRP Publication 62. Ann. ICRP 22 (3).

ICRP, 1998. Radiation dose to patients from radiopharmaceuticals. Addendum 2 to ICRP Publication 53. ICRP Publication 80. Ann. ICRP 28 (3).

Rossetti, C., Vanoli, G., Paganelli, G., Kwiatkowski, M., Zito, F., Colombo, F., Bonino, C., Carpinelli, A., Casati, R., Deutsch, K., Marmion, M., Woulfe, S.R., Lunghi, F., Deutsch, E., Fazio, F., 1994. Human biodistribution, dosimetry and clinical use of technetium (III)-99m-Q12. J. Nucl. Med. 35, 1571–1580.

C.15.3. Biokinetic data for ^{99m}Tc-furifosmin

Organ (S)	F_s	T (h)	a	$\widetilde{A}_s/A_0$(h)
Resting subject				
Heart wall	0.024	6.0	0.67	0.13
		24	0.33	
Lungs	0.04	24	1.0	0.28
Kidneys	0.052	1.0	0.5	0.21
		24	0.5	
Liver	0.07	6.0	1.0	0.30
Other organs and tissues	0.814	0.42	0.48	3.4
		36	0.52	
Gallbladder contents	0.20			0.35
Gastrointestinal tract contents				
Small intestine	0.60			0.72
Upper large intestine	0.60			0.94
Lower large intestine	0.60			0.46
Urinary bladder contents	0.40			
Adult, 15 years, 10 years				0.47
5 years				0.40
1 year				0.26
Exercise				
Heart wall	0.027	6.0	0.67	0.14
		24	0.33	
Lungs	0.04	24	1.0	0.28
Kidneys	0.08	1.3	0.75	0.23
		24	0.25	
Liver	0.06	6.0	1.0	0.26
Other organs and tissues	0.793	1.0	0.45	4.0
		96	0.55	
Gallbladder contents	0.20			0.29
Gastrointestinal tract contents				
Small intestine	0.60			0.59
Upper large intestine	0.60			0.77
Lower large intestine	0.60			0.38
Urinary bladder contents	0.40			
Adult, 15 years, 10 years				0.38
5 years				0.32
1 year				0.21

C.15.4. Absorbed doses for ^{99m}Tc-furifosmin

Resting subject

^{99m}Tc 6.01 h

Organ	Absorbed dose per unit activity administered (mGy/MBq)				
	Adult	15 years	10 years	5 years	1 year
Adrenals	4.3E-03	5.5E-03	8.4E-03	1.2E-02	2.1E-02
Bladder	2.2E-02	2.9E-02	4.2E-02	5.5E-02	7.1E-02
Bone surfaces	5.1E-03	6.2E-03	9.1E-03	1.3E-02	2.4E-02
Brain	1.6E-03	2.0E-03	3.3E-03	5.3E-03	9.3E-03
Breasts	1.8E-03	2.2E-03	3.5E-03	5.7E-03	1.1E-02
Gallbladder	5.1E-02	5.7E-02	7.5E-02	1.3E-01	4.4E-01
Gastrointestinal tract					
Stomach	4.6E-03	6.2E-03	1.0E-02	1.5E-02	2.6E-02
Small intestine	1.9E-02	2.4E-02	3.9E-02	6.1E-02	1.1E-01
Colon	3.2E-02	4.1E-02	6.8E-02	1.1E-01	1.9E-01
(Upper large intestine	3.6E-02	4.7E-02	7.7E-02	1.2E-01	2.2E-01)
(Lower large intestine	2.6E-02	3.3E-02	5.5E-02	8.8E-02	1.6E-01)
Heart	7.8E-03	1.0E-02	1.5E-02	2.3E-02	4.0E-02
Kidneys	1.4E-02	1.7E-02	2.3E-02	3.4E-02	5.8E-02
Liver	6.9E-03	8.8E-03	1.3E-02	1.9E-02	3.4E-02
Lungs	5.5E-03	7.8E-03	1.1E-02	1.7E-02	3.1E-02
Muscles	3.1E-03	3.9E-03	5.8E-03	8.7E-03	1.5E-02
Oesophagus	2.5E-03	3.2E-03	4.6E-03	7.1E-03	1.3E-02
Ovaries	1.0E-02	1.3E-02	1.9E-02	2.8E-02	4.6E-02
Pancreas	5.1E-03	6.6E-03	1.1E-02	1.7E-02	2.7E-02
Red marrow	3.7E-03	4.4E-03	6.4E-03	8.7E-03	1.4E-02
Skin	1.7E-03	2.0E-03	3.1E-03	5.0E-03	9.3E-03
Spleen	3.6E-03	4.7E-03	7.4E-03	1.1E-02	2.0E-02
Testes	2.7E-03	3.5E-03	5.7E-03	8.8E-03	1.5E-02
Thymus	2.5E-03	3.2E-03	4.6E-03	7.1E-03	1.3E-02
Thyroid	2.0E-03	2.6E-03	4.2E-03	6.7E-03	1.2E-02
Uterus	8.8E-03	1.1E-02	1.7E-02	2.5E-02	3.9E-02
Remaining organs	3.8E-03	4.9E-03	7.6E-03	1.2E-02	2.0E-02
Effective dose (mSv/MBq)	1.0E-02	1.3E-02	1.8E-02	3.0E-02	5.7E-02

Exercise

^{99m}Tc 6.01 h

Organ	Absorbed dose per unit activity administered (mGy/MBq)				
	Adult	15 years	10 years	5 years	1 year
Adrenals	4.5E-03	5.7E-03	8.7E-03	1.3E-02	2.2E-02
Bladder	1.8E-02	2.3E-02	3.4E-02	4.4E-02	5.8E-02
Bone surfaces	5.5E-03	6.6E-03	9.7E-03	1.4E-02	2.6E-02
Brain	1.9E-03	2.4E-03	3.9E-03	6.3E-03	1.1E-02
Breasts	2.0E-03	2.5E-03	3.9E-03	6.2E-03	1.2E-02
Gallbladder	4.3E-02	4.9E-02	6.3E-02	1.1E-01	3.6E-01
Gastrointestinal tract					
Stomach	4.6E-03	6.2E-03	1.0E-02	1.5E-02	2.5E-02
Small intestine	1.6E-02	2.1E-02	3.3E-02	5.1E-02	9.2E-02
Colon	2.7E-02	3.4E-02	5.7E-02	8.9E-02	1.7E-01
(Upper large intestine	3.0E-02	3.9E-02	6.4E-02	1.0E-01	1.9E-01)
(Lower large intestine	2.2E-02	2.8E-02	4.7E-02	7.4E-02	1.4E-01)
Heart	8.7E-03	1.1E-02	1.7E-02	2.5E-02	4.4E-02
Kidneys	1.5E-02	1.8E-02	2.5E-02	3.6E-02	6.1E-02
Liver	6.3E-03	7.9E-03	1.2E-02	1.7E-02	3.0E-02
Lungs	5.6E-03	8.0E-03	1.1E-02	1.7E-02	3.1E-02
Muscles	3.2E-03	4.0E-03	6.0E-03	9.0E-03	1.6E-02
Oesophagus	2.9E-03	3.6E-03	5.2E-03	8.1E-03	1.4E-02
Ovaries	9.2E-03	1.2E-02	1.7E-02	2.5E-02	4.2E-02
Pancreas	5.2E-03	6.7E-03	1.1E-02	1.6E-02	2.7E-02
Red marrow	3.7E-03	4.5E-03	6.6E-03	9.1E-03	1.5E-02
Skin	1.8E-03	2.2E-03	3.4E-03	5.5E-03	1.0E-02
Spleen	3.9E-03	4.9E-03	7.8E-03	1.2E-02	2.1E-02
Testes	2.8E-03	3.6E-03	5.7E-03	8.9E-03	1.5E-02
Thymus	2.9E-03	3.6E-03	5.2E-03	8.1E-03	1.4E-02
Thyroid	2.4E-03	3.0E-03	4.9E-03	7.8E-03	1.4E-02
Uterus	7.9E-03	9.9E-03	1.5E-02	2.2E-02	3.6E-02
Remaining organs	3.8E-03	4.9E-03	7.5E-03	1.2E-02	2.0E-02
Effective dose (mSv/MBq)	8.9E-03	1.1E-02	1.6E-02	2.7E-02	5.1E-02

C.16. ^{99m}Tc-labelled monoclonal tumour-associated antibodies
^{99m}Tc

C.16.1. Biokinetic model

(C 45) Radiolabelled monoclonal antibodies against antigenic substances within or on the surface of malignant cells are used in medical research and for diagnosis and treatment of cancer. The antibody is an immunoglobulin, usually IgG_1 or IgG_{2a}, and is used either as the intact molecule (molecular weight 150 kDa) or as fragments $F(ab')_2$ (100 kDa) and Fab′ (50 kDa). Antibodies against a large number of tumour-associated antigens have been produced and investigated, but only a few are now in regular use as commercial products for diagnostic purposes.

(C 46) There is great variation in production with regard to type of antigen, type of cells used (mouse, goat, human etc.), and possible genetic modification (chimeric, humanised). There is also variation in the mode of application of the product, with regard to amount of substance administered, possible pre-treatment with unlabelled antibody or other modifying substances, route of administration (intravenous injection or infusion, subcutaneous or intraperitoneal injection etc.), type of radionuclide used as label, and method of labelling.

(C 47) In spite of these variations, certain common features in the behaviour of the antibodies can be distinguished. Directly after intravenous injection, the highest activity is seen in organs with high vascular perfusion, such as liver, spleen, bone marrow, and kidneys. Organ uptake is mainly a function of molecular size; intact molecules are taken up mainly in the liver and bone marrow, while smaller fragments concentrate to a higher degree in the kidneys. Also, the rate of degradation and elimination is mainly a function of molecular size, being more rapid with the smaller fragments.

(C 48) Based on these general properties, a set of models can be defined, assuming principal uptake in the above-mentioned organs and an even distribution of the remainder in the rest of the body. The quantitative data for uptake and elimination have been defined after an extensive survey of published reports, and are to be looked upon as typical values for the intact antibody and 'large' and 'small' fragments.

(C 49) The antibodies and fragments are metabolised within the body. The technetium thus set free is then assumed to be handled by the body according to the biokinetic model for pertechnetate (ICRP, 1987). The contribution from released technetium can be calculated as:

$$\frac{T_p - T_{eff}}{T_{eff}}$$

where T_p is the physical half-life, and T_{eff} is the effective half-life for the antibody.

C.16.2. References and further reading for ^{99m}Tc-labelled monoclonal antibodies

Bischof Delaloye, A., Delaloye, B., 1995. Radiolabelled monoclonal antibodies in tumour imaging and therapy: out of fashion? Eur. J. Nucl. Med. 22, 571–580.

Britton, K.E., Granowska, M., 1987. Radioimmunoscintigraphy in tumour identification. Cancer Surv. 6, 247–267.

Fishman, A.J., Khaw, B.A., Strauss, H.N., 1989. Quo vadis radioimmune imaging. J. Nucl. Med. 20, 1911–1915.

ICRP, 1987. Radiation dose to patients from radiopharmaceuticals. ICRP Publication 53. Ann. ICRP 18 (1–4).

C.16.3. Biokinetic data for ^{99m}Tc-labelled monoclonal antibodies

Intact antibody

Organ (S)	F_s	T (h)	a	$\widetilde{A}_s/A_0$(h)
Kidneys	0.03	24	0.5	0.23
		96	0.5	
Liver	0.50	24	0.5	3.8
		96	0.5	
Spleen	0.09	24	0.5	0.68
		96	0.5	
Red bone marrow	0.20	24	0.5	1.5
		96	0.5	
Other organs and tissues	0.18	24	0.5	1.4
		96	0.5	
Released technetium	1.0	−24	0.5	*
		−96	0.5	

*To obtain the contribution from released technetium, the cumulated activities given in the pertechnetate model should be multiplied by 0.13.

$F(ab')_2$ fragments

Organ (S)	F_s	T (h)	a	$\widetilde{A}_s/A_0$(h)
Kidneys	0.20	12	1.0	1.2
Liver	0.30	12	1.0	1.7
Spleen	0.06	12	1.0	0.35
Red bone marrow	0.10	12	1.0	0.58
Other organs and tissues	0.34	12	1.0	2.0
Released technetium	1.0	−12	1.0	*

*To obtain the contribution from released technetium, the cumulated activities given in the pertechnetate model should be multiplied by 0.33.

$F(ab')$ fragments

Organ (S)	F_s	T (h)	a	$\widetilde{A}_s/A_0$(h)
Kidneys	0.40	6.0	1.0	1.7
Liver	0.10	6.0	1.0	0.43
Spleen	0.02	6.0	1.0	0.09
Red bone marrow	0.03	6.0	1.0	0.13
Other organs and tissues	0.45	6.0	1.0	2.0
Released technetium	1.0	−6.0	1.0	*

*To obtain the contribution from released technetium, the cumulated activities given in the pertechnetate model should be multiplied by 0.50.

C.16.4. Absorbed doses for ^{99m}Tc-labelled monoclonal antibodies

Intact antibody

^{99m}Tc 6.01 h

Organ	Absorbed dose per unit activity administered (mGy/MBq)				
	Adult	15 years	10 years	5 years	1 year
Adrenals	1.0E-02	1.2E-02	1.8E-02	2.4E-02	3.7E-02
Bladder	3.7E-03	4.9E-03	6.9E-03	9.6E-03	1.6E-02
Bone surfaces	1.2E-02	1.6E-02	2.6E-02	4.4E-02	1.0E-01
Brain	1.4E-03	1.7E-03	2.6E-03	4.2E-03	7.9E-03
Breasts	2.1E-03	2.6E-03	4.3E-03	6.6E-03	1.2E-02
Gallbladder	1.5E-02	1.7E-02	2.4E-02	3.7E-02	6.1E-02
Gastrointestinal tract					
Stomach	8.4E-03	1.1E-02	1.6E-02	2.6E-02	4.6E-02
Small intestine	5.6E-03	7.0E-03	1.1E-02	1.7E-02	2.9E-02
Colon	8.9E-03	1.1E-02	1.9E-02	3.0E-02	5.4E-02
(Upper large intestine	1.2E-02	1.5E-02	2.5E-02	4.1E-02	7.3E-02)
(Lower large intestine	4.9E-03	6.4E-03	1.0E-02	1.6E-02	2.8E-02)
Heart	5.5E-03	6.9E-03	1.0E-02	1.4E-02	2.5E-02
Kidneys	1.9E-02	2.2E-02	3.2E-02	4.5E-02	7.4E-02
Liver	4.5E-02	5.8E-02	8.5E-02	1.2E-01	2.1E-01
Lungs	4.9E-03	6.3E-03	8.7E-03	1.3E-02	2.2E-02
Muscle	2.9E-03	3.7E-03	5.4E-03	7.9E-03	1.4E-02
Oesophagus	2.5E-03	3.0E-03	4.3E-03	6.5E-03	1.1E-02
Ovaries	4.0E-03	5.1E-03	7.6E-03	1.1E-02	1.9E-02
Pancreas	1.1E-02	1.4E-02	2.0E-02	3.0E-02	4.8E-02
Red marrow	1.7E-02	1.9E-02	3.0E-02	5.2E-02	1.1E-01
Salivary glands	4.2E-03	5.4E-03	7.6E-03	1.1E-02	1.7E-02
Skin	1.6E-03	1.9E-03	3.0E-03	4.7E-03	8.9E-03
Spleen	6.0E-02	8.4E-02	1.3E-01	1.9E-01	3.4E-01
Testes	1.3E-03	1.6E-03	2.6E-03	4.2E-03	7.7E-03
Thymus	2.5E-03	3.0E-03	4.3E-03	6.5E-03	1.1E-02
Thyroid	4.0E-03	6.0E-03	9.2E-03	1.9E-02	3.5E-02
Uterus	3.3E-03	4.2E-03	6.6E-03	1.0E-02	1.7E-02
Remaining organs	3.1E-03	4.0E-03	5.8E-03	8.7E-03	1.4E-02
Effective dose (mSv/MBq)	9.8E-03	1.2E-02	1.9E-02	3.0E-02	5.4E-02

$F(ab')_2$ fragments

^{99m}Tc 6.01 h

Organ	Absorbed dose per unit activity administered (mGy/MBq)				
	Adult	15 years	10 years	5 years	1 year
Adrenals	9.1E-03	1.1E-02	1.7E-02	2.4E-02	4.0E-02
Bladder	7.3E-03	9.6E-03	1.3E-02	1.6E-02	2.8E-02
Bone surfaces	8.3E-03	1.0E-02	1.6E-02	2.6E-02	5.6E-02
Brain	1.8E-03	2.3E-03	3.6E-03	5.8E-03	1.0E-02
Breasts	2.0E-03	2.6E-03	4.0E-03	6.4E-03	1.2E-02
Gallbladder	1.1E-02	1.3E-02	1.9E-02	2.9E-02	4.6E-02
Gastrointestinal tract					
Stomach	1.3E-02	1.6E-02	2.3E-02	3.7E-02	7.0E-02
Small intestine	8.1E-03	1.0E-02	1.6E-02	2.4E-02	4.2E-02
Colon	1.6E-02	2.2E-02	3.6E-02	5.7E-02	1.0E-01
(Upper large intestine	2.2E-02	2.9E-02	4.8E-02	7.7E-02	1.4E-01)
(Lower large intestine	9.0E-03	1.2E-02	1.9E-02	3.0E-02	5.5E-02)
Heart	4.4E-03	5.6E-03	8.3E-03	1.2E-02	2.1E-02
Kidneys	6.2E-02	7.4E-02	1.0E-01	1.5E-01	2.5E-01
Liver	2.3E-02	2.9E-02	4.3E-02	6.1E-02	1.1E-01
Lungs	3.9E-03	5.1E-03	7.3E-03	1.1E-02	1.9E-02
Muscles	3.3E-03	4.1E-03	6.0E-03	8.9E-03	1.6E-02
Oesophagus	2.6E-03	3.3E-03	4.8E-03	7.5E-03	1.3E-02
Ovaries	5.6E-03	7.1E-03	1.1E-02	1.6E-02	2.7E-02
Pancreas	9.4E-03	1.2E-02	1.7E-02	2.5E-02	4.1E-02
Red marrow	8.7E-03	9.7E-03	1.5E-02	2.5E-02	4.8E-02
Salivary glands	6.4E-03	7.2E-03	1.1E-02	1.6E-02	2.6E-02
Skin	1.8E-03	2.2E-03	3.5E-03	5.5E-03	1.0E-02
Spleen	3.4E-02	4.7E-02	7.1E-02	1.1E-01	1.9E-01
Testes	2.0E-03	2.6E-03	4.0E-03	6.3E-03	1.2E-02
Thymus	2.6E-03	3.3E-03	4.8E-03	7.5E-03	1.3E-02
Thyroid	8.5E-03	1.3E-02	2.0E-02	4.3E-02	8.0E-02
Uterus	4.8E-03	6.0E-03	9.3E-03	1.4E-02	2.4E-02
Remaining organs	3.6E-03	4.5E-03	6.8E-03	1.0E-02	1.8E-02
Effective dose (mSv/MBq)	9.7E-03	1.2E-02	1.8E-02	2.9E-02	5.2E-02

F(ab′) fragments

^{99m}Tc 6.01 h

Organ	Absorbed dose per unit activity administered (mGy/MBq)				
	Adult	15 years	10 years	5 years	1 year
Adrenals	8.4E-03	1.1E-02	1.6E-02	2.4E-02	4.2E-02
Bladder	1.0E-02	1.3E-02	1.7E-02	2.0E-02	3.7E-02
Bone surfaces	6.3E-03	7.5E-03	1.1E-02	1.7E-02	3.2E-02
Brain	2.0E-03	2.5E-03	4.1E-03	6.5E-03	1.2E-02
Breasts	1.9E-03	2.5E-03	3.8E-03	6.0E-03	1.1E-02
Gallbladder	8.7E-03	1.1E-02	1.7E-02	2.4E-02	3.6E-02
Gastrointestinal tract					
Stomach	1.6E-02	2.1E-02	2.9E-02	4.6E-02	9.0E-02
Small intestine	1.0E-02	1.3E-02	2.0E-02	3.0E-02	5.2E-02
Colon	2.3E-02	3.0E-02	4.9E-02	8.0E-02	1.5E-01
(Upper large intestine	3.1E-02	4.0E-02	6.6E-02	1.1E-01	2.0E-01)
(Lower large intestine	1.2E-02	1.6E-02	2.6E-02	4.1E-02	7.6E-02)
Heart	3.7E-03	4.7E-03	7.1E-03	1.1E-02	1.8E-02
Kidneys	8.9E-02	1.1E-01	1.5E-01	2.1E-01	3.7E-01
Liver	8.7E-03	1.1E-02	1.7E-02	2.4E-02	4.0E-02
Lungs	3.1E-03	4.2E-03	6.2E-03	9.5E-03	1.7E-02
Muscles	3.4E-03	4.2E-03	6.2E-03	9.4E-03	1.7E-02
Oesophagus	2.6E-03	3.3E-03	4.9E-03	7.8E-03	1.4E-02
Ovaries	6.8E-03	8.6E-03	1.3E-02	1.9E-02	3.3E-02
Pancreas	8.1E-03	1.0E-02	1.5E-02	2.2E-02	3.5E-02
Red marrow	4.7E-03	5.5E-03	8.1E-03	1.2E-02	2.0E-02
Salivary glands	7.9E-03	9.8E-03	1.4E-02	1.9E-02	3.1E-02
Skin	1.9E-03	2.3E-03	3.7E-03	5.9E-03	1.1E-02
Spleen	1.4E-02	1.8E-02	2.8E-02	4.1E-02	7.0E-02
Testes	2.5E-03	3.2E-03	4.9E-03	7.5E-03	1.4E-02
Thymus	2.6E-03	3.3E-03	4.9E-03	7.8E-03	1.4E-02
Thyroid	1.2E-02	1.9E-02	2.9E-02	6.2E-02	1.2E-01
Uterus	5.8E-03	7.3E-03	1.1E-02	1.7E-02	2.8E-02
Remaining organs	3.7E-03	4.6E-03	6.9E-03	1.0E-02	1.8E-02
Effective dose (mSv/MBq)	1.1E-02	1.4E-02	2.0E-02	3.2E-02	5.9E-02

C.17. ^{99m}Tc-labelled small colloids (intratumoural injection)
^{99m}Tc

C.17.1. Biokinetic model

(C 50) The typical procedure is to inject approximately 20 MBq ^{99m}Tc-colloid immediately adjacent to the breast tumour that is later to be removed. The patient is investigated with a gamma camera 4 h after injection and then operated on for the removal of the tumour very shortly afterwards. If no uptake of ^{99m}Tc in the lymph nodes is seen on the scan, the tumour and the site(s) of injection of the radioactivity are removed surgically. If lymph node uptake of activity is found, a more radical operation is performed.

(C 51) In either situation, the injected ^{99m}Tc-colloid is removed in its entirety by approximately 6 h after injection (this may be extended to 18 h in some circumstances). The only significant absorbed dose of radiation is that to surrounding tissues, mainly lung, as a result of irradiation from the local deposit of radionuclide in the breast during the few hours of exposure. This dose is generally considered to be very small.

(C 52) Current ICRP dosimetric models do not permit calculations of dose from breast as a source organ, and because the doses are likely to be very small, the Task Group does not consider it necessary to develop a new dosimetric model in which breast is treated as a source organ.

(C 53) Leakage of radionuclide from the injection site into the systemic circulation is not considered likely; should it happen, such leakage would be covered by the existing ^{99m}Tc-colloid model.

C.17.2. Further reading for ^{99m}Tc-labelled small collids

Bronskill, M.J., 1983. Radiation dose estimates for interstitial radiocolloid lymphoscintigraphy. Small colloids Semin. Nucl. Med. 13 (1), 20–25.

Eshima, D., Fauconnier, T., Eshima, L., et al., 2000. Radiopharmaceuticals for lymphoscintigraphy; including dosimetry and radiation considerations. Semin. Nucl. med. 30 (1), 25–32.

Wilhelm, A.J., Mijnhout, G.S., Franssen, .J., 1999. Eur. J.Nucl. Med. 26, S36–S42.

C.17.3. Biokinetic data for ^{99m}Tc-labelled small colloids

Organ (S)	F_s	T (h)	a	$\widetilde{A}_s/A_0$(h)
Time to removal: 6 h				
Breast	1.0			4.3
Time to removal: 18 h				
Breast	1.0			7.6

C.17.4. Absorbed doses for ^{99m}Tc-labelled small colloids

Intratumoural injection

^{99m}Tc 6.01 h

Organ	Absorbed dose per unit activity administered (mGy/MBq)			
	6 h to removal		18 h to removal	
	Adult	15 years	Adult	15 years
Adrenals	7.9E-04	9.3E-04	1.4E-03	1.6E-03
Bladder	2.1E-05	3.9E-05	3.6E-05	6.8E-05
Bone surfaces	1.2E-03	1.5E-03	2.1E-03	2.6E-03
Brain	4.9E-05	5.8E-05	8.7E-05	1.0E-04
Breasts (remaining*)	3.6E-03	3.9E-03	6.4E-03	6.9E-03
Gallbladder	5.3E-04	7.2E-04	9.3E-04	1.3E-03
Gastrointestinal tract				
Stomach	9.2E-04	1.3E-03	1.6E-03	2.3E-03
Small intestine	1.1E-04	1.5E-04	2.0E-04	2.7E-04
Colon	8.3E-05	1.9E-04	1.4E-04	3.3E-04
(Upper large intestine	1.2E-04	2.8E-04	2.0E-04	4.9E-04)
(Lower large intestine	3.8E-05	7.0E-05	6.6E-05	1.2E-04)
Heart	4.1E-03	5.2E-03	7.1E-03	9.1E-03
Kidneys	3.1E-04	4.2E-04	5.4E-04	7.3E-04
Liver	1.1E-03	1.4E-03	1.9E-03	2.4E-03
Lungs	3.6E-03	3.9E-03	6.4E-03	6.9E-03
Muscles	6.6E-04	8.3E-04	1.2E-03	1.5E-03
Oesophagus	3.6E-03	5.0E-03	6.2E-03	8.7E-03
Ovaries	4.1E-05	4.8E-05	7.1E-05	8.3E-05
Pancreas	9.7E-04	1.1E-03	1.7E-03	2.0E-03
Red marrow	8.6E-04	9.2E-04	1.5E-03	1.6E-03
Skin	1.2E-03	1.4E-03	2.1E-03	2.4E-03
Spleen	6.8E-04	8.3E-04	1.2E-03	1.5E-03
Thymus	3.6E-03	5.0E-03	6.2E-03	8.7E-03
Thyroid	4.7E-04	6.2E-04	8.2E-04	1.1E-03
Uterus	4.1E-05	6.4E-05	7.1E-05	1.1E-04
Remaining organs	6.6E-04	8.3E-04	1.2E-03	1.5E-03
Effective dose (mSv/MBq)	1.2E-03	1.4E-03	2.0E-03	2.4E-03

In the model, it is assumed that no leakage occurs.

* Dose to the remaining breast has been assumed to be equal to the dose to the lungs.

C.18. ^{99m}Tc-tetrofosmin

^{99m}Tc

C.18.1. Biokinetic model

(C 54) Technetium-99m-1,2-bis[bis(2-ethoxyethyl)phosphino]ethane is a lipophilic technetium phosphine dioxo cation($[^{99m}Tc(tetrofosmin)_2O_2]^+$) prepared from a freeze-dried kit (Myoview). It is used for studies of myocardial perfusion. Technetium-99m-tetrofosmin accumulates in viable myocardial tissue in proportion to regional blood flow in a manner similar to thallous chloride. After intravenous injection, the substance is cleared rapidly from the blood (<5% left by 10 min) and taken up predominantly in muscular tissues (including heart), liver, kidneys, and salivary glands, with a smaller amount in the thyroid.

(C 55) Biodistribution is generally similar to that of technetium-99m-MIBI (Cardiolite; ICRP, 1991b), but there are some differences that have a bearing on diagnostic technique. Technetium-99m-tetrofosmin shows a heart uptake of 1.2% and is cleared very rapidly from the liver (<4.5% left by 1 h) and lungs. More than 80% of the substance is excreted in 48 h, and the faecal:urinary excretion is 54:46. When the substance is injected in conjunction with an exercise stress test, there is a considerable increase of the uptake in skeletal muscle but little change in heart uptake. Initial rates of urinary and faecal clearance are lower than at rest and the faecal:urinary excretion ratio is 46:54.

(C 56) The quantitative figures for uptake and excretion in man, presented in the table below, are based on reports by Smith et al. (1992) and Higley et al. (1993). Substance excreted by the hepatobiliary system is assumed to leave the body via the intestinal tract according to the *Publication 30* gastrointestinal tract model (ICRP, 1979). The kidney–bladder model presented in *Publication 53* (ICRP, 1987) is used for the substance excreted in urine.

C.18.2. References for ^{99m}Tc-tetrofosmin

Higley, B., Smith, F.W., Smith, T., Gemmell, H.G., Gupta, P.D., Gvozdanovic, D.V., Graham, D., Hinge, D., Davidson, J., Lahiri, A., 1993. Technetium-99m-1,2-bis[bis(2-ethoxyethyl) phosphino]ethane: human biodistribution, dosimetry and safety of a new myocardial perfusion imaging agent. J. Nucl. Med. 34, 30–38.

ICRP, 1979. Limits for intakes of radionuclides by workers. ICRP Publication 30, Part 1. Ann. ICRP 2 (3/4).

ICRP, 1987. Radiation dose to patients from radiopharmaceuticals. ICRP Publication 53. Ann. ICRP 18 (1–4).

ICRP, 1991b. Radiation dose to patients from radiopharmaceuticals. Addendum 1 to ICRP Publication 53, in: Radiological protection in biomedical research. ICRP Publication 62. Ann. ICRP 22 (3).

Smith, T., Lahiri, A., Gemmell, H.G., Davidson, J., Smith, F.W., Pickett, R.D., Higley, B., 1992. Dosimetry of ^{99m}Tc-P53 a new myocardial perfusion imaging agent. In: Schlafke-Stelson, A., Watson, E.E. (Eds.), Fifth International Radiopharmaceutical Dosimetry Symposium. CONF-910529. Oak Ridge Associated Universities, Oak Ridge, TN, pp. 467–481.

C.18.3. Biokinetic data for ^{99m}Tc-tetrofosmin

Organ (S)	F_s	T (h)	a	$\widetilde{A}_s/A_0$(h)
Resting subject				
Thyroid	0.003	2.0	1.00	0.0064
Salivary glands	0.015	24	1.00	0.10
Heart wall	0.012	4.0	0.67	0.055
		24	0.33	
Kidneys	0.07	1.0	0.70	0.21
		24	0.30	
Liver	0.10	0.5	0.85	0.088
		2.0	0.15	
Other organs and tissues	0.80	0.33	0.15	4.8
		24	0.85	
Gallbladder contents	0.18			0.24
Gastrointestinal tract contents				
Small intestine	0.54			0.51
Upper large intestine	0.54			0.67
Lower large intestine	0.54			0.33
Urinary bladder contents	0.46			
Adult, 15 years, 10 years				0.33
5 years				0.28
1 year				0.18
Exercise				
Thyroid	0.002	2.0	1.00	0.0044
Salivary glands	0.01	24	1.00	0.070
Heart wall	0.013	4.0	0.67	0.060
		24	0.33	
Kidneys	0.05	1.0	0.70	0.15
		24	0.30	
Liver	0.05	0.5	0.85	0.045
		2.0	0.15	
Other organs and tissues	0.875	0.33	0.05	5.8
		24	0.95	
Gallbladder contents	0.153			0.18
Gastrointestinal tract contents				
Small intestine	0.46			0.36
Upper large intestine	0.46			0.46
Lower large intestine	0.46			0.23
Urinary bladder contents	0.54			
Adult, 15 years, 10 years				0.25
5 years				0.22
1 year				0.14

C.18.4. Absorbed doses for ^{99m}Tc-tetrofosmin

Resting subject

^{99m}Tc 6.01 h

Organ	Absorbed dose per unit activity administered (mGy/MBq)				
	Adult	15 years	10 years	5 years	1 year
Adrenals	4.4E-03	5.5E-03	8.3E-03	1.2E-02	2.2E-02
Bladder	1.4E-02	1.8E-02	2.7E-02	3.5E-02	4.9E-02
Bone surfaces	6.3E-03	7.5E-03	1.1E-02	1.6E-02	3.0E-02
Brain	2.7E-03	3.4E-03	5.5E-03	8.9E-03	1.6E-02
Breasts	2.3E-03	2.9E-03	4.3E-03	6.9E-03	1.3E-02
Gallbladder	2.7E-02	3.2E-02	4.2E-02	7.3E-02	2.3E-01
Gastrointestinal tract					
Stomach	4.6E-03	6.1E-03	9.8E-03	1.4E-02	2.4E-02
Small intestine	1.1E-02	1.4E-02	2.2E-02	3.4E-02	6.1E-02
Colon	1.8E-02	2.2E-02	3.7E-02	5.8E-02	1.1E-01
(Upper large intestine	2.0E-02	2.5E-02	4.1E-02	6.5E-02	1.2E-01)
(Lower large intestine	1.5E-02	1.9E-02	3.2E-02	4.9E-02	9.2E-02)
Heart	5.2E-03	6.5E-03	9.7E-03	1.5E-02	2.5E-02
Kidneys	1.0E-02	1.2E-02	1.7E-02	2.5E-02	4.3E-02
Liver	3.3E-03	4.1E-03	6.3E-03	9.2E-03	1.6E-02
Lungs	3.2E-03	4.2E-03	6.3E-03	9.6E-03	1.7E-02
Muscles	3.5E-03	4.3E-03	6.5E-03	9.9E-03	1.8E-02
Oesophagus	3.3E-03	4.2E-03	6.2E-03	9.6E-03	1.7E-02
Ovaries	7.7E-03	9.6E-03	1.4E-02	2.1E-02	3.6E-02
Pancreas	5.0E-03	6.3E-03	9.8E-03	1.5E-02	2.5E-02
Red marrow	3.9E-03	4.7E-03	7.1E-03	1.0E-02	1.7E-02
Skin	1.4E-02	1.8E-02	2.4E-02	3.4E-02	5.2E-02
Spleen	4.1E-03	5.2E-03	8.2E-03	1.2E-02	2.2E-02
Testes	3.4E-03	4.3E-03	6.6E-03	1.0E-02	1.8E-02
Thymus	3.3E-03	4.2E-03	6.2E-03	9.6E-03	1.7E-02
Thyroid	4.7E-03	6.8E-03	1.1E-02	2.0E-02	3.7E-02
Uterus	7.0E-03	8.7E-03	1.3E-02	2.0E-02	3.2E-02
Remaining organs	3.8E-03	4.9E-03	7.5E-03	1.2E-02	2.0E-02
Effective dose (mSv/MBq)	6.9E-03	8.8E-03	1.3E-02	2.1E-02	3.9E-02

Exercise

^{99m}Tc 6.01 h

Organ	Absorbed dose per unit activity administered (mGy/MBq)				
	Adult	15 years	10 years	5 years	1 year
Adrenals	4.4E-03	5.5E-03	8.3E-03	1.2E-02	2.2E-02
Bladder	1.4E-02	1.8E-02	2.7E-02	3.5E-02	4.9E-02
Bone surfaces	6.3E-03	7.5E-03	1.1E-02	1.6E-02	3.0E-02
Brain	2.7E-03	3.4E-03	5.5E-03	8.9E-03	1.6E-02
Breasts	2.3E-03	2.9E-03	4.3E-03	6.9E-03	1.3E-02
Gallbladder	2.7E-02	3.2E-02	4.2E-02	7.3E-02	2.3E-01
Gastrointestinal tract					
Stomach	4.6E-03	6.1E-03	9.8E-03	1.4E-02	2.4E-02
Small intestine	1.1E-02	1.4E-02	2.2E-02	3.4E-02	6.1E-02
Colon	1.8E-02	2.2E-02	3.7E-02	5.8E-02	1.1E-01
(Upper large intestine	2.0E-02	2.5E-02	4.1E-02	6.5E-02	1.2E-01)
(Lower large intestine	1.5E-02	1.9E-02	3.2E-02	4.9E-02	9.2E-02)
Heart	5.2E-03	6.5E-03	9.7E-03	1.5E-02	2.5E-02
Kidneys	1.0E-02	1.2E-02	1.7E-02	2.5E-02	4.3E-02
Liver	3.3E-03	4.1E-03	6.3E-03	9.2E-03	1.6E-02
Lungs	3.2E-03	4.2E-03	6.3E-03	9.6E-03	1.7E-02
Muscles	3.5E-03	4.3E-03	6.5E-03	9.9E-03	1.8E-02
Oesophagus	3.3E-03	4.2E-03	6.2E-03	9.6E-03	1.7E-02
Ovaries	7.7E-03	9.6E-03	1.4E-02	2.1E-02	3.6E-02
Pancreas	5.0E-03	6.3E-03	9.8E-03	1.5E-02	2.5E-02
Red marrow	3.9E-03	4.7E-03	7.1E-03	1.0E-02	1.7E-02
Skin	1.4E-02	1.8E-02	2.4E-02	3.4E-02	5.2E-02
Spleen	4.1E-03	5.2E-03	8.2E-03	1.2E-02	2.2E-02
Testes	3.4E-03	4.3E-03	6.6E-03	1.0E-02	1.8E-02
Thymus	3.3E-03	4.2E-03	6.2E-03	9.6E-03	1.7E-02
Thyroid	4.7E-03	6.8E-03	1.1E-02	2.0E-02	3.7E-02
Uterus	7.0E-03	8.7E-03	1.3E-02	2.0E-02	3.2E-02
Remaining organs	3.8E-03	4.9E-03	7.5E-03	1.2E-02	2.0E-02
Effective dose (mSv/MBq)	6.9E-03	8.8E-03	1.3E-02	2.1E-02	3.9E-02

C.19. ^{111}In-labelled monoclonal tumour-associated antibodies
^{111}In

C.19.1. Biokinetic model

(C 57) The models for indium-labelled monoclonal tumour-associated antibodies and fragments are the same as those used for the corresponding technetium-labelled substances, with the modification that released indium is handled by the body according to the model for ionic indium (ICRP, 1987).

> This biokinetic model is not intended to apply to therapeutic use of the substance.

C.19.2. References and further reading for ^{111}In-labelled monoclonal antibodies

Bischof Delaloye, A., Delaloye, B., 1995. Radiolabelled monoclonal antibodies in tumour imaging and therapy: out of fashion? Eur. J. Nucl. Med. 22, 571–580.

Britton, K.E., Granowska, M., 1987. Radioimmunoscintigraphy in tumour identification. Cancer Surv. 6, 247–267.

Fishman, A.J., Khaw, B.A., Strauss, H.N., 1989. Quo vadis radioimmune imaging. J. Nucl. Med. 20, 1911–1915.

ICRP, 1987. Radiation dose to patients from radiopharmaceuticals. ICRP Publication 53. Ann. ICRP 18 (1–4).

C.19.3. Biokinetic data for ^{111}In-labelled monoclonal antibodies

Intact antibody

Organ (S)	F_s	T (h)	a	$\widetilde{A}_s/A_0$(h)
Kidneys	0.03	24	0.5	1.2
		96	0.5	
Liver	0.50	24	0.5	21
		96	0.5	
Spleen	0.09	24	0.5	3.7
		96	0.5	
Red bone marrow	0.20	24	0.5	8.3
		96	0.5	
Other organs and tissues	0.18	24	0.5	7.5
		96	0.5	
Released indium	1.0	−24	0.5	*
		−96	0.5	

*To obtain the contribution from released indium, the cumulated activities given in the model for ionic indium should be multiplied by 0.58.

F(ab′)$_2$ fragments

Organ (S)	F_s	T (h)	a	$\widetilde{A}_s/A_0$(h)
Kidneys	0.20	12	1.0	2.9
Liver	0.30	12	1.0	4.4
Spleen	0.06	12	1.0	0.88
Red bone marrow	0.10	12	1.0	1.5
Other organs and tissues	0.34	12	1.0	5.0
Released indium	1.0	−12	1.0	*

*To obtain the contribution from released indium, the cumulated activities given in the model for ionic indium should be multiplied by 0.85.

F(ab′) fragments

Organ (S)	F_s	T (h)	a	$\widetilde{A}_s/A_0$(h)
Kidneys	0.40	6.0	1.0	3.2
Liver	0.10	6.0	1.0	0.80
Spleen	0.02	6.0	1.0	0.16
Red bone marrow	0.03	6.0	1.0	0.24
Other organs and tissues	0.45	6.0	1.0	3.6
Released indium	1.0	−6.0	1.0	*

*To obtain the contribution from released indium, the cumulated activities given in the model for ionic indium should be multiplied by 0.92.

C.19.4. Absorbed doses for ^{111}In-labelled monoclonal antibodies

Intact antibody

^{111}In 67.9 h

Organ	Absorbed dose per unit activity administered (mGy/MBq)				
	Adult	15 years	10 years	5 years	1 year
Adrenals	3.1E-01	3.7E-01	5.3E-01	7.2E-01	1.2E+00
Bladder	7.8E-02	9.9E-02	1.6E-01	2.4E-01	4.1E-01
Bone surfaces	3.2E-01	3.6E-01	5.7E-01	9.4E-01	1.6E+00
Brain	5.7E-02	7.3E-02	1.1E-01	1.8E-01	3.3E-01
Breasts	6.9E-02	8.5E-02	1.4E-01	2.1E-01	3.8E-01
Gallbladder	3.8E-01	4.3E-01	6.0E-01	9.2E-01	1.6E+00
Gastrointestinal tract					
Stomach	1.6E-01	2.0E-01	3.1E-01	4.8E-01	8.3E-01
Small intestine	1.5E-01	1.8E-01	2.8E-01	4.3E-01	7.1E-01
Colon	1.4E-01	1.7E-01	2.7E-01	4.2E-01	6.9E-01
(Upper large intestine	1.6E-01	2.0E-01	3.2E-01	5.1E-01	8.4E-01)
(Lower large intestine	1.1E-01	1.4E-01	2.1E-01	3.0E-01	4.9E-01)
Heart	1.6E-01	2.0E-01	2.9E-01	4.1E-01	7.3E-01
Kidneys	8.0E-01	9.5E-01	1.3E+00	1.9E+00	3.1E+00
Liver	1.1E+00	1.4E+00	2.0E+00	2.8E+00	4.8E+00
Lungs	1.4E-01	1.8E-01	2.6E-01	3.8E-01	6.7E-01
Muscles	9.6E-02	1.2E-01	1.8E-01	2.6E-01	4.8E-01
Oesophagus	8.6E-02	1.0E-01	1.5E-01	2.2E-01	3.8E-01
Ovaries	1.2E-01	1.5E-01	2.2E-01	3.3E-01	5.5E-01
Pancreas	2.9E-01	3.5E-01	5.3E-01	8.0E-01	1.3E+00
Red marrow	4.1E-01	4.6E-01	6.9E-01	1.2E+00	2.8E+00
Skin	5.4E-02	6.5E-02	1.0E-01	1.6E-01	3.1E-01
Spleen	1.1E+00	1.5E+00	2.2E+00	3.4E+00	5.9E+00
Testes	4.8E-02	6.2E-02	9.5E-02	1.5E-01	2.7E-01
Thymus	8.6E-02	1.0E-01	1.5E-01	2.2E-01	3.8E-01
Thyroid	6.6E-02	8.2E-02	1.2E-01	2.0E-01	3.6E-01
Uterus	1.1E-01	1.3E-01	2.0E-01	3.0E-01	5.0E-01
Remaining organs	1.0E-01	1.3E-01	2.0E-01	3.0E-01	5.1E-01
Effective dose (mSv/MBq)	2.2E-01	2.7E-01	4.1E-01	6.4E-01	1.2E+00

$F(ab')_2$ fragments

^{111}In 67.9 h

Organ	Absorbed dose per unit activity administered (mGy/MBq)				
	Adult	15 years	10 years	5 years	1 year
Adrenals	2.7E-01	3.3E-01	4.7E-01	6.6E-01	1.1E+00
Bladder	8.8E-02	1.1E-01	1.7E-01	2.6E-01	4.4E-01
Bone surfaces	3.2E-01	3.6E-01	5.7E-01	9.3E-01	1.6E+00
Brain	6.5E-02	8.3E-02	1.3E-01	2.0E-01	3.8E-01
Breasts	6.6E-02	8.2E-02	1.3E-01	1.9E-01	3.5E-01
Gallbladder	2.9E-01	3.3E-01	4.6E-01	7.0E-01	1.1E+00
Gastrointestinal tract					
Stomach	1.4E-01	1.7E-01	2.7E-01	4.0E-01	6.8E-01
Small intestine	1.5E-01	1.8E-01	2.8E-01	4.1E-01	6.7E-01
Colon	1.4E-01	1.7E-01	2.6E-01	3.9E-01	6.4E-01
(Upper large intestine	1.5E-01	1.9E-01	2.9E-01	4.5E-01	7.3E-01)
(Lower large intestine	1.2E-01	1.5E-01	2.2E-01	3.2E-01	5.2E-01)
Heart	1.4E-01	1.7E-01	2.5E-01	3.5E-01	6.2E-01
Kidneys	1.2E+00	1.4E+00	1.9E+00	2.7E+00	4.6E+00
Liver	6.7E-01	8.6E-01	1.3E+00	1.7E+00	3.0E+00
Lungs	1.2E-01	1.6E-01	2.3E-01	3.3E-01	5.9E-01
Muscles	9.5E-02	1.2E-01	1.8E-01	2.6E-01	4.7E-01
Oesophagus	8.7E-02	1.1E-01	1.5E-01	2.3E-01	4.0E-01
Ovaries	1.3E-01	1.6E-01	2.3E-01	3.4E-01	5.7E-01
Pancreas	2.3E-01	2.8E-01	4.1E-01	6.2E-01	1.0E+00
Red marrow	4.0E-01	4.5E-01	6.8E-01	1.2E+00	2.7E+00
Skin	5.6E-02	6.7E-02	1.1E-01	1.7E-01	3.1E-01
Spleen	4.9E-01	6.7E-01	1.0E+00	1.5E+00	2.6E+00
Testes	5.7E-02	7.3E-02	1.1E-01	1.7E-01	3.1E-01
Thymus	8.7E-02	1.1E-01	1.5E-01	2.3E-01	4.0E-01
Thyroid	7.5E-02	9.3E-02	1.4E-01	2.2E-01	4.0E-01
Uterus	1.2E-01	1.4E-01	2.1E-01	3.2E-01	5.2E-01
Remaining organs	9.9E-02	1.2E-01	1.8E-01	2.7E-01	4.8E-01
Effective dose (mSv/MBq)	2.0E-01	2.4E-01	3.6E-01	5.5E-01	1.0E+00

F(ab′) fragments

^{111}In 67.9 h

Organ	Absorbed dose per unit activity administered (mGy/MBq)				
	Adult	15 years	10 years	5 years	1 year
Adrenals	2.6E-01	3.2E-01	4.6E-01	6.4E-01	1.1E+00
Bladder	9.0E-02	1.1E-01	1.7E-01	2.6E-01	4.4E-01
Bone surfaces	3.2E-01	3.6E-01	5.7E-01	9.4E-01	1.6E+00
Brain	6.7E-02	8.5E-02	1.3E-01	2.1E-01	3.9E-01
Breasts	6.5E-02	8.0E-02	1.2E-01	1.9E-01	3.4E-01
Gallbladder	2.7E-01	3.0E-01	4.3E-01	6.5E-01	1.0E+00
Gastrointestinal tract					
Stomach	1.3E-01	1.6E-01	2.5E-01	3.8E-01	6.4E-01
Small intestine	1.5E-01	1.8E-01	2.7E-01	4.0E-01	6.6E-01
Colon	1.4E-01	1.7E-01	2.5E-01	3.9E-01	6.2E-01
(Upper large intestine	1.5E-01	1.8E-01	2.8E-01	4.4E-01	7.0E-01)
(Lower large intestine	1.2E-01	1.5E-01	2.2E-01	3.2E-01	5.2E-01)
Heart	1.3E-01	1.6E-01	2.4E-01	3.4E-01	5.9E-01
Kidneys	1.3E+00	1.5E+00	2.0E+00	2.9E+00	4.9E+00
Liver	5.9E-01	7.5E-01	1.1E+00	1.5E+00	2.6E+00
Lungs	1.2E-01	1.5E-01	2.2E-01	3.2E-01	5.7E-01
Muscles	9.5E-02	1.2E-01	1.7E-01	2.6E-01	4.7E-01
Oesophagus	8.7E-02	1.1E-01	1.5E-01	2.3E-01	4.0E-01
Ovaries	1.3E-01	1.6E-01	2.3E-01	3.5E-01	5.7E-01
Pancreas	2.2E-01	2.6E-01	3.9E-01	5.8E-01	9.4E-01
Red marrow	4.0E-01	4.5E-01	6.9E-01	1.2E+00	2.8E+00
Skin	5.6E-02	6.7E-02	1.1E-01	1.7E-01	3.1E-01
Spleen	3.4E-01	4.5E-01	6.8E-01	1.0E+00	1.7E+00
Testes	5.9E-02	7.5E-02	1.1E-01	1.8E-01	3.1E-01
Thymus	8.7E-02	1.1E-01	1.5E-01	2.3E-01	4.0E-01
Thyroid	7.6E-02	9.5E-02	1.4E-01	2.3E-01	4.0E-01
Uterus	1.2E-01	1.4E-01	2.1E-01	3.2E-01	5.2E-01
Remaining organs	9.7E-02	1.2E-01	1.8E-01	2.7E-01	4.7E-01
Effective dose (mSv/MBq)	2.0E-01	2.4E-01	3.5E-01	5.4E-01	1.0E+00

C.20. ^{111}In-octreotide
^{111}In

C.20.1. Biokinetic model

(C 58) In-111-DTPA-D-Phe-1-octreotide (pentatreotide) is a peptide composed of eight amino acids and is an analogue of the active part of the peptide hormone somatostatin. Somatostatin is present in many neurons and endocrine cells, mainly in the brain and in the gastrointestinal tract, and has an inhibitory effect on growth hormone secretion. In-111-DTPA-D-Phe-1-octreotide may be used for visualising tumours containing somatostatin receptors including neuroblastoma, some types of endocrine gastroenteropancreatic tumours, small cell lung cancer, and breast cancer.

(C 59) The biokinetic model is based on scintigraphic studies of a total of 24 humans by Krenning et al. (1992), Forssell Aronsson et al. (1999), and Leide-Svegborn et al. (1999). Tissue samples have been analysed by Forssell Aronsson et al. (1995). These studies have demonstrated uptake in liver, spleen, kidneys, and thyroid. In some patients, there may also be uptake in the pituitary gland. There is a wide variation in uptake values between the subjects. The main route of excretion is via the kidneys and less than 2% is excreted in faeces. Although some degradation seems to occur, the great majority of activity excreted in urine is still peptide bound, even after 48 h. The biokinetic data come from patients with carcinoid tumours and neuroendocrine tumours in the gastrointestinal tract. Uptake in tumour tissue present in any given organ may therefore be included in the published organ uptake values.

(C 60) Intravenously injected In-111-DTPA-D-Phe-1-octreotide is assumed to be taken up immediately in liver, spleen, kidneys, and thyroid, while the rest is assumed to be distributed homogeneously in the remainder of the body. The experimentally found retention data are best described by mono- or bi-exponential functions. The small amount of excretion via the gastrointestinal tract is not included in the model, since its contribution to the absorbed dose in normal circumstances is negligible. According to Claessens et al. (1995) and Koizumi et al. (1989), there is detachment of part of the molecule giving an ^{111}In-substance with long-term retention. The same half-time as for ^{111}In-ions (ICRP, 1987) is assumed for this long-term retention. An observed excretion of 85% via urine after 24 h fits well with the model adopted.

C.20.2. References and further reading for ^{111}In-octreotide

Bajc, M., Palmer, J., Ohlsson, T., Edenbrandt, L., 1994. Distribution and dosimetry of ^{111}In DTPA-D-Phe-octreotide in man assessed by whole body scintigraphy. Acta Radiol. 35, 53–57.

Claessens, R.A.M.J., Koenders, E.B., Boerman, O.C., Oyen, W.J., Borm, G.F., van den Meer, J.W., Corstens, F.H., 1995. Dissociation of indium from indium-111-labelled diethylene triamine pentaacetic acid conjugated non-specific polyclonal human immunoglobulin G in inflammatory foci. Eur. J. Nucl. Med. 22, 212–219.

Forssell Aronsson, E., Fjälling, M., Nilsson, O., Tisell, L.E., Wängberg, B., Ahlman, H., 1995. Indium-111 activity concentration in tissue samples after intravenous injection of indium-111-DTPA-D-Phe-1-octreotide. J. Nucl. Med. 36, 7–12.

Forssell Aronsson, E., Lanhede, B., Fjälling, M., Wängberg, B., Tisell, L.E., Ahlman, H., Mattsson, S., 1999. Pharmacokinetics and dosimetry of ^{111}In-DTPA-D-Phe-1-octreotide in patients with neuroendocrine tumours. In: Schlafke-Stelson, A.T., Stabin, M.G., Sparks, R.B. (Eds.), Proceedings of the Sixth International Radiopharmaceutical Dosimetry Symposium ORISE 99-0164. Oak Ridge Associated Universities, Oak Ridge, TN, pp. 643–655.

ICRP, 1987. Radiation dose to patients from radiopharmaceuticals. ICRP Publication 53. Ann. ICRP 18 (1–4).

Koizumi, M., Endo, K., Watanabe, Y., Saga, T., Sakahara, H., Konishi, H., Yamamuro, T., Toyama, S., 1989. Pharmacokinetics of internally labeled monoclonal antibodies as a gold standard: comparison of biodistribution of 75Se-, 111In-, and 125I-labeled monoclonal antibodies in osteogenic sarcoma xenografts in nude mice. Cancer Res. 49, 1752–1757.

Krenning, E.P., Bakker, W.H., Kooij, P.P.M., Breeman, W.A.P., Oei, H.Y., de Jong, M., Reubi, J.C., Visser, T.J., Bruns, C., Kwekkeboom, D.J., Reijs, A.E.M., van Hagen, P.M., Koper, J.W., Lamberts, S.W.J., 1992. Somatostatin receptor scintigraphy with indium-111-DTPA-D-Phe-1-octreotide in man: metabolism, dosimetry and comparison with iodine-123-Tyr-3-octreotide. J. Nucl. Med. 33, 652–658.

Krenning, E.P., Kwekkeboom, D.J., Bakker, W.H., Breeman, W.A., Kooij, P.P., Oei, H.Y., van Hagen, M., Postema, P.T., de Jong, M., Reubi, J.C., Visser, T.J., Reijs, A.E.M., Hofland, L.J., Koper, J.W., Lamberts, S.W.J., 1993. Somatostatin receptor scintigraphy with (^{111}In-DTPA-D-Phe^{1})- and (^{123}I-Tyr^{3})-octreotide: the Rotterdam experience with more than 1000 patients. Eur. J. Nucl. Med. 20, 716–731.

Leide-Svegborn, S., Nosslin, B., Mattsson, S., 1999. Biokinetics and dosimetry of ^{111}In-DTPA-D-Phe-1-octreotide in patients. In: Schlafke-Stelson, A.T., Stabin, M.G., Sparks, R.B. (Eds.), Proceedings of the Sixth International Radiopharmaceutical Dosimetry Symposium. ORISE 99-0164. Oak Ridge Associated Universities, Oak Ridge, TN, pp. 631–642.

Stabin, M.G., Kooij, P.P., Bakker, W.H., 1997. Radiation dosimetry for indium-111-pentetreotide. J. Nucl. Med. 38, 1919–1922.

C.20.3. Biokinetic data for ^{111}In-octreotide

Organ (S)	F_s	T (h)	a	$\widetilde{A}_s/A_0$(h)
Thyroid	0.001	60	1.0	0.046
Kidneys	0.06	60	1.0	2.8
Liver	0.06	2.0	0.40	2.6
		60	0.30	
		1680	0.30	
Spleen	0.05	60	1.0	2.3
Other organs and tissues	0.829	3.0	0.90	6.9
		60	0.10	
Urinary bladder contents	1.0			
Adult, 15 years, 10 years				1.7
5 years				1.4
1 year				0.91

C.20.4. Absorbed doses for ^{111}In-octreotide

^{111}In 67.9 h

Organ	Absorbed dose per unit activity administered (mGy/MBq)				
	Adult	15 years	10 years	5 years	1 year
Adrenals	5.8E-02	7.5E-02	1.1E-01	1.7E-01	2.9E-01
Bladder	2.0E-01	2.5E-01	3.7E-01	4.6E-01	5.6E-01
Bone surfaces	2.7E-02	3.3E-02	5.0E-02	7.5E-02	1.4E-01
Brain	9.6E-03	1.2E-02	2.0E-02	3.2E-02	5.7E-02
Breasts	1.2E-02	1.5E-02	2.3E-02	3.7E-02	6.7E-02
Gallbladder	5.2E-02	6.3E-02	9.2E-02	1.4E-01	2.2E-01
Gastrointestinal tract					
Stomach	4.3E-02	5.0E-02	7.7E-02	1.1E-01	1.8E-01
Small intestine	2.9E-02	3.7E-02	5.9E-02	9.0E-02	1.5E-01
Colon	2.9E-02	3.5E-02	5.5E-02	8.6E-02	1.4E-01
(Upper large intestine	3.0E-02	3.7E-02	5.8E-02	9.4E-02	1.5E-01)
(Lower large intestine	2.7E-02	3.3E-02	5.2E-02	7.5E-02	1.2E-01)
Heart	2.5E-02	3.2E-02	4.8E-02	7.0E-02	1.2E-01
Kidneys	4.1E-01	4.9E-01	6.7E-01	9.6E-01	1.6E+00
Liver	1.0E-01	1.3E-01	2.0E-01	2.7E-01	4.8E-01
Lungs	2.3E-02	3.0E-02	4.4E-02	6.7E-02	1.2E-01
Muscles	2.0E-02	2.6E-02	3.8E-02	5.6E-02	1.0E-01
Oesophagus	1.4E-02	1.8E-02	2.7E-02	4.3E-02	7.7E-02
Ovaries	2.7E-02	3.5E-02	5.3E-02	8.0E-02	1.3E-01
Pancreas	7.2E-02	8.8E-02	1.3E-01	2.0E-01	3.2E-01
Red marrow	2.2E-02	2.6E-02	3.9E-02	5.3E-02	8.5E-02
Skin	1.1E-02	1.3E-02	2.1E-02	3.2E-02	5.9E-02
Spleen	5.7E-01	7.9E-01	1.2E+00	1.8E+00	3.1E+00
Testes	1.7E-02	2.2E-02	3.7E-02	5.4E-02	8.7E-02
Thymus	1.4E-02	1.8E-02	2.7E-02	4.3E-02	7.7E-02
Thyroid	7.5E-02	1.2E-01	1.8E-01	3.7E-01	6.8E-01
Uterus	3.9E-02	4.9E-02	7.7E-02	1.1E-01	1.6E-01
Remaining organs	2.4E-02	3.2E-02	4.9E-02	8.0E-02	1.3E-01
Effective dose (mSv/MBq)	5.4E-02	7.1E-02	1.1E-01	1.6E-01	2.6E-01

C.21. ^{123}I-labelled fatty acids (^{123}I-BMIPP and ^{123}I-IPPA)
^{123}I

C.21.1. Biokinetic models

(C 61) Free fatty acids are major energy sources for the myocardium, and iodine-labelled free fatty acids are used to study the energy metabolism of the heart. Long-chain fatty acids are taken up rapidly by the heart and metabolised by β-oxidation (Tamaki et al., 2000). The first iodine-labelled free fatty acids that were developed had the disadvantage that the release of radio-iodide was too high. This was overcome by the introduction of ^{123}I-para-iodophenyl pentadecanoic acid (^{123}I-IPPA), a terminally phenylated straight-chain fatty acid, where the iodine was substituted in the phenyl group (Machulla et al., 1980; Reske et al., 1982; Reske, 1985; Dudczak et al., 1986).

(C 62) The rapid clearance of ^{123}I-IPPA from the myocardium is, however, a problem when tomography (SPECT) is performed. This problem has been overcome by the introduction of a methyl group on the 3-carbon of the fatty acid. 3-Methyl-branched fatty acids are metabolised in the peroxisomes by initial alpha-oxidation followed by peroxisomal beta-oxidation, a process that is slower than the mitochondrial beta-oxidation (Casteels et al., 2003). This principle was first utilised by Knapp et al. (1986) by the introduction of beta-methyl-p-(^{123}I)-iodophenylpentadecanoic acid (^{123}I-BMIPP). See also references in Knapp et al. (1995b).

(C 63) After intravenous injection, ^{123}I-IPPA and ^{123}I-BMIPP are cleared rapidly from the blood (biological half-time 2.5–3.0 min) (Knapp et al., 1995a) due to fast uptake in various organs and tissues (Torizuka et al., 1991; Yoshizumi et al., 2000). Whole-body pictures shortly after the injection (Torizuka et al., 1991; Sloof et al., 1997; Yoshizumi et al., 2000; Caveliers et al., 1998) show a concentration of activity in liver and heart, and a uniform distribution in the rest of the body.

(C 64) After the uptake, only some ^{123}I-IPPA and ^{123}I-BMIPP will be metabolised immediately to water-soluble low-molecular-weight products. ^{123}I-IPPA is, to a large extent, metabolised like long-chain fatty acids by rapid mitochondrial beta-oxidation ending up with p-(^{123}I)-iodobenzoic acid, which is excreted in a conjugated form in the urine. The metabolism of ^{123}I-BMIPP is slower than that of ^{123}I-IPPA due to the methyl group on the beta-carbon. The end product is p-(^{123}I)-iodophenyl acetic acid, which is also excreted as a conjugate in the urine. In either case, no release of free iodine has been detected. The initially unmetabolised part of ^{123}I-IPPA and ^{123}I-BMIPP will become incorporated into the fat stores in the body, which have a slow turnover, thus causing considerably delayed metabolism.

(C 65) Time–activity curves for the heart and liver indicate bi-exponential elimination of ^{123}I-BMIPP (Torizuka et al., 1991; De Geeter et al., 1998). Out of these curves, initial uptake in the heart has been calculated to be 5.0–5.7% of the activity administered (excluding blood activity) and 13–14% in the liver. For ^{123}I-BMIPP, the

biological half-time of the fast phase is approximately 1 h and that of the slow phase is approximately 2 days. The fast phase corresponds to a fraction of 0.43 of uptake in the heart. In the liver, the fast-eliminated fraction is 0.33–0.36. The final metabolite is excreted via the kidney and urinary bladder. After 16 h, 15% (Dudczak et al., 1986) has been excreted, and after 24 h, 22.6% has been excreted (Torizuka et al., 1991). There are no data for ^{123}I-BMIPP covering longer time periods, but from studies on labelled fatty acids (Gunnarsson et al., 2003), one must assume uptake into body fat and consequently a slow turnover of part of the administered activity.

(C 66) The biokinetic model for ^{123}I-BMIPP adopted here assumes initial uptake of 6% of the administered activity in the heart and 14% in the liver. The rest is assumed to be distributed uniformly in the remaining organs and tissues. From the heart, 40% is excreted with a biological half-time of 1 h and 60% with a half-time of 48 h. For the liver, the fractions are 30% and 70%, respectively. Elimination from the rest of the body is assumed to be bi-exponential, with a fast phase with a half-time of 48 h and a slow phase with a half-time exceeding 100 h (Gunnarsson et al., 2003).

(C 67) The faster phase corresponds to the combined fast and slow phases of the heart and liver, and represents the turnover of a more dynamic fat pool of the body. The slow phase represents the turnover of the rest of the body fat. The size of the latter long-lasting pool is taken to be 20% of the administered activity; a high value according to data in the literature (Gunnarsson et al., 2003).

(C 68) For ^{123}I-IPPA, data suitable for dose estimations are non-existent. The initial uptake to the heart, liver, and other organs and tissues is assumed to be the same as for ^{123}I-BMIPP. The first phase elimination from heart and liver, however, should be much faster since the beta-oxidation is not inhibited. The model assumes a half-life that is five times lower, i.e. a biological half-time of 10 min for the initial fast phase. For the slow phase of the heart and liver, and for elimination from the rest of the body, the same figures are used as in the ^{123}I-BMIPP model.

Note that the models are intended for ^{123}I alone.

C.21.2. References for ^{123}I-labelled fatty acids

Casteels, M., Foulon, V., Mannaerts, G.P., van Veldhoven, P., 2003. Alpha-oxidation of 3-methyl-substituted fatty acids and its thiamine dependence. Eur. J. Biochem. 270, 1619–1627.

Caveliers, V., Franken, P.R., Florian, F.L., Lou, H., Knapp Jr., F.F., 1998. Intra-individual comparison of 3(R)-BMIPP and 3(S)-BMIPP isomers in humans. J. Nucl. Med. 39, 1672–1675.

De Geeter, F., Caveliers, V., Pansar, I., Bossuyt, A., Franken, P.R., 1998. Effect of oral glucose loading on the biodistribution of BMIPP in normal volunteers. J. Nucl. Med. 39, 1850–1856.

Dudczak, R., Schmoliner, R., Angelberger, P., Knapp, F.F., Goodman, M.M., 1986. Structurally modified fatty acids: clinical potential as tracers of metabolism. Eur. J. Nucl. Med. 12, S45–S48.

Gunnarsson, M., Stenström, K., Leide-Svegborn, S., Faarinen, M., Magnusson, C.E., Åberg, M., Skog, G., Hellborg, R., Mattsson, S., 2003. Biokinetics and radiation dosimetry for patients undergoing a glycerol tri[1-^{14}C]oleate fat malabsorption breath test. Appl. Radiat. Isot. 58, 517–526.

Knapp Jr., F.F., Kropp, J., 1995b. Iodine-123-labelled fatty acids for myocardial single-photon emission tomography: current status and future perspectives. Eur. J. Nucl. Med. 22, 361–381.

Knapp Jr., F.F., Ambrose, K.R., Goodman, M.M., 1986. New radioiodinated methyl-branched fatty acids for cardiac studies. Eur. J. Nucl. Med. 12 (Suppl), S39–S44.

Knapp Jr., F.F., Franken, P., Kropp, J., 1995a. Cardiac SPECT with iodine-123-labeled fatty acids: evaluation of myocardial viability with BMIPP. J. Nucl. Med. 36, 1022–1030.

Machulla, H.J., Marsmann, M., Dutschka, K., 1980. Biochemical concept and synthesis of a radioiodinated phenyl fatty acid for in vivo metabolic studies of the myocardium. Eur. J. Nucl. Med. 5, 171–173.

Reske, S.N., 1985. 123I-phenylpentadecanoic acid as a tracer of cardiac free fatty acid metabolism. Experimental and clinical results. Eur. Heart J. 6 (Suppl B), 39–47.

Reske, S.N., Biersack, H.J., Lackner, K., Machulla, H.J., Knopp, R., Hahn, N., Winkler, C., 1982. Assessment of regional myocardial uptake and metabolism of omega-(p-123I-phenyl) pentadecanoic acid with serial single-photon emission tomography. Nuklearmedizin 21, 249–253.

Sloof, G.W., Visser, F.C., van Lingen, A., Bax, J.J., Eersels, J., Teule, G.J., Knapp Jr., F.F., 1997. Evaluation of heart-to-organ ratios of 123I-BMIPP and the dimethyl-substituted 123I-DMIPP fatty acid analogue in humans. Nucl. Med. Commun. 18, 1065–1070.

Tamaki, N., Morita, K., Kuge, Y., Tsukamoto, E., 2000. The role of fatty acids in cardiac imaging. J. Nucl. Med. 41, 1525–1534.

Torizuka, K., Yonekura, Y., Nishimura, T., Tamaki, N., Uehara, T., Ikekubo, K., Hino, M., 1991. The phase 1 study of β-methyl-p-(^{123}I)-iodophenyl-pentadecanoic acid (^{123}I-BMIPP). Kagu Igaku 28, 681–690.

Yoshizumi, T., Nozaki, S., Fukuchi, K., Yamasaki, K., Fukuchi, T., Maruyama, T., Tomiyama, Y., Yamashita, S., Nishimura, T., Matsuzawa, Y., 2000. Pharamacokinetics and metabolism of ^{123}I-BMIPP fatty acid analog in healthy and CD36-deficient subjects. J. Nucl. Med. 41, 1134–1138.

C.21.3. Biokinetic data for ^{123}I-BMIPP

Organ (S)	F_s	T (h)	a	$\widetilde{A}_s/A_0$(h)
Heart wall	0.06	1	0.40	0.57
		48	0.60	
Liver	0.14	1	0.30	1.5
		48	0.70	
Other organs and tissues	0.80	48	0.75	13
		15,000	0.25	
Urinary bladder contents	1.0			
Adult, 15 years, 10 years				0.41
5 years				0.35
1 year				0.23

(No free iodide is released).

This biokinetic model is intended for ^{123}I alone.

C.21.4. Biokinetic data for ^{123}I-IPPA

Organ (S)	F_s	T (h)	a	$\widetilde{A}_s/A_0$(h)
Heart wall	0.06	0.17	0.40	0.54
		48	0.60	
Liver	0.14	0.17	0.30	1.5
		48	0.70	
Other organs and tissues	0.80	48	0.75	13
		15,000	0.25	
Urinary bladder contents	1.0			
Adult, 15 years, 10 years				0.47
5 years				0.40
1 year				0.27

(No free iodide is released).

This biokinetic model is intended for ^{123}I alone.

C.21.5. Absorbed doses for ^{123}I-labelled fatty acid (BMIPP)

^{123}I 13.2 h

Organ	Absorbed dose per unit activity administered (mGy/MBq)				
	Adult	15 years	10 years	5 years	1 year
Adrenals	1.5E-02	1.9E-02	2.9E-02	4.4E-02	7.9E-02
Bladder	3.9E-02	5.1E-02	7.3E-02	1.1E-01	2.0E-01
Bone surfaces	2.0E-02	2.4E-02	3.8E-02	5.9E-02	1.1E-01
Brain	9.6E-03	1.2E-02	2.0E-02	3.3E-02	5.9E-02
Breasts	8.9E-03	1.1E-02	1.7E-02	2.7E-02	5.3E-02
Gallbladder	1.9E-02	2.3E-02	3.5E-02	5.4E-02	8.7E-02
Gastrointestinal tract					
Stomach	1.3E-02	1.7E-02	2.7E-02	4.2E-02	7.7E-02
Small intestine	1.4E-02	1.7E-02	2.7E-02	4.3E-02	7.9E-02
Colon	1.4E-02	1.8E-02	2.7E-02	4.3E-02	7.7E-02
(Upper large intestine	1.4E-02	1.8E-02	2.7E-02	4.5E-02	7.8E-02)
(Lower large intestine	1.4E-02	1.7E-02	2.7E-02	4.1E-02	7.6E-02)
Heart	5.3E-02	6.8E-02	1.0E-01	1.6E-01	2.8E-01
Kidneys	1.3E-02	1.6E-02	2.6E-02	4.0E-02	7.2E-02
Liver	3.6E-02	4.6E-02	6.9E-02	9.8E-02	1.8E-01
Lungs	1.3E-02	1.7E-02	2.6E-02	4.0E-02	7.4E-02
Muscles	1.1E-02	1.4E-02	2.1E-02	3.3E-02	6.2E-02
Oesophagus	1.3E-02	1.6E-02	2.4E-02	3.8E-02	6.9E-02
Ovaries	1.4E-02	1.8E-02	2.7E-02	4.3E-02	8.0E-02
Pancreas	1.6E-02	2.0E-02	3.1E-02	4.9E-02	8.7E-02
Red marrow	1.1E-02	1.3E-02	2.0E-02	3.0E-02	5.5E-02
Skin	7.5E-03	9.0E-03	1.4E-02	2.3E-02	4.4E-02
Spleen	1.2E-02	1.6E-02	2.5E-02	3.8E-02	7.0E-02
Testes	1.0E-02	1.3E-02	2.0E-02	3.3E-02	6.1E-02
Thymus	1.3E-02	1.6E-02	2.4E-02	3.8E-02	6.9E-02
Thyroid	1.1E-02	1.4E-02	2.3E-02	3.7E-02	6.9E-02
Uterus	1.6E-02	1.9E-02	3.1E-02	4.8E-02	8.7E-02
Remaining organs	1.1E-02	1.4E-02	2.1E-02	3.4E-02	6.2E-02
Effective dose (mSv/MBq)	1.6E-02	2.0E-02	3.1E-02	4.7E-02	8.7E-02

C.21.6. Absorbed doses for ^{123}I-labelled fatty acid (IPPA)

^{123}I 13.2 h

Organ	Absorbed dose per unit activity administered (mGy/MBq)				
	Adult	15 years	10 years	5 years	1 year
Adrenals	1.5E-02	1.9E-02	2.9E-02	4.4E-02	7.9E-02
Bladder	4.3E-02	5.6E-02	8.1E-02	1.1E-01	1.5E-01
Bone surfaces	2.0E-02	2.4E-02	3.8E-02	5.8E-02	1.1E-01
Brain	9.6E-03	1.2E-02	2.0E-02	3.3E-02	5.9E-02
Breasts	8.9E-03	1.1E-02	1.7E-02	2.7E-02	5.2E-02
Gallbladder	1.8E-02	2.3E-02	3.5E-02	5.3E-02	8.5E-02
Gastrointestinal tract					
Stomach	1.3E-02	1.7E-02	2.7E-02	4.2E-02	7.6E-02
Small intestine	1.4E-02	1.7E-02	2.7E-02	4.3E-02	7.8E-02
Colon	1.4E-02	1.8E-02	2.7E-02	4.3E-02	7.6E-02
(Upper large intestine	1.4E-02	1.8E-02	2.7E-02	4.5E-02	7.7E-02)
(Lower large intestine	1.4E-02	1.7E-02	2.7E-02	4.1E-02	7.4E-02)
Heart	5.1E-02	6.5E-02	9.9E-02	1.5E-01	2.7E-01
Kidneys	1.3E-02	1.6E-02	2.6E-02	4.0E-02	7.2E-02
Liver	3.5E-02	4.5E-02	6.7E-02	9.6E-02	1.7E-01
Lungs	1.3E-02	1.7E-02	2.6E-02	4.0E-02	7.4E-02
Muscles	1.1E-02	1.4E-02	2.1E-02	3.3E-02	6.1E-02
Oesophagus	1.3E-02	1.6E-02	2.4E-02	3.8E-02	6.9E-02
Ovaries	1.4E-02	1.8E-02	2.8E-02	4.3E-02	7.8E-02
Pancreas	1.6E-02	2.0E-02	3.1E-02	4.8E-02	8.7E-02
Red marrow	1.1E-02	1.3E-02	2.0E-02	3.0E-02	5.5E-02
Skin	7.5E-03	9.0E-03	1.4E-02	2.3E-02	4.4E-02
Spleen	1.2E-02	1.6E-02	2.5E-02	3.8E-02	7.0E-02
Testes	1.0E-02	1.3E-02	2.0E-02	3.2E-02	5.9E-02
Thymus	1.3E-02	1.6E-02	2.4E-02	3.8E-02	6.9E-02
Thyroid	1.1E-02	1.4E-02	2.3E-02	3.7E-02	6.9E-02
Uterus	1.6E-02	2.0E-02	3.2E-02	4.8E-02	8.2E-02
Remaining organs	1.1E-02	1.4E-02	2.1E-02	3.4E-02	6.2E-02
Effective dose (mSv/MBq)	1.6E-02	2.0E-02	3.1E-02	4.7E-02	8.3E-02

C.22. ^{123}I-labelled brain receptor substances (generic model)
^{123}I

C.22.1. Biokinetic model

(C 69) A large number of radiopharmaceuticals labelled with ^{18}F and ^{123}I have been developed for PET and SPECT studies of different types of receptor in the human brain. For many of these substances, the available biokinetic data are insufficient to construct realistic compound-specific biokinetic models for the calculation of absorbed dose to persons undergoing an investigation. Therefore, a generic model for radionuclide-labelled brain receptor substances that would predict the internal radiation dose with sufficient accuracy for general radiation protection purposes has been developed.

(C 70) A generic model for ^{11}C-labelled brain receptor substances has been published (Nosslin et al., 2003). A review of the literature has identified biokinetic and dosimetric data for five ^{18}F-labelled and 15 ^{123}I-labelled compounds considered to be potential substances for the clinical imaging of brain receptors, e.g. acetylcholinesterase receptors, benzodiazepine receptors, dopamine receptors, dopamine transporters, and serotonin receptors. These data indicate that despite fairly large differences in chemical structure, the patterns of uptake in the human brain, and other tissues for which information is available, appear to be sufficiently similar to justify a generic model for each radionuclide.

(C 71) For some compounds, the published data on the dosimetry of ^{18}F- and ^{123}I-labelled receptor radiopharmaceuticals were derived from PET and SPECT studies in humans, and for other compounds, the biokinetic models were derived, at least in part, from studies of biodistribution in experimental animals.

(C 72) For the ^{123}I model, it is assumed that fractions of 0.06 and 0.003 of the administered activity are distributed instantaneously to brain and thyroid, respectively. The activity is excreted from these tissues with a biological half-time of 100 h, i.e. more than 99% of ^{123}I will decay in situ. It is also assumed that 0.20 of the administered activity is distributed instantaneously to the lungs and then excreted with a biological half-time of 8 h. Fractions of 0.20 and 0.03 are assumed to be deposited in the liver and the kidneys, respectively, and are excreted bi-exponentially with biological half-times of 8 h (50%) and 100 h (50%). Thirty percent (30%) of the activity uptake in liver is eliminated via the gallbladder, and the remainder of the liver uptake is passed directly into the small intestine. It is assumed that 75% of the administered ^{123}I is excreted in the urine and 25% via the gastrointestinal tract.

C.22.2. References and further reading for ^{123}I-labelled brain receptor substances

Booij, J., Sokole, E.B., Stabin, M.G., Janssen, A.G.M., de Bruin, K., van Royen, E.A., 1998. Human biodistribution and dosimetry of [^{123}I]FP-CIT: a potent radioligand for imaging of dopamine transporters, Eur. J. Nucl. Med. 25, 24–30.

Booij, J., Sokole, E.B., Stabin, M.G., Janssen, A.G.M., de Bruin, K., van Royen, E.A., 1998. Human biodistribution and dosimetry of [^{123}I]FP-CIT: a potent radioligand for imaging of dopamine transporters: Erratum. Eur. J. Nucl. Med. 25, 458.

Boundy, K.L., Barnden, L.R., Rowe, C.C., Reid, M., Kassiou, M., Katsifis, A.G., Lambrecht, R.L., 1995. Human dosimetry and biodistribution of iodine-123-iododexetimide: a SPECT imaging agent for cholinergic muscarinic neuroreceptors. J. Nucl. Med. 36, 1332–1338.

Deterding, T.A., Votaw, J.R., Wang, C.K., Eshima, D., Eshima, L., Keil, R., Malveaux, E., Kilts, C.D., Goodman, M.M., Hoffman, J.M., 2001. Biodistribution and radiation dosimetry of the dopamine transporter ligand [^{18}F]FECNT. J Nucl Med. 42, 376–381.

Gründer, G., Siessmeier, T., Lange-Asschenfeldt, C., Vernaleken, I., Buchholz, H.-G., Stoeter, P., Drzezga, A., Lüddens, H., Rösch, F., Bartenstein, P., 2001. [^{18}F]Fluoroethylflumaazenil: a novel tracer for PET imaging of human benzodiazepine receptors. Eur. J. Nucl. Med. 28, 1463–1470.

Gründer, G., Siessmeier, T., Piel, M., Vernaleken, I., Buchholz, H.-G., Zhou, Y., Hiemke, C., Wong, D.P., Rösch, F., Bartenstein, P., 2003. Quantification of D_2-like dopamine receptors in the human brain with [^{18}F]-desmethoxyfallypride. J. Nucl. Med. 44, 109–116.

Kauppinen, T.A., Bergström, K.A., Heikman, P., Hiltunen, J., Ahonen, A.K., 2003. Biodistribution and radiation dosimetry of [^{123}I]ADAM in healthy human subjects: preliminary results. Eur. J. Nucl. Med. 30, 132–136.

Kuikka, J.T., Bergström, K.A., Ahonen, A., Länsimies, E., 1994. The dosimetry of iodine-123 labelled 2β-carbomethoxy-3β-(4-iodophenyl)tropane. Eur. J. Nucl. Med., 21, 53–56.

Mitterhauser, M., Wadsak, W., Wabnegger, L., Mien, L-K., Tögel, S., Langer, O., Sieghart, W., Viernstein, H., Kletter, K., Dudczak, R., 2004. Biological evaluation of 2′-[^{18}F]fluoroflumazenil ([^{18}F]FFMZ) a potential GABA receptor ligand for PET. Nucl. Med. Biol. 31, 291–295.

Mozley, P.D., Stubbs, J.T., Kim, H-J., McElgin, W., Chumpradit, S., Kung, M-P., Romaniallo, G., Kung, H.F., 1995. Dosimetry of a D2/D3 dopamine receptor antagonist that can be used with PET or SPECT. J. Nucl. Med. 36, 1322–1331.

Mozley, P.D., Stubbs, J.T., Kim, H-J., McElgin, W., Kung, M-P., Meegalla, S., Kung, H.F., 1996. Dosimetry of an iodine-123-labeled tropane to image dopamine transporters. J. Nucl. Med. 37, 151–159.

Nosslin, B., Johansson, L., Leide-Svegborn, S., Liniecki, J., Mattsson, S., Taylor, D.M., 2003. A generic model for [^{11}C]-labelled radiopharmaceuticals for imaging receptors in the human brain. Rad. Prot. Dosim. 105, 587–591.

Taylor, D.M., 2000a. Unpublished assessments..

van de Wiele, C., De Vos, F., De Sutter, J., Dumont, F., Slegers, G., Dierkx, R.A., Thierens, H., 1999. Biokinetics and dosimetry of (iodine-123)-iodomethyl-N,N-dimethyltamoxifen, an (anti)oestrogen receptor radioligand. Eur. J. Nucl. Med. 26, 1259–1264.

Verhoeff, N.P., Sokole, E.B., Stabin, M., Hengst, D., Kung, H.F., van Royen, E.A., Janssen, A.G., 1993. Dosimetry of iodine-123 iodobenzamide in healthy volunteers. Eur. J. Nucl. Med. 20, 747–752.

Verhoeff, N.P., Busemann Sokole, E., Hengst, D., Stubbs, J.B., van Royen, E.A., 1993. Dosimetry of iodine-123 iomazenil in humans. Eur. J. Nucl. Med. 20, 580–584.

Versijpt, J., Dumont, F., Thierens, H., Jansen, H., de Vos, F., Slegers, G., Santens, P., Dierckx, R.A., Korf, J., 2000. Biodistribution and dosimetry of [^{123}I]iodo-PK 11195: a potential agent for SPET imaging of the peripheral benzodiazepine receptor. Eur. J. Nucl. Med. 27, 1326–1333.

Volkow, N.D., Ding, Y.-S., Fowler, J.S., Wang, G.-J., Logan, J., Gatley, S.J., Schlyer, D.J., Pappas, N., 1995. A new PET ligand for the dopamine transporter: studies in human brain. J. Nucl. Med. 36, 2162–2168.

Votaw, J.R., Ansari, M.S., Scott Mason, N., Schmidt, D., de Paulis, T., Holburn, G., Clanton, J.A., Votlaw, D.B., Manning, R.G., Kessler, R.M., 1995. Dosimetry of iodine-123-epidepride: a dopamine D2 receptor ligand. J. Nucl. Med. 36, 1316–1321.

Waterhouse, R.N., Stabin, M.G., Page, J.G., 2003. Preclinical acute toxicity studies and rodent-based dosimetry estimates of the novel sigma-1 receptor radiotracer [^{18}F]FPS. Nucl. Med. Biol. 30, 555–563.

C.22.3. Biokinetic data for ^{123}I-labelled brain receptor substances

Organ (S)	F_s	T (h)	a	$\widetilde{A}_s/A_0$(h)
Brain	0.06	100	1.0	1.0
Thyroid	0.003	100	1.0	0.050
Lungs	0.20	8	1.0	1.4
Kidneys	0.03	8	0.50	0.36
		100	0.50	
Kidney excretion	0.75			0.020
Liver	0.20	8	0.50	2.4
		100	0.50	
Stomach wall	0.05	8	1.0	0.36
Other organs and tissues	0.457	8	0.50	5.5
		100	0.50	
Gallbladder contents	0.06			0.67
Gastrointestinal tract contents				
Stomach	0.05			0.030
Small intestine	0.25			1.2
Upper large intestine	0.25			2.3
Lower large intestine	0.25			1.9
Urinary bladder contents	0.75			
Adult, 15 years, 10 years				0.55
5 years				0.47
1 year				0.31

C.22.4. Absorbed doses for ^{123}I-labelled brain receptor substances

^{123}I 13.2 h

Organ	Absorbed dose per unit activity administered (mGy/MBq)				
	Adult	15 years	10 years	5 years	1 year
Adrenals	1.6E-02	2.1E-02	3.2E-02	4.8E-02	8.5E-02
Bladder	5.2E-02	6.6E-02	9.9E-02	1.3E-01	1.9E-01
Bone surfaces	1.7E-02	2.1E-02	3.3E-02	5.1E-02	1.0E-01
Brain	2.9E-02	2.9E-02	3.0E-02	3.4E-02	4.6E-02
Breasts	6.3E-03	7.8E-03	1.3E-02	2.1E-02	4.0E-02
Gallbladder	1.8E-01	2.1E-01	2.7E-01	4.7E-01	1.5E+00
Gastrointestinal tract					
Stomach	5.7E-02	7.6E-02	1.1E-01	1.8E-01	3.8E-01
Small intestine	6.3E-02	8.0E-02	1.3E-01	2.1E-01	3.8E-01
Colon	1.6E-01	2.0E-01	3.4E-01	5.5E-01	1.0E+00
(Upper large intestine	1.5E-01	1.9E-01	3.2E-01	5.2E-01	9.7E-01)
(Lower large intestine	1.7E-01	2.1E-01	3.6E-01	5.8E-01	1.1E+00)
Heart	1.2E-02	1.6E-02	2.5E-02	3.9E-02	7.1E-02
Kidneys	4.6E-02	5.5E-02	7.9E-02	1.2E-01	2.0E-01
Liver	5.8E-02	7.5E-02	1.1E-01	1.6E-01	3.0E-01
Lungs	4.1E-02	5.9E-02	8.3E-02	1.3E-01	2.4E-01
Muscles	1.0E-02	1.3E-02	2.0E-02	3.1E-02	5.8E-02
Oesophagus	7.6E-03	9.8E-03	1.5E-02	2.4E-02	4.4E-02
Ovaries	3.7E-02	4.9E-02	7.6E-02	1.1E-01	2.0E-01
Pancreas	1.9E-02	2.5E-02	4.3E-02	6.9E-02	1.2E-01
Red marrow	1.2E-02	1.4E-02	2.1E-02	2.9E-02	4.7E-02
Skin	5.2E-03	6.3E-03	1.0E-02	1.7E-02	3.2E-02
Spleen	1.2E-02	1.6E-02	2.5E-02	4.0E-02	7.3E-02
Testes	7.0E-03	9.2E-03	1.6E-02	2.6E-02	4.8E-02
Thymus	7.6E-03	9.8E-03	1.5E-02	2.4E-02	4.4E-02
Thyroid	5.5E-02	8.7E-02	1.3E-01	2.9E-01	5.4E-01
Uterus	2.3E-02	3.0E-02	5.0E-02	7.8E-02	1.4E-01
Remaining organs	1.3E-02	1.8E-02	2.9E-02	4.8E-02	7.7E-02
Effective dose (mSv/MBq)	5.0E-02	6.1E-02	9.6E-02	1.5E-01	3.2E-01

C.23. ^{123}I-labelled monoclonal tumour-associated antibodies
^{123}I

C.23.1. Biokinetic model

(C 73) The models for iodine-labelled antibodies and fragments are the same as those used for the corresponding technetium-labelled substances (see Section C.16.1), with the modification that released iodine is assumed to be handled by the body according to the model for iodine with blocking of uptake in the thyroid (ICRP, 1987, p. 275).

This biokinetic model is not intended to apply to therapeutic use of the substance.

C.23.2. References and further reading for ^{123}I-labelled monoclonal antibodies

Bischof Delaloye, A., Delaloye, B., 1995. Radiolabelled monoclonal antibodies in tumour imaging and therapy: out of fashion? Eur. J. Nucl. Med. 22, 571–580.

Britton, K.E., Granowska, M., 1987. Radioimmunoscintigraphy in tumour identification. Cancer Surv. 6, 247–267.

Fishman, A.J., Khaw, B.A., Strauss, H.N., 1989. Quo vadis radioimmune imaging. J. Nucl. Med. 20, 1911–1915.

ICRP, 1987. Radiation dose to patients from radiopharmaceuticals. ICRP Publication 53. Ann. ICRP 18 (1–4).

C.23.3. Biokinetic data for ^{123}I-labelled monoclonal antibodies

Intact antibody

Organ (S)	F_s	T (h)	a	$\widetilde{A}_s/A_0$(h)
Kidneys	0.03	24	0.5	0.44
		96	0.5	
Liver	0.50	24	0.5	7.3
		96	0.5	
Spleen	0.09	24	0.5	1.3
		96	0.5	
Red bone marrow	0.20	24	0.5	2.9
		96	0.5	
Other organs and tissues	0.18	24	0.5	2.6
		96	0.5	
Released iodine	1.0	−24	0.5	*
		−96	0.5	

*To obtain the contribution from released ^{123}I, the cumulated activity given in the model for iodide with blocked thyroid should be multiplied by 0.24.

F(ab′)$_2$ fragments

Organ (S)	F_s	T (h)	a	$\widetilde{A}_s/A_0$(h)
Kidneys	0.20	12	1.0	1.8
Liver	0.30	12	1.0	2.7
Spleen	0.06	12	1.0	0.54
Red bone marrow	0.10	12	1.0	0.91
Other organs and tissues	0.34	12	1.0	3.1
Released iodine	1.0	−12	1.0	*

*To obtain the contribution from released ^{123}I, the cumulated activity given in the model for iodide with blocked thyroid should be multiplied by 0.52.

F(ab′) fragments

Organ (S)	F_s	T (h)	a	$\widetilde{A}_s/A_0$(h)
Kidneys	0.40	6.0	1.0	2.4
Liver	0.10	6.0	1.0	0.60
Spleen	0.02	6.0	1.0	0.12
Red bone marrow	0.03	6.0	1.0	0.18
Other organs and tissues	0.45	6.0	1.0	2.7
Released iodine	1.0	−6.0	1.0	*

*To obtain the contribution from released ^{123}I, the cumulated activity given in the model for iodide with blocked thyroid should be multiplied by 0.69.

C.23.4. Absorbed doses for ^{123}I-labelled monoclonal antibodies

Intact antibody

^{123}I 13.2 h

Organ	Absorbed dose per unit activity administered (mGy/MBq)				
	Adult	15 years	10 years	5 years	1 year
Adrenals	2.7E-02	3.4E-02	5.0E-02	6.9E-02	1.1E-01
Bladder	2.4E-02	3.1E-02	4.6E-02	6.3E-02	8.6E-02
Bone surfaces	3.2E-02	3.7E-02	6.0E-02	1.0E-01	1.8E-01
Brain	4.5E-03	5.8E-03	9.0E-03	1.5E-02	2.8E-02
Breasts	6.0E-03	7.4E-03	1.2E-02	1.9E-02	3.7E-02
Gallbladder	4.0E-02	4.8E-02	6.7E-02	1.0E-01	1.9E-01
Gastrointestinal tract					
Stomach	1.5E-02	1.9E-02	3.2E-02	5.1E-02	9.2E-02
Small intestine	1.2E-02	1.5E-02	2.4E-02	3.9E-02	6.9E-02
Colon	1.2E-02	1.4E-02	2.4E-02	4.0E-02	6.8E-02
(Upper large intestine	1.4E-02	1.7E-02	3.0E-02	5.0E-02	8.6E-02)
(Lower large intestine	8.6E-03	1.1E-02	1.7E-02	2.6E-02	4.4E-02)
Heart	1.4E-02	1.8E-02	2.8E-02	4.2E-02	7.7E-02
Kidneys	5.9E-02	7.2E-02	1.0E-01	1.5E-01	2.5E-01
Liver	1.5E-01	1.9E-01	2.9E-01	4.0E-01	7.3E-01
Lungs	1.4E-02	1.8E-02	2.7E-02	4.0E-02	7.2E-02
Muscles	8.5E-03	1.1E-02	1.6E-02	2.4E-02	4.5E-02
Oesophagus	6.9E-03	8.6E-03	1.3E-02	2.0E-02	3.5E-02
Ovaries	9.4E-03	1.2E-02	1.9E-02	2.9E-02	5.0E-02
Pancreas	3.0E-02	3.7E-02	5.8E-02	8.9E-02	1.5E-01
Red marrow	3.7E-02	4.2E-02	6.7E-02	1.3E-01	3.0E-01
Skin	4.7E-03	5.7E-03	9.1E-03	1.5E-02	2.8E-02
Spleen	2.0E-01	2.9E-01	4.4E-01	6.7E-01	1.2E+00
Testes	4.3E-03	5.6E-03	9.0E-03	1.4E-02	2.6E-02
Thymus	6.9E-03	8.6E-03	1.3E-02	2.0E-02	3.5E-02
Thyroid	5.1E-03	6.5E-03	1.0E-02	1.7E-02	3.1E-02
Uterus	9.3E-03	1.2E-02	1.9E-02	2.9E-02	5.0E-02
Remaining organs	9.0E-03	1.1E-02	1.7E-02	2.6E-02	4.6E-02
Effective dose (mSv/MBq)	2.6E-02	3.3E-02	5.1E-02	8.0E-02	1.5E-01

$F(ab')_2$ fragments

^{123}I 13.2 h

Organ	Absorbed dose per unit activity administered (mGy/MBq)				
	Adult	15 years	10 years	5 years	1 year
Adrenals	2.1E-02	2.7E-02	4.1E-02	6.1E-02	1.1E-01
Bladder	4.7E-02	6.1E-02	8.9E-02	1.3E-01	2.4E-01
Bone surfaces	1.9E-02	2.3E-02	3.6E-02	5.9E-02	1.1E-01
Brain	5.6E-03	7.0E-03	1.1E-02	1.9E-02	3.4E-02
Breasts	5.6E-03	7.0E-03	1.1E-02	1.7E-02	3.3E-02
Gallbladder	2.3E-02	2.8E-02	4.0E-02	6.0E-02	1.0E-01
Gastrointestinal tract					
Stomach	1.2E-02	1.6E-02	2.5E-02	3.8E-02	6.7E-02
Small intestine	1.1E-02	1.4E-02	2.3E-02	3.7E-02	6.5E-02
Colon	1.1E-02	1.4E-02	2.2E-02	3.5E-02	6.2E-02
(Upper large intestine	1.2E-02	1.5E-02	2.4E-02	3.9E-02	6.8E-02)
(Lower large intestine	9.8E-03	1.2E-02	1.9E-02	3.0E-02	5.4E-02)
Heart	1.1E-02	1.3E-02	2.1E-02	3.1E-02	5.7E-02
Kidneys	1.7E-01	2.0E-01	2.8E-01	4.1E-01	7.1E-01
Liver	6.0E-02	7.7E-02	1.2E-01	1.6E-01	2.9E-01
Lungs	1.0E-02	1.3E-02	2.0E-02	3.0E-02	5.6E-02
Muscles	8.3E-03	1.0E-02	1.6E-02	2.4E-02	4.6E-02
Oesophagus	7.0E-03	8.9E-03	1.4E-02	2.1E-02	3.9E-02
Ovaries	1.0E-02	1.3E-02	2.0E-02	3.2E-02	5.8E-02
Pancreas	2.0E-02	2.5E-02	3.9E-02	5.9E-02	1.0E-01
Red marrow	1.7E-02	1.9E-02	3.0E-02	5.2E-02	1.1E-01
Skin	5.0E-03	6.1E-03	9.7E-03	1.6E-02	3.0E-02
Spleen	9.3E-02	1.3E-01	2.0E-01	3.0E-01	5.3E-01
Testes	6.4E-03	8.3E-03	1.3E-02	2.1E-02	4.1E-02
Thymus	7.0E-03	8.9E-03	1.4E-02	2.1E-02	3.9E-02
Thyroid	6.4E-03	8.1E-03	1.3E-02	2.1E-02	4.0E-02
Uterus	1.2E-02	1.5E-02	2.4E-02	3.8E-02	6.8E-02
Remaining organs	8.8E-03	1.1E-02	1.7E-02	2.7E-02	4.8E-02
Effective dose (mSv/MBq)	1.9E-02	2.3E-02	3.5E-02	5.4E-02	9.9E-02

F(ab′) fragments

^{123}I 13.2 h

Organ	Absorbed dose per unit activity administered (mGy/MBq)				
	Adult	15 years	10 years	5 years	1 year
Adrenals	1.7E-02	2.3E-02	3.6E-02	5.5E-02	9.9E-02
Bladder	6.1E-02	7.9E-02	1.1E-01	1.5E-01	1.9E-01
Bone surfaces	1.4E-02	1.7E-02	2.7E-02	4.2E-02	8.3E-02
Brain	5.9E-03	7.4E-03	1.2E-02	2.0E-02	3.6E-02
Breasts	5.2E-03	6.6E-03	9.8E-03	1.6E-02	3.0E-02
Gallbladder	1.4E-02	1.7E-02	2.6E-02	4.0E-02	6.1E-02
Gastrointestinal tract					
Stomach	1.0E-02	1.3E-02	2.1E-02	3.1E-02	5.3E-02
Small intestine	1.1E-02	1.4E-02	2.2E-02	3.4E-02	6.0E-02
Colon	1.1E-02	1.4E-02	2.1E-02	3.2E-02	5.4E-02
(Upper large intestine	1.1E-02	1.4E-02	2.1E-02	3.3E-02	5.6E-02)
(Lower large intestine	1.0E-02	1.3E-02	2.0E-02	3.0E-02	5.2E-02)
Heart	8.5E-03	1.1E-02	1.7E-02	2.5E-02	4.6E-02
Kidneys	2.2E-01	2.6E-01	3.6E-01	5.1E-01	8.9E-01
Liver	1.8E-02	2.3E-02	3.5E-02	5.0E-02	8.8E-02
Lungs	7.8E-03	1.0E-02	1.6E-02	2.4E-02	4.6E-02
Muscles	8.0E-03	9.9E-03	1.5E-02	2.3E-02	4.3E-02
Oesophagus	6.8E-03	8.7E-03	1.3E-02	2.1E-02	3.9E-02
Ovaries	1.1E-02	1.3E-02	2.1E-02	3.2E-02	5.6E-02
Pancreas	1.5E-02	1.8E-02	2.8E-02	4.3E-02	7.4E-02
Red marrow	8.8E-03	1.0E-02	1.6E-02	2.4E-02	4.4E-02
Skin	5.0E-03	6.1E-03	9.7E-03	1.6E-02	2.9E-02
Spleen	3.0E-02	4.1E-02	6.3E-02	9.6E-02	1.7E-01
Testes	7.2E-03	9.3E-03	1.5E-02	2.3E-02	4.1E-02
Thymus	6.8E-03	8.7E-03	1.3E-02	2.1E-02	3.9E-02
Thyroid	6.7E-03	8.6E-03	1.4E-02	2.3E-02	4.2E-02
Uterus	1.3E-02	1.7E-02	2.7E-02	3.9E-02	6.3E-02
Remaining organs	8.1E-03	1.0E-02	1.6E-02	2.4E-02	4.3E-02
Effective dose (mSv/MBq)	1.7E-02	2.1E-02	3.1E-02	4.6E-02	7.8E-02

C.24. ^{131}I-labelled monoclonal tumour-associated antibodies
^{131}I

C.24.1. Biokinetic model

(C 74) The model for iodine-labelled antibodies and fragments is the same as that used for the corresponding technetium-labelled substances (see Section C.16.1), with the modification that released iodine is assumed to be handled by the body according to the model for iodine with blocking of uptake in the thyroid (ICRP, 1987, p. 275).

This biokinetic model is not intended to apply to therapeutic use of the substance.

C.24.2. References and further reading for ^{131}I-labelled monoclonal antibodies

Bischof Delaloye, A., Delaloye, B., 1995. Radiolabelled monoclonal antibodies in tumour imaging and therapy: out of fashion? Eur. J. Nucl. Med. 22, 571–580.

Britton, K.E., Granowska, M., 1987. Radioimmunoscintigraphy in tumour identification. Cancer Surv. 6, 247–267.

Fishman, A.J., Khaw, B.A., Strauss, H.N., 1989. Quo vadis radioimmune imaging. J. Nucl. Med. 20, 1911–1915.

ICRP, 1987. Radiation dose to patients from radiopharmaceuticals. ICRP Publication 53. Ann. ICRP 18 (1–4).

C.24.3. Biokinetic data for ^{131}I-labelled monoclonal antibodies

Intact antibody

Organ (S)	F_s	T (h)	a	$\widetilde{A}_s/A_0$(h)
Kidneys	0.03	24	0.5	1.9
		96	0.5	
Liver	0.50	24	0.5	31
		96	0.5	
Spleen	0.09	24	0.5	5.5
		96	0.5	
Red bone marrow	0.20	24	0.5	12
		96	0.5	
Other organs and tissues	0.18	24	0.5	11
		96	0.5	
Released iodine	1.0	−24	0.5	*
		−96	0.5	

*To obtain the contribution from released ^{131}I, the cumulated activity given in the model for iodide with blocked thyroid should be multiplied by 0.78.

F(ab′)$_2$ fragments

Organ (S)	F_s	T (h)	a	$\widetilde{A}_s/A_0$(h)
Kidneys	0.20	12	1.0	3.3
Liver	0.30	12	1.0	4.9
Spleen	0.06	12	1.0	0.98
Red bone marrow	0.10	12	1.0	1.6
Other organs and tissues	0.34	12	1.0	5.5
Released iodine	1.0	−12	1.0	*

*To obtain the contribution from released ^{131}I, the cumulated activity given in the model for iodide with blocked thyroid should be multiplied by 0.94.

F(ab′) fragments

Organ (S)	F_s	T (h)	a	$\widetilde{A}_s/A_0$(h)
Kidneys	0.40	6.0	1.0	3.4
Liver	0.10	6.0	1.0	0.84
Spleen	0.02	6.0	1.0	0.17
Red bone marrow	0.03	6.0	1.0	0.25
Other organs and tissues	0.45	6.0	1.0	3.8
Released iodine	1.0	−6.0	1.0	*

*To obtain the contribution from released ^{131}I, the cumulated activity given in the model for iodide with blocked thyroid should be multiplied by 0.97.

C.24.4. Absorbed doses for ^{131}I-labelled monoclonal antibodies

Intact antibody

^{131}I 8.04 days

Organ	Absorbed dose per unit activity administered (mGy/MBq)				
	Adult	15 years	10 years	5 years	1 year
Adrenals	2.6E-01	3.2E-01	4.7E-01	6.6E-01	1.1E+00
Bladder	5.0E-01	6.4E-01	9.8E-01	1.3E+00	1.8E+00
Bone surfaces	4.5E-01	4.7E-01	8.1E-01	1.4E+00	2.3E+00
Brain	6.2E-02	7.9E-02	1.3E-01	2.1E-01	4.1E-01
Breasts	8.2E-02	1.0E-01	1.7E-01	2.7E-01	5.2E-01
Gallbladder	3.5E-01	3.9E-01	5.4E-01	8.5E-01	1.6E+00
Gastrointestinal tract					
Stomach	1.6E-01	2.0E-01	3.1E-01	5.0E-01	9.3E-01
Small intestine	1.3E-01	1.7E-01	2.7E-01	4.3E-01	7.5E-01
Colon	1.3E-01	1.6E-01	2.6E-01	4.1E-01	7.3E-01
(Upper large intestine	1.5E-01	1.8E-01	3.0E-01	4.9E-01	8.8E-01)
(Lower large intestine	1.0E-01	1.3E-01	2.0E-01	3.1E-01	5.4E-01)
Heart	1.5E-01	1.9E-01	3.0E-01	4.4E-01	7.9E-01
Kidneys	1.0E+00	1.2E+00	1.7E+00	2.5E+00	4.4E+00
Liver	2.4E+00	3.2E+00	4.9E+00	7.3E+00	1.4E+01
Lungs	1.4E-01	1.8E-01	2.6E-01	3.9E-01	7.2E-01
Muscles	9.8E-02	1.2E-01	1.9E-01	3.0E-01	5.6E-01
Oesophagus	8.8E-02	1.1E-01	1.7E-01	2.6E-01	4.9E-01
Ovaries	1.1E-01	1.4E-01	2.2E-01	3.4E-01	6.1E-01
Pancreas	2.7E-01	3.3E-01	5.1E-01	7.8E-01	1.3E+00
Red marrow	7.4E-01	8.2E-01	1.4E+00	2.7E+00	6.6E+00
Skin	6.8E-02	8.5E-02	1.4E-01	2.2E-01	4.3E-01
Spleen	4.0E+00	5.8E+00	9.0E+00	1.4E+01	2.6E+01
Testes	6.4E-02	8.3E-02	1.4E-01	2.2E-01	4.1E-01
Thymus	8.8E-02	1.1E-01	1.7E-01	2.6E-01	4.9E-01
Thyroid	7.0E-02	8.9E-02	1.4E-01	2.3E-01	4.5E-01
Uterus	1.1E-01	1.4E-01	2.2E-01	3.5E-01	6.1E-01
Remaining organs	1.1E-01	1.4E-01	2.2E-01	3.5E-01	6.2E-01
Effective dose (mSv/MBq)	4.2E-01	5.5E-01	8.6E-01	1.4E+00	2.7E+00

F(ab′)$_2$ fragments

^{131}I 8.04 days

Organ	Absorbed dose per unit activity administered (mGy/MBq)				
	Adult	15 years	10 years	5 years	1 year
Adrenals	9.9E-02	1.2E-01	1.9E-01	2.9E-01	5.2E-01
Bladder	5.6E-01	7.3E-01	1.1E+00	1.5E+00	1.9E+00
Bone surfaces	9.9E-02	1.1E-01	1.8E-01	3.1E-01	5.4E-01
Brain	4.2E-02	5.3E-02	8.9E-02	1.5E-01	2.8E-01
Breasts	4.4E-02	5.6E-02	9.1E-02	1.5E-01	2.9E-01
Gallbladder	1.0E-01	1.2E-01	1.8E-01	2.8E-01	4.9E-01
Gastrointestinal tract					
Stomach	7.1E-02	8.7E-02	1.4E-01	2.2E-01	4.0E-01
Small intestine	6.9E-02	8.7E-02	1.4E-01	2.2E-01	4.0E-01
Colon	6.7E-02	8.4E-02	1.4E-01	2.1E-01	3.8E-01
(Upper large intestine	7.0E-02	8.7E-02	1.4E-01	2.2E-01	4.0E-01)
(Lower large intestine	6.4E-02	7.9E-02	1.3E-01	2.0E-01	3.5E-01)
Heart	6.3E-02	8.1E-02	1.3E-01	2.0E-01	3.7E-01
Kidneys	1.4E+00	1.7E+00	2.4E+00	3.6E+00	6.4E+00
Liver	4.0E-01	5.3E-01	8.2E-01	1.2E+00	2.3E+00
Lungs	5.8E-02	7.5E-02	1.2E-01	1.8E-01	3.5E-01
Muscles	5.4E-02	6.8E-02	1.1E-01	1.7E-01	3.3E-01
Oesophagus	5.0E-02	6.4E-02	1.0E-01	1.6E-01	3.1E-01
Ovaries	6.6E-02	8.4E-02	1.3E-01	2.1E-01	3.7E-01
Pancreas	9.7E-02	1.2E-01	1.9E-01	2.9E-01	5.0E-01
Red marrow	1.3E-01	1.5E-01	2.4E-01	4.5E-01	1.0E+00
Skin	4.2E-02	5.2E-02	8.6E-02	1.4E-01	2.7E-01
Spleen	7.3E-01	1.1E+00	1.6E+00	2.6E+00	4.8E+00
Testes	5.0E-02	6.4E-02	1.1E-01	1.6E-01	3.1E-01
Thymus	5.0E-02	6.4E-02	1.0E-01	1.6E-01	3.1E-01
Thyroid	4.7E-02	6.0E-02	9.7E-02	1.6E-01	3.1E-01
Uterus	7.6E-02	9.5E-02	1.5E-01	2.3E-01	4.0E-01
Remaining organs	5.8E-02	7.5E-02	1.2E-01	2.0E-01	3.7E-01
Effective dose (mSv/MBq)	1.4E-01	1.8E-01	2.8E-01	4.2E-01	7.6E-01

F(ab′) fragments

^{131}I 8.04 days

Organ	Absorbed dose per unit activity administered (mGy/MBq)				
	Adult	15 years	10 years	5 years	1 year
Adrenals	7.1E-02	9.1E-02	1.4E-01	2.3E-01	4.1E-01
Bladder	5.7E-01	7.4E-01	1.1E+00	1.5E+00	1.9E+00
Bone surfaces	5.1E-02	6.2E-02	9.7E-02	1.5E-01	3.0E-01
Brain	3.7E-02	4.7E-02	7.9E-02	1.3E-01	2.5E-01
Breasts	3.6E-02	4.6E-02	7.4E-02	1.2E-01	2.4E-01
Gallbladder	6.3E-02	7.7E-02	1.2E-01	1.8E-01	3.1E-01
Gastrointestinal tract					
Stomach	5.4E-02	6.6E-02	1.1E-01	1.6E-01	3.0E-01
Small intestine	5.7E-02	7.2E-02	1.1E-01	1.8E-01	3.3E-01
Colon	5.5E-02	6.9E-02	1.1E-01	1.7E-01	3.1E-01
(Upper large intestine	5.5E-02	6.9E-02	1.1E-01	1.7E-01	3.1E-01)
(Lower large intestine	5.6E-02	6.9E-02	1.1E-01	1.7E-01	3.0E-01)
Heart	4.7E-02	6.0E-02	9.6E-02	1.5E-01	2.8E-01
Kidneys	1.4E+00	1.7E+00	2.4E+00	3.6E+00	6.6E+00
Liver	8.7E-02	1.1E-01	1.7E-01	2.6E-01	4.7E-01
Lungs	4.3E-02	5.6E-02	8.9E-02	1.4E-01	2.7E-01
Muscles	4.5E-02	5.7E-02	9.1E-02	1.4E-01	2.8E-01
Oesophagus	4.2E-02	5.4E-02	8.6E-02	1.4E-01	2.7E-01
Ovaries	5.7E-02	7.3E-02	1.1E-01	1.8E-01	3.2E-01
Pancreas	6.6E-02	8.2E-02	1.3E-01	2.0E-01	3.6E-01
Red marrow	5.0E-02	5.9E-02	9.3E-02	1.5E-01	2.8E-01
Skin	3.6E-02	4.5E-02	7.4E-02	1.2E-01	2.4E-01
Spleen	1.6E-01	2.2E-01	3.4E-01	5.3E-01	9.6E-01
Testes	4.5E-02	5.9E-02	9.6E-02	1.5E-01	2.8E-01
Thymus	4.2E-02	5.4E-02	8.6E-02	1.4E-01	2.7E-01
Thyroid	4.1E-02	5.3E-02	8.6E-02	1.4E-01	2.7E-01
Uterus	6.8E-02	8.5E-02	1.4E-01	2.0E-01	3.5E-01
Remaining organs	4.6E-02	5.8E-02	9.3E-02	1.5E-01	2.8E-01
Effective dose (mSv/MBq)	1.1E-01	1.4E-01	2.1E-01	3.1E-01	5.3E-01

C.25. ^{201}Tl-ion

^{201}Tl

C.25.1. Biokinetic model

(C 75) Intravenously injected ionic monovalent thallium leaves the blood rapidly by uptake into the cells of all organs and tissues. The distribution is largely determined by the magnitude of the regional blood flow, and is therefore dependent on the degree of physical activity. Compared with the situation at rest, which is considered in the present model, uptake in muscles increases two- to three-fold during exercise, with a corresponding reduction in other tissues.

(C 76) The organ uptake data in the model are based on the reports by Samson et al. (1978), Atkins et al. (1977), and Chen et al. (1983). Bartlett et al. (1984) have shown that 80% of thallium is excreted by way of the gastrointestinal tract and 20% by the renal tract. The whole-body retention curve can be represented by a bi-exponential function, with half-times of 7 days for 63% of the injected activity and 28 days for 37% of the injected activity (Chen et al., 1983). It is assumed here that all organs and tissues have similar retention kinetics, with the exception of the heart which shows more rapid initial clearance (Freeman et al., 1986).

(C 77) The uptake of thallium ions in the testes has been studied extensively. Direct organ measurements at autopsy in two cases (Samson et al., 1978) showed 0.11–0.12%, while Hosain and Hosain (1981) and Gupta et al. (1981) derived values of 0.8–1.0% from gamma camera images of the testicular–scrotal region. More recent studies, however, indicate lower uptake (Rao et al., 1995; Nettleton et al., 2004; Thomas et al., 2005). Thomas et al. (2005) measured testicular uptake in 28 individuals using a collimation method so that the testes were shielded from body background with lead during imaging. However, activity in the scrotum could still influence the measurements. Based on data from Thomas et al. (2005) and Krahwinkel et al. (1988), uptake in the testes of 0.3% has been adopted.

C.25.2. References for ^{201}Tl-ion

Atkins, H.L., Budinger, T.F., Lebowitz, E., Ansari, A.N., Greene, M.W., Fairchild, R.G., Ellis, K.J., 1977. Thallium-201 for medical use. Part 3: Human distribution and physical imaging properties. J. Nucl. Med. 18, 133–140.

Bartlett, R.D., Lathrop, K.A., Faulhaber, P.F., Harper, P.V., 1984. Transfer of thallous ion to and from gastrointestinal sections. J. Nucl. Med. 25, P92.

Chen, C.T., Lathrop, K.A., Harper, P.V., Bartlett, R.D., Stark, V.J., Fultz, K.R., Faulhaber, P.F., 1983. Quantitative measurement of long term in vivo thallium distribution in the human. J. Nucl. Med. 24, P50.

Freeman, M.R., Kanwar, N., Armstrong, P.W., 1986. The variability of thallium half life at rest as compared to exercise. J. Nucl. Med. 27, 997.

Gupta, S.M., Herrera, N., Spencer, R.P., Hosain, F., Crucitti, T.W., 1981. Testicular-scrotal content of ^{201}Tl and ^{67}Ga after intravenous administration. Int. J. Nucl. Med. Biol. 8, 211–213.

Hosain, P., Hosain, F., 1981. Revision of gonadal radiation dose to man from thallium-201. In: Proceedings of the Third International Radiopharmaceutical Dosimetry Symposium, Oak Ridge 1980 (FDA 81-8166). Oak Ridge National Laboratories, Oak Ridge, TN, pp. 333–345.

Krahwinkel, W., Herzog, H., Feinendegen, L.E., 1988. Pharmacokinetics of thallium-201 in normal individuals after routine myocardial scintigraphy. J. Nucl. Med. 29, 1582–1586.

Nettleton, J.S., Lawson, R.S., Prescott, M.C., Morris, I.D., 2004. Uptake, localization, and dosimetry of ^{111}In and ^{201}Tl in human testes. J. Nucl. Med. 45, 138–146.

Rao, D.V., Shepstone, B.J., Wilkins, H.B., Howell, R.W., 1995. Kinetics and dosimetry of thallium-201 in human testes. J. Nucl. Med. 36, 607–609.

Samson, G., Wackers, F.J.Th., Becker, A.E., Busemann Sokole, E., van der Schoot, J.B., 1978. Distribution of thallium-201 in man. In: Oeff, K., Schmidt, H.A.E. (Eds.), Nuklearmedizin und biokybernetik, Vol. 1. Medico-informationsdienste, Berlin, pp. 385–389.

Thomas, S.R., Stabin, M.G., Castronovo, F.P., 2005. Radiation-absorbed dose from ^{201}Tl-thallous chloride. J. Nucl. Med. 46, 502–508.

C.25.3. Biokinetic data for ^{201}Tl-ion

Organ (S)	F_s	T (h)	a	$\widetilde{A}_s/A_0$(h)
Bone	0.06	168	0.63	4.9
		672	0.37	
Thyroid	0.002	168	0.63	0.16
		672	0.37	
Heart wall	0.04	10	0.50	1.9
		168	0.32	
		672	0.18	
Lungs	0.04	168	0.63	3.3
		672	0.37	
Kidneys	0.06	168	0.63	4.9
		672	0.37	
Liver	0.09	168	0.63	7.3
		672	0.37	
Spleen	0.007	168	0.63	0.57
		672	0.37	
Red marrow	0.06	168	0.63	4.9
		672	0.37	
Stomach wall	0.006	168	0.63	0.49
		672	0.37	
Small intestine wall	0.03	168	0.63	2.4
		672	0.37	
Muscles	0.41	168	0.63	33
		672	0.37	
Ovaries	0.0003	168	0.63	0.024
		672	0.37	
Testes	0.003	168	0.63	0.24
		672	0.37	
Other organs and tissues	0.19	168	0.63	16
		672	0.37	
Gastrointestinal tract contents				
Small intestine	0.80			0.77
Upper large intestine	0.80			2.2
Lower large intestine	0.80			3.3
Urinary bladder contents	0.20			
Adult, 15 years, 10 years				0.087
5 years				0.074
1 year				0.050

C.25.4. Absorbed doses for ^{201}Tl-ion

^{201}Tl 3.05 days

Organ	Absorbed dose per unit activity administered (mGy/MBq)				
	Adult	15 years	10 years	5 years	1 year
Adrenals	5.7E-02	7.0E-02	1.0E-01	1.5E-01	2.7E-01
Bladder	3.9E-02	5.4E-02	7.9E-02	1.2E-01	2.2E-01
Bone surfaces	3.8E-01	3.9E-01	6.9E-01	1.2E+00	1.9E+00
Brain	2.2E-02	2.4E-02	3.6E-02	5.4E-02	1.0E-01
Breasts	2.4E-02	2.7E-02	4.4E-02	6.6E-02	1.3E-01
Gallbladder	6.5E-02	8.1E-02	1.3E-01	1.9E-01	3.1E-01
Gastrointestinal tract					
Stomach	1.1E-01	1.5E-01	2.2E-01	3.5E-01	7.3E-01
Small intestine	1.4E-01	1.8E-01	3.1E-01	5.0E-01	9.4E-01
Colon	2.5E-01	3.2E-01	5.5E-01	9.2E-01	1.8E+00
(Upper large intestine	1.8E-01	2.3E-01	3.9E-01	6.4E-01	1.2E+00)
(Lower large intestine	3.4E-01	4.5E-01	7.6E-01	1.3E+00	2.5E+00)
Heart	1.9E-01	2.4E-01	3.8E-01	6.0E-01	1.1E+00
Kidneys	4.8E-01	5.8E-01	8.2E-01	1.2E+00	2.2E+00
Liver	1.5E-01	2.0E-01	3.1E-01	4.5E-01	8.4E-01
Lungs	1.1E-01	1.6E-01	2.3E-01	3.6E-01	6.9E-01
Muscles	5.2E-02	8.2E-02	1.6E-01	4.5E-01	7.6E-01
Oesophagus	3.6E-02	4.2E-02	6.0E-02	9.0E-02	1.6E-01
Ovaries	1.2E-01	1.2E-01	2.9E-01	4.9E-01	1.1E+00
Pancreas	5.7E-02	7.0E-02	1.1E-01	1.6E-01	2.8E-01
Red marrow	1.1E-01	1.3E-01	2.2E-01	4.5E-01	1.1E+00
Skin	2.1E-02	2.4E-02	3.8E-02	5.8E-02	1.1E-01
Spleen	1.2E-01	1.7E-01	2.6E-01	4.1E-01	7.4E-01
Testes	1.8E-01	4.1E-01	3.1E+00	3.6E+00	4.9E+00
Thymus	3.6E-02	4.2E-02	6.0E-02	9.0E-02	1.6E-01
Thyroid	2.2E-01	3.5E-01	5.4E-01	1.2E+00	2.3E+00
Uterus	5.0E-02	6.2E-02	9.9E-02	1.5E-01	2.7E-01
Remaining organs	5.4E-02	8.2E-02	1.6E-01	3.4E-01	5.5E-01
Effective dose (mSv/MBq)	1.4E-01	2.0E-01	5.6E-01	7.9E-01	1.3E+00

ANNEX D. RECOMMENDATIONS ON BREAST-FEEDING INTERRUPTIONS

D.1. Introduction

(D 1) Since many radiopharmaceuticals are secreted in breast milk, it is safest to assume that, unless there are data to the contrary, some radioactive compound will be found in the breast milk when a radiopharmaceutical is administered to a lactating female. Consideration should be given to postponing the procedure. If the procedure is performed, the child should not be breast fed until the radiopharmaceutical is no longer secreted in an amount estimated to give an effective dose >1 mSv to the child. It is therefore recommended that the following actions should be taken for various radiopharmaceuticals, and that the milk expressed during this interruption period should be discarded.

Radiopharmaceutical	Interruption
^{14}*C-labelled*	
Triolein	No
Glycocholic acid	No
Urea	No
^{99m}*Tc-labelled*	
DISDA	No[*,†]
DMSA	No[*,†]
DTPA	No[*,†]
ECD	No[*,†]
Phosphonates (MDP)	No[*,†]
Gluconate	No[*,†]
Glucoheptonate	No[*,†]
HM-PAO	No[*,†]
Sulphur colloids	No[*,†]
MAA	12 h
MAG3	No[*,†]
MIBI	No[*,†]
Microspheres (HAM)	12 h
Pertechnetate	12 h
PYP	No[*,†]
RBC (in vivo)	12 h
RBC (in vitro)	No[*,†]
Technegas	No[*,†]
Tetrofosmin	No[*,†]
WBC	12 h

Radiopharmaceutical	Interruption
I-labelled	
^{123}I-BMIPP	>3 weeks[‡,§]
^{123}I-HSA	>3 weeks[‡,§]
^{123}I-iodo hippurate	12 h
^{123}I-IPPA	>3 weeks[‡,§]
^{123}I-MIBG	>3 weeks[‡,§]
^{123}I-NaI	>3 weeks[‡,§]
^{125}I-HSA	>3 weeks[‡]
^{125}I-iodo hippurate	12 h
^{131}I-iodo hippurate	12 h
^{131}I-MIBG	>3 weeks[‡]
^{131}I-NaI	>3 weeks[‡]
Others	
^{11}C-labelled	No[¶]
^{13}N-labelled	No[¶]
^{15}O-labelled	No[¶]
^{18}F-FDG	No
^{22}Na	>3 weeks[‡]
^{51}Cr-EDTA	No
^{67}Ga-citrate	>3 weeks[‡]
^{75}Se-labelled agents	>3 weeks[‡]
^{81m}Kr-gas	No
^{111}In-octreotide	No
^{111}In-WBC	No
^{133}Xe	No
^{201}Tl-chloride	48 h

[*] 'No', interruption not essential.

[†] 'No' for most of the ^{99m}Tc-labelled compounds, under the circumstance that no free pertechnetate exists in the radiopharmaceutical. An interruption of 4 h during which one meal is discarded can be advised to be on the safe side.

[‡] 3 weeks (504 h) at least. However, difficult to maintain the milk supply → cessation.

[§] ^{123}I, all substances labelled with ^{123}I (except iodo-hippurate): >3 weeks due to the risk of contamination of other iodine isotopes.

[¶] ^{11}C, ^{13}N, and ^{15}O-labelled substances, interruption not essential due to short physical half-life.

D.2. References and further reading for Annex D

Ahlgren, L., Ivarsson, S., Johansson, L., Mattsson, S., Nosslin, B., 1985. Excretion of radionuclides in human breast milk after the administration of radiopharmaceuticals. J. Nucl. Med. 26, 1085–1090.

Castronovo Jr., F.P., Stone, H., Ulanski, J., 2000. Radioactivity in breast milk following ^{111}In-octreotide. Nucl. Med. Commun. 21, 695–699.

Evans, J.L., Mountford, P.J., Herring, A.N., Richardson, M.A., 1993. Secretion of radioactivity in breast milk following administration of $^{99}Tc^{m}$-MAG3. Nucl. Med. Commun. 14, 108–111.

Johnston, R.E., Mukherji, S.K., Perry, R.J., Stabin, M.G., 1996. Radiation dose from breastfeeding following administration of thallium-201. J. Nucl. Med. 37, 2079–2082.

McCauley, E., Mackie, A., 2002. Breast milk activity during early lactation following maternal $^{99}Tc^{m}$ macroaggregated albumin lung perfusion scan. Br. J. Radiol. 75, 464–466.

Mountford, P.J., Coakley, A.J., 1989. A review of the secretion of radioactivity in human breast milk: data, quantitative analysis and recommendations. Nucl. Med. Commun. 10, 15–27.

Rose, M.R., Prescott, M.C., Herman, K.J., 1990. Excretion of iodine-123-hippuran, technetium-99m-red blood cells, and technetium-99m-macroaggregated albumin into breast milk. J. Nucl. Med. 31, 978–984.

Rubow, S., Klopper, J., Wasserman, H., Baard, B., van Niekerk, M., 1994. The excretion of radiopharmaceuticals in human breast milk: additional data and dosimetry. Eur. J. Nucl. Med. 21, 144–153.

Stabin, M.G., Breitz, H.B., 2000. Breast milk excretion of radiopharmaceuticals: mechanisms, findings, and radiation dosimetry. J. Nucl. Med. 41, 863–873.

Tobin, R.E., Schneider, P.B., 1976. Uptake of ^{67}Ga in the lactating breast and its persistence in milk: case report. J. Nucl. Med. 17, 1055–1056.

ANNEX E. RADIATION EXPOSURE OF HANDS IN RADIOPHARMACIES: MONITORING OF DOSES AND OPTIMISATION OF PROTECTION

E.1. Introduction

(E 1) The preparation of radiopharmaceuticals takes place in a radiopharmacy, which may serve a single nuclear medicine unit or may distribute radiopharmaceuticals to users in several hospitals. The radiopharmaceuticals are then administered to patients for diagnostic tests or therapy. The most common radionuclide used in nuclear medicine is ^{99m}Tc, which is added to manufactured pharmaceutical kits. The high activity of the radionuclide used for labelling forms a source of radiation exposure to radiopharmacists. The distribution of dose across the hands is often highly non-homogenous. Whereas personal dose equivalents, recorded by dosimeters placed at the thorax, show yearly values well below the dose limits, the dose equivalents to hands and fingers may reach values up to two orders of magnitude greater than the thorax and have the potential to exceed the annual dose limit of 500 mSv.

(E 2) ^{99m}Tc is obtained from ^{99}Mo/^{99m}Tc generators by controlled elution, and the radionuclide is used subsequently for preparation of various radiopharmaceuticals, using appropriate ligands and following specific labelling protocols. The activities of ^{99m}Tc administered to individual patients vary from approximately 70 to 1300 MBq. In a busy nuclear medicine department, the daily usage of ^{99m}Tc activity may reach 50 GBq, and radiopharmacies that serve a number of nuclear medicine departments may handle over 200 GBq.

(E 3) The activities dispensed have been increasing over the last 20 years due to the rise in the number of patients investigated and also due to some increase in the activity administered to an average patient to allow single photon emission computed tomographic (SPECT) imaging procedures to be performed (Gemmell and Staff, 1988; ARSAC, 2006). Doses to the hands of operators have also increased with the activities handled.

(E 4) Medical physicists have been aware for some time that exposure of the hands of radiopharmacists could be significant (Neil, 1969; Anderson et al., 1972; Bjurman et al., 1982), and more detailed studies were carried out in the late 1980s (Harding et al., 1985; Koback and Plato, 1985; Clarke and Brisco, 1986; Williams et al., 1987; Stuardo, 1990; Batchelor et al., 1991a,b). However, these studies aimed to determine the average dose to the hands to demonstrate compliance with earlier ICRP recommendations (ICRP, 1977).

(E 5) Systematic studies to determine the dose to specific parts of the hand to demonstrate compliance with later ICRP recommendations were initiated in the UK, where a large radiopharmacy in the Western Infirmary, Glasgow was preparing radiopharmaceuticals for nuclear medicine departments in 12 hospitals (Montgomery et al., 1997, 1999; Dhanse et al., 2000). Observations made over several years showed that exposure of the hands had been rising steadily because of the increased

activities being handled. The use of shielding devices enabled some dose reduction (Montgomery et al., 1997), but the systems available for automating the preparation of ^{99m}Tc radiopharmaceuticals could not be used as they were unable to dispense the large numbers of patient vials within the time scale required in a large radiopharmacy (Montgomery et al., 1999).

(E 6) Other radiopharmaceutical developments have occurred over the last ten years which may contribute to hand exposure. There is some (very limited) information indicating that a similar problem may be encountered in positron emission tomography (PET) units; however, automation of the synthesis and dispensing of positron emitting radiopharmaceuticals, together with use of appropriate shielding, may alleviate the problem. There has been increased interest in the use of high-energy beta-emitting radionuclides, particularly ^{90}Y, for treatment of malignant and non-malignant conditions as new radiopharmaceuticals have become available. The aim of this report is to review the data that are currently available, and to recommend strategies for protection of the hands and for monitoring dose to the hands. The text will concentrate explicitly on hand exposure from ^{99m}Tc and high-energy beta-emitters (^{90}Y, ^{32}P) explicitly, but some general comments about protection for ^{18}F-FDG and other PET radiopharmaceuticals will be included.

(E 7) The assessment of average absorbed doses to the hands does not satisfy dosimetry requirements from a radiation protection point of view, since the non-uniformity of the dose distribution is pronounced, and it is the maximum local skin exposure which is important, because it is linked to potential deterministic effects. Therefore, it is the maximum dose that should be evaluated and tested for conformity with the dose limits recommended by the Commission for the most exposed parts of the skin of the hands. For practical purposes, this has been defined as 500 mSv averaged over 1 cm^2 (ICRP, 1991a; 2007).

E.2. Methods of dose assessment

(E 8) Measurements of doses to the hands of radiopharmacists have been based on two methods: thermoluminescent dosimetry (Harding et al., 1990; Batchelor et al., 1991a,b; Chiesa et al., 1997; Hastings et al., 1997; Mackenzie, 1997; Dhanse et al., 2000; Jankowski et al., 2003; Berus et al., 2004; Paul et al., 2006; Vanhavere et al., 2006; Covens et al., 2007; Wrzesień et al., 2008) and electronic monitoring (Montgomery et al., 1997, 1999; Dhanse et al., 2000; Whitby and Martin, 2002, 2003, 2005; Donadille et al., 2005; Guy et al., 2005).

E.2.1. Thermoluminescent dosimeters

(E 9) Several studies have attached thermoluminescent dosimeters (TLDs) to various sites on the skin of the hands, with dose readings recorded after a given procedure or time span of exposure. This method has proved particularly suitable for studies of dose distribution across the skin of the hands and fingers, and comparing

the dose to the most exposed part of the hand with that recorded at the position used for routine monitoring.

(E 10) A recent systematic investigation has been carried out in Poland in which TLDs were fixed on the finger tips (nails, pulps), the second phalanges of all fingers, the bases of the middle fingers on the back of the hand where a dosimetric ring is routinely worn in these departments, and on various points on the palm and wrist on both hands (Wrzesień et al., 2008). In this study, measurements were obtained from 19 TLDs on each hand, exposed over 42 daily shifts of radiopharmacy practice performed by 13 radiopharmacists from five nuclear medicine departments. The large volume of collected data has permitted evaluation of the dose distribution over the hands and parts of the fingers. Other studies have measured dose distributions and made comparisons with monitoring positions on the palm side of the hand (Berus et al., 2004; Vanhavere et al., 2006), or made measurements over many years comparing the dose to the finger tip with that recorded by a ring dosimeter (Dhanse et al., 2000).

E.2.2. Electronic monitoring

(E 11) A second method for dose assessment was employed at the Regional Dispensary of the Western Infirmary in Glasgow, where the majority of activity is dispensed into vials for single-patient administrations. The dosimetric method for the measurement and recording of dose rates to various parts of the hands utilised an instrument known as AEGIS (Advance Extremity Gamma Instrumentation System; Montgomery et al., 1997; Dhanse et al., 2000; Whitby and Martin, 2003, 2005). This instrument is based on a semiconductor detector, which is sensitive to gamma-ray photons, and the electronic signals are stored by a logger and transmitted to a processor linked to a personal computer. The detectors respond linearly to the dose rate from photons of a given energy, and were calibrated for primary and scattered photons from ^{99m}Tc.

(E 12) The main advantage of this device is the ability to observe instantaneous changes in the dose rate, and to record them almost in real time so that doses received from single actions can be identified. Variable positioning enables observations of exposure rate for the fingers to which the detector is attached to be determined during different phases of radiopharmaceutical preparation and dispensing. The simultaneous review of videos of dispensing with the dose rate data recorded at the time is particularly useful (Guy et al., 2005).

E.3. Dispensing technique

(E 13) Workers who prepare and dispense in a radiopharmacy perform a series of similar procedures, often for a large number of patient administrations. The basic manipulation consists of withdrawing into a syringe activity from a vial containing eluate that has been produced in the ^{99}Mo/^{99m}Tc generator. This is transferred to a second vial for labelling a ligand. Different techniques for withdrawal have been encountered in several departments studied in the UK, and are described in detail by Whitby and Martin (2005). Common techniques are described below.

Fig. E.1. Positions of hands used for dispensing radiopharmaceutical with the inversion technique, showing the arrangement commonly used with the index finger pushing against the syringe barrel as the plunger is pulled by the thumb and middle finger (Martin and Whitby, 2005) (with permission from Lippincott Williams and Wilkins).

E.3.1. Inversion technique

(E 14) Use of an inverted vial with the syringe needle inserted into liquid pooled near the neck. A typical application of the technique, in which the thumb and middle finger withdraw the plunger with the index finger pushing against the barrel of the syringe, is shown in Fig. E.1.

E.3.2. V-technique

(E 15) The vial is held at 20–40° to the horizontal, and the syringe angled at 20–40° in the opposite direction to form a V-configuration (Fig. E.2). In a modification to

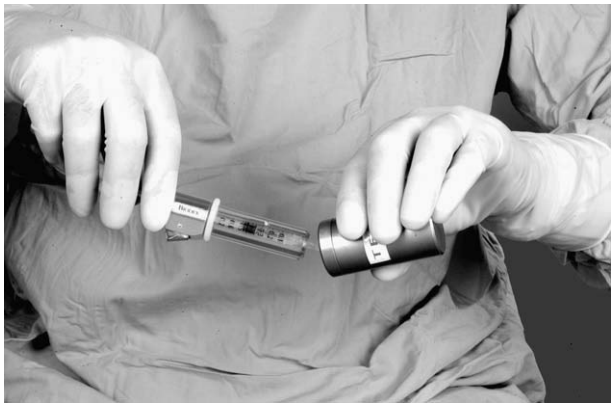

Fig. E.2. Positions of hands used for dispensing radiopharmaceutical with the V-technique (Martin and Whitby, 2005) (with permission from Lippincott Williams and Wilkins).

Fig. E.3. Positions of hands used for dispensing radiopharmaceutical with the vial tipped at 45° over a bench and withdrawing liquid using a longer syringe needle (Martin and Whitby, 2005) (with permission from Lippincott Williams and Wilkins).

the V-technique, the vial may be held at a steeper angle (50–70°) to the horizontal, while the syringe is angled downwards at 10–30° below the horizontal.

E.3.3. 45° Table top

(E 16) The vial is not inverted but tipped at 45° over a bench, and liquid is withdrawn using a longer syringe needle (Fig. E.3). This technique may be used where there are larger amounts of liquid in the dispensing vial.

E.3.4. Purpose-built jig

(E 17) In some departments, a purpose-built jig is used to hold a vial containing eluted activity at a defined position to avoid direct contact of the vial with the hand of the worker.

(E 18) The dispensing technique employed is less important in determining the magnitude of the dose than the skill of the operator and the use made of local shielding devices (see Section E.5). Doses can be increased considerably if the procedure takes a longer time, for example if the radiopharmacist needs to make small adjustments to remove air bubbles (Berus et al., 2004). Thus, it is important that staff undergo an extensive period of training and practice with non-radioactive liquids prior to dispensing radiopharmaceuticals for the first time. Although the dispensing technique is less important in determining the magnitude of doses received, it does affect the fingers which receive the highest doses. Therefore, it should be taken into account when determining the positions on the fingers at which monitoring should be carried out.

(E 19) There has been some debate regarding the size of syringe that is most appropriate for dispensing. A 1-ml syringe is perhaps the best choice, as it allows the volume of radiopharmaceutical to be judged more readily so that manipulations can be performed more rapidly, but this results in the fingers being closer to the radiopharmaceutical. A 2-ml syringe is often recommended, as the radiopharmaceutical in the base of a larger syringe will be further away from the fingers manipulating the plunger. However, amounts of solution in the syringe are more difficult to judge and this may increase the time taken to dispense. Thus, there is a balance between competing factors about which the radiopharmacist and radiation protection expert should liaise to assess the risk and determine the best approach.

E.4. Hand exposure and dose distribution

(E 20) Results of studies on hand exposure are often expressed in terms of dose to a given location on either hand, related to the amount of ^{99m}Tc activity processed (μSv/GBq). A study of several UK radiopharmacies showed that doses to the most exposed parts of the hands from dispensing radiopharmaceuticals varied from 4 to 40 μGy/GBq (Whitby and Martin, 2005). A substantial amount of other data (Koback and Plato, 1985; Williams et al., 1987; Chiesa et al., 1997; Hastings et al., 1997; Mackenzie, 1997; Dhanse et al., 2000; Harding et al., 1990; Jankowski et al., 2003; Paul et al., 2006; Tandon et al., 2007; Covens et al., 2007; Wrzesień et al., 2008) for individual pharmacists or other staff members dispensing ^{99m}Tc-labelled radiopharmaceuticals shows doses varying from a few μGy to more than 100 μGy per GBq handled.

(E 21) All studies demonstrate the importance of the skill of the radiopharmacist and the speed with which syringe manipulations are performed. As a rule, workers with limited experience receive doses to the fingers which are significantly higher than those of highly skilled radiopharmacists who can perform the manipulations more rapidly. The dispensing time will be kept to a minimum by close attention to staff training.

(E 22) During the dispensing process, the majority of the exposure to the hand originates from activity within the syringe, as the radiopharmaceutical is drawn up and dispensed (Dhanse et al., 2000; Whitby and Martin, 2003). The tip of the index finger on the dominant hand is likely to receive the highest dose. The exposure to the tip of the thumb can also be significant and may be similar to that of the index finger, especially where a syringe shield is used (Whitby and Martin, 2005).

(E 23) As the active volume is drawn into the syringe, it is often the thumb and middle finger which draw back the plunger (Fig. E.1), with the index finger pushing against the end of the syringe shield. Therefore, the index finger tends to be nearer to the active volume than any other part of the hand. However, the finger placement used by different individuals varies, even when the same dispensing technique is used, and the distribution of dose across the hand varies for every individual as it is related to the exact position that the fingers adopt during the dispensing process. Some individuals place the tip of the index finger further along the barrel of the syringe when withdrawing or dispensing a volume of activity, so it will not be as highly exposed as other fingers. Thus, when a syringe shield is employed, small differences in the positions of the index finger and thumb relative to the active volume within the syringe can have a significant effect on exposure.

(E 24) The dose to the non-dominant hand, which holds the vial, also depends on the use of a syringe shield and dispensing technique. Staff employing the inversion technique (Fig. E.1) or modified V-technique have the potential to expose the non-dominant hand to a greater dose than those employing the V- or 45° table top techniques (Figs. E.2 and E.3; Whitby and Martin, 2005). This is because the vial is held with the neck towards the bottom of the hand, so the wrist lies closer to the radiation field from the vial and syringe (Fig. E.1). As the user inverts the vial, the active volume collects near the neck of the vial, increasing the exposure by broadening the radiation field (Whitby and Martin, 2003). Using the V- and 45° table top techniques, the non-dominant hand is largely to the rear of the top of the vial and is further from the radiopharmaceutical in the syringe, so exposure is less significant than that to the fingers of the dominant hand.

(E 25) For procedures where dispensing is undertaken from vials containing more liquid, the vial does not have to be inverted and a long syringe needle can be used to reach the base of the vial. Although there will be more activity in the vial, the hand dose will tend to be lower because the radiopharmaceutical is in the bottom of the vial, further from the hand, and the protection offered by the vial shield or lead pot is more effective.

(E 26) There is general agreement that, irrespective of local differences in technique, **the most exposed parts of the hands are likely to be the tips of the index and middle fingers, and the thumb of the dominant hand**. The hand that manipulates the syringe will tend to receive a higher dose, and the dose to the non-dominant hand will typically be approximately half this value. The differences in handling techniques, including ways of manipulating the syringe, and the relative positions of the syringe and vial for withdrawal of active solutions are of secondary importance for the magnitude of doses to hands compared with the use of syringe shielding.

(E 27) Similar issues to those discussed above also apply to staff members in nuclear medicine departments. Although radiopharmaceuticals may be dispensed by the radiopharmacist directly into syringes, ready for injection, it is more usual, particularly where one radiopharmacy serves several hospitals, to dispense into a vial which is then sent to the nuclear medicine department. Thus, withdrawal of radiopharmaceuticals into a syringe may also be undertaken by a nurse/technician or a physician prior to injection into the patient, although the activities handled will be much lower. Doses from giving the injection are variable, but again use of a syringe shield is the most effective way of keeping these to a minimum. The non-dominant hand is sometimes used to support the syringe needle, and if this is done the tips of the fingers on this hand are likely to receive the highest doses (Covens et al., 2007). If a Venflon needle is inserted into the patient's vein beforehand, the injection may proceed more rapidly and the dose to the hand of the nurse or physician kept to a minimum.

E.5. Use of syringe and vial shields

(E 28) The application of shielding for the syringe and vial is the single most important factor in reducing the magnitude of doses to the finger tips. Syringe shields have the disadvantage that they are heavy and make manipulations more difficult, but they provide the most effective method for reducing hand doses. Doses to the fingers for the parts of procedures for which syringe shields are used are only 10–25% of those for similar parts when a shield is not used. The maximum dose rates (averaged over 1-s intervals) are reduced to approximately 40% of those where no shield is used, and the lengths of the periods of exposure to high dose rates are reduced from 6–10 s to 2–4 s.

(E 29) The reason for this is that the syringe shield provides protection around the barrel of the syringe, but there is still a narrow pencil beam of radiation emerging from the end in the direction in which the fingers are positioned in order to manipulate the plunger. The maximum dose rates are smaller because of the shielding, but the periods of exposure, as the fingers move through the high dose rate parts of the field, are also shorter because the lateral extent of the field with high dose rates is less (Whitby and Martin, 2003).

(E 30) Due to the dose reduction that is achieved, syringe shields should also be used for intravenous injection of patients. The poor visibility of the pharmaceutical within traditional syringe shields, which only have narrow lead glass windows, may increase the time to dispense, and some reports have suggested that this may outweigh the shielding advantage (Berus et al., 2004). Syringe shields made entirely from lead glass are now available, which provide good visibility and so should not slow down the procedure (Figs. E.1–3). They allow the technician to check volumes of liquid more quickly and determine whether there are any bubbles present in the syringe. The disadvantage of glass shields is that they are relatively brittle, they often break, and they are more expensive to replace. The metal syringe shields with windows are more substantial, but as stated above, they limit the view of the liquid in the syringe and may therefore slow down procedures.

(E 31) Vials from which radioactivity is drawn will always be handled in shielded containers, which may be simple lead pots or specialist vial shields. Tungsten vial shields, which have screw-top lids with an aperture through which the syringe needle is inserted, provide more effective shielding against exposure from activity in the vial from which the radiopharmaceutical is being withdrawn. The radiation field is restricted to the region immediately in front of the shield aperture (Whitby and Martin, 2003). The screw-top lid on the shield holds the vial firmly in place, and this facilitates the manipulation as the operator does not need to hold the vial in place with the syringe needle. It also avoids the temptation, when a simple lead pot is used, for the operator to hold the vial in place with a finger tip, which would increase the dose to that finger significantly.

(E 32) The disadvantage of a vial shield is that it does not allow the amount of liquid in the vial to be viewed. Effective shielding of vials is essential when high activity levels in the eluate vial are transferred to the kit vials; for this, tungsten vial shields provide the best option for gamma-emitting radionuclides. When the activity from kit vials is divided into individual patient administrations of radiopharmaceuticals (much lower activity), use of a vial shield is preferable for the kit vial. Simple lead pots provide adequate protection for the transport and drawing up of radiopharmaceutical for individual patient administrations.

E.6. Dispensing cabinets

(E 33) The average time taken to dispense radiopharmaceuticals during a session varies between centres. This depends on the number of patient administrations dispensed, the protocol, and the technique adopted. Preparatory procedures, such as the sequence of adding active solution and saline to the preparation involved in labelling, may be optimised more or less effectively.

(E 34) The design of the dispensing cabinet is also an important factor. In some radiopharmacies, the radiopharmaceuticals are prepared in shielded laminar flow cabinets which form part of an aseptic suite. The cabinets have thick lead walls which protect the body of the user, and a lead glass shield in the upper part of the cabinet protects the head and neck. In one common design, the users work over the top of the wall, through a slit between the lower wall and upper glass shield that runs the length of the cabinet. This gives the user a relatively free range of movement within the cabinet and enables the radiopharmaceuticals to be dispensed rapidly, while minimising the dose to the body. Careful positioning of vials and materials within the cabinet is important for streamlining the procedure and minimising doses to the hands.

(E 35) Some centres use isolator hot cell cabinets, in which the working space is completely sealed and the operator is required to put both hands through sealed, gloved entry ports. The range of movement open to the user in this arrangement is more restricted, and this is reflected in increased session times. However, it is not the time spent working with activity, i.e. the time spent per manipulation, that is increased by use of an isolator hot cell, but the additional time required for

operators to insert and withdraw their hands from the gloved area in order to perform other tasks within the room.

(E 36) The dose data available from centres where hand doses have been studied in detail with a heavy workload dispensing of the order of 100–200 GBq/day led to the conclusion that there is a potential for approaching, and possibly exceeding, the annual dose limit to the pulp of fingers (500 mSv) if appropriate protection measures are not in place (Dhanse et al., 2000; Jankowski et al., 2003; Whitby and Martin, 2005; Wrzesień et al., 2008).

E.7. Hand doses from beta-emitting therapy radionuclides

(E 37) Significant doses to the hands can be received during the administration of radionuclides which emit high-energy beta-radiation. Medical staff often are not aware of the high risk from exposure to beta particles, and the 500 mSv annual dose limit can easily be exceeded if appropriate protection measures are not in place. Treatments for a variety of malignancies are now undertaken in major radiotheraoy centres, of which the application of radioimmunotherapy for non-Hodgkins lymphoma with ^{90}Y Zevalin is the most widely used (Aubert et al., 2002; Zhu, 2004; Cremonesi et al., 2006; Rimpler et al., 2007; Rimpler and Barth, 2007). In addition, radiosynovectomy using ^{90}Y and other beta emitters has been applied to the treatment of rheumatoid arthritis for over 40 years (Mielcarek and Barth, 2002; Liepe et al., 2005). These therapies require one or more GBq of ^{90}Y. They present significant protection problems, since the dose rates at 5 cm and 30 cm from a 1 Gbq point source are 3500 mGy h^{-1} and 100 mGy h^{-1}, respectively (Shleien et al., 1998), and the skin dose equivalent rate from a contamination level of 1 MBq cm^{-2} is 2000 mSv h^{-1} (Delacroix et al., 2002).

(E 38) A wide range of finger doses from 1 μSv to over 100 μSv per MBq handled have been reported (Mielcarek and Barth, 2002; Liepe et al., 2005; Rimpler et al., 2007; Rimpler and Barth, 2007), which implies that there are significant options for improving radiation protection practices. Measurements performed in a number of hospitals during therapy with Zevalin have shown mean/median finger doses of 3 to 6 mSv per patient for the preparation stage and 0.5 to 1 mSv per patient for the administration of 1 – 2 GBq of 90Y (Cremonesi et al., 2006; Rimpler et al., 2007). For the administration of therapies such as peptide receptor radiotherapy with 90Y, which are performed using an infusion pump, a median dose to the finger tip of 5.5 mSv and a range of 2 – 29 mSv were reported by Rimpler et al. (2007).

(E 39) Direct handling of any vessel containing a high-energy beta emitter may give rise to high localised skin doses. Therefore, particular care should be taken in the planning of administrations. Shields of 10 mm thick polymethylmethacrylate (PMMA) must be used to absorb the beta radiation and reduce bremsstrahlung production in order to ensure that doses are kept to a minimum, and dedicated hot cells may be used for radiopharmaceutical preparation. The mean and maximum ranges of 90Y beta particles in PMMA are 4.0 mm and 9.2 mm, respectively. Specialised syringe shields made of 5 – 10 mm thick PMMA should always be used. Forceps

should be used for manipulations of syringes and vials where close contact with any thin-walled vessel containing radiopharmaceutical would otherwise occur. If the injection or infusion is carried out through tubing, then the length should be minimised, since the local unshielded dose rate may be tens of mSv per minute for administrations of GBq activities, and PMMA shields should be used for infusion pumps. The wearing of disposable gloves is essential for all procedures involving unsealed radionuclides. However, for beta emitters it can be critical in avoiding tissue reactions, since the skin dose rate would be 1350 mSv h^{-1} if a 0.05 ml droplet containing 1 Mbq of 90Y were left on the skin (Delacroix et al., 2002).

(E 40) If adequate protection measures are not in place, the exposure of the fingers will be high, and doses of many tens and even hundreds of mSv have been reported from single patient administrations for a number of different 90Y therapies (Mielcarek and Barth, 2002; Liepe et al., 2005; Rimpler et al., 2007; Rimpler and Barth, 2007). For example, during administration of 90Y for radiosynovectomy treatment of the knee, doses of 20 to 100 μSv per MBq were received when the non-dominant hand was used to hold the syringe needle in position for the injection (Liepe et al., 2005). The use of grasp forceps to hold the needle reduced the dose to the hands to less than 1 μSv per MBq.

E.8. Radiopharmaceuticals for PET imaging

(E 41) Studies reported to date for preparation of ^{18}F-FDG are limited (Liemann et al., 2000; Laffont et al., 2001; Cronin, 2002; Guillet et al., 2005; Vanhavere et al., 2006; Visseaux et al., 2007; Tandon et al., 2007; Husak et al., 2007; Covens et al., 2007). It is difficult to determine how representative the limited amount of published data is for PET-radiopharmaceutical preparation in general. Results suggest dose rates of 100–600 μGy/GBq handled, but shielding of the fingers at these centres was more limited. Dose rates reported for ^{99m}Tc preparation in some of these studies were substantially greater than those in this report, so the results may not represent dose levels for techniques that have been optimised.

(E 42) There is more scope for automation of the dispensing process because the numbers of vials prepared at one time is usually more limited. However, there are issues of protection in the handling and administration, so some notes on shielding are included here. Moreover, as ^{18}F-FDG production increases, doses could easily approach the dose limit if procedures are not optimised. Some of the shorter half-life radionuclides require the injection of higher activities, and a manual injection of 2.3 GBq of ^{15}O for a single scan can give a finger dose approaching 1 mSv (Cronin, 2002).

(E 43) Dispensing technique is important for PET radiopharmaceuticals because of the higher dose rates and the short ranges of positrons. If the radiopharmaceutical is drawn up by hand, the inversion and V-techniques, in which the liquid is in the mouth of the vial, are not recommended (Cronin, 2002). Instead, the 45° table top technique should be employed, with the vial held in the lead pot or vial shield using

a pair of long-handled forceps, in order to keep both hands out of the main radiation field.

(E 44) Since the energy of annihilation photons is 511 keV, for which the half value thickness of lead is 4 mm, thicker shields are required for PET radiopharmaceuticals. Vial shields should be made typically from 20–35-mm-thick lead or 20–25-mm-thick tungsten, and syringe shields from 15-mm-thick lead and 10–12-mm-thick tungsten, and should be handled behind a 50–60-mm-thick lead shield to minimise the dose to the body. Since such vial and syringe shields are too heavy to manipulate safely, mechanical supports are normally required for both dispensing and injecting PET radiopharmaceuticals (Towsen, 2003).

(E 45) The possibility of producing bremsstrahlung x rays from positron interactions should be considered. Most of the 0.63-MeV positrons emitted by ^{18}F, which have ranges of 0.9 mm and 1.7 mm in glass and PMMA, respectively, will be absorbed in the walls of the vial or syringe. However, higher energy positrons emitted by ^{11}C (0.96 MeV), ^{13}N (1.2 MeV), and ^{15}O (1.7 MeV) have ranges of several millimetres, and to absorb these, PMMA or plastic liners may be incorporated within vial and syringe shields.

(E 46) Bremsstrahlung x rays make up <5% of the energy converted to radiation, and may therefore not be considered important. However, the liners will increase the distance of the fingers from the source as well as reducing the number of higher energy photons which are more difficult to shield against. An alternative to the lead and tungsten shields that has been used is a 10-mm-thick PMMA shield, which absorbs all the positrons and increases the distance between the syringe and the technologists' hands, but the syringe must be placed in a shielded container as soon as the radiopharmaceutical has been drawn up until it is injected (Cronin, 2002).

(E 47) The subject of finger doses from PET radiopharmaceuticals merits further systematic study to determine and document the dose levels, most appropriate administration methods, and recommendations for dosimetry.

E.9. Relative importance of different aspects of protection

(E 48) In summary, the protection benefit derived from the technique used involves a balance between various factors. For example, use of shielding devices or increasing the distance from the source will reduce the dose rate but may increase the exposure time, so the impact on the dose to the fingers is more difficult to assess. The relative importance of different aspects of working techniques, together with the protection methodologies that they affect and an indication of the likely impact on dose reduction based on experience gained, are set out in Table E.1. (Martin and Whitby, 2003).

(E 49) In view the factors already discussed, it is understandable that doses to the hands recorded and reported in the literature are highly variable. The most appropriate quantity to use for making comparisons is the assessed dose at the finger tips per unit of activity processed during preparation of radiopharmaceuticals. These data vary between different locations by at least an order of magnitude, and there

Table E.1. Protection factors.

Methodology	Protection	Impact
Whether or not a syringe shield is used	S and T	High
Shielding employed for the vial	S	High
Position of the fingers of the hand holding the syringe	D and T	Medium/high
The speed with which unshielded manipulations are performed	T	Medium/High
Whether the vial from which the radiopharmaceutical is being withdrawn is angled with a long needle extending to the base, or whether the vial is inverted and the needle inserted only 1–2 mm within the cap	D and T	Medium
Size of syringe and length of needle	D and T	Medium
Whether the radiopharmacy product is a vial containing radiopharmaceutical for a single patient or several patients, or a syringe containing the radiopharmaceutical	T	Medium
Design of the dispensing cabinet	S and T	Medium
Ease with which manipulations can be performed within the dispensing cabinet	D and T	Low/medium
Speed with which shielded manipulations are performed	T	Low

T, time; D, distance; S, shielding; high, >40% reduction; medium, 20–40% reduction; low <20% reduction.

is also an order of magnitude variation in the workloads in different radiopharmacies. Predicting the magnitude of exposure on the basis of a qualitative description of technology, mean workload, and working practice is an impossible task.

E.10. Exposure monitoring

(E 50) Monitoring of hand exposure for radiopharmacists is highly recommended. The most appropriate method is dose measurement for pulps of the most exposed fingers of the dominant hand. However, an individual's technique should be observed in order to determine whether other fingers are likely to receive higher doses. If a suitable method can be determined, this should be adopted. Finger stalls, which incorporate a dosimeter near the tip and can fit over a finger, are available (e.g. Health Protection Agency, UK) and are suitable for regular monitoring. These dosimeters can be worn continuously and so provide the ideal dosimetry technique, which is recommended for all departments that handle large quantities of radioactivity in which there is a risk that the dose limit to the finger may be approached.

(E 51) Some workers find that using a dosimeter on the tip of the finger is not acceptable due to impairment of comfort and dexterity of manipulations. In these situations, where it is considered that any dose is unlikely to approach the limit, an alternative solution is to monitor the exposure of the hands at monthly intervals by a conventional TLD ring, worn at the base of the middle finger, and to estimate the highest doses (pulps of index, middle and thumb finger) by means of an empirical ratio.

(E 52) When the dosimeter element in the ring is worn on the palm side, the ratio between the dose to the finger tip and that to the ring element is between 1.5 and 3.5

(Batchelor et al., 1991a; Dhanse et al., 2000; Berus et al., 2004; Whitby and Martin, 2005; Vanhavere, 2006; Covens et al., 2007), although there may be specific manipulations for which it is higher (Berus et al., 2004; Covens et al., 2007). On the other hand, in studies in which the dosimeter is worn on the back of the hand, the ratio is between 4 and 7 (Wresień et al., 2008). The reasons for this difference can be surmised from the positions of the hands manipulating the syringes shown in Figs. E.1–E.3 with respect to the radiation field associated with a shielded syringe.

(E 53) Based on this work, it is recommended that a ring dosimeter should be worn on the middle finger with the element positioned on the palm side, and that a factor of three should be applied to derive an estimate of the dose to the tip. If the dosimeter element is worn facing towards the back of the hand, a factor of six should be applied. The ratio will vary with the technique of the individual, but confirmation that this ratio is applicable to the individual or department might be achieved through the wearing of a ring dosimeter and a second dosimeter at the finger tip for a trial period.

(E 54) If undertaking such measurements, it must be borne in mind that the potential errors are large; dosimeters must be calibrated accurately and a methodology that is consistent with contemporary standards must be employed. If conditions for such measurements cannot be fulfilled and monitoring of the finger tip is not carried out, the appropriate multiplying factor as stated above may be applied to measurements from a ring dosimeter to obtain an assessment of the dose to the finger tip. In the early stages of any programme of finger monitoring, the dispensing technique used by each individual should be reviewed to confirm whether the positions chosen for dosimeters to be worn are the most appropriate. Practical recommendations for a monitoring strategy are given in Table E.2. (Martin and Whitby, 2003).

(E 55) Preliminary monitoring should be undertaken for anyone handling >2 GBq of ^{99m}Tc/day. Individuals handling over 10 GBq/day are likely to exceed the dose

Table E.2. Recommendations for protection and monitoring strategy.

Monthly absorbed dose (mSv)			Recommended monitoring and optimising of protection
Tip or most exposed part	Ring dosimeter element on palm side	Ring dosimeter element on dorsal aspect	
<1	<0.3	<0.2	Regular monitoring not required.
1–6	0.3–2	0.2–1	Initial monitoring to establish the dose level; periodic (twice a year) check whether the levels have changed. High variability of results requires more frequent checks.
6–20	2–7	1–3	Regular monitoring necessary. Optimisation measures for protection required (changes of working conditions, equipment, shielding, etc.).
>20	>7	>3	Regular monitoring of finger tip or most exposed area with obligatory monthly review of doses, and review of work and protection strategy aiming at lowering the doses; use of an electronic dosimeter is highly recommended.

levels above which it is recommended that regular monitoring is undertaken unless effective optimisation has been adopted.

(E 56) During therapies involving the administration of radionuclides emitting high-energy beta-radiation, finger dosimeters should always be worn on the tip or the most exposed area. It may be appropriate for separate dosimeters to be worn for single higher dose therapy administrations. A ring dosimeter will not provide an adequate reflection of the maximum dose, since the dose to the finger tip can be up to 100 times greater than that to the ring (Liepe et al., 2005), so the use of a ratio is not appropriate. Rimpler and Barth (2007) have reported a ratio of three between the finger and ring dosimeter when work was performed at high protection standards, but found ratios of 30 or 40 when some shields were not used. Therefore, the dose to the finger tip should always be monitored.

E.11. Summary of recommendations

(E 57) Finger doses for staff in larger radiopharmacies may approach or exceed dose limits. A number of conclusions and recommendations can be drawn up based on the studies that have been undertaken:

- The dispensing protocol and the use of shielding devices in any radiopharmacy should be assessed carefully to optimise the strategy.
- Shielding of the syringe is the most important factor affecting finger dose, and syringe shields should be used as much as possible.
- Vials from which radioactive liquid is withdrawn should always be shielded.
- The choice of manipulation technique only has a minor influence on finger dose; the most important factor is that staff are able to use the technique effectively.
- All staff should undergo a period of intense training in which they practice manipulations using non-radioactive liquid prior to undertaking any dispensing of radioactive liquid.
- Careful positioning of materials within the dispensing cabinet is important for streamlining the procedure and minimising doses to the hands.
- The most exposed parts of the hands are likely to be the tips of the index and middle fingers, and the thumb of the dominant hand, with exposure for the index finger being highest.
- Preliminary finger dose monitoring should be undertaken for any person handling >2 GBq/day, and regular monitoring should be carried out if doses to the most exposed part of the hand exceed 6 mSv/month.
- The finger tip or most exposed part of the hand should be monitored wherever possible, particularly if the dose is likely to approach a dose limit.
- If it is not possible to monitor the dose to the most exposed finger tip, an empirical multiplying factor may be applied to doses recorded by ring dosimeters worn on the middle finger of the dominant hand to estimate this dose. Factors of three or six should be used for the dosimeter element on the palm or back of the hand, respectively.

- The dispensing technique should be reviewed to confirm that the positions where dosimeters are worn are the most appropriate.
- For injections, prior venous cannulation allows the injection to proceed more rapidly; if the syringe is shielded, the dose to the hand of the nurse or physician will be kept to a minimum.
- Significant doses can be received from a single administration of a therapy involving a high-energy beta-particle emitter, and the following precautions are recommended:
- Administrations of beta-emitting therapy radiopharmaceuticals should be carefully planned.
- 5–10 mm thick PMMA syringe shields should always be used for administration of ^{90}Y or similar high-energy beta-emitting therapy radionuclides.
- Close contact with any thin-walled vessel containing therapeutic levels of ^{90}Y should be avoided through the use of forceps or PMMA shielding.
- Doses to the most exposed finger tips should be monitored directly for each session in which ^{90}Y or similar high-energy beta-emitting therapy radionuclides are administered.

REFERENCES

Anderson, D.W., Richter, C.W., Ficken, V.J., et al., 1972. Use of thermoluminescent dosimeters for measurement of dose to the hands of nuclear medicine technicians. J. Nucl. Med. 13, 627–629.

ARSAC, 2006. Notes for guidance on the clinical administration of radiopharmaceuticals and use of sealed radioactive sources. Administration of Radioactive Substances Advisory Committee. Health Protection Agency, Chilton, UK.

Aubert, B., Guilabert, N., Lamon, A., et al., 2002. Which protection against radiation for new protocols of internal radiotherapy by yttrium-90? Sixth European ALARA Network Workshop in Occupational Exposure Optimization in Medical Field and Radiophamaceutical Industry, pp. 44–49 (http://www.eu-alara.net/images/stories/pdf/program6/Session%20B/B_Aubert.pdf).

Batchelor, S., Baldock, C., Webber, D., 1991a. Radiation dose to the hands of a radiopharmacist. J. Hosp. Pharm. 247 (Suppl.), 38–39.

Batchelor, S., Penfold, A., Huggins, R., 1991b. Radiation dose to the hands in nuclear medicine. Nucl. Med. Commun. 12, 439–444.

Berus, D., Covens, P., Buls, N., et al., 2004. Extremity doses of workers in nuclear medicine: Mapping hand doses in function of manipulation. Proceedings of the 11th International Congress of the IRPA, Madrid, Spain, 2004; 5f8 (http://irpa11.irpa.net/papers/papers.php).

Bjurman, B., Ahlgren, B., Mattsson, S., et al, 1982. Radiation dose to staff handling 99mTc in hospitals. III International Symposium, Radiological Protection Advances in Theory and Practice, Inverness 6–11 June 1982. Proceedings, Vol. 2, pp. 588–593.

Chiesa, C., de Sanctis, V., Crippa, F., et al., 1997. Radiation dose to technicians per nuclear medicine procedure: comparison between technetium–99m, gallium-67 and iodine-131 radiotracers and fluorine-18 fluorodeoxyglucose. Eur. J. Nucl. Med. 24, 1380–1389.

Clarke, E.A., Brisco, S.L., 1986. Dispensing, injecting or imaging? A question of radiation doses. Nucl. Med. Commun. 7, 319.

Covens, P., Berus, D., Buls, N., et al., 2007. Personal dose monitoring in hospitals: Global assessment, critical applications and future needs. Rad. Prot. Dosim. 124, 250–259.

Cremonesi, M., Ferrari, M., Paganelli, G., et al., 2006. Radiation protection in radionuclide therapies with ^{90}Y-conjugates: risks and safety. Eur. J. Nuc. Med. Mol. Im. 33, 1321–1327.

Cronin, B.F., 2002. The technologist's perspective. In: Valk, P.E., Bailey, D.L., Townsend, D.W., et al. (Eds.), Positron Emission Tomography; Basic Science and Clinical Practice. Springer-Verlag, London, pp. 777–791.

Delacroix, D., Guerre, J.P., Leblanc, P., et al., 2002. Radionuclide and radiation protection data handbook. Rad. Prot. Dosim. 98, 1–168.

Dhanse, S., Martin, C.J., Hilditch, T.E., et al., 2000. A study of doses to the hands during dispensing of radiopharmaceuticals. Nucl. Med. Commun. 21, 511–519.

Donadille, L., Bouachri, A.El., Lahaye, T., et al., 2005. Feasibility study of an activity extremity dosimetry prototype. Radiat. Prot. Dosim. 115, 548–552.

Gemmell, H.G., Staff, R.T., 1998. Single-photon emission-computed tomography (SPECT). In: Sharp, P.F., Gemmell, H.G., Smith, F.W. (Eds.), Practical nuclear medicine, 2nd ed. Oxford University Press, Oxford, UK, pp. 13–24.

Guillet, B., Quentin, P., Waultier, S., et al., 2005. Technologist radiation exposure in routine clinical practice with ^{18}F FDG PET. J. Nucl. Med. Technol. 33, 175–179.

Guy, M.J., Greaves, C.D., Morton, R.J., et al., 2005. Development of a combined audiovisual and extremity dose monitoring software tool for use in nuclear medicine. Nucl. Med. Comm. 26, 1147–1153.

Harding, L.K., Hesslewood, S., Ghose, S.K., et al., 1985. The value of syringe shields in a nuclear medicine department. Nucl. Med. Commun. 6, 449–454.

Harding, L.K., Mostafa, A.B., Thomson, W.H., 1990. Staff radiation doses associated with medicine procedures – a review of some recent measurements. Nucl. Med. Commun. 11, 272–277.

Hastings, D.L., Hillel, P.G., Jeans, S.P., et al., 1997. An assessment of finger doses received by staff while preparing and injecting radiopharmaceuticals. Nucl. Med. Commun. 18, 785–790.

Husak, V., Ptacek, J., Drymlova, J., et al., 2007. Radiation dose to the hands of nuclear medicine staff preparing radiopharmaceuticals with gamma emitters including positron radionuclide 18F. Česka Radiologie 61, 80–84.

ICRP, 1977. Recommendations of the International Commission on Radiological Protection. ICRP Publication 26. Ann. ICRP 1(3).

ICRP, 1991a. 1990 Recommendations of the International Commission on Radiological Protection. ICRP Publication 60. Ann. ICRP 21(1–3).

ICRP, 2007. The 2007 Recommendations of the International Commission on Radiological Protection. ICRP Publication 103. Ann. ICRP 37 (2–4).

Jankowski, J., Olszewski, J., Kluska, K., 2003. Distribution of equivalent doses to skin of the hands of nuclear medicine personnel. Radiat. Prot. Dosim. 106, 177–180.

Koback, R., Plato, P., 1985. Influence of dosemeter positioning on reported doses to the upper extremities. Radiat. Prot. Dosim. 11, 257–262.

Laffont, S., Deuvillers, A., Garin, E., et al., 2001. Radiation protection and radiation dose to technicians and patient during PET study (18FDG). Medecine Nucleaire 25, 395–400.

Liemann, H., Will, E., Beuthien-Baumann, B., 2000. Investigations of radiation exposure of the medical personnel during F-18 FDG PRT studies. Nuklear Medizin 39, 77–81, [in German].

Liepe, K., Andreeff, M., Wunderlich, G., et al., 2005. Radiation protection in radiosynovectomy of the knee. Health Phys. 89, 151–154.

Mackenzie, A., 1997. Reduction of extremity dose in the radiopharmacy. Nucl. Med. Commun. 18, 578–581.

Martin, C.J., Whitby, M., 2003. Application of ALARP to extremity doses for hospital workers. J. Radiol. Prot. 23, 405–421.

Mielccarek, J., Barth, I., 2002. Occupational beta radiation exposure during radiosynoviorthesis. Sixth European ALARA Network Workshop in Occupational Exposure Optimization in Medical Field and Radiophamaceutical Industry, pp. 43–46 (http://www.eu-alara.net/images/stories/pdf/program6/Session%20B/I_Barth.pdf).

Montgomery, A., Martin, C.J., Anstee, D., et al., 1997. Application of a gamma extremity monitoring system in a radiopharmaceutical dispensary. Nucl. Med. Commun. 18, 673–679.

FULL BIBLIOGRAPHY

Ahlgren, L., Ivarsson, S., Johansson, L., Mattsson, S., Nosslin, B., 1985. Excretion of radionuclides in human breast milk after the administration of radiopharmaceuticals. J. Nucl. Med. 26, 1085–1090.

Anderson, D.W., Richter, C.W., Ficken, V.J., et al., 1972. Use of thermoluminescent dosimeters for measurement of dose to the hands of nuclear medicine technicians. J. Nucl. Med. 13, 627–629.

Armbrecht, J.J., Burton, D.B., Schelbert, H.R., 1990. Validation of [1-^{11}C]acetate as a tracer for non-invasive assessment of oxidative metabolism with positron emission tomography in normal, ischemic, postischemic and hyperaemic canine myocardium. Circulation 81, 1594–1605.

ARSAC, 2006. Notes for Guidance on the Clinical Administration of Radiopharmaceuticals and Use of Sealed Radioactive Sources. Administration of Radioactive Substances Advisory Committee, Health Protection Agency, Chilton, UK.

Atkins, H.L., Christman, D.R., Fowler, J.S., et al., 1972. Organic radiopharmaceuticals labeled with isotopes of short half-life. V. 18F-Labeled 5- and 6-Fluorotryptophan. J. Nucl. Med. 13, 713–719.

Atkins, H.L., Cloutier, R.J., Lathrop, K.A., et al., 1975. Technetium-99m-sulfur colloid in various liver conditions. MIRD Dose Estimate Report No. 3. J. Nucl. Med. 16, 108A–108B.

Atkins, H.L., Budinger, T.F., Lebowitz, E., et al., 1977. Thallium-201 for medical use. Part 3: Human distribution and physical imaging properties. J. Nucl. Med. 18, 133–140.

Aubert, B., Guilabert, N., Lamon, A., et al., 2002. What protection against radiation for new protocols of internal radiotherapy by yttrium-90? Sixth European ALARA Network Workshop in Occupational Exposure Optimization in Medical Field and Radiophamaceutical Industry, pp. 44–49 (http://www.eu-alara.net/images/stories/pdf/program6/Session%20B/B_Aubert.pdf).

Bajc, M., Palmer, J., Ohlsson, T., et al., 1994. Distribution and dosimetry of ^{111}In DTPA-D-phe-octreotide in man assessed by whole body scintigraphy. Acta Radiol. 35, 53–57.

Barthel, H., Wiener, M., Dannenberg, C., Bettin, S., Sattler, B., Knapp, W.H., 1997. Age-specific cerebral perfusion in 4- to 15-year-old children: a high-resolution brain SPET study using ^{99m}Tc-ECD. Eur. J. Nucl. Med. 24, 1245–1252.

Bartlett, R.D., Lathrop, K.A., Faulhaber, P.F., Harper, P.V., 1984. Transfer of thallous ion to and from gastrointestinal sections. J. Nucl. Med. 25, P92.

Batchelor, S., Baldock, C., Webber, D., 1991a. Radiation dose to the hands of a radiopharmacist. J. Hosp. Pharm. 247 (Suppl.), 38–39.

Batchelor, S., Penfold, A., Huggins, R., 1991b. Radiation dose to the hands in nuclear medicine. Nucl. Med. Commun. 12, 439–444.

Berg, G., Nyström, E., Jacobsson, L., et al., 1998. Radioiodine treatment of hyperthyroidism in a pregnant woman. J. Nucl. Med. 39, 357–361.

Bergmann, R., Brust, P., Kampf, G., Coenen, H.H., Stöcklin, G., 1995. Evaluation of radioselenium labeled selenomethionine, a potential tracer for brain protein synthesis by PET. Nucl. Med. Biol. 22, 475–481.

Berman, M., 1977. Kinetic Models for Absorbed Dose Calculation. Medical Internal Radiation Committee (MIRD) Pamphlet No. 12. Society of Nuclear Medicine, New York, NY.

Berridge, M.S., Adler, L.P., Rao, P.S., 1991. Radiation absorbed dose for O-15-butanol and O-15 water estimated by positron emission tomography. J. Nucl. Med. 32, 1043.

Berus, D., Covens, P., Buls, N., et al., 2004. Extremity doses of workers in nuclear medicine: mapping hand doses in function of manipulation. Proceedings of the 11th International Congress of the IRPA, Madrid, 2004; 5f8 (http://irpa11.irpa.net/papers/papers.php).

Bingham, D., Gardin, I., Hoyes, K.P., 2000. The problem of Auger emitters for radiological protection. Radiat. Prot. Dosim. 92, 219–228.

Bischof Delaloye, A., Delaloye, B., 1995. Radiolabelled monoclonal antibodies in tumour imaging and therapy: out of fashion? Eur. J. Nucl. Med. 22, 571–580.

Bjurman, B., Ahlgren, B., Mattsson, S., et al, 1982. Radiation dose to staff handling 99mTc in hospitals. III International Symposium, Radiological Protection Advances in Theory and Practice, Inverness 6–11 June 1982. Proceedings, Vol. 2, pp. 588–593.

Booij, J., Sokole, E.B., Stabin, M.G., Janssen, A.G.M., de Bruin, K., van Royen, E.A., 1998. Human biodistribution and dosimetry of [^{123}I]FP-CIT: a potent radioligand for imaging of dopamine transporters. Eur. J. Nucl. Med. 25, 24–30.

Booij, J., Sokole, E.B., Stabin, M.G., Janssen, A.G.M., de Bruin, K., van Royen, E.A., 1998. Human biodistribution and dosimetry of [^{123}I]FP-CIT: a potent radioligand for imaging of dopamine transporters: erratum. Eur. J. Nucl. Med. 25, 458.

Bouchet, L.G., Bolch, W.E., Weber, D.A., Atkins, H.L., Poston Sr., J.W., 1999. Radionuclide S-values in a revised dosimetric model of the adult head and brain. MIRD Pamphlet No. 15. J. Nucl. Med. 40, 62S–101S.

Bouchet, L.G., Bolch, W.E., Howell, R.W., Rao, D.V., 2000. S values for radionuclides localized within the skeleton. J. Nucl. Med. 41, 189–212.

Boundy, K.L., Barnden, L.R., Rowe, C.C., et al., 1995. Human dosimetry and biodistribution of iodine-123-iododexetimide: a SPECT imaging agent for cholinergic muscarinic neuroreceptors. J. Nucl. Med. 36, 1332–1338.

Boyes, R.E., Cumming, P., Martin, W.R.W., McGeer, E.G., 1986. Determination of plasma [^{18}F]-6-fluorodopa during positron emission tomography; elimination and metabolism in carbidopa treated subjects. Life Sci. 39, 2243–2252.

Brihaye, C., Depresseux, J.C., Comar, D., 1995. Radiation dosimetry for bolus administration of oxygen-15 water. J. Nucl. Med. 36, 651–656.

Britton, K.E., Granowska, M., 1987. Radioimmunoscintigraphy in tumour identification. Cancer Surv. 6, 247–267.

Bronskill, M.J., 1983. Radiation dose estimates for interstitial radiocolloid lymphoscintigraphy. Semin. Nucl. Med. 13(1), 20–25.

Brown, P.H., Krishnamurthy, G.T., Bobba, V.R., Kingston, E., 1981. Radiation-dose calculation for Tc-99m HIDA in health and disease. J. Nucl. Med. 22, 177–183.

Brown, P.H., Krishnamurthy, G.T., Bobba, V.R., Kingston, E., Turner, F.E., 1982. Radiation-dose calculation for five Tc-99m IDA hepatobiliary agents. J. Nucl. Med. 23, 1025–1030.

Brown, W.D., Oakes, T.R., DeJesus, O.T., et al., 1998. Fluorine-18-fluoro-L-DOPA dosimetry with carbidopa pretreatment. J. Nucl. Med. 39, 1884–1891.

Burns, H.D., Dannals, R.F., Langström, B., et al., 1984. 3-N-[^{11}C]methylspiperone, a ligand binding to dopamine receptors: radiochemical synthesis and biodistribution studies in mice. J. Nucl. Med. 25, 1222–1227.

Casteels, M., Foulon, V., Mannaerts, G.P., van Veldhoven, P., 2003. Alpha-oxidation of 3-methyl-substituted fatty acids and its thiamine dependence. Eur. J. Biochem. 270, 1619–1627.

Castronovo Jr., F.P., Stone, H., Ulanski, J., 2000. Radioactivity in breast milk following ^{111}In-octreotide. Nucl. Med. Commun. 21, 695–699.

Caveliers, V., Franken, P.R., Florian, F.L., Lou, H., Knapp Jr., F.F., 1998. Intra-individual comparison of 3(R)-BMIPP and 3(S)-BMIPP isomers in humans. J. Nucl. Med. 39, 1672–1675.

Chen, C.T., Lathrop, K.A., Harper, P.V., et al., 1983. Quantitative measurement of long term in vivo thallium distribution in the human. J. Nucl. Med. 24, P50.

Chiesa, C., de Sanctis, V., Crippa, F., et al., 1997. Radiation dose to technicians per nuclear medicine procedure: comparison between technetium–99m, gallium-67 and iodine-131 radiotracers and fluorine-18 fluorodeoxyglucose. Eur. J. Nucl. Med. 24, 1380–1389.

Claessens, R.A.M.J., Koenders, E.B., Boerman, O.C., et al., 1995. Dissociation of indium from indium-111-labelled diethylene triamine penta-acetic acid conjugated non-specific polyclonal human immunoglobulin G in inflammatory foci. Eur. J. Nucl. Med. 22, 212–219.

Clarke, E.A., Brisco, S.L., 1986. Dispensing, injecting or imaging? A question of radiation doses. Nucl. Med. Commun. 7, 319.

Cloutier, R.J., Watson, E.E., Rohrer, R.H., Smith, E.M., 1973. Calculating the radiation dose to an organ. J. Nucl. Med. 14, 53–55.

Cloutier, R.J., Freeman, L.M., McAfee, J.G., et al., 1975. Summary of current radiation dose estimates to humans with various liver conditions from ^{198}Au colloidal gold. MIRD Dose Estimate Report No. 4. J. Nucl. Med. 16, 173–174.

Coenen, H.H., Kling, P., Stöcklin, G., 1989. Cerebral metabolism of l-[2-^{18}F]fluorotyrosine, a new PET tracer of protein synthesis. J. Nucl. Med. 30, 1367–1372.

Coffey, J.L., Watson, E.E., 1979. Calculating doses from remaining body activity. A comparison of two methods. Med. Phys. 6, 307–308.

Comar, D., Catron, J.C., Maziere, M., Marazanop, C., 1976. Labelling and metabolism of methionine-methyl-^{11}C. Eur. J. Nucl. Med. 1, 11–14.

Cottrall, M.F., Taylor, D.M., McElwain, T.J., 1973. Investigations of ^{18}F-p-fluorophenylalanine for pancreas scanning. Br. J. Radiol. 46, 277–288.

Covens, P., Berus, D., Buls, N., et al., 2007. Personal dose monitoring in hospitals: Global assessment, critical applications and future needs. Rad. Prot. Dosim. 124, 250–259.

Cremonesi, M., Ferrari, M., Paganelli, G., et al., 2006. Radiation protection in radionuclide therapies with ^{90}Y-conjugates: risks and safety. Eur. J. Nuc. Med. Mol. Im. 33, 1321–1327.

Cronin, B.F., 2002. The technologist's perspective, in Valk, P.E., Bailey, D.L., Townsend, D.W., et al. (Eds.), Positron Emission Tomography; Basic Science and Clinical Practice. Springer-Verlag, London, pp. 777–791.

Cristy, M., Eckerman, K., 1987. Specific Absorbed Fractions of Energy at Various Ages from Internal Photon Sources. Oak Ridge National Laboratory, Oak Ridge, TN.

De Geeter, F., Caveliers, V., Pansar, I., Bossuyt, A., Franken, P.R., 1998. Effect of oral glucose loading on the biodistribution of BMIPP in normal volunteers. J. Nucl. Med. 39, 1850–1856.

Delacroix, D., Guerre, J.P., Leblanc, P., et al., 2002. Radionuclide and Radiation Protection Data Handbook. Rad. Prot. Dosim. 98(1). Nuclear Technology Publishing, Ashford.

Deloar, H.M., Fujiwara, T., Shidahara, M., et al., 1998a. Estimation of absorbed dose for 2-[F-18]fluoro-2-deoxy-D-glucose using whole-body positron emission tomography and magnetic resonance imaging. Eur. J. Nucl. Med. 25, 565–574.

Deloar, H.M., Fujiwara, T., Nakamura, T., et al., 1998. Estimation of internal absorbed dose of l-[methyl-^{11}C]-methionine using whole body positron emission tomography. Eur. J. Nucl. Med. 25, 629–633.

Deterding, T.A., Votaw, J.R., Wang, C.K., et al., 2001. Biodistribution and radiation dosimetry of the dopamine transporter ligand [^{18}F]FECNT. J. Nucl. Med. 42, 376–381.

Dhanse, S., Martin, C.J., Hilditch, T.E., et al., 2000. A study of doses to the hands during dispensing of radiopharmaceuticals. Nucl. Med. Commun. 21, 511–519.

Dhawan, V., Belakhlef, A., Robeson, W., et al., 1996. Bladder wall radiation dose in humans from fluorine-18-FDOPA. J. Nucl. Med. 37, 1850–1852.

Donadille, L., Bouachri, A.El., Lahaye, T., et al., 2005. Feasibility study of an activity extremity dosimetry prototype. Radiat. Prot. Dosim. 115, 548–552.

Dudczak, R., Schmoliner, R., Angelberger, P., Knapp, F.F., Goodman, M.M., 1986. Structurally modified fatty acids: clinical potential as tracers of metabolism. Eur. J. Nucl. Med. 12, S45–S48.

Eckerman, K.F., Stabin, M.G., 2000. Electron absorbed fractions and dose conversion factors for marrow and bone by skeletal region. Health Phys. 78, 199–214.

Eichling, J.O., Bergman, S.R., Schwarz, S.W., et al., 1997. Equivalent dose estimates in adults for intravenously administered O-15 water. Unpublished; personal communication through S. Schwarz.

Evans, J.L., Mountford, P.J., Herring, A.N., Richardson, M.A., 1993. Secretion of radioactivity in breast milk following administration of ^{99}Tc^{m}-MAG3. Nucl. Med. Commun. 14, 108–111.

Eshima, D., Fauconnier, T., Eshima, L., et al., 2000. Radiopharmaceuticals for lymphoscintigraphy; including dosimetry and radiation considerations. Semin. Nucl. Med. 30(1) 25–32.

Farde, L., Hall, H., Ehrin, E., Sedvall, G., 1986. Quantitative analysis of D2 dopamine receptor binding in the living human brain. Science 231, 258–261.

Farde, L., Suhara, T., Nyberg, S., et al., 1997. A PET study of [^{11}C]FLB 457 binding to extrastriatal D_2-dopamine receptors in healthy subjects and antipsychotic drug-treated patients. Psychopharmacology 133, 394–404.

Feinendegen, L.E., Neumann, R.D., 2004. Dosimetry and risk from low- versus high-LET radiation of Auger events and the role of nuclide carriers. Int. J. Radiat. Biol. 80, 813–822.

Fishman, A.J., Khaw, B.A., Strauss, H.N., 1989. Quo vadis radioimmune imaging. J. Nucl. Med. 20, 1911–1915.

Forssell Aronsson, E., Fjälling, M., Nilsson, O., et al., 1995. Indium-111 activity concentration in tissue samples after intravenous injection of indium-111-DTPA-D-Phe-1-octreotide. J. Nucl. Med. 36, 7–12.

Forssell Aronsson, E., Lanhede, B., Fjälling, M., et al., 1996. Pharmacokinetics and dosimetry of ^{111}In-DTPA-D-Phe-1-octreotide in patients with neuroendocrine tumours, in: Schlafke-Stelson, AT., Stabin, M.G., Sparks, R.B. (Eds.), Proceedings of the Sixth International Radiopharmaceutical Dosimetry Symposium. Oak Ridge Associated Universities, Oak Ridge, TN, pp. 643–655.

Freeman, M.R., Kanwar, N., Armstrong, P.W., 1986. The variability of thallium half life at rest as compared to exercise. J. Nucl. Med. 27, 997.

Frost, J.J., Mayberg, H.S., Sadzot, B., et al., 1990. Comparison of [^{11}C]diprenorphine and [^{11}C]carfentanil binding to opiate receptors in humans by positron emission tomography. J. Cereb. Blood Flow Metab. 10, 484–492.

Gardin, I., Faraggi, M., Le Guludec, D., Bok, B., 1999. Cell irradiation caused by diagnostic nuclear medicine procedures: dose heterogeneity and biological consequences. Eur. J. Nucl. Med. 26, 1617–1626.

Gelfand, M.J., Thomas, S.R., Kereiakes, J.G., 1983. Absorbed radiation dose from routine imaging of the skeleton in children. Ann. Radiol. 26, 421–423.

Gemmell, H.G., Staff, R.T. 1998. Single-photon emission-computed tomography (SPECT) In: Practical Nuclear Medicine 2nd Edition, ed. P.F. Sharp, H.G. Gemmell, F.W. Smith, Oxford University press, Oxford, pp 13–24.

Gerson, M.C., Lukes, J., Deutsch, E., et al., 1994. Comparison of technetium 99m Q12 and thallium 201 for detection of angiographically documented coronary artery disease in humans. J. Nucl. Cardiol. 1, 499–508.

Goddu, S.M., Howell, R.W., Rao, D.V., 1994. Cellular dosimetry: absorbed fractions for monoenergetic electron and alpha particle sources and S-values for radionuclides uniformly distributed in different cell compartments. J. Nucl. Med. 35, 303–316.

Goddu, S.M., Howell, R.W., Bouchet, L.G., Bolch, W.E., Rao, D., 1997. MIRD Cellular S Values. Society of Nuclear Medicine, Inc, Reston, VA.

Gössner, W., Masse, R., Stather, J.W., 2000. Cells at risk for dosimetric modelling relevant to bone tumour induction. Radiat. Prot. Dosim. 92, 209–213.

Groshar, D., Slobodin, G., Zuckerman, E., 2002. Quantitation of liver and spleen uptake of 99mTc-phytate colloid using SPECT: detection of liver cirrhosis. J. Nucl. Med. 43, 312–317.

Gründer, G., Siessmeier, T., Lange-Asschenfeldt, C., et al., 2001. [^{18}F]Fluoroethylflumaazenil: a novel tracer for PET imaging of human benzodiazepine receptors. Eur. J. Nucl. Med. 28, 1463–1470.

Gründer, G., Siessmeier, T., Piel, M., et al., 2003. Quantification of D_2-like dopamine receptors in the human brain with [^{18}F]-desmethoxyfallypride. J. Nucl. Med. 44, 109–116.

Guillet, B., Quentin, P., Waultier, S., et al., 2005. Technologist radiation exposure in routine clinical practice with ^{18}F FDG PET. J. Nucl. Med. Technol. 33, 175–179.

Gunnarsson, M., Stenström, K., Leide-Svegborn, S., et al., 2003. Biokinetics and radiation dosimetry for patients undergoing a glycerol tri[1-^{14}C]oleate fat malabsorption breath test. Appl. Radiat. Isot. 58, 517–526.

Gupta, S.M., Herrera, N., Spencer, R.P., et al., 1981. Testicular-scrotal content of ^{201}Tl and ^{67}Ga after intravenous administration. Int. J. Nucl. Med. Biol. 8, 211–213.

Guy, M.J., Greaves, C.D., Morton, R.J., et al., 2005. Development of a combined audiovisual and extremity dose monitoring software tool for use in nuclear medicine. Nucl. Med. Comm. 26, 1147–1153.

Harding, L.K., Hesslewood, S., Ghose, S.K., et al., 1985. The value of syringe shields in a nuclear medicine department. Nucl. Med. Commun. 6, 449–454.

Harding, L.K., Mostafa, A.B., Thomson, W.H., 1990. Staff radiation doses associated with medicine procedures – a review of some recent measurements. Nucl. Med. Commun. 11, 272–277.

Harvey, J., Firnau, G., Garnett, E.S., 1985. Estimation of the radiation dose in man due to 6-[^{18}F]fluoro-L-dopa. J. Nucl. Med. 26, 931–935.

Hastings, D.L., Hillel, P.G., Jeans, S.P., et al., 1997. Assessment of finger doses received by staff while preparing and injecting radiopharmaceuticals. Nucl. Med. Commun. 18, 785–790.

Hays, M.T., Segall, G.M., 1999. A mathematical model for the distribution of fluorodeoxyglucose in humans. J. Nucl. Med. 40, 1358–1366.

Hays, M.T., Watson, E.E., Thomas, S.R., Stabin, M., 2002. Radiation absorbed dose estimates from ^{18}F-FDG. MIRD Dose Estimate Report No. 19. J. Nucl. Med. 43, 210–214.

Heiss, W.D., Wienhard, K., Wagner, R., et al., 1996. F-DOPA as an amino acid tracer to detect brain tumors. J Nucl. Med. 37, 1180–1182.

Herscovitch, P., Carson, R.E., Stabin, M., et al., 1993. A new kinetic approach to estimate the radiation dosimetry of flow-based radiotracers. J. Nucl. Med. 34, 155P.

Herscovitch, P., Schmall, B., Doudet, D., Carson, R., Eckelman, W., 1997. Biodistribution and radiation dose estimates for [^{11}-C]raclopride (abstract). J. Nucl. Med. 5 (Suppl.), 224.

Herzog, H., Spohr, G., Notohamiprodjo, G., Feinendegen, L.E., 1987. Absolute quantification of pharmacokinetic distribution of RES colloids in individuals with normal liver function. Nucl. Med. Commun. 8, 157–175.

Higley, B., Smith, F.W., Smith, T., et al., 1993. Technetium-99m-1,2-bis[bis(2-ethoxyethyl) phosphino]ethane: human biodistribution, dosimetry and safety of a new myocardial perfusion imaging agent. J. Nucl. Med. 34, 30–38.

Hofer, K.G., 1996. Biophysical aspects of Auger processes. A review. Acta Oncol. 35, 789–796.

van den Hoff, J., Burchert, W., Wolpers, H.G., Meyer, G.J., Hundeshagen, H., 1996. A kinetic model for cardiac PET with [1-^{11}C]acetate. J. Nucl. Med. 37, 521–529.

Hoffman, J.M., Melega, W.P., Hawk, T.C., et al., 1992. The effects of carbidopa administration of 6-[^{18}F]fluoro-L-DOPA kinetics in positron emission tomography. J. Nucl. Med. 33, 1472–1477.

Holman, B.L., Hellman, R.S., Goldsmith, S.J., et al., 1989. Biodistribution, dosimetry and clinical evaluation of technetium-99m ethyl cysteinate dimer in normal subjects and in patients with chronic cerebral infarction. J. Nucl. Med. 30, 1018–1024.

Hosain, P., Hosain, F., 1981. Revision of gonadal radiation dose to man from thallium-201, in: Proceedings of the Third International Radiopharmaceutical Dosimetry Symposium, Oak Ridge 1980 (FDA 81-8166) Oak Ridge National Laboratories, Oak Ridge, TN, pp. 333–345.

Houle, S., DaSilva, J.N., Wilson, A.A., 2000a. Imaging the 5-HT_{1A} receptors with PET: WAY-100635 and analogues. Nucl. Med. Biol. 27, 463–466.

Houle, S., Ginovart, N., Hussey, D., Meyer, J.H., Wilson, A.A., 2000b. Imaging the serotonin transporter system with positron emission tomography: initial human studies with [^{11}C]DAPP and [^{11}C]DASB. Eur. J. Nucl. Med. 27, 1719–1722.

Husak, V., Ptacek, J., Drymlova, J., et al., 2007. Radiation dose to the hands of nuclear medicine staff preparing radiopharmaceuticals with gamma emitters including positron radionuclide 18F. Česka Radiologie 61, 80–84.

IAEA, 2006. Quality Assurance for Radioactivity Measurement in Nuclear Medicine. Technical Report Series No. 454. International Atomic Energy Agency, Vienna.

Inoue, T., Tomiyoshi, K., Higuichi, T., et al., 1996. Biodistribution studies on l-3-[fluorine-18]fluoro-α-methyl tyrosine: a potential tumor-detecting agent. J. Nucl. Med. 39, 663–667.

ICRP, 1971. Protection of the Patient in Radionuclide Investigations. ICRP Publication 17. Pergamon Press, Oxford.

ICRP, 1973. Alkaline Earth Metabolism in Adult Man. ICRP Publication 20. Pergamon Press, Oxford.

ICRP, 1975. Report of the Task Group on Reference Man. ICRP Publication 23. Pergamon Press, Oxford.

ICRP, 1977. Recommendations of the International Commission on Radiological Protection. ICRP Publication 26. Ann. ICRP 1(3).

ICRP, 1979. Limits for intakes of radionuclides by workers. ICRP Publication 30, Part 1. Ann. ICRP 2(3/4).

ICRP, 1980. Limits for intakes of radionuclides by workers. ICRP Publication 30, Part 2. Ann. ICRP 4(3/4).

ICRP, 1981. Limits for intakes of radionuclides by workers. ICRP Publication 30, Part 3. Ann. ICRP 6(2/3).
ICRP, 1987. Radiation dose to patients from radiopharmaceuticals. ICRP Publication 53. Ann. ICRP 18(1–4).
ICRP, 1991a. 1990 Recommendations of the International Commission on Radiological Protection. ICRP Publication 60. Ann. ICRP 21(1–3).
ICRP, 1991b. Radiation dose to patients from radiopharmaceuticals. Addendum 1 to ICRP Publication 53. ICRP Publication 62. Ann. ICRP 22(3).
ICRP, 1993. Age-dependent doses to members of the public from intake of radionuclides. Part 2: ingestion dose coefficients. ICRP Publication 67. Ann. ICRP 23(3/4).
ICRP, 1994. Dose coefficients for intake of radionuclides by workers. ICRP Publication 68. Ann. ICRP 24(4).
ICRP, 1996. Age-dependent doses to members of the public from intake of radionuclides. Part 5. ICRP Publication 72. Ann. ICRP 26(1).
ICRP, 1998. Radiation dose to patients from radiopharmaceuticals. Addendum 2 to ICRP Publication 53. ICRP Publication 80. Ann. ICRP 28(3).
ICRP, 2001a. Doses to the embryo and fetus from intake of radionuclides by the mother. ICRP Publication 88. Ann. ICRP 31(1–3).
ICRP, 2001b. Radiation dose to patients from radiopharmaceuticals. Addendum 4 to ICRP Publication 53.
ICRP, 2002. Basic anatomical and physiological data for use in radiological protection: reference values. ICRP Publication 89. Ann. ICRP 31(3/4).
ICRP, 2003. Relative biological effectiveness (RBE), quality factor (Q) and radiation weighting factor (w_R). ICRP Publication 92. Ann. ICRP 33(4).
ICRP, 2004. Doses to infants from ingestion of radionuclides in mothers' milk. ICRP Publication 95. Ann. ICRP 34(3/4).
ICRP, 2006. Human alimentary tract model for radiological protection. ICRP Publication 100. Ann. ICRP 35(1/2).
ICRP, 2007. The 2007 Recommendations of the International Commission on Radiological Protection. ICRP Publication 103. Ann. ICRP 37(2–4).
ICRU, 1979. Methods of Assessment of Absorbed Dose in Clinical Use of Radionuclides. ICRU Report 32. International Commission on Radiation Units and Measurements, Bethesda, MD.
ICRU, 2002. Absorbed-dose specification in nuclear medicine. ICRU Report 67. J. ICRU 2, 1–110.
Iyo, M., Namba, H., Fukushi, K., et al., 1997. Measurement of acetylcholinesterase by positron emission tomography in the brains of healthy controls and patients with Alzheimer's disease. Lancet 349, 1805–1809.
Jankowski, J., Olszewski, J., Kluska, K., 2003. Distribution of equivalent doses to skin of the hands of nuclear medicine personnel. Radiat. Prot. Dosim. 106, 177–180.
Johansson, L., Mattsson, S., Nosslin, B., Leide-Svegborn, S., 1992. Effective dose from radiopharmaceuticals. Eur. J. Nucl. Med. 19, 933–938.
Johansson, L., 1996. Absorbed dose in the salivary glands from technetium-99m labeled radiopharmaceuticals, in: Schlafke-Stelson, A, Stabin, M.G., Sparks, R.B. (Eds.), Sixth International Radiopharmaceutical Dosimetry Symposium, Gatlinburg, TN. Oak Ridge Institute for Science and Education, pp. 513–521.
Johnston, R.E., Mukherji, S.K., Perry, R.J., Stabin, M.G., 1996. Radiation dose from breastfeeding following administration of thallium-201. J. Nucl. Med. 37, 2079–2082.
Jönsson, L., Ljungberg, M., Strand, S.E., 2005. Evaluation of accuracy in activity calculations for the conjugate view method from Monte Carlo simulated scintillation camera images using experimental data in an anthropomorphic phantom. J. Nucl. Med. 46, 1679–1686.
Kassis, A.M., 2004. The amazing world of Auger electrons. Int. J. Radiat. Biol. 80, 789–903.
Kaul, A., Krauss, O., Petrausch, G., 1985. Strahlenexposition durch Tc-99m-Methylendiphosphonat — lokale Dosisverteilung in Wachstum zonen des kindlichen Skelett und Organdosen, in: Poretti, G. (Ed.), Medizinische Physik. Deutsche Gesellschaft für medizinische Physik, Bern.

Kauppinen, T.A., Bergström, K.A., Heikman, P., Hiltunen, J., Ahonen, A.K., 2003. Biodistribution and radiation dosimetry of [^{123}I]ADAM in healthy human subjects: preliminary results. Eur. J. Nucl. Med. 30, 132–136.

Kim, S., Wagner Jr., H.N., Villemagne, V.L., et al., 1997. Longer occupancy of opioid receptors by nalmefene compared to naloxone as measured in vivo by a dual detector system. J. Nucl. Med. 38, 1726–1731.

Knapp Jr., F.F., Ambrose, K.R., Goodman, M.M., 1986. New radioiodinated methyl-branched fatty acids for cardiac studies. Eur. J. Nucl. Med. 12 (Suppl.), S39–S44.

Knapp Jr., F.F., Franken, P., Kropp, J., 1995a. Cardiac SPECT with iodine-123-labeled fatty acids: evaluation of myocardial viability with BMIPP. J. Nucl. Med. 36, 1022–1030.

Knapp Jr., F.F., Kropp, J., 1995b. Iodine-123-labelled fatty acids for myocardial single-photon emission tomography: current status and future perspectives. Eur. J. Nucl. Med. 22, 361–381.

Koback, R., Plato, P., 1985. Influence of dosemeter positioning on reported doses to the upper extremities. Radiat. Prot. Dosim. 11, 257–262.

Koizumi, M., Endo, K., Watanabe, Y., et al., 1989. Pharmacokinetics of internally labeled monoclonal antibodies as a gold standard: comparison of biodistribution of 75Se-, 111In-, and 125I-labeled monoclonal antibodies in osteogenic sarcoma xenografts in nude mice. Cancer Res. 49, 1752–1757.

Krahwinkel, W., Herzog, H., Feinendegen, L.E., 1988. Pharmacokinetics of thallium-201 in normal individuals after routine myocardial scintigraphy. J. Nucl. Med. 29, 1582–1586.

Krenning, E.P., Bakker, W.H., Kooij, P.P.M., et al., 1992. Somatostatin receptor scintigraphy with indium-111-DTPA-D-Phe-1-octreotide in man: metabolism, dosimetry and comparison with iodine-123-Tyr-3-octreotide. J. Nucl. Med. 33, 652–658.

Krenning, E.P., Kwekkeboom, D.J., Bakker, W.H., et al., 1993. Somatostatin receptor scintigraphy with (^{111}In-DTPA-D-Phe^{1})- and (^{123}I-Tyr^{3})-octreotide: the Rotterdam experience with more than 1000 patients. Eur. J. Nucl. Med. 20, 716–731.

Kuikka, J.T., Bergström, K.A., Ahonen, A., Länsimies, E., 1994. The dosimetry of iodine-123 labelled 2β-carbomethoxy-3β-(4-iodophenyl)tropane. Eur. J. Nucl. Med. 21, 53–56.

Laffont, S., Deuvillers, A., Garin, E., et al., 2001. Radiation protection and radiation dose to technicians and patient during PET study (18FDG). Medecine Nucleaire 25, 395–400.

Leggett, R.W., Williams, L.R., 1991. Suggested reference values for regional blood volumes in humans. Health Phys., 139–154.

Leggett, R.W., Williams, L.R., 1995. A proposed blood circulation model for reference man. Health Phys. 69, 187–201.

Leide-Svegborn, S., Nosslin, B., Mattsson, S., 1996. Biokinetics and dosimetry of ^{111}In-DTPA-D-Phe-1-octreotide in patients, in: Schlafke-Stelson, AT., Stabin, M.G., Sparks, R.B. (Eds.), Proceedings of the Sixth International Radiopharmaceutical Dosimetry Symposium. Oak Ridge Associated Universities, Oak Ridge, TN, pp. 631–642.

Léveillé, J., Demonceau, G., Walovitch, R.C., 1992. Intrasubject comparison between technetium-99m-ECD and technetium-99m-HMPAO in healthy human subjects. J. Nucl. Med. 33, 480–484.

Liemann, H., Will, E., Beuthien-Baumann, B., 2000. Investigations of radiation exposure of the medical personnel during F-18 FDG PRT studies. Nuklear Medizin 39, 77–81, [in German].

Liepe, K., Andreeff, M., Wunderlich, G., et al., 2005. Radiation protection in radiosynovectomy of the knee. Health Phys. 89, 151–154.

Liniecki, J., 1998. Private communication. Department of Nuclear Medicine. Medical University of Lodz, Lodz.

Loevinger, R., Berman, M., 1968. A schema for absorbed-dose calculations for biologically distributed radionuclides. MIRD Pamphlet No. 1. J. Nucl. Med. 9 (Suppl. 1), 7–14.

Loevinger, R., Budinger, T.F., Watson, E.E., 1991. MIRD Primer for Absorbed Dose Calculations. Revised edition. Society of Nuclear Medicine, New York, NY.

Lu, E., Meyer, E., Kuwabara, H., Ma, Y., Shiraishi, M., Evans, A.C., 1995. Reduction of radiation absorbed dose in F-18-DOPA PET studies by hydration-induced voiding. J. Nucl. Med. 36 (Suppl.), 98P.

Luxen, A., Guillaume, M., Melega, W.P., Pike, V.W., Solin, O., Wagner, R., 1992. Production of 6[^{18}F]fluoro-L-DOPA and its metabolism in vivo – a critical review. Nucl. Med. Biol. 19, 149–158.

Machulla, H.J., Marsmann, M., Dutschka, K., 1980. Biochemical concept and synthesis of a radioiodinated phenyl fatty acid for in vivo metabolic studies of the myocardium. Eur. J. Nucl. Med. 5, 171–173.

Mackenzie, A., 1997. Reduction of extremity dose in the radiopharmacy. Nucl. Med. Commun. 18, 578–581.

Martin, C.J., Whitby, M., 2003. Application of ALARP to extremity doses for hospital workers. J. Radiol. Prot. 23, 405–421.

McClain, D.A., Hug Jr., C.C., 1980. Intravenous fentanyl kinetics. Clin. Pharmacol. Ther. 28, 106–114.

McCauley, E., Mackie, A., 2002. Breast milk activity during early lactation following maternal ^{99}Tc^{m} macroaggregated albumin lung perfusion scan. Br. J. Radiol. 75, 464–466.

Meija, A.A., Nakamura, T., Masatoshi, I., Hatazawa, J., Mazaki, M., Watanuki, S., 1991. Estimation of absorbed doses in humans due to intraveneous administration of fluorine-18-fluorodeoxyglucose in PET studies. J. Nucl. Med. 32, 699–706.

Melega, W.P., Hoffman, J.M., Luxen, A., Nissenson, C.H.K., Phelps, M.E., Barrio, J.P., 1990. The effects of carbidopa on the metabolism of 6-[^{18}F]fluoro-L-dopa in rats, monkeys and humans. Life Sci. 47, 149–157.

Meyer, G.-J., Waters, S.L., Coenen, H.H., Luxen, A., Maziere, B., Långström, B., 1995. PET radiopharmaceuticals in Europe: current use and data relevant for the formulation of summaries of product characteristics (SPCs). Eur. J. Nucl. Med. 22, 1420–1432.

Mielcarek, J., Barth, I., 2002. Occupational beta radiation exposure during radiosynoviorthesis. Sixth European ALARA Network Workshop in Occupational Exposure Optimization in Medical Field and Radiophamaceutical Industry, pp. 43–46 (http://www.eu-alara.net/images/stories/pdf/program6/Session%20B/I_Barth.pdf).

Mitterhauser, M., Wadsak, W., Wabnegger, L., et al., 2004. Biological evaluation of 2′-[^{18}F]fluoroflumazenil ([^{18}F]FFMZ): a potential GABA receptor ligand for PET. Nucl. Med. Biol. 31, 291–295.

Montgomery, A., Martin, C.J., Anstee, D., et al., 1997. Application of a gamma extremity monitoring system in a radiopharmaceutical dispensary. Nucl. Med. Commun. 18, 673–679.

Montgomery, A., Anstee, D.E., Martin, C.J., et al., 1999. Reduction in finger dose for radiopharmaceutical dispensing afforded by a syringe shield and an automatic dose dispenser. Nucl. Med. Commun. 20, 189–194.

Mountford, P.J., Coakley, A.J., 1989. A review of the secretion of radioactivity in human breast milk: data, quantitative analysis and recommendations. Nucl. Med. Commun. 10, 15–27.

Mozley, P.D., Stubbs, J.T., Kim, H-J., et al., 1995. Dosimetry of a D2/D3 dopamine receptor antagonist that can be used with PET or SPECT. J. Nucl. Med. 36, 1322–1331.

Mozley, P.D., Stubbs, J.T., Kim, H-J., et al., 1996. Dosimetry of an iodine-123-labeled tropane to image dopamine transporters. J. Nucl. Med. 37, 151–159.

Mulholland, G.K., Kilbourn, M.R., Sherman, P., et al., 1995. Synthesis, in vivo biodistribution and dosimetry of [^{11}C]N-methylpiperidyl benzilate ([^{11}C]NMPB), a muscarinic acetylcholine receptor antagonist. Nucl. Med. Biol. 22, 13–17.

NCRP, 1982. Nuclear Medicine – Factors Influencing the Choice and Use of Radionuclides in Diagnosis and Therapy. NCRP Report No. 70. National Council on Radiation Protection and Measurements, Bethesda, MD.

NCRP, 1985. General Concepts for the Dosimetry of Internally Deposited Radionuclides. NCRP Report No. 84. National Council on Radiation Protection and Measurements, Bethesda, MD.

Neil, C.M., 1969. The question of radiation exposure to the hand from handling 99mTc. J. Nucl. Med. 10, 732–734.

Nettleton, J.S., Lawson, R.S., Prescott, M.C., Morris, I.D., 2004. Uptake, localization, and dosimetry of ^{111}In and ^{201}Tl in human testes. J. Nucl. Med. 45, 138–146.

Norrgren, K., Svegborn, S.L., Areberg, J., Mattsson, S., 2003. Accuracy of the quantification of organ acticity from planar gamma camera images. Cancer Biother. Radiopharm, 18.

Nosslin, B., Johansson, L., Leide-Svegborn, S., Liniecki, J., Mattsson, S., Taylor, D., 2003. A generic model for 11C-labelled radiopharmaceuticals for imaging receptors in the human brain. Rad. Prot. Dosim. 105, 587–591.

Olsson, H., Halldin, C., Swahn, G., Farde, L., 1999. Quantification of [^{11}C]FLB 457 binding to extrastriatal dopamine receptors in the human brain. J. Cereb. Blood Flow Metab. 19, 1164–1173.

Osman, S., Lundkvist, C., Pike, V.W., et al., 1996. Characterization of the radioactive metabolites of the 5-HT_{1A} receptor radioligand, [O-methy-^{11}C]WAY-100635, in monkey and human plasma by HPLC: comparison of the behaviour of an identified radioactive metabolite with parent radioligand in monkey using PET. Nucl. Med. Biol. 23, 627–634.

Pappata, S., Samson, Y., Chavoix, C., Prenant, C., Mazière, M., Baron, J.C., 1988. Regional specific binding of [^{11}C]RO 15 1788 to central type benzodiazepine receptors in human brain: quantitative evaluation by PET. J. Cereb. Blood Flow Metab. 8, 304–313.

Paul, G.S., Sharma, S.K., Rath, G.K., 2006. Finger doses for staff handling radiopharmaceuticals in nuclear medicine. J. Nucl. Med. Technol. 34, 169–173.

Pauwels, T., Dethy, S., Goldman, S., Monclus, M., Luxen, A., 1994. Effect of catechol-O-methyl transferase inhibition on peripheral and central metabolism of 6-[^{18}F]fluoro-L-DOPA. Eur. J. Pharmacol. 257, 53–58.

Persson, A., Pauli, S., Swahn, C.G., Halldin, C., Sedvall, G., 1989. Cerebral uptake of ^{11}C-Ro 15 1788 and its acid metabolite ^{11}C-Ro 15 3890: PET study in human volunteers. Human Psychopharmacol. 4, 215–220.

Pike, V.W., McCarron, J.A., Hume, S.P., et al., 1995. Preclinical development of a radioligand for studies of central 5-HT1A receptors in vivo – [^{11}C]WAY-100635. Med. Chem. Res. 5, 208–227.

Rao, D.V., Shepstone, B.J., Wilkins, H.B., Howell, R.W., 1995. Kinetics and dosimetry of thallium-201 in human testes. J. Nucl. Med. 36, 607–609.

Reske, S.N., Biersack, H.J., Lackner, K., et al., 1982. Assessment of regional myocardial uptake and metabolism of omega-(p-123I-phenyl) pentadecanoic acid with serial single-photon emission tomography. Nuklearmedizin 21, 249–253.

Reske, S.N., 1985. 123I-phenylpentadecanoic acid as a tracer of cardiac free fatty acid metabolism. Experimental and clinical results. Eur. Heart J. 6 (Suppl. B), 39–47.

Rimpler, A., Barth, I., Senftleben, S., et al., 2007. Beta radiation exposure of staff during therapies with Y-90 labeled substances. Beta-Days in Capri (Italy), 20–22 Sept. 2007 (http://www.uznuclear.rug.ac.be/betadayscapri/).

Rimpler, A., Barth, I., 2007. Beta radiation exposure of medical staff and implications for extremity dose monitoring. Rad. Prot. Dosim. 125, 335–339.

Roedler, H.D., 1980. Accuracy of Internal Dose Calculations with Special Consideration of Radiopharmaceutical Biokinetics. Third International Radiopharmaceutical Dosimetry Symposium, Oak Ridge, TN. HHS Publication (FDA 81-8166). Department of Health and Human Welfare, Bureau of Radiological Health, Rockville, MD.

Roedler, H.D., Kaul, A., 1976. Dose to Target Organs from Remaining Body Activity: Results of the Formally Exact and Approximate Solution. Radiopharmaceutical Dosimetry Symposium, Oak Ridge, TN. HEW Publication (FDA 76-8044). pp. 155–163.

Roedler, H.D., Kaul, A., Hine, G.J., 1978. Internal Radiation Dose in Diagnostic Nuclear Medicine. Hoffman, Berlin.

Rose, M.R., Prescott, M.C., Herman, K.J., 1990. Excretion of iodine-123-hippuran, technetium-99m-red blood cells, and technetium-99m-macroaggregated albumin into breast milk. J. Nucl. Med. 31, 978–984.

Rossetti, C., Vanoli, G., Paganelli, G., et al., 1994. Human biodistribution, dosimetry and clinical use of technetium (III)-99m-Q12. J. Nucl. Med. 35, 1571–1580.

Rubow, S., Klopper, J., Wasserman, H., Baard, B., van Niekerk, M., 1994. The excretion of radiopharmaceuticals in human breast milk: additional data and dosimetry. Eur. J. Nucl. Med. 21, 144–153.

Russell, J.R., Stabin, M.G., Sparks, R.B., Watson, E.E., 1997. Radiation absorbed dose to the embryo/fetus from radiopharmaceuticals. J. Nucl. Med. 73, 756–769.

Ryan, J., Cooper, M., Loberg, M., Harvey, E., Sikorski, S., 1977. Technetium-99m-labelled N-(2,6-dimethylphenyl carbamoylmethyl)-iminodiacetic acid (Tc99mHIDA): a new radiopharmaceutical for hepatobiliary imaging studies. J. Nucl. Med. 18, 997–1004.

Samson, G., Wackers, F.J.Th., Becker, A.E., et al., 1978. Distribution of thallium-201 in man, in: Oeff, K, Schmidt, H.A.E. (Eds.), Nuklearmedizin und biokybernetik, Vol. 1. Medico-informationsdienste, Berlin, pp. 385–389.

Schmidt, D., Langen, K-J., Herzog, H., et al., 1997. Whole-body kinetics and dosimetry of l-3-[^{123}I]iodo-α-methyltyrosine. Eur. J. Nucl. Med. 24, 1162–1166.

Shleien, B., Slaback, L.A.S, Jr., Birky, B.K., 1998. Handbook of Health Physics and Radiological Health. Williams and Wilkins, Baltimore, MD.

Shoup, T.M., Olson, J., Hoffman, J.M., et al., 1999. Synthesis and evaluation of [^{18}F]1-amino-3-fluorocyclobutane-1-carboxylic acid to image brain tumours. J. Nucl. Med. 40, 331–338.

Shreve, P., Chiao, P.C., Humes, H.D., Schwaiger, M., Gross, M.D., 1995. Carbon-11-acetate PET imaging in renal disease. J. Nucl. Med. 36, 1595–1601.

Shreve, P.D., Gross, M.D., 1997. Imaging of the pancreas and related diseases with PET carbon-11-acetate. J. Nucl. Med. 38, 1305–1310.

Sloof, G.W., Visser, F.C., van Lingen, A., et al., 1997. Evaluation of heart-to-organ ratios of 123I-BMIPP and the dimethyl-substituted 123I-DMIPP fatty acid analogue in humans. Nucl. Med. Commun. 18, 1065–1070.

Smith, T., Veall, N., Wootton, R., 1982. Bladder wall dose from administered radiopharmaceuticals: the effect of variation in urine flow rate, voiding interval and initial bladder content. Radiat. Prot. Dosim. 2, 183–189.

Smith, T., Lahiri, A., Gemmell, H.G., et al., 1992. Dosimetry of ^{99m}Tc-P53, a new myocardial perfusion imaging agent, in: Schlafke-Stelson, A, Watson, E.E. (Eds.), Fifth International Radiopharmaceutical Dosimetry Symposium. CONF-910529. Oak Ridge Associated Universities, Oak Ridge, TN, pp. 467–481.

Smith, T., Tong, C., Lammertsma, A.A., et al., 1994. Dosimetry of intravenously administered oxygen-15 labelled water in man: a model based on experimental human data from 21 subjects. Eur. J. Nucl. Med. 21, 1126–1134.

Snyder, W.S., Ford, M.R., Warner, G.G., Fisher Jr, H.R., 1969. Estimates of absorbed fractions for monoenergetic photon sources uniformly distributed in various organs of a heterogeneous phantom. MIRD Pamphlet No. 5. J. Nucl. Med. 10 (Suppl. 3).

Snyder, W.S., Ford, M.R., Warner, G.G., Watson, S.B., 1975. "S" Absorbed Dose per Unit Cumulated Activity for Selected Radionuclides and Organs. MIRD Pamphlet No. 11. Society of Nuclear Medicine, New York, NY.

Snyder, W.S., Ford, M.R., 1976. Estimation of doses to the urinary bladder and to the gonads, in: Cloutier, R.J., et al., (Eds.), Radiopharmaceutical Dosimetry Symposium, Oak Ridge, TN. HEW Publication (FDA 76-8044). Department of Health, Education and Welfare, Bureau of Radiological Health, Rockville, MD, pp. 313–349.

Snyder, W.S., Ford, M.R., Warner, G.G., 1978. Estimates of Specific Absorbed Fractions for Photon Sources Uniformly Distributed in Various Organs of a Heterogeneous Phantom. Medical Internal Radiation Dose Committee (NM/MIRD) Pamphlet No. 5, revised. Society of Nuclear Medicine, New York, NY.

Stabin, M.G., 1996. MIRDOSE: personal computer software for internal dose assessment in nuclear medicine. J. Nucl. Med. 37, 538–546.

Stabin, M.G., Kooij, P.P., Bakker, W.H., 1997. Radiation dosimetry for indium-111-pentetreotide. J. Nucl. Med. 38, 1919–1922.

Stabin, M.G., Breitz, H.B., 2000. Breast milk excretion of radiopharmaceuticals: mechanisms, findings, and radiation dosimetry. J. Nucl. Med. 41, 863–873.

Stabin, M.G., Siegel, J.A., 2003. Physical models and dose factors for use in internal dose assessment. Health Phys. 83, 294–310.

Stabin, M.G., Sparks, R.B., Crowe, E., 2005. OLINDA/EXM: the second-generation personal computer software for internal dose assessment in nuclear medicine. J. Nucl. Med. 46, 1023–1027.

Stenhouse, M.J., Baxter, M.S., 1977. Bomb ^{14}C as a biological tracer. Nature (Lond.) 267, 828–832.

Stenström, K., Leide-Svegborn, S., Erlandsson, B., et al., 1996. Application of accelerator mass spectrometry (AMS) for high-sensitivity measurements of $^{14}CO_2$ in long-term studies of fat metabolism. Appl. Radiat. Isot. 47, 417–422.

Stepanek, J., Larsson, B., Weinreich, R., 1996. Auger-electron spectra of radionuclides for therapy and diagnostics. Acta Oncol. 35, 863–868.

Stuardo, E., 1990. Hand dose levels in Chilean nuclear medicine laboratories. Radiat. Prot. Dosim. 34, 127–130.

Sun, K.T., Chen, K., Huang, S-C., et al., 1997. Compartment model for measuring myocardial oxygen consumption using [1-^{11}C]acetate. J. Nucl. Med. 38, 459–466.

Surma, M.J., Wiewiora, J., Liniecki, J., 1994. Usefulness of ^{99m}Tc-N,N′-ethylene-1-dicysteine complex for dynamic kidney investigations. Nucl. Med. Comm. 15, 628–635.

Surma, M.J., 1998a. Verification of ^{99m}Tc-ethylenedicysteine (^{99m}Tc-EC) distribution model in the organism. Nucl. Med. Rev. 1, 29–32.

Surma, M.J., 1998b. ^{99m}Tc-Ethylenedicysteine (^{99m}Tc-EC) renal clearance determination error for the multiple- and single-sample methods. Nucl. Med. Rev. 1, 33–40.

Syed, I.B., 1976. Dosimetry of indium-113m radiopharmaceuticals with special attention to the urinary bladder, in: Cloutier, R.J., et al., (Eds.), Radiopharmaceutical Dosimetry Symposium, Oak Ridge, TN. HEW Publication (FDA 76-8044). Department of Health, Education and Welfare, Bureau of Radiological Health, Rockville, MD, pp. 360–369.

Szabo, Z., Scheffel, U., Mathews, W.B., et al., 1999. Kinetic analysis of [^{11}C]McN5652: a serotonin transporter radioligand. J. Cereb. Blood Flow Metab. 19, 967–981.

Taavitsainen, M., Riihimäki, E., Tähti, E., 1980. Body disappearance and liver mean transit time of 99m-Tc-diethyl-IDA. Eur. J. Nucl. Med. 5, 147–150.

Taillefer, R., Edell, S., Innes, G., Lister-James, J., 2000. Acute thromboscintigraphy with (99m)Tc-apcitide: results of the phase 3 multicenter clinical trial comparing 99mTc-apcitide scintigraphy with contrast venography for imaging acute DVT. Multicenter trial investigators. J. Nucl. Med. 41, 1214–1223.

Tamaki, N., Morita, K., Kuge, Y., Tsukamoto, E., 2000. The role of fatty acids in cardiac imaging. J. Nucl. Med. 41, 1525–1534.

Tanaka, N., Fukushi, K., Shinotoh, H., et al., 2001. Positron emission tomographic measurement of brain acetylcholinesterase activity using N-[^{11}C]methylpiperidin-4-yl acetate without arterial blood sampling: methodology of shape analysis and its diagnostic power for Alzheimer's disease. J. Cereb. Blood Flow Metab. 21, 295–306.

Tandon, P., Venkatesh, M., Bhatt, B.C., 2007. Extremity dosimetry for radiation workers handling unsealed radionuclides in nuclear medicine departments in India. Health Phys. 92, 112–118.

Taylor, D.M., 2000a. Unpublished assessments.

Taylor, D.M., 2000b. Generic models for radionuclide dosimetry: ^{11}C, ^{18}F or ^{75}Se-labelled amino acids. Appl. Radiat. Isot. 52, 911–922.

Taylor, D.M., 2000c. Subcellular distribution of gallium-67 and other Auger-emitting radionuclides in human and animal tissues. Radiat. Prot. Dosim. 92, 229–231.

Taylor, D.M., Cottrall, M.F., 1973. Evaluation of amino acids labelled with ^{18}F for pancreas scanning, in: Radiopharmaceuticals and Labelled Compounds, Vol. I. IAEA, Vienna, pp. 441–443.

Thomas, S.R., Stabin, M.G., Chen, C.-T., Samaratunga, R.C., 1999. A dynamic urinary bladder model for radiation dose calculations. MIRD Pamphlet No. 14, revised. J. Nucl. Med. 40, 102S–123S.

Thomas, S.R., Stabin, M.G., Castronovo, F.P., 2005. Radiation-absorbed dose from ^{201}Tl-thallous chloride. J. Nucl. Med. 46, 502–508.

Tobin, R.E., Schneider, P.B., 1976. Uptake of ^{67}Ga in the lactating breast and its persistence in milk: case report. J. Nucl. Med. 17, 1055–1056.

Torizuka, K., Yonekura, Y., Nishimura, T., et al., 1991. The phase 1 study of β-methyl-p-(^{123}I)-iodophenyl-pentadecanoic acid (^{123}I-BMIPP). Kagu Igaku 28, 681–690.

Towsen, J.E.C., 2002. Radiation dosimetry and protection in PET, in: Valk, PE., Bailey, D.L., Townsend, D.W., et al. (Eds.), Positron Emission Tomography; Basic Science and Clinical Practice. Springer-Verlag, London, pp. 265–279.

Vallabhajosula, S., Zimmerman, R.E., Picard, M., et al., 1989. Technetium-99m ECD: a new brain imaging agent: in vivo kinetics and biodistribution studies in normal human subjects. J. Nucl. Med. 30, 599–604.

Vanhavere, F., Berus, D., Buls, N., et al., 2006. Use of extremity dose meters in a hospital environment. Radiat. Prot. Dosim. 118, 190–195.

Verhoeff, N.P., Sokole, E.B., Stabin, M., et al., 1993. Dosimetry of iodine-123 iodobenzamide in healthy volunteers. Eur. J. Nucl. Med. 20, 747–752.

Verhoeff, N.P., Busemann Sokole, E., Hengst, D., Stubbs, J.B., van Royen, E.A., 1993. Dosimetry of iodine-123 iomazenil in humans. Eur. J. Nucl. Med. 20, 580–584.

Versijpt, J., Dumont, F., Thierens, H., et al., 2000. Biodistribution and dosimetry of [^{123}I]iodo-PK 11195: a potential agent for SPET imaging of the peripheral benzodiazepine receptor. Eur. J. Nucl. Med. 27, 1326–1333.

Visseaux, H., Vuillez, J.P., Giraud, J.Y., 2007. Dosimetric study and radioprotection optimization in 18F-FDG scintigraphy. Medecine Nucleaire 28, 205–217.

Votaw, J.R., Ansari, M.S., Scott Mason, N., et al., 1995. Dosimetry of iodine-123-epidepride: a dopamine D2 receptor ligand. J. Nucl. Med. 36, 1316–1321.

Volkow, N.D., Ding, Y.S., Fowler, J.S., et al., 1995. A new PET ligand for the dopamine transporter: studies in human brain. J. Nucl. Med. 36, 2162–2168.

Waterhouse, R.N., Stabin, M.G., Page, J.G., 2003. Preclinical acute toxicity studies and rodent-based dosimetry estimates of the novel sigma-1 receptor radiotracer [^{18}F]FPS. Nucl. Med. Biol. 30, 555–563.

Watson, E.E., Stabin, M.G., Eckerman, K.F., 1989. A model of the peritoneal cavity for use in internal dosimetry. J. Nucl. Med. 30, 2002–2011.

Wester, H.J., Herz, M., Senkowitsch-Schmidtke, R., Schwaiger, M., Stöcklin, G., Hamacher, K., 1999a. Preclinical evaluation of 4-[^{18}F]fluoroprolines: diasteromeric effect on metabolism and uptake in mice. Nucl. Med. Biol. 26, 259–265.

Wester, H.J., Herz, M., Weber, W., et al., 1999b. Synthesis and radiopharmacology of O-(2-[^{18}F]fluoroethyl)-L-tyrosine for tumor imaging. J. Nucl. Med. 40, 205–212.

Westera, G., Buck, A., Burger, C., Leenders, K.L., von Schultness, G.K., Schubiger, A.P., 1996. Carbon-11 and iodine-123 labelled iomazenil: a direct PET-SPECT comparison. Eur. J. Nucl. Med. 23, 5–12.

Whitby, M., Martin, C.J., 2002. Options for shielding the hand during dispensing and administration of radiopharmaceuticals. Sixth European ALARA Network Workshop in Occupational Exposure Optimization in Medical Field and Radiopharmaceutical Industry, pp. 167–170 (http://www.eualara.net/images/stories/pdf/program6/Session%20C/M_Whithy.pdf).

Whitby, M., Martin, C.J., 2003. Investigation using an advanced extremity gamma instrumentation system of options for shielding the hand during the preparation and injection of radiopharmaceuticals. J. Radiol. Prot. 23, 79–96.

Whitby, M., Martin, C.J., 2005. A multi-centre study of dispensing methods and hand doses in hospital radiopharmacies. Nucl. Med. Commun. 26, 49–60.

van de Wiele, C., De Vos, F., De Sutter, J., et al., 1999. Biokinetics and dosimetry of (iodine-123)-iodomethyl-N,N-dimethyltamoxifen, an (anti)oestrogen receptor radioligand. Eur. J. Nucl. Med. 26, 1259–1264.

Wilhelm, A.J., Mijnhout, G.S., Franssen, E.J., 1999. Radiopharmaceuticals in sentinel lymph-node detection - an overview. Eur. J. Nucl. Med. 26, S36–S42.

Williams, E.D., Laird, E.E., Forster, E., 1987. Monitoring radiation dose to the hands in nuclear medicine: location of dosemeters. Nucl. Med. Commun. 8, 449–503.

Williams, L.R., Leggett, R.W., 1989. Reference values for resting blood flow to organs of man. Clin. Phys. Physiol. Meas. 10, 187–217.

Wilson, A.A., Inaba, T., Fischer, N., et al., 1998. Derivatives of WAY 100635 as potential imaging agents for 5-HT1A receptors: syntheses, radiosyntheses, and in vitro and in vivo evaluation. Nucl. Med. Biol. 25, 769–776.

Winchell, H.S., Horst, W.D., Braun, L., Oldendorf, W.H., Hattner, R., Parker, H., 1980. N-Isopropyl (^{123}I)*p*-iodoamphetamine: single-pass brain uptake and washout; binding to brain synaptosomes; and localisation in dog and monkey brain. J. Nucl. Med. 21, 947–952.

Wistow, B.W., Subramanian, G., Van Heertum, R.L., et al., 1977. An evaluation on ^{99m}Tc-labeled hepatobiliary agents. J. Nucl. Med. 18, 455–461.

Wrzesień, M., Olszewski, J., Jankowski, J., 2008. Hand exposure to ionising radiation of nuclear medicine workers. Rad. Prot. Dosim. 130, 325–330.

Wu, R.K., Siegel, J.A., Rattner, Z., Malmud, L.S., 1984. Tc-99m HIDA dosimetry in patients with various hepatic disorders. J. Nucl. Med. 25, 905–912.

Yeh, S.H., Liu, R.S., Wu, L.C., Yen, S.H., Chang, C.W., Chen, K.Y., 1999. ^{11}C-acetate clearance in nasopharyngeal carcinoma. Nucl. Med. Commun 20, 131–134.

Yoshizumi, T., Nozaki, S., Fukuchi, K., et al., 2000. Pharamacokinetics and metabolism of ^{123}I-BMIPP fatty acid analog in healthy and CD36-deficient subjects. J. Nucl. Med. 41, 1134–1138.

Zanzonico, P.B., 2000. Internal radionuclide radiation dosimetry: a review of basic concepts and recent developments. J. Nucl. Med. 41, 297–308.

Zhu, X., 2004. Radiation safety considerations with yttrium-90 ibritumomab tiuxetan (Zevalin). Semin. Nucl. Med. 34, 20–23.

Montgomery, A., Anstee, D.E., Martin, C.J., et al., 1999. Reduction in finger dose for radiopharmaceutical dispensing afforded by a syringe shield and an automatic dose dispenser. Nucl. Med. Commun. 20, 189–194.

Neil, C.M., 1969. The question of radiation exposure to the hand from handling 99mTc. J. Nucl. Med. 10, 732–734.

Paul, G.S., Sharma, S.K., Rath, G.K., 2006. Finger doses for staff handling radiopharmaceuticals in nuclear medicine. J. Nucl. Med. Technol. 34, 169–173.

Rimpler, A., Barth, I., Senftleben, S., et al., 2007. Beta radiation exposure of staff during therapies with Y-90 labeled substances. Beta-Days in Capri (Italy), 20–22 Sept. 2007 (http://www.uznuclear.rug.ac.be/betadayscapri/).

Rimpler, A., Barth, I., 2007. Beta radiation exposure of medical staff and implications for extremity dose monitoring. Rad. Prot. Dosim. 125, 335–339.

Shleien, B., Slaback Jr., L.A.S., Birky, B.K., 1998. Handbook of Health Physics and Radiological Health. Williams and Wilkins, Baltimore, MD.

Stuardo, E., 1990. Hand dose levels in Chilean nuclear medicine laboratories. Radiat. Prot. Dosim. 34, 127–130.

Tandon, P., Venkatesh, M., Bhatt, B.C., 2007. Extremity dosimetry for radiation workers handling unsealed radionuclides in nuclear medicine departments in India. Health Phys. 92, 112–118.

Towsen, J.E.C., 2002. Radiation dosimetry and protection in PET. In: Valk, P.E., Bailey, D.L., Townsend, D.W., et al. (Eds.), Positron Emission Tomography; Basic Science and Clinical Practice. Springer-Verlag, London, pp. 265–279.

Vanhavere, F., Berus, D., Buls, N., et al., 2006. Use of extremity dose meters in a hospital environment. Radiat. Prot. Dosim. 118, 190–195.

Visseaux, H., Vuillez, J.P., Giraud, J.Y., 2007. Dosimetric study and radioprotection optimization in 18F-FDG scintigraphy. Medecine Nucleaire 28, 205–217.

Whitby, M., Martin, C.J., 2002. Options for shielding the hand during dispensing and administration of radiopharmaceuticals. Sixth European ALARA Network Workshop in Occupational Exposure Optimization in Medical Field and Radiopharmaceutical Industry, pp. 167–170 (http://www.eu-alara.net/images/stories/pdf/program6/Session%20C/M_Whithy.pdf).

Whitby, M., Martin, C.J., 2003. Investigation using an advanced extremity gamma instrumentation system of options for shielding the hand during the preparation and injection of radiopharmaceuticals. J. Radiol. Prot. 23, 79–96.

Whitby, M., Martin, C.J., 2005. A multi-centre study of dispensing methods and hand doses in hospital radiopharmacies. Nucl. Med. Commun. 26, 49–60.

Williams, E.D., Laird, E.E., Forster, E., 1987. Monitoring radiation dose to the hands in nuclear medicine: location of dosemeters. Nucl. Med. Commun. 8, 449–503.

Wrzesień, M., Olszewski, J., Jankowski, J., 2008. Hand exposure to ionising radiation of nuclear medicine workers. Rad. Prot. Dosim. 130, 325–330.

Zhu, X., 2004. Radiation safety considerations with yttrium-90 ibritumomab tiuxetan (Zevalin). Semin. Nucl. Med. 34, 20–23.